Shaking Table Testing of Cyclic Behaviour of Fine-Grained Soils Undergoing Cementation: Cemented Paste Backfill

IMAD HAZIM ALAINACHI

A thesis submitted in partial fulfilment of the requirements for the Doctorate in Philosophy degree in Civil Engineering

under the supervision of

Dr. Mamadou Fall

Department of Civil Engineering
Faculty of Engineering
University of Ottawa

ABSTRACT

Cemented paste backfill (CPB) is a novel technology developed in the past few decades to better manage mining wastes (such as tailings) in environmentally friendly way. It has received prominent interest in the mining industry around the world. In this technology, up to 60% of the total amount of tailings is reused and converted into cemented construction material that can be used for secondary support in underground mine openings (stopes) and to maximize the recovery of ore from pillars. CPB is an engineered mixture of tailings, water, and hydraulic binder (such as cement), that is mixed in the paste plant and delivered into the mine stopes either by gravity or pumping. During and after placing it into the mine stopes, the performance of CPB mainly depends on the role of the hydraulic binder, which increases the mechanical strength of the mixture through the process of cement hydration. Similar to other fine-grained soils undergoing cementations, CPB's behavior is affected by several conditions or factors, such as cement hydration progress (curing time), chemistry of pore water, mixing and curing temperature, and filling strategy. Also, it has been found that fresh CPB placed in the mine stopes can be susceptible to many geotechnical issues, such as liquefaction under ground shaking conditions. Liquefaction-induced failure of CPB structure may cause injuries and fatalities, as well as significant environmental and economic damages. Many researches studied the effect of the aforementioned conditions on the static mechanical behavior of CPB. Other researches have evaluated the liquefaction behavior of natural soils and tailings (without cement) during cyclic loadings using shaking table test technique. Only few studies investigated the CPB liquefaction during dynamic loading events using the triaxial tests. Yet, there are currently no studies that addressed the liquefaction behavior of CPB under the previous conditions by using the shaking table technique. In this Ph.D. study, a series of shaking table tests were conducted on fresh CPB samples (75 cm × 75 cm ×70 cm), which were mixed and poured into a flexible laminar shear box (that was designed and build for the purpose of this research). Some of these shaking table tests were performed at different maturity ages of 2.5 hrs, 4.0 hrs, and 10.0 hrs, to investigate the effect of cement hydration progress on the liquefaction potential of CPB. Another set of tests were conducted to assess the effect of the chemistry (sulphate content) of the pore-water on the cyclic response of fresh CPB by exposing cyclic loads on couple of CPB models that contain different concertation of sulphate ions of 0.0 ppm and 5000 ppm. Moreover, as part of this study, series of shaking table test was conducted on CPB samples that were prepared and cured at different temperatures of 20^{o}C and 35^{o}C, to evaluate the effect of temperature of the cyclic behavior of CPB. Furthermore, the effect of filling strategy on the cyclic behavior of fresh CPB was assessed by conducting set of shaking tables tests on CPB models that were prepared at different filling strategies of continuous filling, and sequential or discontinuous (layered) filling. The results obtained show that CPB has different cyclic behavior and performance under these different conditions. It is observed that the progress of cement hydration (longer curing time) enhances the liquefaction resistance of CPB, while the presence of sulphate ions diminishes it. It is also found that CPB mixed and cured in low temperature is more prone to liquefaction than those prepared at higher temperatures. Moreover, the obtained results show that adopting the discontinuous (layered) filling strategy will improve the liquefaction resistance of

CPB. The finding presented in this thesis will contribute to efficient, cost effective and safer design of CPB structures in the mine areas, and will help in minimizing the risks of liquefaction-induced failure of CPB structures.

DEDICATION

To the soul of my Father "**HAZIM ALAINACHI**". I have kept my promise to you, and I hope that this work makes you happy and proud.

To all members of my beloved family, especially to my mother **TAROUB AL AREF**, my wife, **GHADA**, and my children, **HAZIM**, **AHMED**, and **MAYAR**.

Thank you all for your love, support, and patience during times of my study.

ACKNOWLEDGMENTS

First and foremost, Alhamdulillah (praise and thanks to my God), for providing me with the strength, opportunity to study and learn, and for the endless generosity in all aspects of life.

I would like also to express my immense and heartful thanks and appreciation to my supervisor, Dr. Mamadou Fall, for his enduring, encouragement, guidance, support and constructive feedback during my Ph.D. research study.

I would like to sincerely acknowledge and give special thanks to Dr. Muslim Majeed and Dr. Rozalina Dimitrova at the University of Ottawa, and Dr. Mohammad Al-Umar at the University of Thi-Qar for their invaluable advices and unconditional support during my study. I would like also to take this opportunity to express my thanks and appreciation to all of those who provided friendship, support and assistance. They include Mr. Ahmed Bahlol, Dr. Alaa Abdulridha, Dr. Gamal Elnavelsya, Mrs. Ghada Ali, Mr. Kun Fang, Mr. Jean-Claude Célestin, Mr. Luc Cloutier, Dr. Mohammed Al-Khazaali, Mrs. Najlaa Abdul-Hussain, Dr. Othman Nasir, Mr. Sada Haruna, and Dr. Zaid Aldhafeeri. In addition, my sincere thanks to all my colleagues at the University of Ottawa, as they have offered invaluable encouragement and support.

Last, but not least, I am extremely thankful for my mother “Taroub”, wife “Ghada”, and children “Hazim, Ahmed, and Mayar”, for their love and encouragement that allowed me to finish this journey. I also want to thank every single member of my family and my in-laws’ who always supported me during my life, specially during my study. This accomplishment would not have been possible without your love. Finally, I want to pray for the soul of my father. I have kept my promise to you, and I hope that this work makes you happy and proud.

LIST OF CONTENTS

LIST OF FIGURES

LIST OF TABLES

LIST OF SYMBOLS AND ABBREVIATIONS

9MT : Nine Mine Tailings
AMD :Acid Mine Drainage
BPT : Break Penetration Test
CF : Continuous Filling
CPB : Cemented Paste Backfill
CPT : Cone Penetration Test
CT : Cable Transducer
CVR : Critical Void Ratio
D : Direction
DAQS : Data Acquisition System
DF : Discontinuous Filling
DTG : Differential Thermogravimetry
E : Electrical
EC : Electrical Conductivity
ELM : Extream Learning Machine
Fc : Fine Content
FLSB : Flexible Laminar Shear Box
g : Ground Acceleration (9.81 m/sec^2)
Gs : Specific Gravity
H : Hydraulic
HD : Horizontal Displacement
HDA : Horizontal Displacement Amplitude
hrs : Hours
LVDT : Linear Variable Differential Transformer
M : Manual
min : Minutes
OPC : Ordinary Portland Cement
PC : Portland Cement
PCI : Portland Cement – type I
PLMD : Post Loading Monitoring Duration
ppm : Parts-Per-Million (10^{-6})
PWP : Pore-Water Pressure
S : Degree of Saturation
SD : Shaking Duration
sec : Seconds
SEM : Scanning Electron Microscopy
SLF : Sinusoidal Loading Frequency
SPHA : Shaking Peak Horizontal Acceleration

SPT : Standard Penetration Test
ST : Silica Tailings
Temp. : Temperature
TG : Thermal Gravimetry
VD : Vertical Displacement
VWC : Volumetric Water Content
w/c : Water-to-Cement Ratio
XRD : X-ray Diffraction

R_u : Pore-Water Pressure Ratio
σ' : Effective Stress
σ'_o : Initial Effective Stress
Δu : Change in Pore-Water Pressure Ratio
A : Deformation Amplitude
T : Loading Cycle Time
a : Peak Ground Acceleration
f : Circular Loading Frequency
g : Ground Acceleration
u : Pore Water Pressure
θ : Diffraction Angle
σ : Total Stress
ω : Radial Loading Frequency

CHAPTER 1 General Introduction

1.1 Background and Problem Statement

Mining is one of the industries that highly influences the evolution and development of human societies around the world. It significantly contributes to the economy and remarkably boosts the employment market. For instant, in 2017, the worldwide revenue produced by mining activities was around 600 billion USD. Canada is one of the leading countries in mining industry, producing more than 60 kinds of minerals and metals. The total Canada-wide production of minerals in 2018 was 47 billion CAD (Aldhafeeri 2018, Natural Resources Canada 2019, Statista 2019).

On the other hand, mining activities might be associated with several engineering and environmental problems that have negative impacts, such as the production of huge quantities of soil wastes (e.g. tailings) as a result of ore extraction during mining. For example, the annual worldwide production of mine waste in 1982 exceeded 4500 million tons, and it was around 650 million tons in Canada in 1991 (Moncur 2006). These tailings were found to be a potential source of environmental hazards when poorly disposed of, as they can generate acid mine drainage (AMD), which causes detrimental effects on underground and surface water bodies if deported from mine disposal site. Also, surface disposal of tailings in the form of tailings dams and/or tailing ponds might cause geotechnical engineering problems (e.g., dam failure) when subjected to earthquakes. For instant, 20 events of tailings dam failure were recorded around the world between 2000 and 2010 (Azam and Li 2010). Moreover, mining extraction creates large underground openings (stopes) that expose the surrounding areas to various geotechnical engineering problems, such as ground subsidence. In addition, the instability of these underground openings might put the safety of workers in the mine workplace at risk and people in the surrounding area (Coumans 2003, Kesimal et al. 2005, Hesketh et al. 2010).

A novel method of underground mine waste disposal named Cemented Paste Backfill (CPB) was developed in the past few decades to minimize the risks associated with mining activities. The CPB technique can be summarized by mixing the tailings with water and binders, and then pumping the mixture back into the underground mine stope. CPB is considered to be an environmentally friendly waste management technique, because it allows large quantities of the mine waste to be returned to the mine stope. Also, it was found that using CPB as backfill will increase the stability of the underground mine in the long term. Thus, CPB became a common practice in underground mine backfill process around the world (Brakebusch 1995, Belem and Benzaazoua 2004, Fall et al. 2005, Ercikdi et al. 2009, Thompson et al. 2009, Aldhafeeri and Fall 2016).

However, several geotechnical engineering issues were identified that occurred owing to fresh CPB placed in mine stopes. These issues include mechanical instability when it is exposed

to static loadings and liquefaction when it is exposed to dynamic loading (such as seismic activities or blasting loading). Failure of CPB in mine stopes might cause injuries and fatalities within the mine workers besides the negative environmental impacts and economic damages (Poulos et al. 1985, Fall and Samb 2008, Abdelaal 2011, Becker et al. 2014).

Considerable amount of research has been undertaken to assess the mechanical behavior or stability of CPB exposed to static loading conditions (e.g. Kesimal et al. 2005, Nasir and Fall 2010, Abdelaal 2011, Li and Aubertin 2012, Ghirian and Fall 2013, Ghirian and Fall 2014, Cui and Fall 2016, Ghirian and Fall 2016a, Cihangir et al. 2018). Yet, only a few studies (Saebimoghaddam 2010, Lu and Fall 2017) evaluated the liquefaction response of fresh CPB exposed to dynamic loading conditions, particularly cyclic loadings. Thus, and as the frequency of seismic events occurring in underground mines is increasing (Cook 1976), the need of more studies to understand the cyclic induced liquefaction of early aged CPB has become critically important.

In the past decades, several seismic activities were recorded in mine areas. These activities were initiated either owing to natural earthquake events or the mining activities itself (Hasegawa et al. 1989, Ahn et al. 2017). This fact increases the frequency of CPB structures to be exposed to cyclic loading, which increases the risk of seismic-induced liquefaction of CPB at early age.

Like any cementitious material, the engineering properties of CPB (such as the mechanical, thermal, and hydraulic behavior etc.) are affected by the progress of cement hydration. With the passage of time, the better mechanical behavior is expected in these materials (Saebimoghaddam 2010, Bullard et al. 2011, Scrivener et al. 2015, Aldhafeeri and Fall 2016). On the other hand, previous studies have found that CPB may contain various (uncontrollable) minerals and chemical components (such as the sulphate), which might come from the mine processing water or from the composition of the mine tailings itself (Pokharel and Fall 2011). The initial content of these chemicals could significantly influence the mechanical behavior of CPB (Ercikdi et al. 2009, Fall and Pokharel 2011). Other studies have found that the temperature of fresh CPB placed in mine stopes is affected by several heat sources (Wu et al. 2012), which might affect mechanical, thermal, and hydraulic properties of CPB besides its geochemical and environmental properties (Aldhafeeri et al. 2016, Cui and Fall 2016). Accordingly, it can be obviously expected that the progress of cement hydration with time, initial content of chemical components and heat variation can significantly affect the liquefaction behavior of early age CPB.

Typically, most of the mines follow a sequential filling strategy at which the mine stope will be filled up in two or more layers. The first layer (plug fill) is typically 2-3 m thick. Afterword, the main part of the stope will be filled continuously or in layers (based on the size of the stope). Implementing this strategy can reduce the stresses on the stope barricade (Yumlu and Guresci 2007, Ghirian and Fall 2016b). Previous studies found that the static mechanical strength of CPB is affected by filling the stope continuously or in stages (Ghirian and Fall 2016b). However, there is a lack of knowledge on the influence of dynamic loadings on the behavior of CPB that is sequentially filled in the mine stopes.

Considering the facts mentioned above, there is a need to acquire a sufficient understanding of the behavior of CPB under dynamic (cyclic) loading, particularly its of comprehensive study of the mechanical stability of CPB structures under dynamic loadings, particularly cyclic loadings, at the early ages by assessing the behavior and liquefaction potential of early age CPB subjected to these loadings under the effect of different conditions, such as the effect of progress of cement hydration with time, effect of initial content of uncontrolled chemical elements, the effect of temperature variation, and the effect of different filling strategies.

1.2 Objectives

Bearing in mind the paucity of understanding of the geotechnical behavior and response, particularly liquefaction potential, of early aged CPB exposed to cyclic loadings and the influence of various conditions on this response, the main objective of this Ph.D. study is to use the shaking table testing technique to understand the behavior and response of fresh CPB under cyclic conditions, in relation to the following conditions:

1. The influence of progress of cement hydration process (progress of curing time) on this behavior

2. The influence of the initial content of chemical elements, particularly sulphate ions, on this behavior

3. The influence of the backfill temperature (mixing and curing temperature) on this behavior

4. The influence of continuous filling and discontinuous filling on this behavior

1.3 Research Approaches and Methods

1.3.1 Research Approaches

The research approaches adopted in this study are illustrated in the schematic flowchart in Figure 1.1. To better understand the cyclic behavior of CPB under the influence of the aforementioned conditions, this study was conducted in five main phases:

Phase 1 – This phase includes the definition of the studied problem, and determining the research objectives.

Phase 2 – This phase includes a comprehensive literature review of (i) the material to be tested (CBP), (ii) the dynamic response of this material, (iii) the susceptibility of liquefaction and its assessment criteria, and (iv) the experimental approach (shaking table test).

Phase 3 – This phase consists of determining the cyclic parameters that are applied in the experimental tests. These parameters have been chosen giving due consideration to (i) the historical seismic events in underground mine areas, (ii) parameters that were used in similar

experimental approach in the literature, and (iii) the capacities and limitations of instruments to be used in this experiment.

Phase 4 - Conducting the experimental program that are divided into four sub-phases to better understand the influence of each condition or factor mentioned above. These sub-phases are:

1. Conducting shaking table tests on three CPB samples which were cured to different maturity ages (curing time) of 2.5 hrs, 4.0 hrs, and 10.0 hrs.

2. Conducting shaking table tests on two CPB samples, 4.0 hrs old, which were prepared with different initial concentration of sulphate (0 ppm and 5000 ppm).

3. Conducting shaking table tests on two CPB samples, 2.5 hrs old, which were prepared and cured at different temperatures (20°C and 35°C).

4. Conducting shaking table tests on three CPB samples which were prepared by following different filling strategy of (i) continuous filling, 2.5 hrs old, (ii) continuous filling, 4.0 hrs old, and (iii) discontinuous (layered) filling at which the first layer (plug) is 4.0 hrs old and the second layer (residual fill) is 2.5 hrs old.

Phase 5 - Analyzing the experimental results and assessing the seismic-induced liquefaction potential of CPB with respect to the tested conditions.

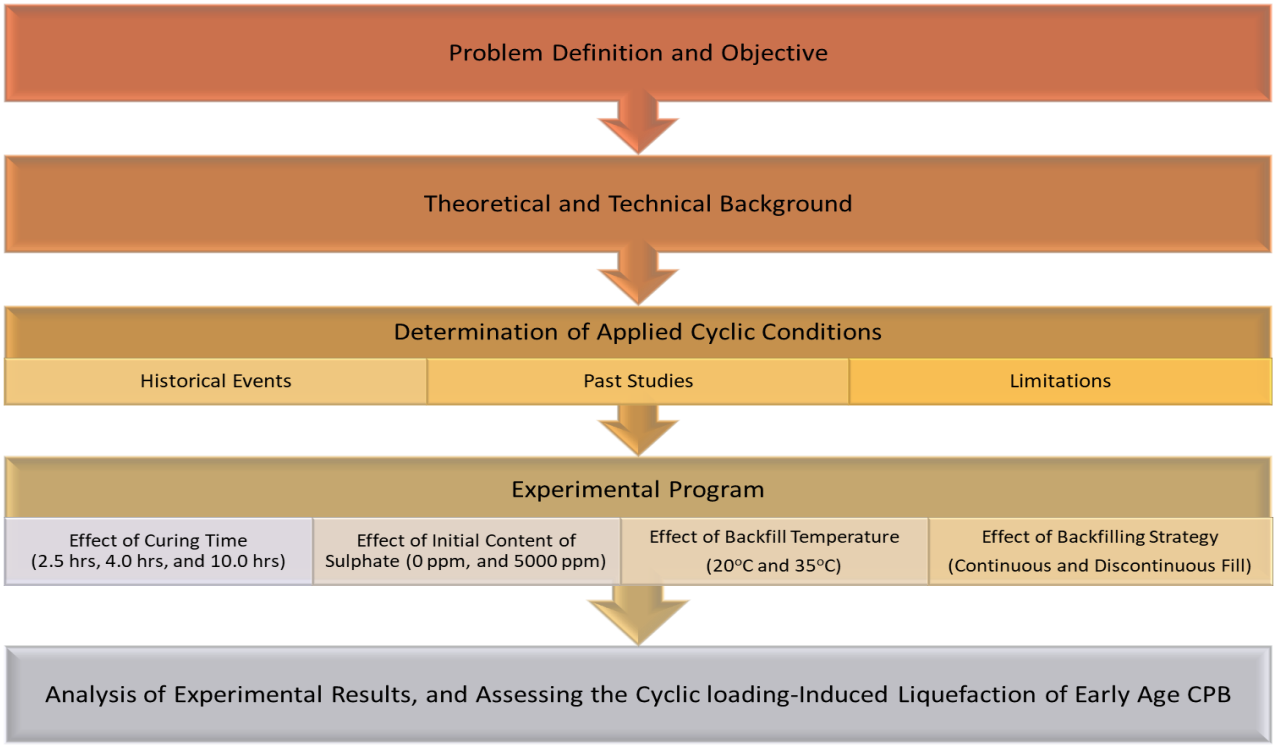

Figure 1.1 Flowchart of research approach

1.4 Thesis Outline

This thesis is mainly organized in the form of technical papers and contains eight chapters (Figure 1.2), as described below:

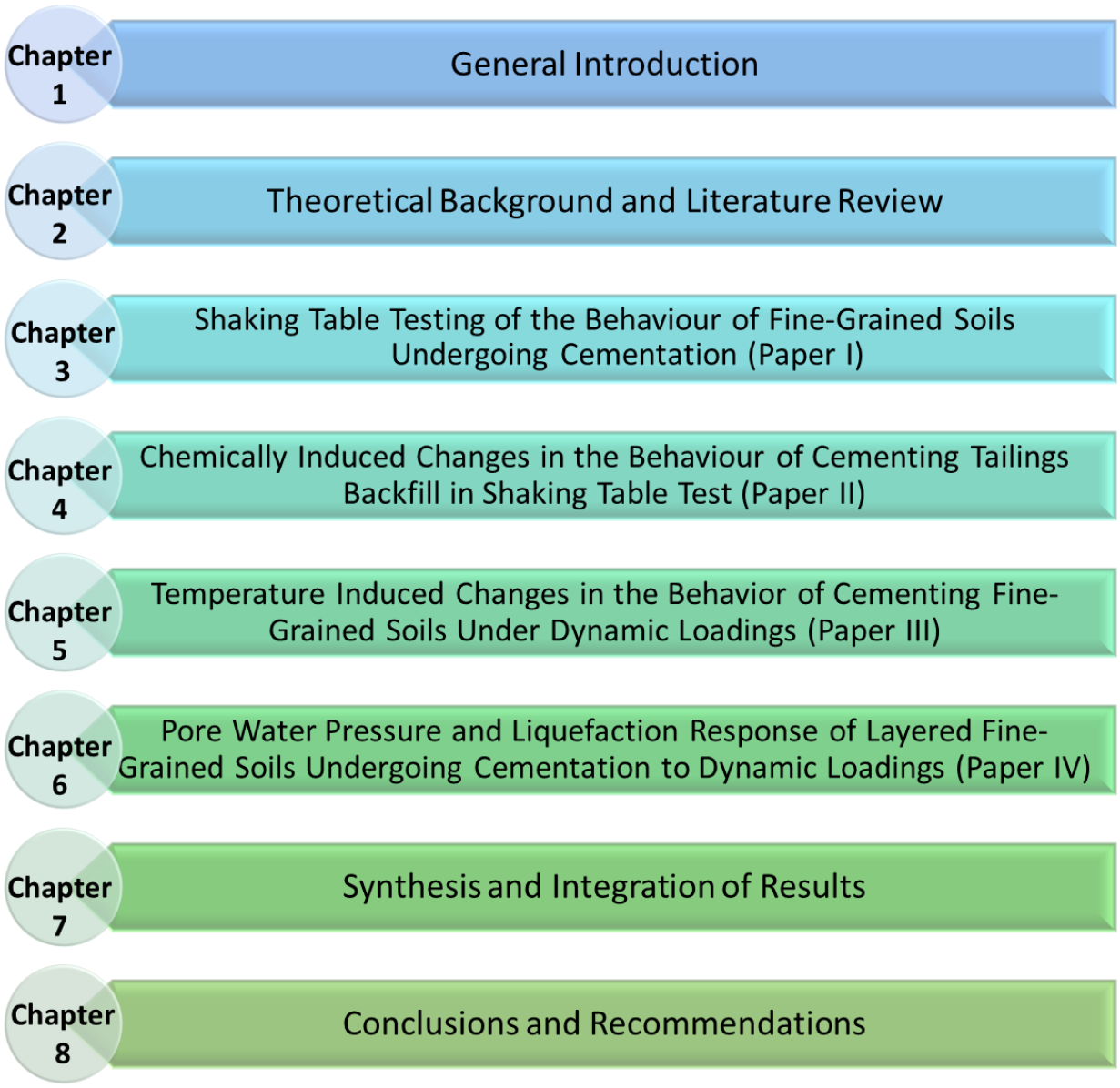

Figure 1.2 Organization of the thesis

Chapter 1: provides a general introduction to the PhD study. The problem statements, objectives, and research approaches and methods adopted in this study.

Chapter 2: includes a literature review and a review of the fundamental technical and theoretical background information on Cemented Paste Backfill (CPB), seismic events in underground mines,

Portland cement, liquefaction and shaking table testing technique. This information is necessary to facilitate the understanding of the technical issues addressed in this thesis. Moreover, previous studied of shaking table tests on natural fine-grained soils and tailings are reviewed and discussed.

Chapter 3: presents the technical paper on shaking table testing of the cyclic behavior of fine-grained soils (cementing paste backfill) undergoing cementation.

Chapter 4: deals with the assessment of cyclic-induced liquefaction susceptibility of cementing paste backfill with various sulphate contents.

Chapter 5: studies the effect of initial temperature of cementing paste backfill on its cyclic behavior.

Chapter 6: discusses the effect of continuous filling and discontinuous (layered) filling on the cyclic behavior of CPB.

Chapter 7: syntheses the overall thesis results.

Chapter 8: presents the summary and conclusions on this thesis.

Moreover, detailed explanation on the experimental setup of this research is presented in the **Appendix** of this dissertation.

It should be emphasized that since a paper-based thesis format is adopted, some of the contents in the papers may be repeated as each paper is independently written, and crafted according to manuscript instructions for the specified publication.

1.5 References

Abdelaal, A. (2011) *Early age mechanical behavior and stiffness development of cemented paste backfill with sand*, Doctoral dissertation, University of Toronto.

Ahn, K. S., Zhang, C. and Canbulat, I. (2017) 'Study of seismic activities associated with Australian underground coal mining', in *Coal Operators' Conference*, University of Wollongong, Australia,

Aldhafeeri, Z. (2018) *Reactivity of Cemented Paste Backfill*, University of Ottawa.

Aldhafeeri, Z. and Fall, M. (2016) 'Time and damage induced changes in the chemical reactivity of cemented paste backfill', *Journal of Environmental Chemical Engineering*, 4(4), 4038-4049.

Aldhafeeri, Z., Fall, M., Pokharel, M. and Pouramini, Z. (2016) 'Temperature dependence of the reactivity of cemented paste backfill', *Applied Geochemistry,* 72, 10-19.

Azam, S. and Li, Q. (2010) 'Tailings dam failures: a review of the last one hundred years', *Geotechnical news,* 28(4), 50-54.

Becker, D., Cailleau, B., Kaiser, D. and Dahm, T. (2014) 'Macroscopic Failure Processes at Mines Revealed by Acoustic Emission (AE) Monitoring', *Bulletin of the Seismological Society of America,* 104(4), 1785-1801.

Belem, T. and Benzaazoua, M. (2004) *An overview on the use of paste backfill technology as a ground support method in cut and fill mines,* translated by Perth, Australia: CRC Press, 637–650.

Brakebusch, F. W. (1995) 'Basics of paste backfill systems', *International Journal of Rock Mechanics and Mining Sciences and Geomechanics Abstracts,* 3(32), 122A.

Bullard, J. W., Jennings, H. M., Livingston, R. A., Nonat, A., Scherer, G. W., Schweitzer, J. S., Scrivener, K. L. and Thomas, J. J. (2011) 'Mechanisms of cement hydration', *Cement and Concrete Research,* 41(12), 1208-1223.

Cihangir, F., Ercikdi, B., Kesimal, A., Ocak, S. and Akyol, Y. (2018) 'Effect of sodium-silicate activated slag at different silicate modulus on the strength and microstructural properties of full and coarse sulphidic tailings paste backfill', *Construction and Building Materials,* 185, 555-566.

Cook, N. G. W. (1976) 'Seismicity associated with mining', *Engineering Geology,* 10(1976), 99-122.

Coumans, C. (2003) *Mining in Canada: the bigger picture Presentation for Philippine delegation to Ottawa.*

Cui, L. and Fall, M. (2016) 'Mechanical and thermal properties of cemented tailings materials at early ages: Influence of initial temperature, curing stress and drainage conditions', *Construction and Building Materials,* 125, 553-563.

Ercikdi, B., Kesimal, A., Cihangir, F., Deveci, H. and Alp, İ. (2009) 'Cemented paste backfill of sulphide-rich tailings: Importance of binder type and dosage', *Cement and Concrete Composites,* 31(4), 268-274.

Fall, M., Benzaazoua, M. and Ouellet, S. (2005) 'Experimental characterization of the influence of tailings fineness and density on the quality of cemented paste backfill', *Minerals Engineering*, 18(1), 41-44.

Fall, M. and Pokharel, M. (2011) 'Strength development and sorptivity of tailings shotcrete under various thermal and chemical loads', *Canadian Journal of Civil Engineering*, 38(7), 772-784.

Fall, M. and Samb, S. S. (2008) 'Pore structure of cemented tailings materials under natural or accidental thermal loads', *Materials Characterization*, 59(5), 598-605.

Ghirian, A. and Fall, M. (2013) 'Coupled thermo-hydro-mechanical–chemical behaviour of cemented paste backfill in column experiments. Part I: Physical, hydraulic and thermal processes and characteristics', *Engineering Geology*, 164, 195-207.

Ghirian, A. and Fall, M. (2014) 'Coupled thermo-hydro-mechanical–chemical behaviour of cemented paste backfill in column experiments', *Engineering Geology*, 170, 11-23.

Ghirian, A. and Fall, M. (2016a) 'Influence of Curing Stress on Long-term Hydro-Mechanical Response of Cemented Paste Backfill', in *Tailings and Mine Waste*, Keystone, Colorado, USA,

Ghirian, A. and Fall, M. (2016b) 'Strength evolution and deformation behaviour of cemented paste backfill at early ages: Effect of curing stress, filling strategy and drainage', *International Journal of Mining Science and Technology*, 26(5), 809-817.

Hasegawa, H. S., Wetmiller, R. J. and Gendzwill, D. J. (1989) 'Induced seismicity in mines in Canada—an overview', *Pure and applied geophysics*, 129(3-4), 423-453.

Hesketh, A. H., Broadhurst, J. L. and Harrison, S. T. L. (2010) 'Mitigating the generation of acid mine drainage from copper sulfide tailings impoundments in perpetuity: A case study for an integrated management strategy', *Minerals Engineering*, 23(3), 225-229.

Kesimal, A., Yilmaz, E., Ercikdi, B., Alp, I. and Deveci, H. (2005) 'Effect of properties of tailings and binder on the short-and long-term strength and stability of cemented paste backfill', *Materials Letters*, 59(28), 3703-3709.

Li, L. and Aubertin, M. (2012) 'A modified solution to assess the required strength of exposed backfill in mine stopes', *Canadian Geotechnical Journal*, 49(8), 994-1002.

Lu, G. and Fall, M. (2017) 'Simulation of Blast Induced Liquefaction Susceptibility of Subsurface Fill Mass', *Geotechnical and Geological Engineering*, 36(3), 1683-1706.

Moncur, M. C. (2006) 'Acid mine drainage: past, present...future?', *Wat on Earth*,

Nasir, O. and Fall, M. (2010) 'Coupling binder hydration, temperature and compressive strength development of underground cemented paste backfill at early ages', *Tunnelling and Underground Space Technology*, 25(1), 9-20.

Natural Resources Canada (2019) 'Earthquake Reports for 2019', [online], available: http://www.seismescanada.rncan.gc.ca/recent/2019/index-en.php 2019].

Poulos, S. J., Robinsky, E. I. and Keller, T. O. (1985) 'Liquefaction Resistance of Thickened Tailings', *Journal of Geotechnical Engineering*, 111(12), 1380-1394.

Saebimoghaddam, A. (2010) *Liquefaction of Early Age Cemented Paste Backfill*, Doctoral dissertation: University of Toronto.

Scrivener, K. L., Juilland, P. and Monteiro, P. J. M. (2015) 'Advances in understanding hydration of Portland cement', *Cement and Concrete Research*, 78, 38-56.

Statista (2019) 'Total revenue of the top mining companies worldwide from 2002 to 2017', [online], available: https://www.statista.com/statistics/208715/total-revenue-of-the-top-mining-companies/ 2019].

Thompson, B. D., Grabinsky, M. W., Bawden, W. F. and Counter, D. B. (2009) *In-situ measurements of cemented paste backfill in long-hole stope*, translated by Toronto, ON, Canada.

Yumlu, M. and Guresci, M. (2007) 'Paste backfill bulkhead monitoring: A case study from Inmet's Cayeli Mine, Turkey', in *In Proceedings of the 9th International Symposium in Mining with Backfill*, Montréal, QC, Canada,

CHAPTER 2 Theoretical Background and Literature Review

2.1 Introduction

In order to facilitate the understanding of the experiments and results presented in this thesis manuscript, this chapter provides a review of the fundamental theoretical and technical background information on CPB and other relevant topics. Section 2.2 provides background information on CPB technology, including the mix design and preparation, delivery means, backfilling strategy, and the design of CPB from geotechnical point of view as well as the source of sulphate and temperature in backfill operations. In section 2.3, the sources of seismic events in underground mines are discussed narrating some relevant historical events. Afterwards, the current knowledge on binder hydration (Portland Cement) and some of the factors that affect binder hydration are reviewed and discussed in section 2.4. The background information to understand the liquefaction, its susceptibility and assessment criteria are provided in section 2.5. Furthermore, background of shaking table testing technique and a review of the previous studies that used this technique on natural fine-grained soils and tailings are described in sections 2.6 and 2.7, respectively.

2.2 Background of Cemented Paste Backfill (CPB)

The underground mining operations often create large underground openings that may cause many geotechnical engineering problems in the mine and the surrounding areas. These problems include ground subsidence and instability of the underground mine openings. Moreover, extracting ores from underground mine may produce large amount of mine wastes (tailings). Traditional mine waste management technologies are used to dispose of tailings on the ground surface (such as tailings pond and tailings dams). In addition to the high cost, these disposal methods were found to be a source of significant environmental hazards, such as acid mine drainage (Abdul-Hussain 2011, Jamali 2012, Cui 2017). Alternatively, a novel waste management method was developed in the early 1980s in Germany, where the mine wastes were turned into cemented backfill. This technology is called the cemented paste backfill (CPB). This practice was implemented in North America around the 1990s and was adopted in several underground mining industries around the world as it allows big quantities of tailings to be re-used and returned to the mine stopes. Also, the use of CPB increases the stability of the underground mine stopes. Furthermore, CPB reduces the mining cycle and consequently increases the mine productivity (Belem and Benzaazoua 2004, Kesimal et al. 2005, Abdul-Hussain and Fall 2012, Yilmaz et al. 2015, Cui and Fall 2016, Aldhafeeri 2018).

2.2.1 CPB mix design and preparation

Typically, CPB mixture consists of mine tailings with a solid percentage of 70% - 85% and around 3% - 7% (by total weight of solid) of hydraulic binder (usually cement). These ingredients are

often mixed with fresh water with a water-to-cement ratio (w/c) that can range between 5.5 and 9.6. The content of these ingredients is often selected based on the tailings fineness and density, which affect CPB transportability (slump) (Figure 2.1). These components are prepared in paste backfill plant commonly located at the surface of the mine (Benzaazoua et al. 2004, Yilmaz et al. 2011, Aldhafeeri 2018, Xu et al. 2020).

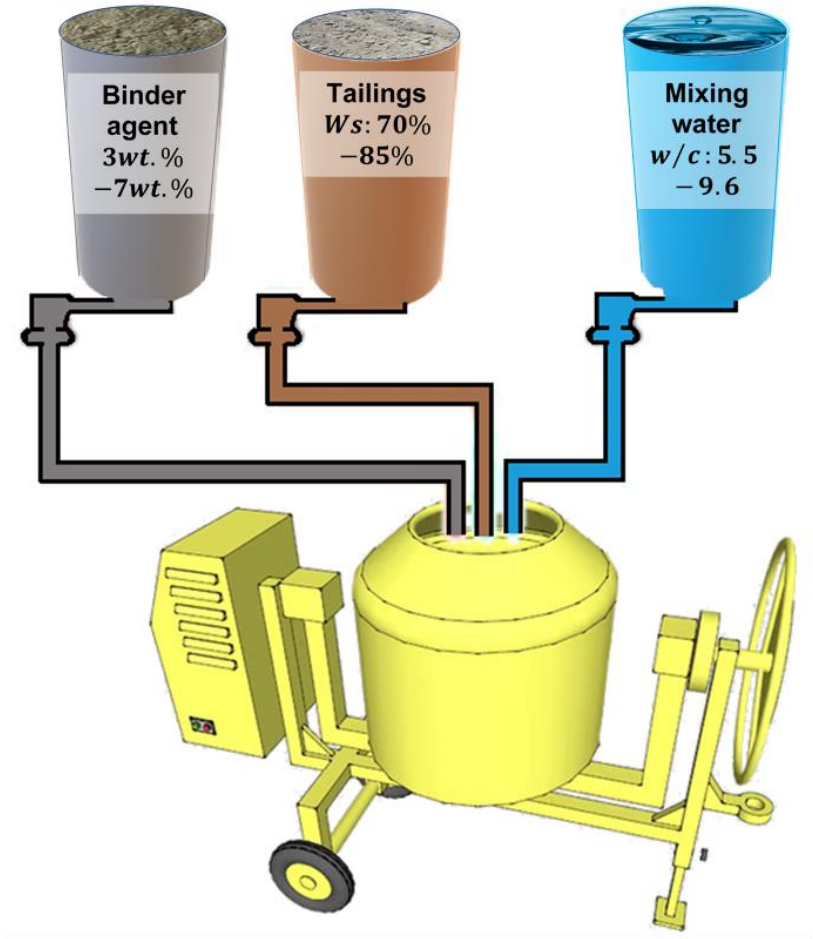

Figure 2.1 Cemented paste backfill components

2.2.2 Transportation and underground delivery systems

After being prepared in the paste plant on the mine surface (often), produced paste fill is then delivered into the mine stope by gravity, pumping and/or a combination of both, through underground distribution system. This system consists of boreholes, pipes, pumps, and cleaning system (Figure 2.2) (Cui 2017, Aldhafeeri 2018). Rheological properties of fresh CPB represent a key factor in CPB transportation into the mine stope, as pipelines' clogging might occur if the transported material did not have suitable flowability (Ali et al. 2021). Pipeline clogging will cause flow delays and/or temporary discontinuity of the progress of CPB production, which will lead to significant financial losses as well as the high cost of possible pipelines' replacements (Wu et al.

2013, Haruna and Fall 2019). To maintain suitable flowability, the pumping pressure of fresh CPB must be larger than the yield stress of the produced paste. Yield stress and viscosity are the most common properties for analyzing flowability. Slump flow test is also commonly practiced in mining industry to determine CPB flowability. In general, the rheological properties and the flowability of CPB are influenced by several factors, such as temperature, binder type and content, and elapsed time after mix preparation. On the other hand, pumping velocity must be balanced with pipe diameter and relative density of the fill in order to optimize the delivery system (Belem and Benzaazoua 2004, Wu et al. 2013, Cui 2017, Ali et al. 2021).

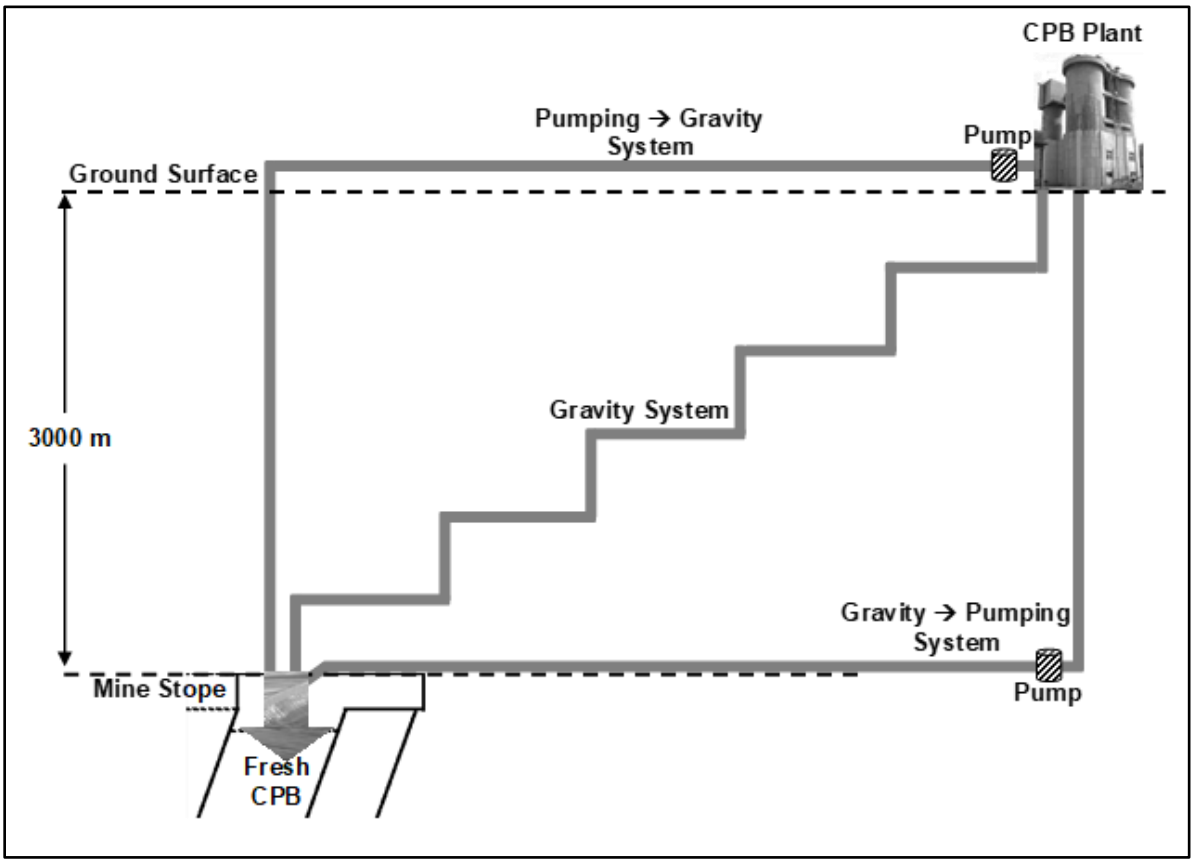

Figure 2.2 CPB delivery systems

2.2.3 Mine backfill strategy and rate

After the placement of fresh CPB in the mine stope and prior to filling completion, retaining wall structure (named barricade) must be constructed (at the drawpoint drifts that access the mining stope) to hold the backfill in place (Figure 2.3). However, it is imperative to ensure that the pressure applied by fresh CPB does not exceed the barricade strength or capacity. Otherwise, the barricade might fail and jeopardize the safety of workers. Accordingly, most mines have implemented a sequential filling strategy to fill up the mine stope in their operation. This strategy begins with pouring a plug fill, which is typically a layer of 2 – 3 meters that consists of CPB with high binder content. The plug layer is often cured with sufficient time, then the main CPB fill (typically with

low binder content) will be poured to fill the rest of the underground stope (Yumlu and Guresci 2007, Abdul-Hussain and Fall 2012).

On the other hand, it is crucial to control the rate of filling the stope with CPB (backfilling rate) with respect to the volume (m^3/h) or the height (m/h) of the stope. Despite the fact that the increase in backfilling rate will accelerate the mining cycle and consequently improve the mine production or productivity, it is obvious that rapid backfilling will potentially increase the pressure that acts on barricade and might lead to barricade failure. Backfilling rate can also vary from one mine to another based on the operation sequence of each mine. Furthermore, selecting a suitable backfilling rate depends on the content of CPB mix ingredients, backfill setting time, and arching effect (Nasir and Fall 2010, Cui 2017).

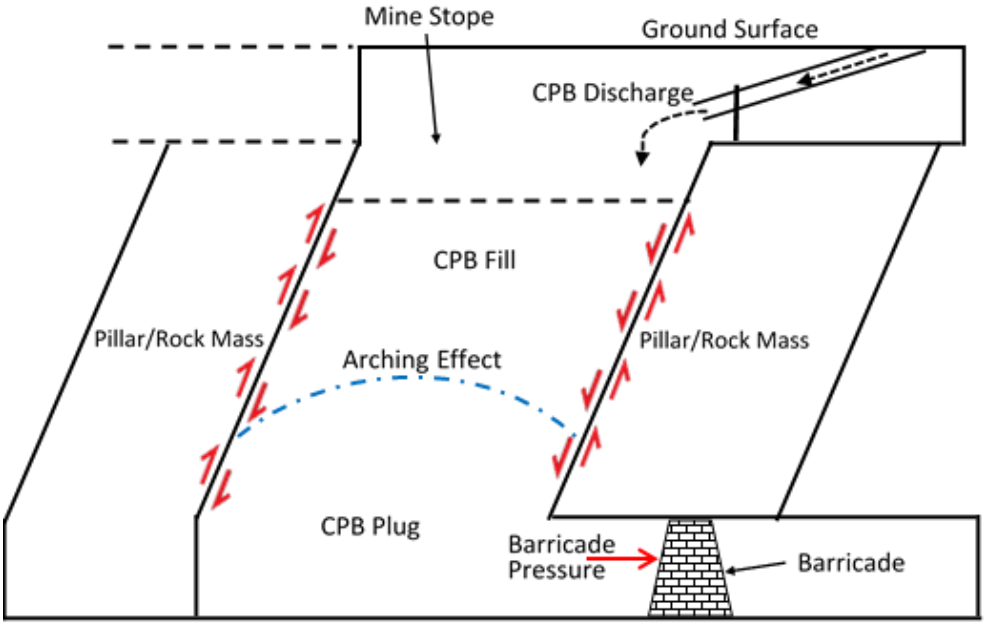

Figure 2.3 Schematic view of CPB placement common strategy and stress distribution

2.2.4 Geotechnical design of CPB

The design of CPB structures depends on two main factors; (i) the economic efficiency in matter of the quick completion of backfill process in order to reduce the mining cycle time, which consequently enhances the mine production, and (ii) safety of the workers in the mine workplace and surrounding area, as the CPB structures placed in the mine stope have to develop sufficient strength to provide a safe and stable platform for mine workers besides facilitating the removal of the adjacent rocks. Thus, ensuring the strength and stability of CPB structures with respect to mine productivity is significantly important in CPB design (Belem and Benzaazoua 2004, Lu 2017).

In general, the strength development of CPB is affected by several factors, such as cement hydration, and self-desiccation (as explained in section 2.4 below). In addition, the continuous backfilling process produces consolidation pressure on the fill mass, and subsequently increases

the strength of CPB. This will gradually cause a relative displacement along the rock mass/backfill interface, and consequently make the interface able to resist the self-weight stresses and generate interface shear stress. Coherently, continuous backfilling process will maximize the confinement at the base of the stope, leading to arching effect (Figure 2.3), which will limit the overburden pressure and transfer additional vertical stress to the adjacent rock walls via shear (Rankine and Sivakugan 2007, Galaa et al. 2011). Accordingly, in order to reach the desired performance, CPB structures must be designed to accommodate any additional static and dynamic loads, especially when the CPB backfill is still in the early ages (Cui 2017). Furthermore, previous studies (e.g. Fall and Benzaazoua 2005, Fall et al. 2010, Fall and Pokharel 2010, Nasir and Fall 2010, Pokharel and Fall 2013, Cui and Fall 2016, Li and Fall 2016, Li and Fall 2018) have revealed that the strength of CPB is significantly affected by internal and external conditions. These conditions include (i) the presence of sulphate ions in the backfill mix, which can jeopardize the strength of CPB, and (ii) the initial and curing temperature of the CPB mix, which is directly proportional to the improvement of CPB strength. Thus, designing early ages CPB structure should give due consideration to the effect of these factors on the mechanical strength of CPB under static and dynamic loadings.

2.2.5 Source of sulphate in backfill operations

In many hard rock mines, tailings materials are known to contain significant amount of sulphide minerals, such as pyrite (FeS_2), which is commonly found in several types of igneous, sedimentary, and metamorphic rocks. These minerals become chemically unstable (reactive) and oxidize when they are disposed under atmospheric conditions (O_2 and H_2O) (Ercikdi et al. 2017, Aldhafeeri 2018). Therefore, CPB material often contains sulphate ions in a quantity that is much higher than that found in other cementitious materials subjected to sulphate attacks. Previous studies have found several sources of sulphate ions in CPB systems. These sources include (i) ingredient-related sources, such as the oxidization of sulphide minerals contained in tailings and/or the mine processing water (which are often rich in sulphate) used as the mixing water in CPB preparation; and (ii) operation-related sources, such as Sulphur dioxide and air method which is done to remediate cyanide in some mines (such as gold mines) as well as the chemical additives (such as gypsum and anhydrite), which are often added to the clinker to control the cement setting (Ercikdi et al. 2009, Pokharel and Fall 2013). The initial content of sulphate in CPB can vary from as low as 5,000 ppm to as high as 25,000 ppm (Fall and Pokharel 2010).

2.2.6 Source of temperature in backfill operations

Previous studies have found various heat sources that may significantly affect the temperature of CPB structures in the mine stope. These sources include (i) internal heat generated during the process of cement hydration; (ii) external heat sources which are related to the temperature variation with the depth, geological conditions, and geographic location of the mine; and (iii) human-induced temperature. Moreover, during its transportation and delivery processes, CPB temperature might be affected by the thermal interactions between rock temperature and CPB temperature in the pipelines and the frictional heating of the fresh CPB with the pipelines (Fall et

al. 2007, Fall et al. 2010, Fall and Pokharel 2010, Wu et al. 2013, Aldhafeeri et al. 2016, Ali et al. 2021)

2.3 Seismic Events in Underground mines

Concurrently, with the booming in the mining industry in several regions of the world, there is an apparent reduction in ore bodies available at shallow depths in many underground mines. Furthermore, the rate of volume extraction is growing significantly in order to satisfy global demands. Thus, underground mining operations are being accomplished to a greater extent at greater depths and with greater volume (Johnson 2015). On the other hand, mining excavation was found to be a potential source of seismic activities, as it redistributes the stress in the earth's crust, which increases or decreases the stresses around the mine. This stress disturbance causes stress concentration in deep rocks that release seismic pulses when it exceeds the strength of these rocks. Accordingly, failure in rock masses near mining excavations induced by the changes in its stress states will cause seismic events to occur in these underground mines, and the rate of occurrence and seriousness of mine-induced seismic events tend to rise with a growing rate of volume extraction and depth of mining. So, seismicity monitoring has become an important tool for many mine operations. Thus, as part of its productivity and safety, seismic events in underground mining have become an iconic subject in related studies, either to improve the stability of mine excavation or in understanding the seismic phenomena in underground mining (Cook 1976, Hasegawa et al. 1989, Lasocki and Orlecka-Sikora 2008, Gibowicz and Kijko 2013). Based on the aforementioned, CPB structures will be progressively exposed to more frequent and severe seismic loadings. So, due to the paucity of related studies, there is a great need to understand the behavior of early age CPB subjected to seismic loadings.

2.3.1 Sources and characteristics

Besides exposing to natural fault slip (earthquakes), CPB structures in underground mines can be exposed to seismic or cyclic loadings from various sources. The underground mining seismicity can occur in the form of (i) rockburst at which the rocks will be severely ejected into the mine opening, (ii) sudden slip of coal towards the face of the mine which is known as outburst, and (iii) pillar burst (or bump) referring to the ground shaking of unknown origin or the sudden slip of coal (or other semi-viscous seams) at great depths. Furthermore, the high rated rock faulting (tensional fault and/or thrust fault) owing to mining processes, which may occur along the weakened faults either above or below the mine, are also considered as other source of seismic loading in underground mines (McGarr 1971, Smith et al. 1974, Milne and Berry 1976, Hasegawa et al. 1989, Hinzen 1982). Figure 2.4 below presents examples of underground mine-induced seismicity in Canada.

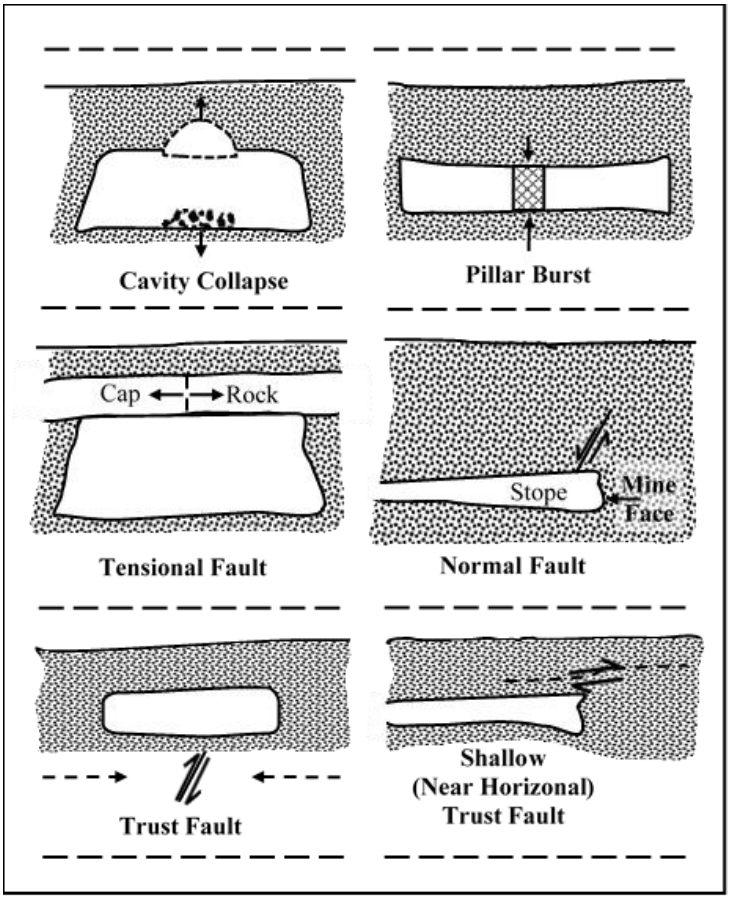

Figure 2.4 Underground mine-induced seismicity in Canada (modified from: Hasegawa et al. 1989)

It has been widely agreed that the seismic or cyclic behavior of soil (natural and/or man-made) is significantly affected by the parameters of seismic or cyclic loads (e.g., earthquake characteristics). These characteristics include shaking peak horizontal acceleration, duration of shaking (number of cyclic loads), loading frequency (number of cycles per second), and the maximum amplitude of motion (Chopra 2005, Das and Ramana 2010, Humar 2012).

2.3.1.1 Shaking peak horizontal acceleration

Shaking peak horizontal acceleration (SPHA) is the most common way of expressing the ground motion parameter and is one of the main factors used in seismic hazard analysis, because it is closely related to the largest dynamic forces inflicted during seismic activities. It describes the ground motion, the seismic-induced damages in surface and/or underground structures, and soil behavior (e.g., liquefaction) when exposed to dynamic loads (Hashash et al. 2001, Saebimoghaddam 2010). For instant, past earthquake records show that several structures were severely damaged when they were exposed to an earthquake with an acceleration of 0.5g. It was also found that a peak acceleration of as low as 0.05g can cause soil liquefaction (Gopikrishna 2000, James et al. 2003).

2.3.1.2 Shaking duration

Although the duration of ground motion cannot be used in isolation to analyze seismic hazard and estimate earthquake damages, yet these damages were found to be significantly affected by the duration of strong-ground motion as long duration may cause fatigue failure and large deformation (Hancock and Bommer 2006, Hashash et al. 2001). For instant, the number of load or stresses reversals (i.e. shaking duration) during an earthquake has great impact on the generation of excess pore-water pressure in loose, unsaturated sands, which might cause liquefaction (Saebimoghaddam 2010). In general, strong-motion duration is directly proportional to the damage magnitude of an earthquake. It was noted that long duration motion of moderate amplitude can produce enough load reversals to cause substantial damages, while high amplitude motion in low duration may not cause considerable damages as it might not produce enough load reversals (Kramer 1996).

2.3.1.3 Cyclic frequency

Cyclic frequency in seismology refers to the number of load cycles that may occur in a period of one second. The frequency of a possible future earthquake, in reality, cannot be predicted with certainty and can only be probabilistically estimated. However, the dynamic response of structures and soil deposits are reliant on the cyclic frequency (Hashash et al. 2001, Humar 2012). For example, severe damages of structures were recorded in the past when they were exposed to an earthquake with a frequency of 1 to 5 Hz. It indicates that the frequency of exciting forces has reached the natural frequency of these structure (i.e. resonant frequency) (Gopikrishna 2000, Humar 2012). Likewise, the natural frequency of a soil (which depends on the properties of the soil material) may decrease during dynamic excitation of high frequency to a certain level at which the soil might experience a degradation of effective stress due to the buildup of pore-water pressure, and consequently liquefy (Popescu et al. 2006). Hence, studying and/or estimating motion cyclic frequency will help in understanding the effect of earthquake-induced ground vibration on these structures and soil.

2.3.1.4 Maximum amplitude of motion

Maximum motion amplitude, which might also be referred to as horizontal displacement amplitude (HDA), is generally a function of wavelength, as the longer the wavelengths, the larger the displacement amplitude (Kuesel 1969). Typically, the displacement amplitude of ground motion cannot be measured directly. Instead, it can be computed by integrating the earthquake acceleration. Also, to better estimate the displacement amplitude of possible future earthquake, it is crucial to consider the predicted earthquake characteristics as well as the subsurface conditions of the examined area (Kramer 1996, Hashash et al. 2001).

2.3.2 Historical events

In the past century, numerous earthquakes events were recorded in mining regions around the world. In North America, for example, around forty-eight mine-induced earthquakes were recorded in the United States and around twenty-five events in Canada between 1984 and 2000.

Moreover, more than ten mine-induced seismic events were recorded in Ontario and Quebec (Canada) in the last ten years (U.S. Geological Survey 2000, Natural Resources Canada 2019).

Among the worldwide mine-induced seismic events, several events lead to environmental and economic disasters. For instance, the Samarco mine in Brazil, in 2015, was exposed to three small-magnitude seismic shocks in 90 minutes, causing the collapse of the Fundão tailing dam due to liquefaction. This accident resulted in the fatality of 19 persons and around 40 million cubic meter of mining waste washed the neighboring area, resulting in a total loss of around 6.4 billion US dollars. Moreover, this accident completely disrupted a facility that was producing 44% of Brazilian (5% of world's) production of iron ore pellets. This event was perceived to be the worst disaster ever happened in Brazil (Agurto-Detzel et al. 2016, Phillips 2016, Siegler et al. 2016). On the other hand, the Saguenay earthquake 1988 in Quebec was one of the largest recorded earthquakes in eastern North America. The liquefaction-related damages to the homes of this area were documented immediately following the earthquake of 0.13g ground acceleration (magnitude of 5.9 on Richter scale). Also, regarding the 2006 earthquake of Sudbury, Ontario was considered the strongest recorded earthquake in northeastern Ontario as it had a ground acceleration of 0.0027g (magnitude of 4.1 on Richter scale) (Tuttle et al. 1990, Atkinson et al. 2008, Saebimoghaddam 2010, Natural Resources Canada 2019).

Recent studies (e.g. Saebimoghaddam 2010, Abdelaal 2011) indicated that mine backfill, particularly early age CPB, is considered a liquefiable material. So, as the mine areas are significantly prone to seismic activities, it is crucially important to study the seismic behavior of fresh CPB placed in the mine stopes.

2.4 Background of Portland cement, its hydration and key influential factors

One of the main components of CPB is the hydraulic binder. The major role of these binders is to bond the tailings particles, leading to the increase in the strength of the mixture (Belem and Benzaazoua 2004). Ordinary Portland cement – type I (PCI) is the most common binder used in the preparation of CPB as it is easily used in many parts of the world. In the prances of water, the PCI components will go through a series of complex reactions which are responsible for bonding the tailings particles within the CPB. These reactions are known as the cement hydration process (Aldhafeeri 2018). A brief description of PCI, the basic hydration reactions and the key influential factors are discussed in the following subsections.

2.4.1 Portland cement

Ordinary Portland Cement (OPC) is a hydraulic cement that hardens by reacting with water and forms water-resistant products including calcium silicate hydrate (C-S-H), calcium hydroxide ($Ca(OH)_2$ or CH), and calcium sulphoaluminate (AKA ettringite) ($3CaO.Al_2O_3.3CaSo_4.31H_2O$) (Cui 2017, ASTM C150/C50M-19a 2019). Around 60% (by volume) of the total cement hydration products in hardened cement is the amorphous, poorly crystalline gel of C-S-H, which is formed by the hydration of C_3S and C_2S. On the other hand, the thin to large hexagonal crystals of CH

occupy around 20% (by volume) of the total cement hydration products. CH is a by-product of the hydration of calcium silicate. The rest of the cement hydration products is the needle-like morphological crystals of ettringite, which is the product of the hydration of the aluminate phases and gypsum (Abdul-Hussain 2011, Cui 2017).

2.4.2 Cement hydration process

The mechanism of cement hydration was explained by several researches (e.g. Bullard et al. 2011, Scrivener et al. 2015). They pointed out that the progress of cement hydration with time passes through four stages. The heat flow (Figure 2.5) and consequently the magnitude of cement hydration (Figure 2.6) varies with time at each stage. These stages are presented as follows:

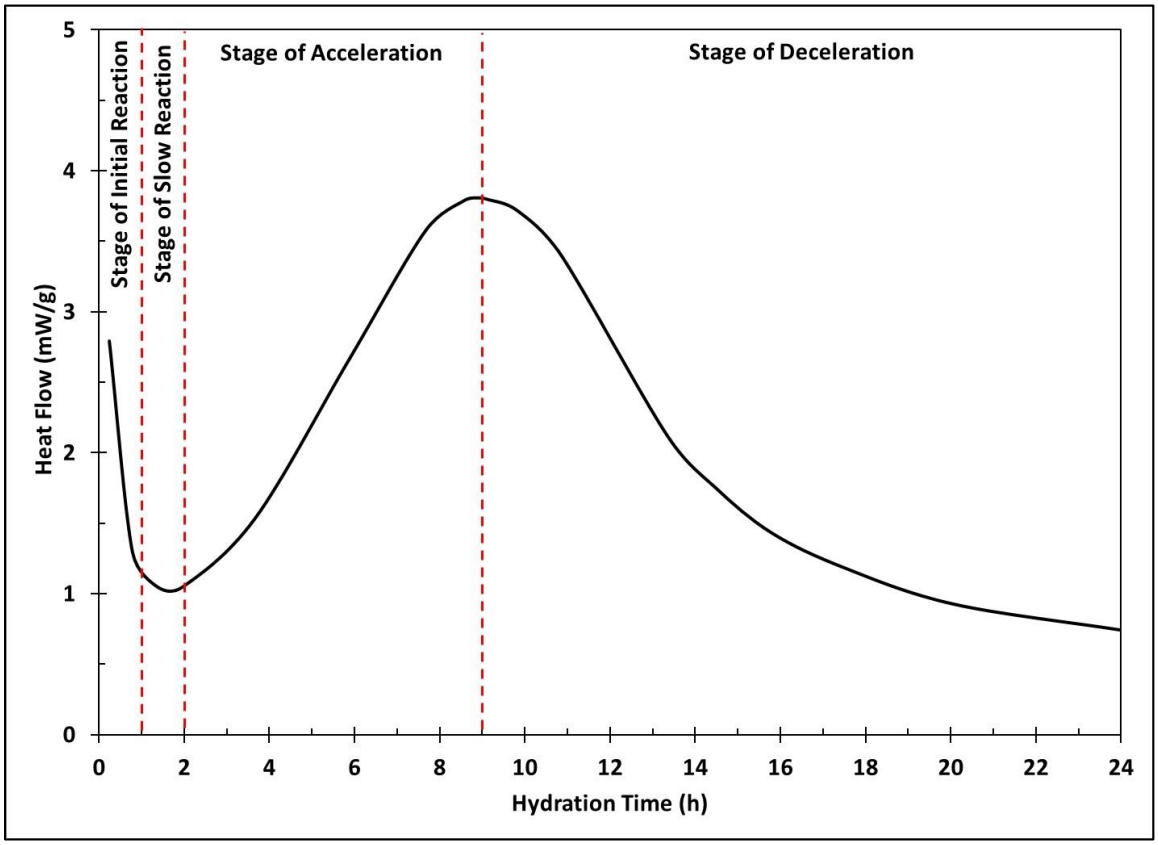

Figure 2.5 Progress of cement hydration with time (modified from: Bullard et al. 2011)

(a) Stage of initial reaction (up to 1 hour after mixing): In this stage, the cement will start to act immediately after exposed to mixing water as the aluminite and gypsum dissolve rapidly and release a significant amount of heat.

(b) Stage of slow reaction (between 1 and 2 hours after mixing): In this stage, the magnitude of cement hydration will start to increase at a slow rate with minimal heat release as C-S-H and ettringite will be formed around the calcium silicate. During this period the cement paste will be in plastic state.

(c) Stage of acceleration (between 2 and 9-10 hours after mixing): In this stage, significant amount of heat will be generated and the hydration magnitude rapidly increases and reaches the peak magnitude as the pore spaces will be further refined, so the bond strength will be enhanced exceedingly.

(d) Stage of deceleration (more than 10 hours after mixing): In this stage, the continuous formation of C-S-H and CH around the particles will decrease the heat flow. Consequently, the magnitude of cement hydration will decrease with time until it reaches its minimum values at around 24 hours age.

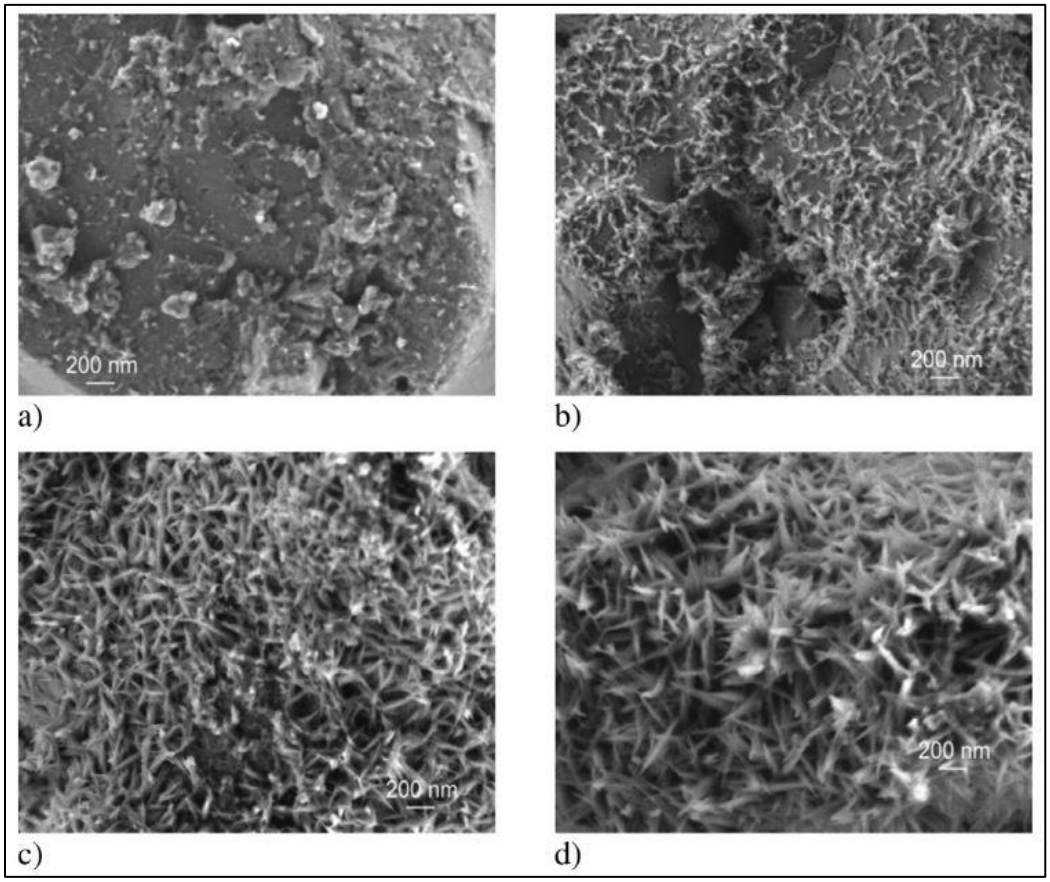

Figure 2.6 SEM observation of C_3H hydration through different stages of cement hydration. (a) reaction stage, (b) slow reaction stage, (c) acceleration stage and (d) declaration stage (Scrivener et al. 2015).

2.4.3 Key factors that affect cement hydration

There are several factors that affect cement hydration. These factors include w/c ratio, fineness of the cement, temperature, and chemistry of mixing water (Bentz 2006, Lin and Meyer 2009, Fall et al. 2010, Li and Fall 2016, Wu et al. 2016).

Bentz (2006) indicated that the degree of cement hydration is inversely proportional to w/c ratio as the reduction in w/c will decrease the porosity and hydraulic conductivity of the cementitious material, and consequently enhance the mechanical strength of these materials.

Similarly, fineness of cement particles was found to be another factor that accelerates the cement hydration process and, thus, improves the mechanical strength of the soils undergoing cementation. The finer cement particles have larger surface area, which provides the mixing water higher contact area. This allows more water to react with cement particles. Moreover, hydration of fine cement particles produces less thick cement hydration products. Thus, the setting time of cemented particles will be reduced. Hence, the reaction between water and fine cement particles (cement hydration) accelerates and the mechanical strength improves (Bentz 2006, Lin and Meyer 2009).

Moreover, it has been found that high initial and/or curing temperature of cementitious material will accelerate the cement hydration process because high temperature will reduce the pore spaces between particles and reduce the water content. This will accelerate the cement hydration process and lead to more cement hydration products to be precipitated within the pores between the particles. Thus, high initial and/or curing temperature will enhance the mechanical strength of cemented soil or material at early ages (Lin and Meyer 2009, Fall et al. 2010, Wang et al. 2016). However, Maltais and Marchand (1997), Elkhadiri et al. (2009) specified that the mechanical strength of cementitious material can be reduced at advanced ages when cured at a curing temperature that exceeds 85^{o}C, because this range of curing temperature will lead to less uniform microstructure, higher porosity, and coarser pore structure within the soil particles.

Also, cement hydration process was found to be affected by the chemistry of mixing water. The presence of some chemical components in mixing water (such as sodium silicate) might increase the rate of the cement hydration process and improve the mechanical strength of cementitious soils (Abdul-Hussain and Fall 2012). On the other hand, the presence of other chemical components (such as sulphate) might inhibit the cement hydration process. The inhibition is attributed to the reaction between the sulphate anions in the mixture and C_3A grains which will form a thin coating of anhydrated cement particles and prevent the C_3A from quickly reacting with water (Li and Fall 2016).

2.5 Liquefaction

Problematic soils are the soils that change their engineering behavior or properties in different conditions, causing many problems in engineering practice. Problematic soils are widely distributed around the world and can be found either in shallow or deep deposits. Liquefiable soils are one of the most common problematic soils, especially in the seismically active areas of the world, such as Japan and North America (Iwasaki 1986, Tuttle et al. 1990, Ali 2010).

In the following subsection, liquefaction will be briefly described, focusing on its definition, mechanism, susceptibility, and assessment criteria.

2.5.1 Definition of liquefaction

Liquefaction can be defined as the rapid change in the engineering behavior or properties of a soil when exposed to external conditions, such as earthquakes or blasting conditions, at which the soil will behave like a liquid. When disturbed, the liquefiable soils will temporarily lose their strength as a result of rapid development of excessive pore-water pressure (PWP). Soil liquefaction causes sudden deformation in engineering structures, foundations, and road pavements (Seed and Idriss 1971, Chern and Chang 1995, United States Geological Survey 2019).

Remarkable amounts of economic damages and significant human fatalities were recorded around the world due to liquefaction and related phenomena associated with ground vibration and earthquake shaking. For instance, on June 14, 1964, a 7.6 magnitude earthquake with 55 km epicenter was recorded in Niigata, Japan, causing death of 36 persons, injury of 385 persons, smashing of 3,534 and damage to 11,000 houses. In this earthquake, soil supporting the 307 m long bridge of Showa that crosses the river of Shinano was exposed to lateral spreading due to an extensive liquefaction causing the collapse of the bridge (Figure 2.7) within 2 minutes of the maximum acceleration of the ground movement (Kawasumi 1968, Bhattacharya et al. 2014). On the other hand, irrecoverable damages to around 400,00 building and 6,434 fatalities were caused by the Great Hanshin-Awaji earthquake that took place on January 17, 1995 in Kobe port in the southern part of Hyōgo Prefecture, Japan, with a magnitude of 6.9. In this event, the two major man-made islands in Kobe port (Port Island and Rokko Island) were exposed to a combination of extensive liquefaction and large lateral movements of breakwater structures, destroying the sea-wall (Figure 2.8) and other structures constructed along the two islands shore-line. In addition, the liquefaction of this accident resulted in ground settlement of 5-60 cm depth and 2-3 m horizontal movement of the shoreline, causing damages to many foundations of bridges and other facilities connecting the two islands to the mainland (Okimura et al. 1996).

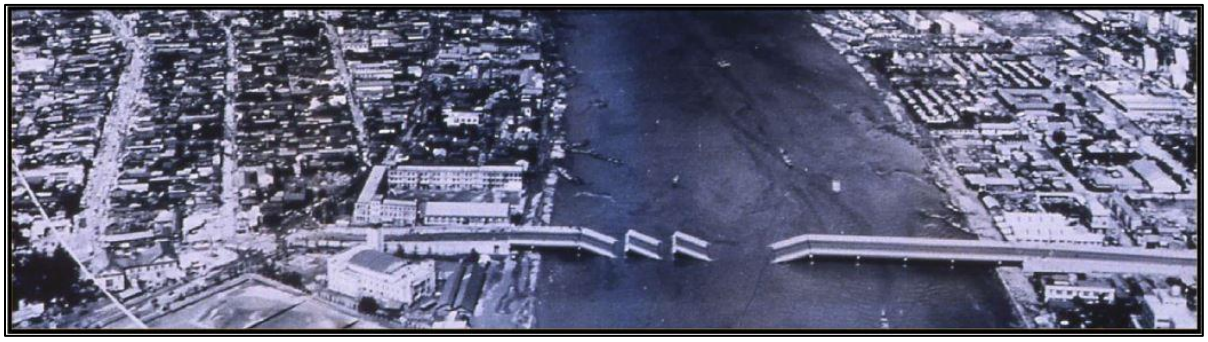

Figure 2.7 Liquefaction induced collapse of Showa bridge during Niigata earthquake 1964 (Bhattacharya et al. 2014).

Between 2010 and 2011, Canterbury earthquake occurred in Christchurch, New Zealand, and resulted in variable degrees of liquefaction over a very wide range of areas of naturally-sedimented soil formations, causing significant damages to residential houses in the area (Orense et al. 2014). Also, the Bento Rodrigues town in Brazil, in 2014, experienced a disaster when the

tailing dam of Samarco mine collapsed (Figure 2.9) due to liquefaction as a result of three mining-induced earthquakes. This accident caused the death of around 19 people and a loss of around 6.4 billion dollars (Phillips 2016, Siegler et al. 2016).

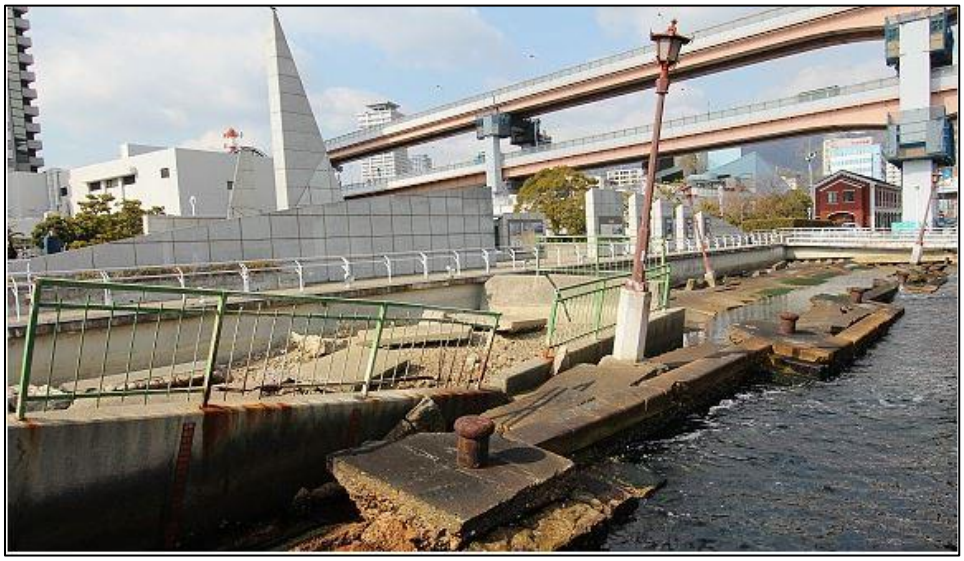

Figure 2.8 Sea-wall collapse due to liquefaction after the Great Hanshin-Awaji Earthquake in 1995 (Japan-guide 2016)

Figure 2.9 The tailing dam failure in Bento Rodrigues Town, Brazil in 2015 (Resourceful Paths 2016)

2.5.2 Contractive and dilative behavior

Depending on soil characteristics, the behavior of liquefiable soil due to exterior disturbance (such as ground shaking) will vary between contractive and dilative behavior.

For example, when the shearing or shaking confines saturated loose granular soil, volume of the soil will decrease (contraction) as soil particles will consolidate and become denser than its initial packing. This will rapidly increase the pore-water pressure as the pore water will not be able to leave the pores immediately. The rapid increase in pore-water pressure will virtually reduce the solid-to-solid contact pressure between the grains, and the soil will behave like fluid. In other words, the undrained loading of this type of soils will increase the pore-water pressure and reduce the soil effective stress. Accordingly, there is a common consent between engineering studies that soils flows are a result of contractive soil liquefaction, as the soil liquefaction produces high pore-water pressures, forcing the materials to flow like fluid (Poulos et al. 1985, Fleming et al. 1989). On the other hand, although shearing of dense soils to small strain will generate some excess pore-water pressure, increasing the shear to large strain will reduce the pore-water pressure as the soil particles will start to pile on each other, causing increase in soil volume (dilation). It will, therefore, increase the soil effective stress (Rauch 1997, Kramer et al. 2011). If the rate of volumetric expansion of dilative sand exceeds the sand expansion rate, soil will become unstable as the effective confining pressure will decrease and the materials will be unable to accommodate the applied pressure. In other words, the stability of soil materials depends on the rate of volume strain (whether positive, zero, or negative) forced on the material and the rate of the allowable volume change of the material itself (Peters 1991, Lade and Yamamuro 2011).

Casagrande (1976) mentioned the boundary line between contractive and dilative behavior of liquefiable soils as the Critical Void Ratio (CVR). He defined the CVR as the void ratio or relative density at which liquefaction advances in flow structure. In other words, liquefiable soil remains in dilative zone regardless of the minor principle stress as long as it is below the CVR line. Otherwise, upon passing the CVR line, soil will become contractive (Figure 2.10). Ishihara et al. (1975), on the other hand, defined the boundary between gradually stiffening and compliant unloading as the stress threshold between contractive and dilative monotonic shearing.

Fleming et al. (1989) studied different methods to differentiate between the contractive and dilative behavior of liquefiable soils in the field. They found that landslide transformation into a flow in one session is a good evidence that the slope is consisted of contractive material, emphasizing that the excess pore-water pressure will be high enough to develop the debris flow in saturation condition. On the other hand, in the presence of dilative material, the landslide will convert into debris flow in multiple episodes. Furthermore, the quick generation of debris flow (i.e. the immediate transformation from landslide into debris flow) is another evidence of the contractive behavior of soil, as the pore-water needs some time to escape from the pores of dilative materials. In other words, the landslide of dilative materials will take some time before it becomes a debris flow.

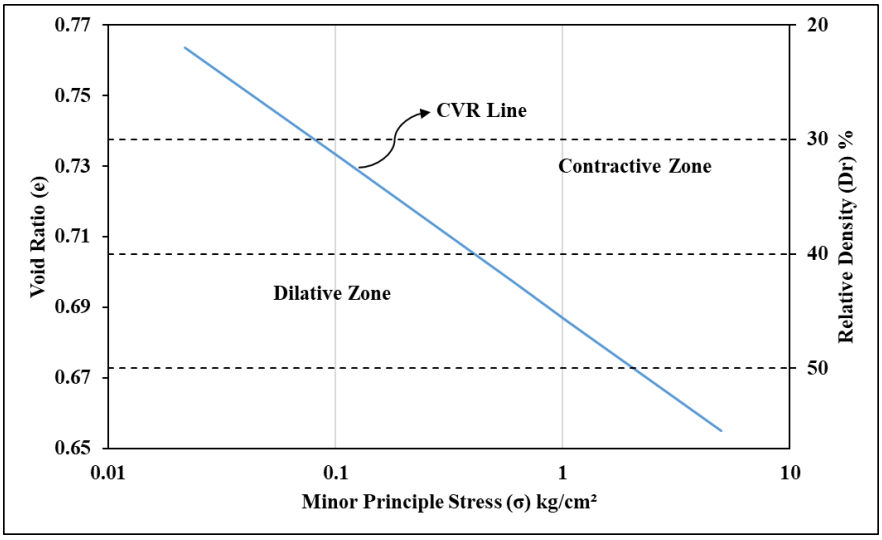

Figure 2.10 Contractive and dilative zones of liquefiable soils (modified from: Casagrande 1976)

In the lab, the differentiation between contractive and dilative behavior of liquefiable sand can be observed by applying drained direct shear stress on soils of different initial densities (Figure 2.11). As strain begins, the shear stress of dense sand will rapidly increase and reach a peak value, and then the stress will decrease gradually with the continuous increase in displacement (dilative behavior). While in the loose sand, shear stress will continue increasing gradually with continuous increase in displacement (contractive behavior). Furthermore, the void ratio of dense (dilative) sand is directly proportional to displacement, while the loose (contractive) sand is inversely proportional to displacement (Ellen et al. 1982). Moreover, increasing shear on dry sand or silt in one direction (monotonic shear) causes two steps of volumetric strain (Figure 2.12), starting with volume decrease (contraction), followed by volume increase (dilation) (De Groot et al. 2006).

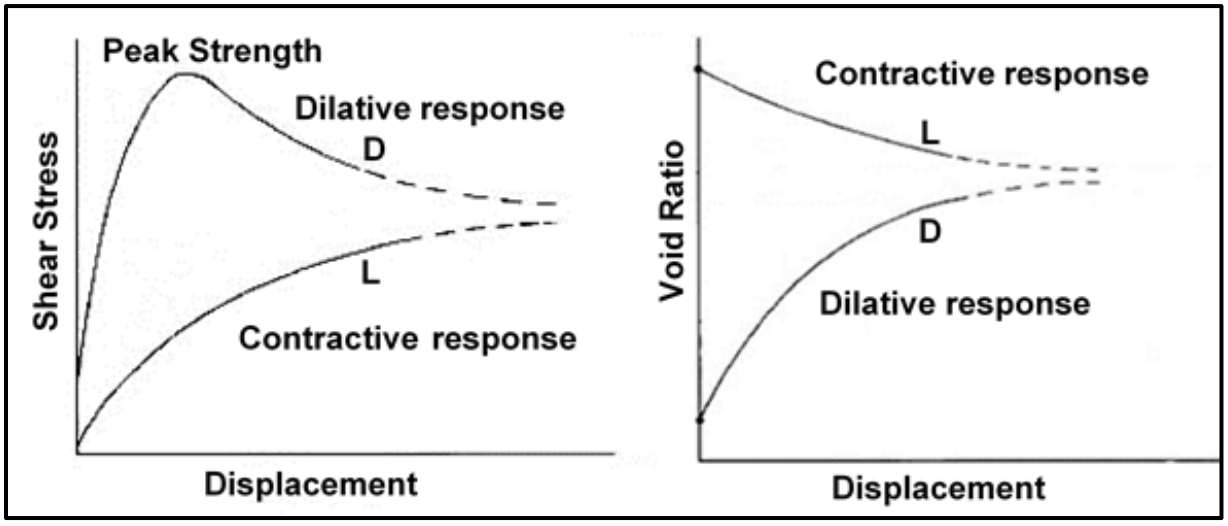

Figure 2.11 Contractive and dilative response of liquefiable sand during direct shear stress

D: Dense sand, L: Loose sand (modified from: Ellen et al. 1982)

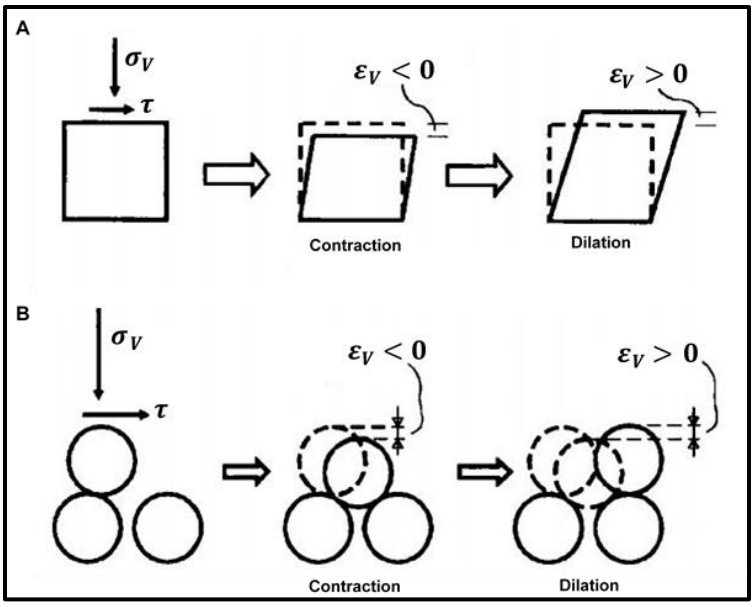

Figure 2.12 Contractive and dilative response of liquefiable dry sand and silt under monotonic shear A: volume change, B: grains contraction and dilation (modified from: De Groot et al. 2006)

2.5.3 Liquefaction Susceptibility and Assessment Criteria

The disastrous earthquake of Niigata in 1965 became an iconic event for many researchers to assess the susceptibility of liquefaction-induced phenomenon. Seed and Idriss (1971) identified the significant factors that lead to liquefaction of sand during earthquake and proposed a "simplified procedure" to evaluate the liquefaction resistance of soils. They validated this model by comparing the actual liquefaction and non-liquefaction behavior in the field (which provides good guidance to evaluate the past liquefaction incidents) with the soil performance evaluated by the model (which can appropriately link the previous field observation with the new situations). The outcome of this study showed that limited field data will also work in providing a base for predicting the performance of other sand deposits. North America and many other counties in the world have used this procedure as a practice standard.

Based on the observations from recorded earthquakes, Wang (1979) provided two conditions for soil to be considered as liquefiable soil. He proposed that clayey soils are susceptible to liquefaction if they contain less than 15 % of particles that are finer than 5 μm and have water content of more than 0.9– liquid limit ratio. Seed (1982) developed the liquefaction criteria (Wang 1979) and produced new criteria termed as "Chinese criteria", wherein they stated that in addition to the previous conditions, clayey soils can be susceptible to liquefaction only if their liquid limit is less than 35%. They also proposed a specific magnitude scaling factor. Seed et al. (1983) used field data gathered from SPT and CPT tests in different countries around the world (such as the United States, Japan, China, Guatemala, etc.) with the aim of standardizing the "simplified procedure" to evaluate the liquefaction potential in sandy soils during an earthquake of different magnitudes. In addition, the cross-hole shear velocity test was also used in this regard. This study

highlighted advantages and disadvantages of using the stress ratio approach (SPT and/or CPT methods) and the strain approach (Shear velocity method). The advantages include easy implementation, simplicity, cost-effectiveness, higher accuracy towards ground motion, and wide comprehensiveness of the SPT and CPT methods, while the disadvantage includes the inefficiency of these approaches in soils with large particles (gravel, cobles, and/or boulders).

Referring to different studies, such as (Seed et al. 1983), Robertson and Campanella (1985) presented a modified CPT-based method to evaluate the liquefaction potential in sandy soils using field and laboratory data collected from Canada, Japan, China, and the United States. Their study revealed that the liquefaction resistance of soil, as well as the soil resistance to penetration spawned by the SPT and CPT apparatus, are both influenced by soil compositional and environmental variables (such as soil density, soil structure, stress states and history, aging, and cementation). Accordingly, a correlation between soil resistance towards CPT as well as liquefaction can be provided by studying the effects of these variables on the CPT resistance (Figure 2.13).

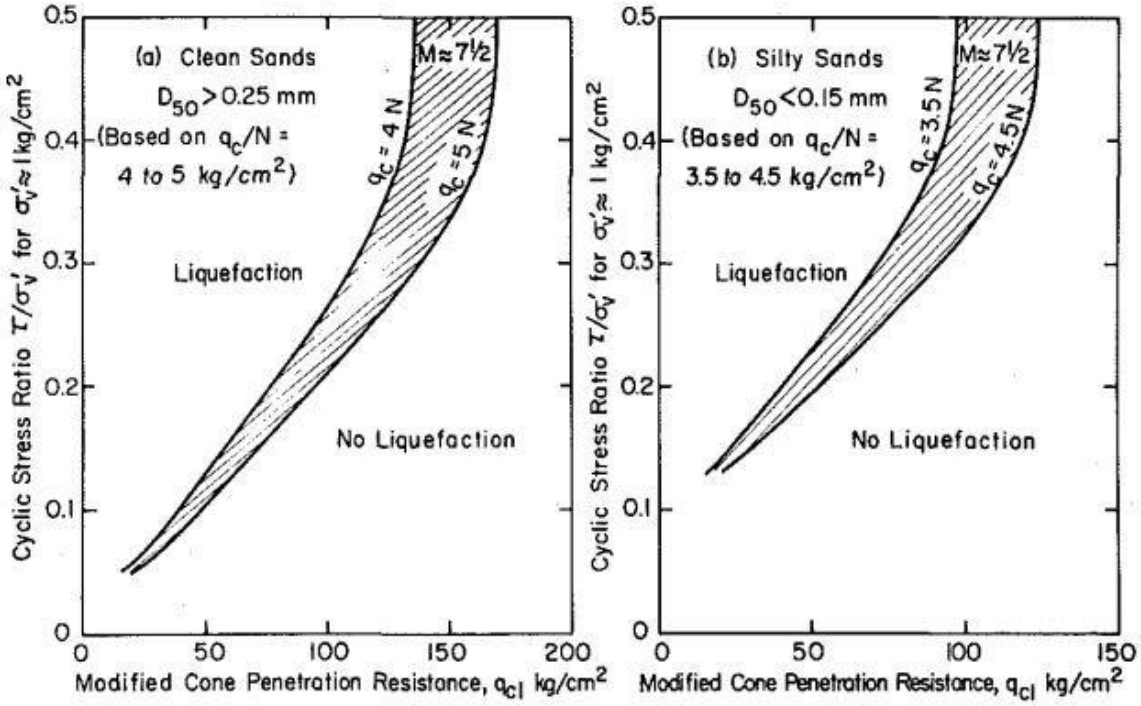

Figure 2.13 Correlation between liquefaction resistance and modified CPT resistance in two sands. (a) clean sands, and (b) silty sands, (modified from: Robertson and Campanella 1985)

Youd (1988) argued about Chinese criterion believing that it is very conservative soil screening criterion. He claimed that the liquefaction occurs only on soils that have a liquid limit less than 35%, and plasticity index less than 7%, provided that it is not classified as a "C" in the USCS classification (i.e. not CH, CL, SC, or GC). In other words, clayey soils are not susceptible to liquefaction. This exclusion of clayey soils was also assented by (Martin and Lew 1999).

Youd and Idriss (2001) summarized different studies that were conducted to assess liquefaction and liquefiable soils. They concluded that standard penetration test (SPT), cone penetration test (CPT), shear wave velocity test and Becker penetration test (BPT) (for gravelly soils) are the recommended field tests to evaluate liquefaction. They also proposed that in liquefaction assessment, a great attention should be applied to magnitude of movement moment, peak acceleration, and the possibility of liquefaction underneath grounds of more than 6% of slope. They also recommended that for engineering practice, a range of magnitude scaling factors should be applied with less conservatory than the factors proposed by (Seed and Idriss 1982).

To avoid sudden drop in shear strength of silty sands during static and/or cyclic earthquake events that will cause significant damages to civil engineering structures due to liquefaction, or to mitigate these damages, Taiba et al. (2016) underlined the significance of identifying the factors influencing soil liquefaction, with special attention to the shape and gradation of the particles of granular sandy soils. For this reason, they performed series of undrained compression triaxial tests with initial confining pressure of 100 kPa on samples of soils with low plastic fines (0% – 40%) and relative density of 52%, which were obtained from Algeria and France in order to assess liquefaction susceptibility of these soils. They found great influence of particles shape and gradation on the liquefaction resistance of different soils. In addition, their study found that a correlation exists between the grading characteristics and liquefaction resistance (undrained peak shear strength), as a result of which they found that the undrained peak shear strength is (linearly and logarithmically) directly proportional to the grain size, and (linearly and logarithmically) inversely proportional to the fine content (Figure 2.14). They also introduced new granulometric characteristics on the static liquefaction susceptibility of silty sand soils.

Taking into consideration that soil liquefaction is a “classification problem”, alternative method for evaluating soil liquefaction susceptibility was proposed by Samui et al. (2015), wherein the extreme learning machine (ELM) was applied in six different models relying on magnitude of the ground vibration, cone resistance during CPT test, mean grain size, total and effective (vertical) stress, normalized (horizontal) peak ground acceleration, and cyclic stress ratio. This approach succeeded in illustrating the relationship between soil parameters and earthquake parameters in assessing soil liquefaction susceptibility. Therefore, the ELM method can be considered as a suitable tool for predicting the soil liquefaction susceptibility.

Modern academic studies and engineering practices of soil liquefaction have based their liquefaction assessment on the “energy principles” of excess pore-water pressure (PWP), shear strength, and shear strain/deformation of the soil (Wu et al. 2004). For instance, Figueroa et al. (1994) explained the mechanism of liquefaction by the tendency of soil particles to decrease in volume when subjected to seismic shear stresses. Thus, the stresses will be transferred to the pore water and reduce the normal stress among soil particles. So, the soil loses shear strength when the increase in PWP becomes equal to the normal pressure, causing collapse and extensive damages to the engineering structures supported by these soils. Also, Obermeier et al. (2001) adopted the approach of counting dissipated energy, which is the area bounded by the stress-strain curve during

cyclic loading, as another criterion for liquefaction assessment. Moreover, The PWP ratio criterion is another liquefaction assessment criterion based on the change in PWP. Liquefaction susceptibility is evaluated in this criterion by the high values of PWP ratio (R_u), which is the ratio of the change in PWP (Δu) and the initial effective stress (σ'_o). There is liquefaction if $R_u \geq 1$, and if $R_u < 1$, there is no liquefaction (Wu et al. 2004). This criterion was adopted in several researches, such as (Pépin et al. 2009).

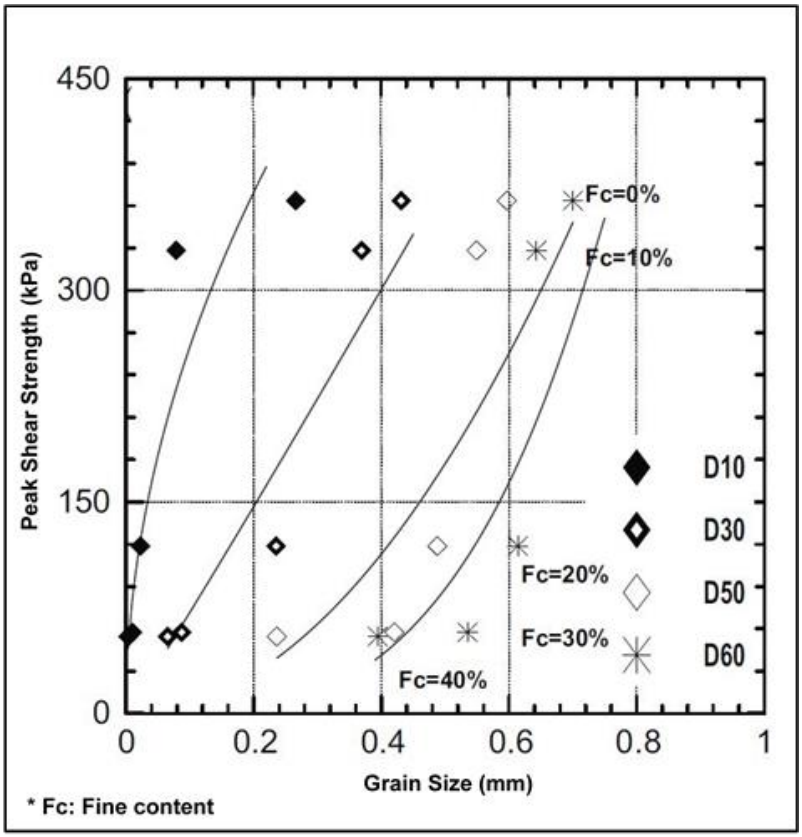

Figure 2.14 Correlation between liquefaction resistance, grain size and fine content in sandy soils. (modified from: Taiba et al. 2016)

It is worth admitting that the existing liquefaction susceptibility and assessment criteria have some limitations, as these approaches determine liquefaction, whereby samples that were obtained from critical strata in sites were historically exposed to earthquakes. Moreover, these approaches are challenged by the fact that observations from ground surface at damaged sites do not provide full insight into the mechanics behavior of the affected soil (Boulanger and Idriss 2006). However, Desai (2000) found that the aforementioned energy principles gathered from filed and/or laboratory data (such as the excess PWP and confining pressure) might provide a suitable indication of the initiation of liquefactions during seismic conditions. Accordingly, as the change in PWP can be considered an essential component of liquefaction process as defined by (Figueroa et al. 1994) and based on the justification of (Desai 2000), this study adopted the PWP-based criterion to assess liquefaction behavior of early aged CPB under seismic loading.

2.5.4 Liquefaction of Cemented Paste Backfill

Over the past three decades, researches have suggested that cemented paste backfill (CPB) with unconfined compressive strength of 100 kPa or more will be resistant to liquefaction (Le Roux et al. 2004). However, CPB is perceived to be susceptible to liquefaction when it is exposed to dynamic loading at early ages, leading to excessive horizontal loads that might cause barricade collapse (Saebimoghaddam 2010, Ercikdi et al. 2017, Cihangir et al. 2018). This consideration was based on the contractive and dilative behaviors that the CPB samples exhibited when exposed to different loading values during the triaxial test (Moghaddam and Grabinsky 2010).

Although the liquefaction of fresh CPB placed in mine stopes was cited in several publications as one of the CPB design challenges, there were only few studies that discussed this issue in detail (Shahsavari et al. 2014). For instance, Grabinsky and Simms (2006) evaluated the mechanical and hydraulic properties of CPB, including reviewing some results related to the cyclic loading in CPB. This study found that the development of suction (negative PWP) will reduce the excess PWP, which will allow stope filling process to be faster, minimizing the risk of liquefaction under the self-weight loading. Also, Saebimoghaddam (2010) studied the liquefaction of CPB at early age under dynamic loading by applying cyclic triaxial loading on CPB samples cured to different curing time. This study concluded that the cyclic failure increases with the increase in loads magnitude and decreases with the increase in curing time. It was found that CPB samples cured to 4 hrs or more were highly resistant to liquefaction as it produced insignificant axial strain and excess PWP. Abdelaal (2011), on the other hand, used the triaxial testing apparatus to study the influence of mixing CPB with high proportion of sand on liquefaction susceptibility, and the combined effect of adding sand to the cyclic response of CPB under undrained conditions. It was revealed that the presence of sand increases the effectiveness of cement within the mixture and enhances the cyclic resistant. Furthermore, Suazo et al. (2017) studied the cyclic response of CPB using a constant-volume direct simple shear apparatus. Several factors, such as curing age, cement content as well as the initial soil content within the CPB mixture, were investigated in this study in order to evaluate their effect on liquefaction resistance of CPB. It was found that the increase in these factors enhances the liquefaction resistance of CPB. Also, during the loading and unloading of shear stress, most of the tested specimens showed contractive shear response along with steady development of excess PWP.

Despite that the above cited literature provided important background of cyclic behavior of CPB, it was noted that no study (up to date) has considered the assessment of cyclic-induced liquefaction behavior of fresh (early age) CPB material using shaking table testing method, which (as discussed below) provides more realistic assessment of material response under cyclic loads.

2.6 Shaking Table Test

Shaking tables are apparatuses that can be used in engineering practices to evaluate the effects of any seismic event that occurred in the past or might occur in the future. Since the sixties of the last

century, shaking tables were considered as a very influential and most realistic tool to assess and simulate the response of different construction foundations and their supporting soils towards dynamic and ground motions' loads that impose these structures (Bairro and Vaz 2000, Ngadimon 2006). In order to conduct a shaking table test, the model of the foundation under study and its supporting soils need to be contained together in a container. These containers are designed to be attached to the shaking table. During the test, the tested material will be exposed to shear stress that will be interpreted to evaluate the behavior of the tested material towards the dynamic loads. These containers are commonly known as the shear boxes in several literatures (Ueng et al. 2006, Mohamed 2014).

In the following subsection, an overview of the types of shaking tables is provided, and a brief description on various types of shear boxes is presented. The shaking table used and the laminar shear box developed in this thesis are presented in the technical papers, I-IV as well as detailed in the Appendix.

2.6.1 Types of shaking table

Based on previous studies (e.g. Tokimatsu and Seed 1987, Iai 1989, Jafarzadeh 2004, Prasad et al. 2004, Ngadimon 2006, Bhattacharya et al. 2012), shaking tables types are classified based on several criteria, as discussed in succeeding paragraphs:

i. Method of vibration actuation: Shaking tables were classified into three types; manual, hydraulically, and electrically driven shaking tables. It was proven by several previous studies that hydraulically driven shaking table has more advantages than the other two types. For example, it is capable of conducting the test for any size of load, while the manual and electrically driven tables can be used for only small and small to medium size loads respectively. On the other hand, while using the hydraulically driven shaking tables, it is possible to change some of the controlling parameters (according to the purpose of the test), such as shaking velocity, stroke, and frequency, while it is difficult and not possible in case of manual and electrically driven tables, respectively.

ii. Direction of movement (loading direction): Shaking tables are classified into one directional shaking tables and multi directional shaking tables. The advantages and disadvantages of each type depend on the application that the shaking table is used for. Although the multi directional shaking table might give (in some cases) more accurate results (if it was used properly), the factors of one directional movement shaking table are easier to be controlled.

iii. The gravity field: Shaking tables are differentiated into shaking tables that use (1-g) gravity field and shaking tables of (N-g) augmented gravity field (geotechnical centrifuge at N times earth's gravity). Again, depending on the application of the shaking table test, each one of these types is more useful. Using (N-g) centrifuge shaking tables leads to more applicable results corresponding to stress levels in real

situations. On the other hand, the use of (1-g) shaking table is much easier, as it has fewer deficiencies and the errors are more controlled. Nevertheless, it does not correspond to the stress levels in real situations and its results are less authentic than that of the centrifuge shaking tables. In addition, the design and the use of shaking table of (1-g) gravity are less expensive than the centrifuge devices.

iv. The range of maximum load that the table can handle: Shaking tables are classified into three types; small scale tables (up to 1 Ton max. load), medium scale tables (max. load of 1 - 5 Tons), and large-scale tables (more than 5 Tons).

v. The geometry of the shaking table and the soil container (shear box) that is used in the experiment: Shaking tables are differentiated into small, medium and large size tables and rectangular or square shaking tables.

Shaking table was extensively used in previous researches. Table 2.1 below summarizes some shaking tables that were used in previous studies.

Table 2.1 Shaking tables reported in some literatures

Table Shape	Vibration Actuation	Dimensions		Used in	Loading Direction	Reported by
		L (m)	W (m)			
Square	H	4.00	4.00	N-g	2-D	Jafarzadeh (2004)
Rectangular	M	1.80	0.60	1-g	2-D	Prasad et al. (2004)
Square	H	3.60	3.60	1-g	2-D	Thevanayagam et al. (2009)
Square	E/H	1.22	1.22	1-g	1-D	Turan et al. (2009)
Square	H	2.00	2.00	1-g	2-D	Motamed et al. (2010)
Square	E/H	4.00	4.00	1-g	2-D	Haeri et al. (2012)
Square	E	1.00	1.00	1-g	1-D	Pathak et al. (2013)
Square	H	1.00	1.00	1-g	1-D	Mohamed (2014)
Rectangular	E/H	4.86	3.36	1-g	1-D	Guoxing et al. (2015)
Rectangular	E/H	4.86	3.36	N-g	1-D	Wang et al. (2015)

H: Hydraulic, **M:** Manual, **E:** Electrical, **g:** ground acceleration (9.81 m/sec^2), **D:** Direction

2.6.2 Shear box

Shear box or soil container is designed to be used to test soils under cyclic induced shear strain which will help in assessing liquefaction behavior of soil during the seismic activities. Accordingly, beside calling them in most of the literature as “Shear Box”, some other literatures (e.g. Eseller-Bayat et al. 2013) might also call them “Liquefaction box”.

Similar to the shaking tables, there are different types of the shear box, depending on the application that is used for. Bhattacharya et al. (2012) summarized the different types of soil containers into six types:

i. Rigid container which is a rough box as its end walls and base have shear stiffness significantly higher than the stiffness of the contained soil, in order to ensure the that the shear stresses are developed vertically between the soil and the container walls. However, this type of shear boxes has some limitations such as the reflection of waves by the rigid walls.

ii. Rigid container with flexible boundary at which soft materials (such as sponge) are glued along the rigid end walls to partially reduce the waves reflection and the lateral stiffness of the end walls. Yet, this type has a limitation of the uncertainty of the actual boundary condition.

iii. Rigid container with hinged end-walls at which the end walls are permitted to rotate about the base to allow the evaluation of lateral earth pressure.

iv. Equivalent shear beam container at which a flexible material (such as rubber) is attached to the end walls so the wall stiffness will match the stiffness of the contained soil. This will help to eliminate the interaction between the container and the soil. However, the limitation of this type of boxes are the conflict between the linear elastic stress-strain relationship of the rubber and the non-linear behaviour of soil under cyclic loading.

v. Laminar container: which consist of a stack of laminae, which are individually supported by bearings and a steel guide connected to an external frame. Using this type of boxes minimizes the lateral stiffness of the box, so the response of the soil-box system is governed by the soil itself.

vi. Active boundaries container: which is a laminar box but with an external actuator that is connected to each individual lamina. This allows different pressure to be applied at each lamina, to accommodate the variation of soil stiffness during earthquake.

Each research in the literature that used these containers (or boxes) have selected the kind of the container based on the goal of the research as well as the experimental limitation that might appear in every experiment. For instance, in order to investigate the effect of the shear box

geometry, simulate the real effect of earthquake on the soil deformation and stress conditions and accommodate the limitation of swinging platform of the centrifuge shake table, Takahashi et al. (2001) designed an active type (flexible) shear box (Figure 2.15) that is consisted of thirteen aluminum laminae of inner size of around (450 x 200 x 24 mm), and the height of the box was designed to be 325 mm. Each lamina contains grooves at which roller bearings were mounted to support the laminae. Soil samples in this box were designed to be tested under loading of one direction movement and a gravity of 100-g. So, in order to force laminae to move in only the same loading direction, the box was surrounded by external columns with rollers. To avoid soil particles from spreading in the gaps between laminae, a rubber rectangular sleeve was used to contain the soil inside the box. Hydraulic actuators were connected to the box in three different leveled laminae, and linear variable differential transformers (LVDTs) were attached to the actuators in order to collect their signals to provide the required data to investigate the behavior of structures under the condition of large soil movement using a simple finite element analysis.

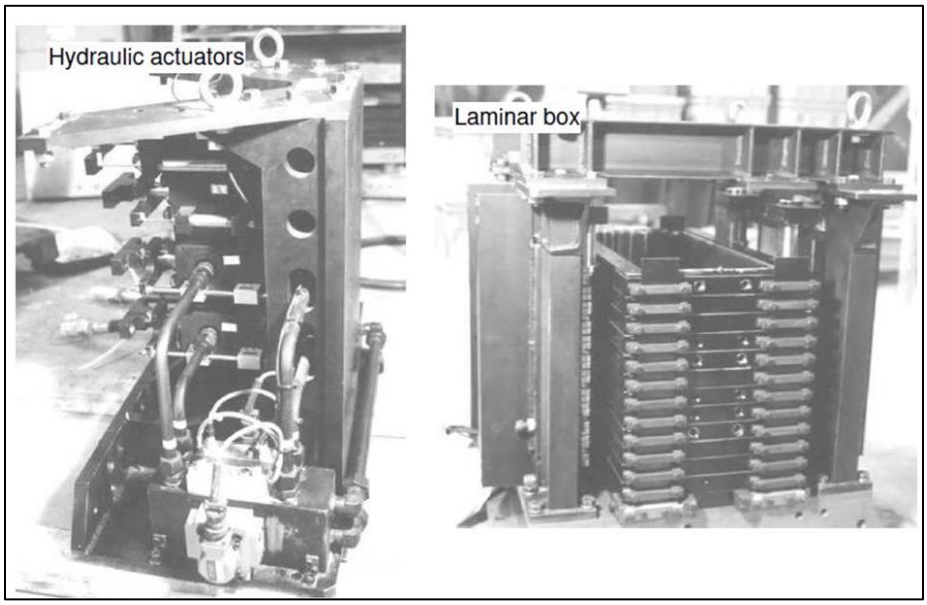

Figure 2.15 Laminer shear box (Takahashi et al. 2001)

James et al. (2003) constructed a mid-size rigid sample box within a series of shaking table tests to investigate the liquefaction behavior of tailings during seismic activities. The sample box (Figure 2.16) of around 1 cubic meter size was made of enclosed, rigid, reinforced, welded aluminum frame on a reinforced aluminum base plate. In order to confine sample inside the box, the box walls were made of aluminum sheets on three sides and one side of acrylic sheet to help observe the sample during test. The box was bolted to a shake table.

Figure 2.16 Rigid shear box (James et al. 2003)

El-Emam and Bathurst (2004) used rigid rectangular shear box of (1.4 x 2.7 m) dimensions bolted to shaking table of steel platform, with (2.7 x 2.7 m) dimensions, and servo-hydraulic actuator to perform series of dynamic shaking table tests to find out the seismic behavior of reduced-scale reinforced soil walls made of synthetic, olivine, angular to sub-angular grained, silica-free sand. Ueng et al. (2006) developed a laminar shear box to study the liquefaction behavior of saturated sand and soil-water interaction under two-dimensional ground shaking. 15 layers of (1880 x 1520 mm) inner dimension, each layer consisting of two nested aluminum frames, were attached to surrounding rigid steel walls, and whole assembly was placed on top of 2-D shaking table (Figure 2.17). To avoid the rubber membrane inside the box (that contains the soil sample) from rupturing and the excessive building of expanded soil on the side of the membrane, the 15 layers (lamiae) were placed at the top of each other with a 20 mm gap between each layer. In order to allow the biaxial motion, the center of mass of each layer of soil and each lamina was designed not to be in the same geometrical center of the horizontal cross section. Also, the vertical alignments of the center of mass of different layers were designed not to match each other, especially during the shear deformation.

Dihoru et al. (2010) investigated the dynamic behavior of soil in two different sized shear boxes to understand the limitations associated with each design, evaluate soil behavior of each box in relation to a known idealized behavior, and to provide design improvement solutions and new design concepts. In this study, they used small scale laminar shear box of (1200 x 500 x 800 mm) size, and a large-scale laminar shear box of (5000 x 1200 x 1200 mm) size (Figure 2.18). Dry sand payload was placed in both boxes to compare the behavior in both cases. Both boxes were subjected to one directional seismic load with multi amplitude values. The study concluded that the behavior of a laminar shear box differs greatly from the idealized behavior, and these behaviors vary with different load amplitude values.

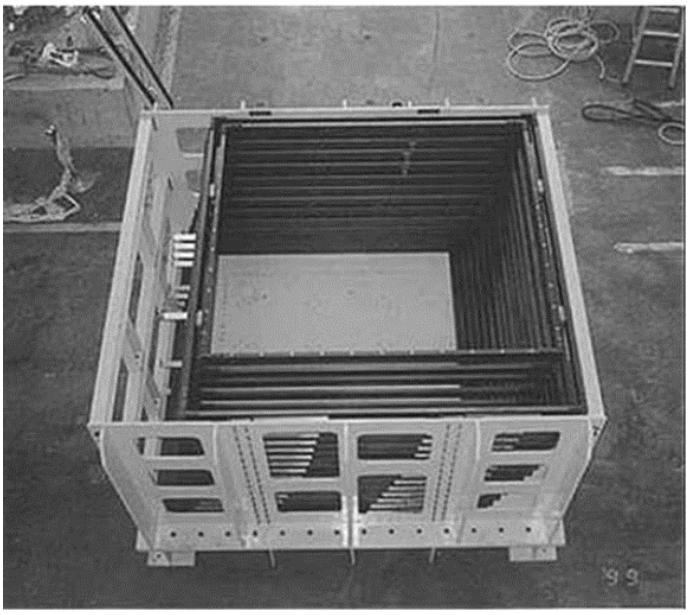

Figure 2.17 Biaxial laminer shear box (Ueng et al. 2006)

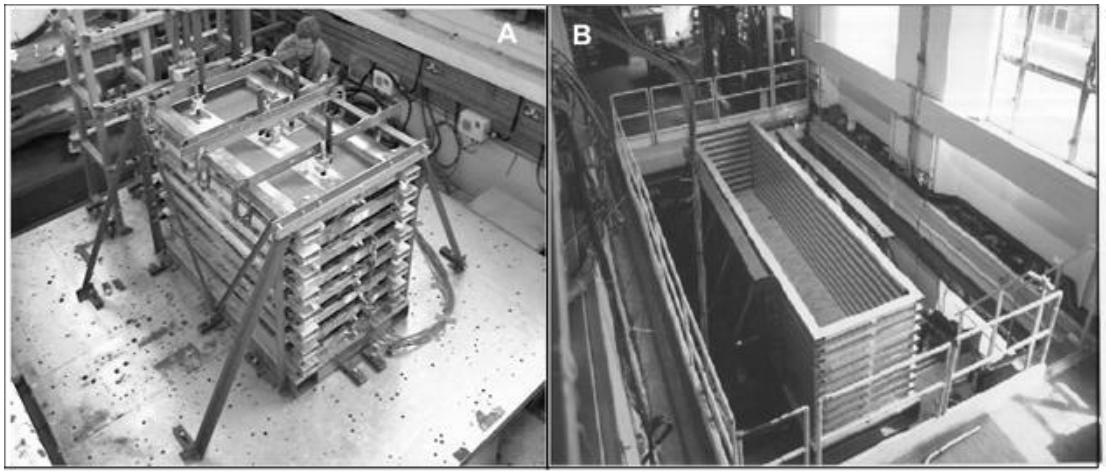

Figure 2.18 Laminar shear box with different size scale (Dihoru et al. 2010)

A: small scale, B: Large scale

Eseller-Bayat et al. (2013) designed a cyclic simple shear liquefaction box of (300 x 270 x 490 mm) dimensions (Figure 2.19) in order to test the liquefaction behavior of sand under controlled cyclic shear strain in saturated condition. The box contains two rotating walls connected to two translating rigid walls with a flexible sealant. Two sets of transducers were placed inside the box, one for pore-water pressure and the other for the liner variable displacement. The box was fixed to a shaking table in order to simulate the seismic activity. Eseller-Bayat et al. (2013) concluded that this box can be re-designed to accommodate tests for samples of different sizes and different consistency (such as silt, re-formed clay, and gravelly soils).

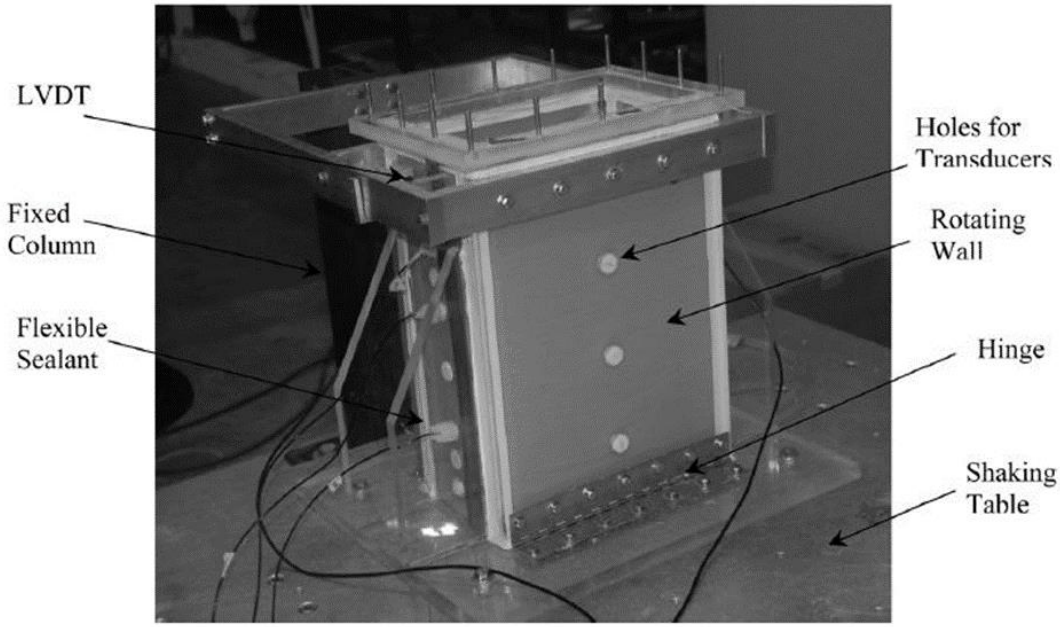

Figure 2.19 Cyclic simple shear liquefaction box (Eseller-Bayat et al. 2013)

To study the deformation and liquefaction behavior of poorly graded sand and a footing model during earthquake events under saturated and unsaturated conditions in different scenarios, Mohamed (2014) designed a square flexible laminar shear box (FLSB) (Figure 2.20A) with inner dimensions of (800 x 800 x 807 mm). It consisted of 24 laminae of 31 mm thickness, with 2mm spacing between laminae to ensure independency of movement of each lamina. To ensure single axis movement (parallel to the shaking direction), linear bearing system was attached to the FLSB, and an external frame was mounted to the FLSB to help secure the box into the shake table. To hold the soil inside the FLSB, a flexible plastic bag of small stiffness in comparison with the tested soil was used (Figure 2.20B).

Rollins et al. (2019) studied the liquefaction mitigation of prefabricated vertical plastic drain piles in liquefiable sand under seismic loadings using a large-scale laminar shear box that consisted of 40 stacked rectangular shear lamina with dimensions of (500 cm x 275 cm x 15 cm) of each lamina.

In the current study, a Flexible Laminar Shear Box (FLSB) was designed and fabricated in the facilities of the University of Ottawa solely for the purpose of this research. To the best knowledge of the author, this FLSB is the first of its kind that is used to study the liquefaction behavior of cemented fine soils such as CPB under seismic conditions at early ages of maturity. Further details of the shaking table and FLSB used in this research as well as the methodology, experimental conditions, instrumentations, and accessories are briefly described in the following chapters.

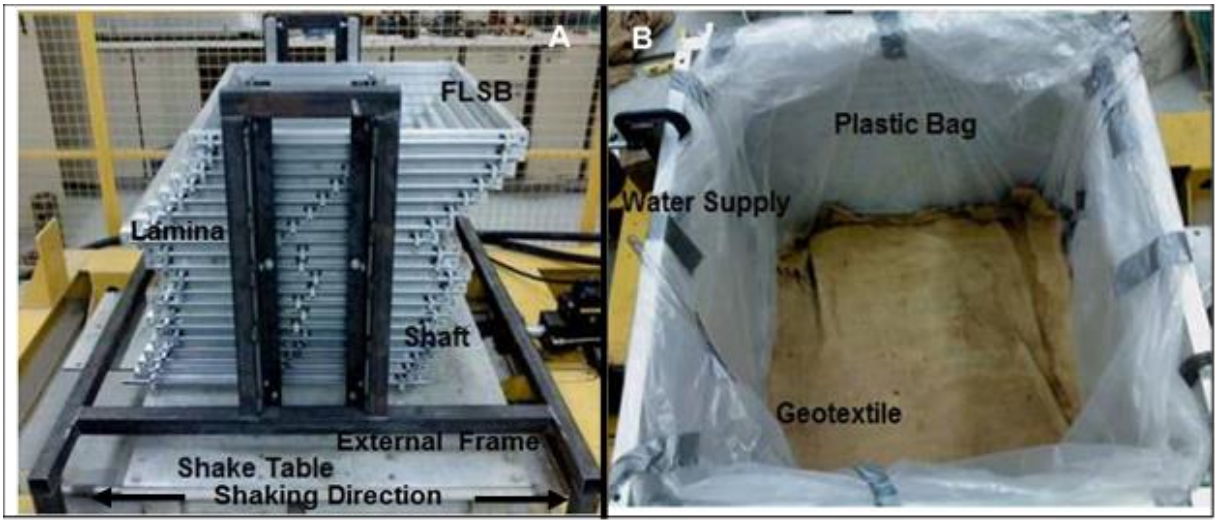

Figure 2.20 Flexible laminar shear box (FLSB) (modified from: Mohamed 2014)

A: the FLSB, B: Flexible plastic bag.

2.7 Previous Studies of Shaking Table Tests on Natural Fine-Grained Soils and Tailings

In addition to the studies mentioned in previous sections, there were many other researches that were conducted on the liquefaction response of natural fine-grained soils and tailings (without cement) using the shaking table technique. The following subsections summarize some of the most recent studies.

2.7.1 Shaking table test of liquefaction on natural fine-grained soils

A series of large-scale shaking table test was conducted by (Chen et al. 2020) to explore the liquefaction effect of soft silty clay and liquefiable sand on irregular subway structures. In this study, laminar shear box of 35 cm × 20 cm × 17 cm (L×W×H) was used and the soil samples were subjected to a series of 1-D seismic loading of 1.0g acceleration, 0.1 – 50 Hz frequency, and shaking durations of 30 – 180 seconds. During the tests, the buildup of pore pressure, acceleration response and horizontal displacement of the model soils were evaluated along with the settlement of the ground surface and the strain deformation of the model. As a result, the liquefiable soil exhibited multiple peaks of acceleration with significant amplification while applying medium to low frequency and liquefaction-induced uplift of the structure occurred. Moreover, it was found that sand liquefaction played a natural isolation role and minimized the underground structure damage as compared to the response within the soft soils.

To determine the dynamic response and the mechanism of pile-soil interaction of Puqian Bridge in China, (Dong et al. 2019) conducted shaking table test of 50 seconds duration and 0.15g – 0.6g acceleration, using a 37 cm × 28 cm × 20 cm laminar shear box. The tested soil model consisted of 47 cm thick mucky clay layer overlaying layers of coarse sand, gravel, and bedrock respectively. Each layer of the physical model contained set of strain gages and accelerometers as well as a displacement gage that was placed on top of the clay layer (underneath the pile cap of

the structure) to monitor the seismic-induced relative horizontal displacement of the top of the pile. It was concluded that the overburden layer amplified the seismic wave and increased the peak acceleration along the pile length. The fundamental frequency decreased with increase in seismic intensity, while the horizontal displacement of the pile top increased with increase in seismic intensity, and crack damage was developed at the interface between the soft and hard soil layers.

Centrifuge test operated by electro-hydraulic shaking table was conducted by (Huang et al. 2019) to explore the liquefaction mitigation effectiveness on sand foundation treated with nanoparticles. The test was conducted using a laminar shear box of 50 cm × 40 cm × 55 cm and applying sinusoidal and earthquake waves with 45g rotational acceleration for 35 second duration on clean medium- to fine-grained sand. In this study, piezoelectrical accelerometers were attached to the model and the shaking table to monitor the seismic wave propagation. The excess pore pressure was captured using pore pressure transducers placed at different levels within the sample. Moreover, laser displacement transducer was fixed to the top surface and the sides of the model to measure settlement and lateral displacement. The study revealed that adding nanoparticles to the sand foundation enhances the liquefaction resistance by reducing the excess pore pressure, shear strain, and lateral displacement, as the nanoparticles will delay the dynamic-induced propagation of excess pore pressure due to the dispersion of nanoparticles in water and forming the pore fluid gel.

Onur (2018) evaluated the liquefaction of non-plastic fine-grained silty sand soil by conducting shaking table test using a laboratory-scale shaking table test device (Figure 2.21A), which is controlled by a computer. The test was performed after applying a vertical stress of 50 kPa (using a rigid mass) on the surface of the fully saturated soil model (Figure 2.21B). Applying the dynamic loading resulted in excess pore-water generation and the occurrence of settlement with different values. Owing to the upward movement of water and downward displacement of the rigid mass, the liquefaction potential was higher in the conditions of high shaking acceleration and low relative density of soil.

Zhan et al. (2014) used a 23 layered large-scale laminar shear box (Figure 2.22) to study the dynamic characteristics of saturated silty soils ground subgrade with the inclusion of stone columns. This study was carried out by conducting set of shaking tables tests with different loading accelerations (0.161g, 0.252g, and 0.325g). It was found that there was no visible sign of settlement during ground shaking of less than 0.161g acceleration, while there was an obvious uplift on ground surface during the 0.252g accelerated shaking. Ground shaking of 0.325g acceleration caused damage to the subgrade. It was also noted that there was almost no shear displacement in silty soils under 0.161g ground shaking acceleration, while there was significant shear displacement under 0.252g and 0.325g loading acceleration. However, the shear displacement was less significant when applying the same seismic loading on silty soils that contain stone columns (Figure 2.23). The inclusion of stone columns also significantly reduced the accumulated settlement and nonuniform settlement of the ground (Figure 2.24).

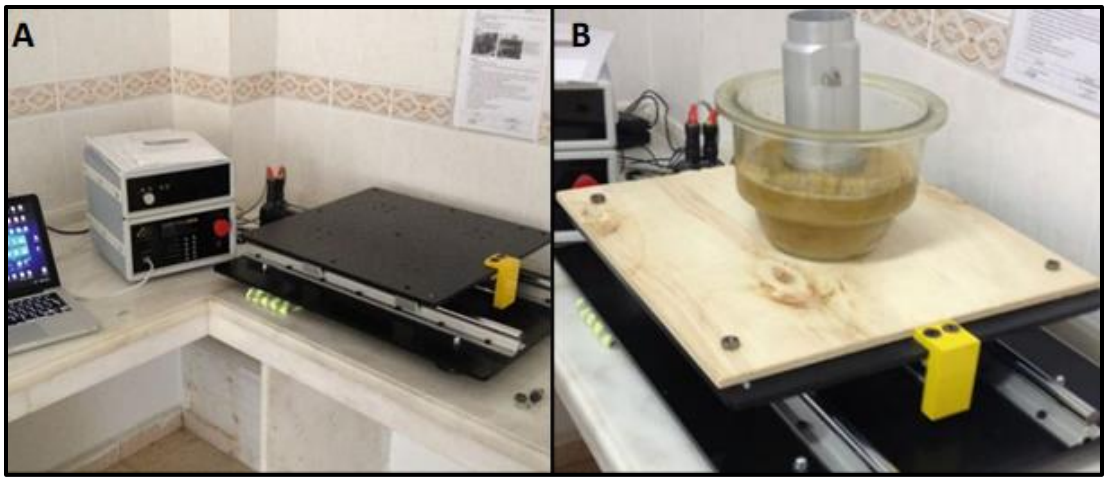

Figure 2.21 Laboratory scale-shaking table test (modified from: Onur 2018)

A: Shaking table B: Soil model.

Figure 2.22 Large-scale laminar shear box used by (Zhan et al. 2014).

In order to verify their three dimensional, numerical model which was developed to simulate static and seismic loads to investigate the liquefaction triggers of soil under mat foundation, Cetin et al. (2012) used the results of centrifuge and shaking table tests that was performed by (Unutmaz and Cetin 2012), wherein a simplified procedure that includes laboratory-based cyclic shear and volumetric-strain relationship was applied to evaluate settlement and tilting potential of mat foundation due to seismic activities. The laboratory shaking table results were calibrated against values of settlement and foundation tilting potentials recorded from the 1999 earthquake of Kocaeli, Turkey.

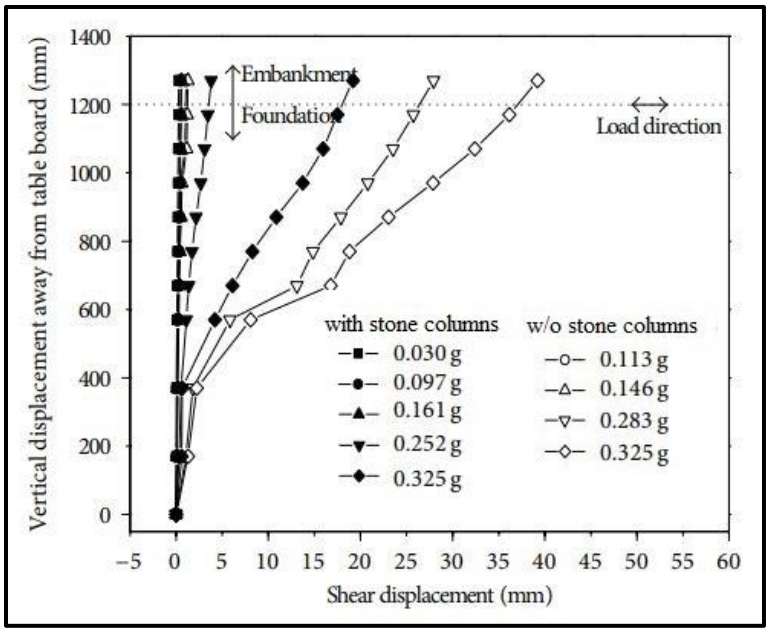

Figure 2.23 Dynamic-induced shear displacement of silty soils with and without stone columns (modified from: Zhan et al. 2014).

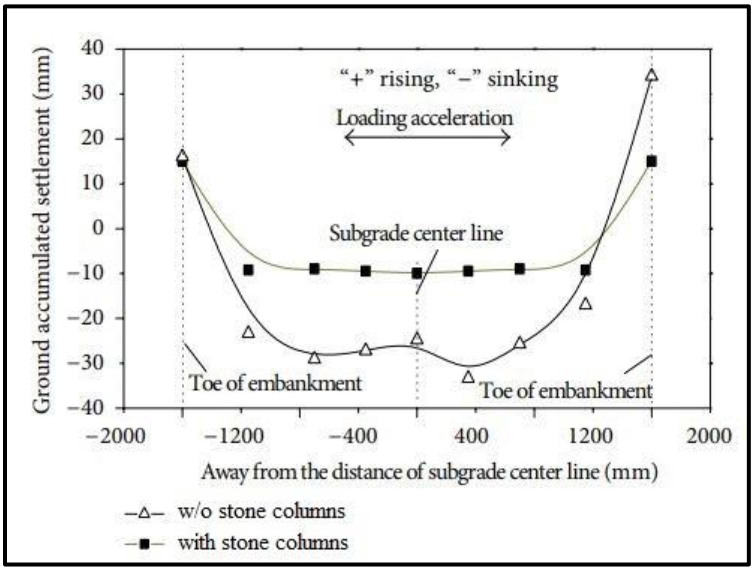

Figure 2.24 Dynamic-induced accumulated settlement of silty soils with and without stone columns (modified from: Zhan et al. 2014).

Chen et al. (2010) conducted a series of shaking table tests to assess the behavior of liquefiable unsaturated clay under non-uniform ground movement waves in order to investigate the response of a utility tunnel that is proposed to be constructed in similar conditions. In this study, the authors used "dual multi-axis shaking table system" that is consisted of two shear boxes that are fixed to two different sized shaking tables (small scale fixed table and large-scale moveable table).

Jiang et al. (2007) conducted shaking table test using a large-scale laminar shear box (4 m × 1.5 m × 2.5 m) to evaluate the influence of two reinforcement systems (compacted gravel, and fly-ash gravel) on saturated silty soils along high-speed railway. to meet its objectives, the study used accelerometers, PWP transducers, displacement transducers, and LVDTs. The results of this study indicated that the compacted gravel will effectively improve the liquefaction countermeasure ability of the ground by restraining the excess PWP development. Also, both reinforcement systems were able to improve the anti-shear displacement capacity by resisting the ground shear displacement. They can also significantly reduce the liquefaction-induced amplification of response acceleration, and they can reduce the seismic-induced settlement.

Adalier et al. (2003) assessed the liquefaction mitigation mechanisms of non-plastic silty soils due to the deployment of stone columns as an anti-liquefaction factor. Series of (N-g) shaking table (centrifuge) tests were conducted in this research at which stone columns of different sizes were placed within the silt deposit. First test was conducted on pure saturated silt (without stone column) which was placed in (1-D) laminar soil container of 25 cm ×45 cm ×25 cm dimensions (W×H×L), and was equipped with accelerometers, LVDTs, and PWP transducers (Figure 2.25). It was found from this test that the relative density of silt was reduced by 3% during shaking. The acceleration records showed significant attenuation of soil strength and stiffness duo to liquefaction as the soil acceleration gradually decreased after couple of shaking cycles. This gradual decrease in acceleration refers to gradual strength degradation due to excess PWP development. Then, after 9-10 cycles of shaking, the acceleration virtually disappeared referring to full attenuation of motion (total loss of shear strength) in the entire silt stratum due to liquefaction. The acceleration attenuation was accompanied with around 10 cm of settlement leading to a 1.3% of permanent volumetric strain of silt layer thickness. Acceleration, excess PWP, and settlement data gathered from the other tests (with different size of stone columns) showed stiffening of the material foundation response during shaking. This was attributed to the role of stone columns in retarding the excess PWP buildup, reduced the surcharged-footing settlement by about 50%, and consequently enhanced the foundation soil overall stiffness.

Holchin and Vallejo (1995) conducted set of shaking tables tests (1-D) to assess the seismic behavior of clay embankments that contain cavities filled with sand lenses. The amplitude of the shaking was around 0.4 cm, and the cyclic frequency ranged from 6 to 35 Hz. A rigid soil container of 35 cm × 10 cm × 30 cm made of 0.5 cm thick clear plexiglass was used in this experiment. As a result, the cyclic loading caused liquefaction of the sand lenses, which in turn exerted pressure on their containing cavities, leading to cavity walls deformation. This deformation caused tensile cracks in the clay, demonstrating the seismic-induced failure of clay embankments due to liquefaction of sand lenses.

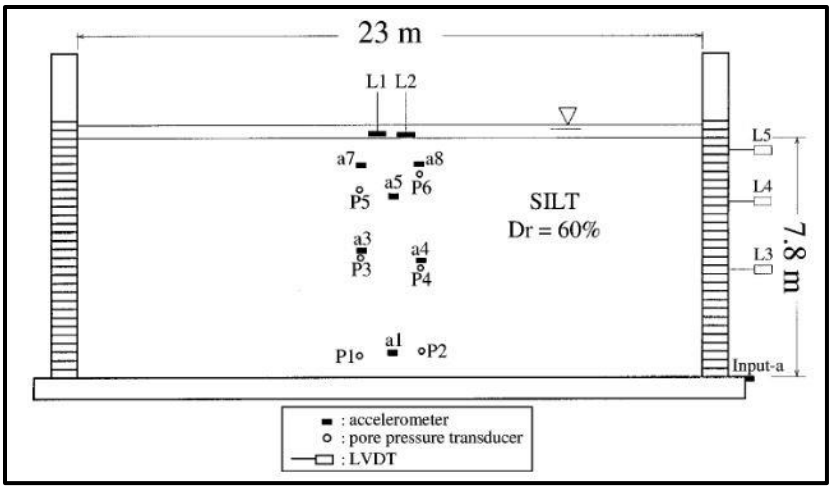

Figure 2.25 Instrumentations setup of centrifuge shaking table test conducted by (Adalier et al. 2003).

2.7.2 Shaking table test of liquefaction on tailings

There were few studies till now that used the shaking table test to evaluate the seismic response of tailings. For example, Jin et al. (2018) investigated the dynamic behavior of tailings reservoir under seismic loading using the shaking table test. In this test, a model tailing dam was constructed in a model box (Figure 2.26). Drainage pipes and piezometric tubes were installed within the model besides sets of accelerometers, pore pressure sensors and displacement sensors that were used to monitor the tailings behavior during shaking. The model box was mounted over the shaking table and multiple seismic loadings with 0.1g – 0.6g accelerations were applied. The study found that the acceleration amplification factor decreased with increase in dam height when increasing the peak acceleration. Also, PWP inside the slope height was greater than the lateral PWP. Thus, the vertical PWP ratio was less than the horizontal PWP ratio, which means that the tailings were easy to liquefy in the air facing section. Moreover, the measured peak values of the earth pressure in the inner section of the dam were higher than the peak values measured near the air surface. The study also contained some numerical simulation in this regard.

Ren et al. (2018) conducted numerical modeling and physical experiment to study the dynamic response of Xiangchong tailings impoundment in China. The physical experiment was conducted using earthquake shaking table by constructing a laboratory model with geometric scale of 1:300 of the real dam in two different water content conditions. At each water content condition, multiple shaking sessions with different load levels were conducted. The results show that the input peak accelerations are negatively correlated with the acceleration magnification factor. The numerical modeling results were slightly different as compared to the results of the physical experiment, which was attributed by the authors to the limitation of the reduced scale of the physical model. Both numerical modeling and physical model agreed that the lower elastic modulus is correlated with weaker response of the dynamic behavior as a result of the conservation of energy. In other words, the input earthquake energy dissipates in the form of elastic vibration, plastic deformation, and damping.

Figure 2.26 Shaking table test of tailing dam (Jin et al. 2018)

Shaking table test was conducted by (Antonaki et al. 2016) to evaluate the liquefaction potential of mildly sloped consolidate mine tailings. Centrifuge test was conducted in the research with 80g acceleration on 20-25 m high tailing deposit placed in laminar container. The initial water content of the tailing model was adjusted to 59%. Settlement gauges, PWP sensors, accelerometers and LVDTs were used in this test to monitor the parameters of soil behavior under dynamic loadings. Coarse waste rocks were deposited within the tailing slayers to investigate its effect on enhancing the soil behavior, and it was found that the mine tailing exhibited a significant higher buildup of PWP as compared to the mixed deposit. It was also observed that the behavior of both deposits was similar with respect to the lateral displacement and the slight deformation of the slope. However, the mine tailing deposit deformed in the direction of the toe of the slope, while the mixture deposit deformed in the opposite side.

Pépin et al. (2009) used the rigid shear box bolted to 3-g, 1-D shaking table to determine the effect of drainage inclusion on pore-water development in order to evaluate the dynamic behavior of hard rock mine tailings against liquefaction under ground motion conditions, which might cause failure in retaining dikes. Tests were conducted under the influence of the variation of tailing density, drainage inclusion, and some other factors. In this study, results of previously tested sand were used as a reference in assessing the response of hard rock tailing tested under those conditions. Various instruments were installed with the sample inside the shear box at different levels in order to monitor the changes in dynamic properties (Figure 2.27). For example, pressure sensor was used to measure the variation of pore-water pressure with depth, and LVDTs

were installed to measure the vertical displacement of the tailing at different depths. On the other hand, a perforated plastic plate was installed at different levels to reduce the seepage pressure effect on the displacement. Furthermore, metal plate was installed at different depths to determine changes in bearing capacity with depth due to the development of excess pore-water pressure and consequent liquefaction by measuring the heave in tailing sample. It was concluded from this study that hard rock mine tailings are liquefiable material with liquefaction resistance that is less than sand's resistance. It was also noted that maximum excess water pressure is reached at the top of the sample first, and then progresses downward. However, the presence of drainage will decrease the excess pre-water pressure development, which will reduce the liquefaction potential. Although it is less effective approach, reinforcing the tailings with rigid inclusions (such as columns or waste rock) in tailings impoundment might be used to increase the tailings' resistance against liquefaction.

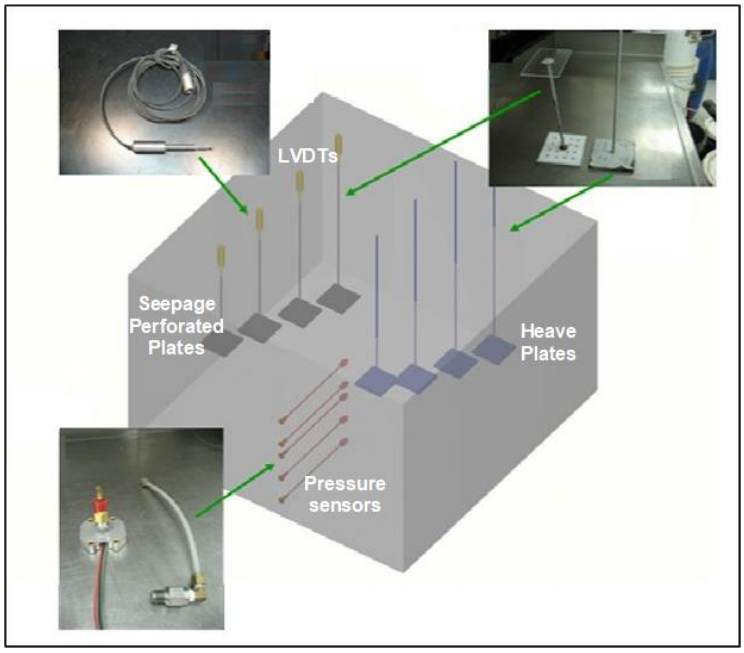

Figure 2.27 Instruments installed within tailings experimented by shaking table test (modified from: Pépin et al. 2009).

James et al. (2003) conducted a preliminary investigation by applying 1-D (horizontal) shaking table test in order to understand factors influencing the resistance of mine tailings against liquefaction besides evaluating the mitigation measures such as creating drainage inclusions by including rock fill wastes within the tailings impoundments. Tests were conducted giving due consideration to the effect of factors influencing liquefaction, such as the material density, grain size distribution, particles angularity structure, and confining stresses (vertical and lateral) in addition to the common agreement that tailings liquefy as they contain sufficient water content to do so. The study revealed that the pore-water pressure increases with the increase in shaking time. After shaking stops, pore-water pressure starts to decrease for some time and then becomes constant. It was also found that the applied seismic loading (in this experiment) was not enough to

induce complete liquefaction through the deep layers of the sample, so only the upper layers of the sample were exposed to significant settlement (i.e. loss in bearing capacity). Accordingly, the water started to expel during the test from the top of the sample.

2.8 Conclusions

Over the past few decades, cemented paste backfill (CPB) has become a noticeable interesting method of tailing management around the world. It allows around up to 60% of hazardous mining waste (tailings) to be reused and returned into the underground mine opening (mine stope). CPB is considered as a fine soil undergoing cementation, as it consists of fine-grained mine tailings mixed with hydraulic binder (such as cement) and water (fresh or mine processed). CPB mixture is prepared in paste plants located in the mine area, and the fresh CPB mixture is delivered into the mine stope through related pipelines. There are different strategies, wherein the fresh CPB is placed in the mine stope, including filling the mine stope with CPB in one layer or in two layers (plug and main fill).

From the theoretical and technical background information, it was learnt that cement hydration is one of the key factors in the backfilling role of CPB. Also, it is understood that CPB in the field might be subjected to different sources of heat, which affects the mechanical behavior of CPB. Moreover, CPB may contain different types of chemical elements (such as sulphate), which was found to have an effect on the characteristics of CPB.

Besides being subjected to static loads, mining areas are highly prone to seismic activities. It was learnt from the literature that fine-grained soil might be susceptible to seismic-induced liquefaction, based on the contractive and dilative behavior of the disturbed material. Disturbing liquefiable soils leads to the propagation of excess pore-water pressure, which reduces the effective stress and consequently reduces the shear strength of these soils. CPB is considered a liquefiable soil, especially when it is in the young maturity ages. This may make CPB structures prone to liquefaction-induced failure causing injuries and fatalities in the mine area as well as the negative impacts to the environment and the economic loss.

From the reviewed studies, it can be observed that researchers studied the seismic or cyclic loading-induced liquefaction of natural soils and/or tailings (without cement) using the shaking table testing method, which is a realistic tool in simulating seismic or cyclic conditions. It was also observed that only few studies that investigated the liquefaction potential of CPB under dynamic loadings. However, these studies have used only the triaxial test in this regard. Since no study till now has used the shaking table test, so there is a great need to assess the cyclic response of fresh CPB using the shaking table test. Furthermore, similar to the mechanical properties of the CPB, the cyclic response might also be affected by some parameters (such as the temperature and chemistry of the CPB mixture as well as the filling strategy). There is, therefore, a great need to understand the effect of these parameters on the liquefaction response of fresh CPB under dynamic loadings in order to fill the gap of previous studies. Also, a better understanding will contribute to

more efficient design of CPB structures at early age and help in minimizing liquefaction-induced failure and related impacts and damages.

2.9 References

Abdelaal, A. (2011) *Early age mechanical behavior and stiffness development of cemented paste backfill with sand*, Doctoral dissertation, University of Toronto.

Abdul-Hussain, N. (2011) *Experimental Study on the Engineering Properties of Gelfil*, Masters thesis, University of Ottawa.

Abdul-Hussain, N. and Fall, M. (2012) 'Thermo-hydro-mechanical behaviour of sodium silicate-cemented paste tailings in column experiments', *Tunnelling and Underground Space Technology*, 29, 85-93.

Adalier, K., Elgamal, A., Meneses, J. and Baez, J. I. (2003) 'Stone columns as liquefaction countermeasure in non-plastic silty soils', *Soil Dynamics and Earthquake Engineering*, 23(7), 571-584.

Agurto-Detzel, H., Bianchi, M., Assumpção, M., Schimmel, M., Collaço, B., Ciardelli, C., Barbosa, J. R. and Calhau, J. (2016) 'The tailings dam failure of 5 November 2015 in SE Brazil and its preceding seismic sequence', *Geophysical Research Letters*, 43(10), 4929-4936.

Aldhafeeri, Z. (2018) *Reactivity of Cemented Paste Backfill*, University of Ottawa.

Aldhafeeri, Z., Fall, M., Pokharel, M. and Pouramini, Z. (2016) 'Temperature dependence of the reactivity of cemented paste backfill', *Applied Geochemistry*, 72, 10-19.

Ali, G., Fall, M. and Alainachi, I. (2021) 'Time- and temperature-dependence of rheological properties of cemented tailings backfill with sodium silicate', *ASCE's Journal of Materials in Civil Engineering*, DOI: 10.1061/(ASCE)MT.1943-5533.0003605.

Ali, M. M. (2010) 'Identifying and Analyzing Problematic Soils', *Geotechnical and Geological Engineering*, 29(3), 343-350.

Antonaki, N., Abdoun, T. and Sasanakul, I. (2016) 'Centrifuge Modeling of Mine Tailings and Waste Rock Co-Disposal, Consolidation, and Dynamic Loading', in *Geo-Chicago*, American Society of Civil Engineering, 245-254.

ASTM C150/C50M-19a (2019) 'Standard Specification for Portland Cement',

Atkinson, G. M., Kaka, S. I., Eaton, D., Bent, A., Peci, V. and Halchuk, S. (2008) 'A very close look at a moderate earthquake near Sudbury, Ontario', *Seismological Research Letters*, 79(1), 119-131.

Bairro, R. and Vaz, C. (2000) *Shaking table testing of civil engineering structures-The LNEC 3D simulator experience*, translated by Auckland, New Zeland.

Belem, T. and Benzaazoua, M. (2004) *An overview on the use of paste backfill technology as a ground support method in cut and fill mines*, translated by Perth, Australia: CRC Press, 637–650.

Bentz, D. P. (2006) 'Influence of water-to-cement ratio on hydration kinetics: Simple models based on spatial considerations', *Cement and Concrete Research*, 36(2), 238-244.

Benzaazoua, M., Fall, M. and Belem, T. (2004) 'A contribution to understanding the hardening process of cemented pastefill', *Minerals Engineering*, 17(2), 141-152.

Bhattacharya, S., Lombardi, D., Dihoru, L., Dietz, M. S., Crewe, A. J. and Taylor, C. A. (2012) 'Model Container Design for Soil-Structure Interaction Studies' in *Role of Seismic Testing Facilities in Performance-Based Earthquake Engineering*, 135-158.

Bhattacharya, S., Tokimatsu, K., Goda, K., Sarkar, R., Shadlou, M. and Rouholamin, M. (2014) 'Collapse of Showa Bridge during 1964 Niigata earthquake: A quantitative reappraisal on the failure mechanisms', *Soil Dynamics and Earthquake Engineering*, 65, 55-71.

Boulanger, R. W. and Idriss, I. M. (2006) 'Liquefaction Susceptibility Criteria for Silts and Clays', *Journal of Geotechnical and Geoenvironmental Engineering*, 132(11)(11), 1413-1426.

Bullard, J. W., Jennings, H. M., Livingston, R. A., Nonat, A., Scherer, G. W., Schweitzer, J. S., Scrivener, K. L. and Thomas, J. J. (2011) 'Mechanisms of cement hydration', *Cement and Concrete Research*, 41(12), 1208-1223.

Casagrande, A. (1976) 'Liquefaction and cyclic deformation of sands-a critical review', *Harvard Soil Mechanics Series, Harvard University, Cambridge, Massachusetts.*, No. 88.

Cetin, K. O., Unutmaz, B. and Jeremic, B. (2012) 'Assessment of seismic soil liquefaction triggering beneath building foundation systems', *Soil Dynamics and Earthquake Engineering*, 43, 160-173.

Chen, J., Shi, X. and Li, J. (2010) 'Shaking table test of utility tunnel under non-uniform earthquake wave excitation', *Soil Dynamics and Earthquake Engineering*, 30(11), 1400-1416.

Chen, S., Tang, B., Zhao, K., Li, X. and Zhuang, H. (2020) 'Seismic response of irregular underground structures under adverse soil conditions using shaking table tests', *Tunnelling and Underground Space Technology*, 95.

Chern, S. and Chang, T. (1995) 'Simplified procedure for evaluating soil liquefaction characteristics', *Journal of Marine Science and Technology*, 3(1)(1), 35-42.

Chopra, A. K. (2005) *Earthquake Dynamics of Structures - a Primer*, Earthquake Engineering Research Institute (EERI), USA.

Cihangir, F., Kesimal, A., Yilmaz, T., Koc, E. and Akyol, Y. (2018) 'Investigation of the effect of tailings characteristics on paste backfill properties', in *International Multidisciplinary Scientific GeoConference: SGEM: Surveying Geology & mining Ecology Management*, Sofia, Bulgaria,

Cook, N. G. W. (1976) 'Seismicity associated with mining', *Engineering Geology*, 10(1976), 99-122.

Cui, L. (2017) *Multiphysics Modeling and Simulation of the Behavior of Cemented Tailings Backfill*, Doctoral dissertation: University of Ottawa.

Cui, L. and Fall, M. (2016) 'Mechanical and thermal properties of cemented tailings materials at early ages: Influence of initial temperature, curing stress and drainage conditions', *Construction and Building Materials*, 125, 553-563.

Das, B. M. and Ramana, G. V. (2010) *Principles of soil dynamics*, 2nd ed., Cengage Learning. Inc, Boston.

De Groot, M. B., Bolton, M. D., Foray, P., Meijers, P., Palmer, A. C., Sandven, R., Sawicki, A. and Teh, T. C. (2006) 'Physics of liquefaction phenomena around marine structures', *Journal of Waterway, Port, Coastal, and Ocean Engineering*, 132(4)(4), 227-243.

Desai, C. S. (2000) 'Evaluation of liquefaction using disturbed state and energy approaches', *Journal of Geotechnical and Geoenvironmental Engineering*, 126(7)(7), 618-631.

Dihoru, L., Crewe, A. J., Dietz, M., Bhattacharya, S. and Taylor, C. A. (2010) 'Laminar Shear Box Design for Soil-Structure Interaction Studies', in *International Workshop on Role of Research Infrastructures in Performance-Based Earthquake Engineering, 14th European Conference in Earthquake Engineering*, Ohrid, Macedonia,

Dong, Y., Feng, Z., He, J., Chen, H., Jiang, G. and Yin, H. (2019) 'Seismic Response of a Bridge Pile Foundation during a Shaking Table Test', *Shock and Vibration*, 2019, 1-16.

El-Emam, M. M. and Bathurst, R. J. (2004) 'Experimental Design, Instrumentation and Interpretation of Reinforced Soil Wall Response Using a Shaking Table', *International Journal of Physical Modelling in Geotechnics*, 4(4), 13-32.

Elkhadiri, I., Palacios, M. and Puertas, F. (2009) 'Effect of curing temperature on cement hydration', *Ceram Silik*, 53(2)(2), 65-75.

Ellen, S. D., Algus, M. A., Cannon, S. H., Fleming, R. W., Lahr, P. C., Peterson, D. M. and Reneau, S. L. (1982) *Description and mechanics of soil slip/debris flows in the storm*, 1434, U.S. Geolological Survey Profissional Paper

Ercikdi, B., Cihangir, F., Kesimal, A. and Deveci, H. (2017) 'Practical Importance of Tailings for Cemented Paste Backfill' in Yilmaz, E. and Fall, M., eds., *Paste Tailings Management*, Cham: Springer International Publishing, 7-32.

Ercikdi, B., Kesimal, A., Cihangir, F., Deveci, H. and Alp, İ. (2009) 'Cemented paste backfill of sulphide-rich tailings: Importance of binder type and dosage', *Cement and Concrete Composites*, 31(4), 268-274.

Eseller-Bayat, E., Gokyer, S., Yegian, M. K., Ortakci, E. and Alshawabkeh, A. (2013) 'Design and Application of Simple Shear Liquefaction Box', *Geotechnical Testing Journal*, 36(3).

Fall, M. and Benzaazoua, M. (2005) 'Modeling the effect of sulphate on strength development of paste backfill and binder mixture optimization', *Cement and Concrete Research*, 35(2), 301-314.

Fall, M., Célestin, J. C., Pokharel, M. and Touré, M. (2010) 'A contribution to understanding the effects of curing temperature on the mechanical properties of mine cemented tailings backfill', *Engineering Geology*, 114(3-4), 397-413.

Fall, M., Nasir, O. and Celestine, J. (2007) 'Paste backfill responses in deep mine temperature conditions', in Symposium minefill, Montreal, Canada, CD-Room,

Fall, M. and Pokharel, M. (2010) 'Coupled effects of sulphate and temperature on the strength development of cemented tailings backfills: Portland cement-paste backfill', *Cement and Concrete Composites*, 32(10), 819-828.

Figueroa, J. L., Saada, A. S., Liang, L. and Dahisaria, N. M. (1994) 'Evaluation of soil liquefaction by energy principles', *Journal of Geotechnical Engineering*, 120(9)(9), 1554-1569.

Fleming, R. W., Ellen, S. D. and Algus, M. A. (1989) 'Transformation of dilative and contractive landslide debris into debris flows—an example from Marin County, California.', *Engineering Geology*, 27(1-4)(1-4), 201-223.

Galaa, A. M., Thompson, B. D., Grabinsky, M. W. and Bawden, W. F. (2011) 'Characterizing stiffness development in hydrating mine backfill using ultrasonic wave measurements', *Canadian Geotechnical Journal*, 48(8), 1174-1187.

Gibowicz, S. J. and Kijko, A. (2013) *An Introduction to Mining Seismology*, Elsevier.

Gopikrishna, K. (2000) *An Approach to assess severity of site damage using accelerograms*, M. Tech dissertation, Visvesvaraya Technological University, Karnataka, India.

Grabinsky, M. and Simms, P. (2006) 'Self-Desiccation of Cemented Paste Backfill and Implications for Mine Design' in *Proceedings of the Ninth International Seminar on Paste and Thickened Tailings*, Australian Centre for Geomechanics., 323-332.

Guoxing, C., Su, C., Xi, Z., Xiuli, D., Chengzhi, Q. I. and Zhihua, W. (2015) 'Shaking-table tests and numerical simulations on a subway structure in soft soil', *Soil Dynamics and Earthquake Engineering*, 76, 13-28.

Haeri, S. M., Kavand, A., Rahmani, I. and Torabi, H. (2012) 'Response of a group of piles to liquefaction-induced lateral spreading by large scale shake table testing', *Soil Dynamics and Earthquake Engineering*, 38, 25-45.

Hancock, J. and Bommer, J. J. (2006) 'A State-of-Knowledge Review of the Influence of Strong-Motion Duration on Structural Damage', *Earthquake Spectra,* 22(3), 827-845.

Haruna, S. and Fall, M. (2019) 'Time- and temperature-dependent rheological properties of cemented paste backfill that contains superplasticizer', *Powder Technology*.

Hasegawa, H. S., Wetmiller, R. J. and Gendzwill, D. J. (1989) 'Induced seismicity in mines in Canada—an overview', *Pure and applied geophysics*, 129(3-4), 423-453.

Hashash, Y. M., Hook, J. J., Schmidt, B., John, I. and Yao, C. (2001) 'Seismic design and analysis of underground structures', *Tunnelling and Underground Space Technology,* 16(4)(4), 247-293.

Hinzen, K. G. (1982) 'Source parameters of mine tremors in the eastern part of the Ruhr-District (West-Germany)', *Journal of geophysics,* 51, 105-112.

Holchin, J. D. and Vallejo, L. E. (1995) 'The Liquefaction of Sand Lenses Due to Cyclic Loading', in *Third International Conferences on Recent Advances in Geotechnical Earthquake Engineering and Soil Dynamics*, St. Louis, Missouri, Missouri University of Science and Technology, 253-259.

Huang, Y., Wen, Z., Wang, L. and Zhu, C. (2019) 'Centrifuge testing of liquefaction mitigation effectiveness on sand foundations treated with nanoparticles', *Engineering Geology,* 249, 249-256.

Humar, J. (2012) *Dynamics of structures,* 3rd ed., CRC Press.

Iai, S. (1989) 'Similitude for shaking table tests on soil-structure-fluid model in 1g gravitational field', *Soils and Foundations,* 29(1)(1), 105-118.

Ishihara, K., Tatsuoka, F. and Yasuda, S. (1975) 'Undrained deformation and liquefaction of sand under cyclic stresses.', *Soils and Foundations,* 15(1)(1), 29-44.

Iwasaki, T. (1986) 'Soil liquefaction studies in Japan: state-of-the-art', *Soil Dynamics and Earthquake Engineering,* 5(1)(1), 2-68.

Jafarzadeh, B. (2004) 'Design and evaluation concepts of laminar shear box for 1g shaking table tests', in *The 13th world conference on earthquake engineering*, Vancouver, BC, Canada,

Jamali, M. (2012) *Effect of Binder Content and Load History on the One dimensional Compression of Williams Mine Cemented Paste Backfill,* Master of Applied Science dissertation: University of Toronto.

James, M., Jolette, D., Aubertin, M. and Bussière, B. (2003) *An Experimental Set-up to Investigate Tailings liquefaction and control measures*, translated by Montréal, QC, Canada.

Japan-guide (2016) 'Meriken Park', [online], available: http://www.japan-guide.com/e/e3552.html 2019].

Jiang, G., Liu, X., Zhang, J. and Zhao, R. (2007) 'Shaking table test of composite foundation reinforcement of saturated silty soil for high speed railway', *Frontiers of Architecture and Civil Engineering in China,* 1(3), 353-360.

Jin, J., Song, C., Liang, B., Chen, Y. and Su, M. (2018) 'Dynamic characteristics of tailings reservoir under seismic load', *Environmental Earth Sciences,* 77(18).

Johnson, D. B. (2015) 'Biomining goes underground', *Nature Geoscience,* 8(3)(3), 165-166.

Kawasumi, H. (1968) *General report on the Niigata Earthquake of 1964,* Tokyo Electrical Engineering College Press, Tokyo, Japan.

Kesimal, A., Yilmaz, E., Ercikdi, B., Alp, I. and Deveci, H. (2005) 'Effect of properties of tailings and binder on the short-and long-term strength and stability of cemented paste backfill', *Materials Letters,* 59(28), 3703-3709.

Kramer, S. (1996) *Geotechnical Earthquake Engineering,* Pren-tice Hall, New Jersey, USA.

Kramer, S. L., Hartvigsen, A. J., Sideras, S. S. and Ozener, P. T. (2011) 'Site response modeling in liquefiable soil; Deposits', in *In 4th IASPEI/IAEE International Symposium: Effects of Surface Geology on Seismic Motion,* University of California Santa Barbara, 13-24.

Kuesel, T. R. (1969) 'Earthquake design criteria for subways', *Journal of the structural division,* ASCE ST6, 1213-11231.

Lade, P. V. and Yamamuro, J. A. (2011) 'Evaluation of static liquefaction potential of silty sand slopes', *Canadian Geotechnical Journal*, 48(2), 247-264.

Lasocki, S. and Orlecka-Sikora, B. (2008) 'Seismic hazard assessment under complex source size distribution of mining-induced seismicity', *Tectonophysics*, 456(1-2), 28-37.

Le Roux, K., Bawden, W. F. and Grabinsky, M. W. (2004) 'Liquefaction analysis of early age cemented paste backfill' in *Proceedings of the 8th International Symposium on Mining with Backfill*, Beijing, China: 19-21.

Li, W. and Fall, M. (2016) 'Sulphate effect on the early age strength and self-desiccation of cemented paste backfill', *Construction and Building Materials*, 106, 296-304.

Li, W. and Fall, M. (2018) 'Strength and self-desiccation of slag-cemented paste backfill at early ages: Link to initial sulphate concentration', *Cement and Concrete Composites*, 89, 160-168.

Lin, F. and Meyer, C. (2009) 'Hydration kinetics modeling of Portland cement considering the effects of curing temperature and applied pressure', *Cement and Concrete Research*, 39(4), 255-265.

Lu, G. (2017) *Modelling the Response of Evolutive Granular Media to Blast Loading: Cemented Tailings Backfill*, Doctoral dissertation, University of Ottawa.

Maltais, Y. and Marchand, J. (1997) 'Influence of curing temperature on cement hydration and mechanical strength development of fly ash mortars', *Cement and Concrete Research*, 27(7)(7), 1009-1020.

Martin, G. R. and Lew, M. (1999) *Recommended procedures for implementation of DMG special publication 117, Guidelines for analyzing and mitigating landslide hazards in California*, The Southern California Earthquake Center, University of Southern California.

McGarr, A. (1971) 'Violent deformation of rock near deep-level, tabular excavations—seismic events', *Bulletin of the Seismological Society of America*, 61(5)(5), 1453-1466.

Milne, W. G. and Berry, M. J. (1976) 'Induced seismicity in Canada', *Engineering Geology*, 10(2-4)(2-4), 219-226.

Moghaddam, A. and Grabinsky, M. F. (2010) 'Monotonic triaxial response of early age cemented paste backfill' in *Proceedings 63rd Canadian Geotechnical Conference & 6th Canadian Permafrost Conference.*, Calgary, AB, Canada: 119-126.

Mohamed, F. M. O. (2014) *Bearing Capacity and Settlement Behaviour of Footings Subjected to Static and Seismic Loading Conditions in Unsaturated Sandy Soils*, Doctoral dissertation: University of Ottawa.

Motamed, R., Sesov, V., Towhata, I. and Anh, N. T. (2010) 'Experimental modeling of large pile groups in sloping ground subjected to liquefaction-induced lateral flow: 1-G shaking table tests', *Soils and Foundations*, 50(2)(2), 261-279.

Nasir, O. and Fall, M. (2010) 'Coupling binder hydration, temperature and compressive strength development of underground cemented paste backfill at early ages', *Tunnelling and Underground Space Technology*, 25(1), 9-20.

Natural Resources Canada (2019) 'Earthquake Reports for 2019', [online], available: http://www.seismescanada.rncan.gc.ca/recent/2019/index-en.php 2019].

Ngadimon, K. (2006) *Design and Simulation of Hydraulic Shaking Table*, Doctoral dissertation: University of Technology.

Obermeier, S., Pond, E. C. and Olson, S. M. (2001) *Paleoliquefaction studies in continental settings: Geologic and geotechnical factors in interpretations and back-analysis*, US Geological Survey.

Okimura, T., Takada, S. and Koid, T. H. (1996) 'Outline of the great Hanshin earthquake, Japan 1995', *Natural hazards*, 14(1)(1), 39-71.

Onur, M. İ. (2018) 'Liquefaction Analysis by Using Laboratory Scale Shaking Table Test Device' in *Proceedings of 3rd International Sustainable Buildings Symposium (ISBS 2017)*, 554-562.

Orense, R. P., Towhata, I. and Chouw, N. (2014) *Soil Liquefaction during Recent Large-Scale Earthquakes*, CRC Press.

Pathak, S. R., Kshirsagar, M. P. and Joshi, M. S. (2013) 'Liquefaction triggering criterion using shake table test', *International Journal of Engineering Technology*, 5, 4439-4449.

Pépin, N., Aubertin, M. and James, M. (2009) *An Investigation of the Cyclic Behaviour of tailings using shaking table tests - effect of a drainage inclusion on porewater development,* translated by Halifax, N.S., Canada.

Peters, J. F. (1991) ' Discussion of "Instability of Granular Materials with Nonassociated Flow" by Poul V. Lade, Richard B. Nelson, and Y. Marvin Ito (December, 1988, Vol. 114, No. 12)', *Journal of Engineering Mechanics,* 117(4)(4), 934-936.

Phillips, D. (2016) 'Samarco dam collapse: One year on from Brazil's worst environmental disaster', *The Guardian,*

Pokharel, M. and Fall, M. (2013) 'Combined influence of sulphate and temperature on the saturated hydraulic conductivity of hardened cemented paste backfill', *Cement and Concrete Composites,* 38, 21-28.

Popescu, R., Prevost, J. H., Deodatis, G. and Chakrabortty, P. (2006) 'Dynamics of nonlinear porous media with applications to soil liquefaction', *Soil Dynamics and Earthquake Engineering,* 26(6-7), 648-665.

Poulos, S. J., Robinsky, E. I. and Keller, T. O. (1985) 'Liquefaction Resistance of Thickened Tailings', *Journal of Geotechnical Engineering,* 111(12), 1380-1394.

Prasad, S. K., Towhata, I., Chandradhara, G. P. and Nanjundaswamy, P. (2004) 'Shaking table tests in earthquake geotechnical engineering', *Current science,* 1398-1404.

Rankine, R. M. and Sivakugan, N. (2007) 'Geotechnical properties of cemented paste backfill from Cannington Mine, Australia', *Geotechnical and Geological Engineering,* 25(4), 383-393.

Rauch, A. F. (1997) *EPOLLS: an empirical method for prediciting surface displacements due to liquefaction-induced lateral spreading in earthquakes,* Doctoral dissertation, Virginia Tech.

Ren, Z., Wang, K., Zhang, Q.-s., Xu, Z.-m., Tang, Z.-g., Chen, J.-p., Yang, J.-q. and Xu, Z.-h. (2018) 'Earthquake dynamic response behavior of Xiangchong valley type tailings impoundment in Yunnan, China', *Journal of Mountain Science,* 15(1), 82-99.

Resourceful Paths (2016) 'Lessons from Samarco Fundao failure and integrated approaches to reduce tailings risk', [online], available:

http://www.resourcefulpaths.com/blog/2016/11/06/lessons-from-the-samarco-fundao-failure-and-integrated-approaches-to-reduce-tailings-risk 2019].

Robertson, P. K. and Campanella, R. G. (1985) 'Liquefaction potential of sands using the CPT', *Journal of Geotechnical Engineering*, 111(3)(3), 384-403.

Rollins, K. M., Oakes, C. and Meservy, T. (2019) 'Liquefaction Mitigation Potential of Prefabricated Vertical Drains from Large-Scale Laminar Shear Box Testing', in *Proceedings of 16th Panamerican conference on soil mechanics and geotechnical engineering*, Cancun, Mexico, IOS Press, 2104-2115.

Saebimoghaddam, A. (2010) *Liquefaction of Early Age Cemented Paste Backfill*, Doctoral dissertation: University of Toronto.

Samui, P., Jagan, J. and Hariharan, R. (2015) 'An Alternative Method for Determination of Liquefaction Susceptibility of Soil', *Geotechnical and Geological Engineering*, 34(2), 735-738.

Scrivener, K. L., Juilland, P. and Monteiro, P. J. M. (2015) 'Advances in understanding hydration of Portland cement', *Cement and Concrete Research*, 78, 38-56.

Seed, H. B. (1982) *Ground motions and soil liquefaction during earthquakes*, Earthquake engineering research insititue.

Seed, H. B. and Idriss, I. M. (1971) 'Simplified procedure for evaluating soil liquefaction potential', *Journal of Soil Mechanics & Foundations Div*, 97(9)(9), 1249-1273.

Seed, H. B. and Idriss, I. M. (1982) *Ground motions and soil liquefaction during earthquakes*, Earthquake Engineering Research Institute. Monograph, Oakland, California.

Seed, H. B., Idriss, I. M. and Arango, I. (1983) 'Evaluation of liquefaction potential using field performance data', *Journal of Geotechnical Engineering*, 109(3)(3), 458-482.

Shahsavari, M., Moghaddam, R. and Grabinsky, M. (2014) 'Liquefaction Screening Assessment for As-placed Cemented Paste Backfill', in *The 67th Canadian Geotechnical Conference.*, Regina, SK, Canada,

Siegler, J., Ravara, A., Pereira, S. and Flynn, B. B. (2016) 'The Samarco Accident in Brazil: Industry and Supply Chain Impacts', in *5th World Production and Operations Management Conference P&OM*, Havana,

Smith, R. B., Winkler, P. L., Anderson, J. G. and Scholz, C. H. (1974) 'Source mechanisms of microearthquakes associated with underground mines in eastern Utah', *Bulletin of the Seismological Society of America*, 64(4)(4), 1295-1317.

Suazo, G., Fourie, A. and Doherty, J. (2017) 'Cyclic Shear Response of Cemented Paste Backfill', *Journal of Geotechnical and Geoenvironmental Engineering*, 143(1).

Taiba, A. C., Belkhatir, M., Kadri, A., Mahmoudi, Y. and Schanz, T. (2016) 'Insight into the Effect of Granulometric Characteristics on the Static Liquefaction Susceptibility of Silty Sand Soils', *Geotechnical and Geological Engineering*, 34 (1)(1), 367-382.

Takahashi, A., Takemura, J., Suzuki, A. and Kusakabe, O. (2001) 'Development and performance of an active type shear box in a centrifuge', *International Journal of Physical Modelling in Geotechnics*, 1(2), 1-17.

Thevanayagam, S., Kanagalingam, T., Reinhorn, A., Tharmendhira, R., Dobry, R., Pitman, M., Abdoun, T., Elgamal, A., Zeghal, M., Ecemis, N. and El Shamy, U. (2009) 'Laminar box system for 1-g physical modeling of liquefaction and lateral spreading', *Geotechnical Testing Journal*, 32(5)(5), 438-449.

Tokimatsu, K. and Seed, H. B. (1987) 'Evaluation of settlements in sands due to earthquake shaking', *Journal of Geotechnical Engineering*, 113(8)(8), 861-878.

Turan, A., Hinchberger, S. D. and El Naggar, H. (2009) 'Design and commissioning of a laminar soil container for use on small shaking tables', *Soil Dynamics and Earthquake Engineering*, 29(2), 404-414.

Tuttle, M., Law, K. T., Seeber, L. and Jacob, K. (1990) 'Liquefaction and ground failure induced by the 1988 Saguenay, Quebec, qrthquakel', *Canadian Geotechnical Journal*, 27(5), 580-589.

U.S. Geological Survey, U. (2000) 'Routine United States Mining Seismicity', [online], available: https://www.usgs.gov/faqs/how-should-i-cite-a-usgs-website?qt-news_science_products=0#qt-news_science_products 2019].

Ueng, T. S., Wang, M. H., Chen, M. H., Chen, C. H. and Peng, L. H. (2006) 'A large biaxial shear box for shaking table test on saturated sand', *Geotechnical Testing Journal*, 29(1), 1-8.

United States Geological Survey (2019) 'Earthquake Glossary - Liquefaction', [online], available: https://earthquake.usgs.gov/learn/glossary/?term=liquefaction 2019].

Unutmaz, B. and Cetin, K. O. (2012) 'Post-cyclic settlement and tilting potential of mat foundations', *Soil Dynamics and Earthquake Engineering*, 43, 271-286.

Wang, L., Chen, G. and Chen, S. (2015) 'Experimental study on seismic response of geogrid reinforced rigid retaining walls with saturated backfill sand', *Geotextiles and Geomembranes*, 43(1), 35-45.

Wang, W. (1979) *Some findings in soil liquefaction*, Earthquake Engineering Department, Water Conservancy and Hydroelectric Power Scientific Research Institute.

Wang, Y., Fall, M. and Wu, A. (2016) 'Initial temperature-dependence of strength development and self-desiccation in cemented paste backfill that contains sodium silicate', *Cement and Concrete Composites*, 67, 101-110.

Wu, A., Wang, Y., Zhou, B. and Shen, J. (2016) 'Effect of Initial Backfill Temperature on the Deformation Behavior of Early Age Cemented Paste Backfill That Contains Sodium Silicate', *Advances in Materials Science and Engineering*, 2016, 1-10.

Wu, D., Fall, M. and Cai, S. J. (2013) 'Coupling temperature, cement hydration and rheological behaviour of fresh cemented paste backfill', *Minerals Engineering*, 42, 76-87.

Wu, J., Kammerer, A. M., Riemer, M. F., Seed, R. B. and Pestana, J. M. (2004) *Laboratory Study of Liquefaction Triggering Criteria*, translated by Vancouver, BC, Canada.

Xu, X., Fall, M., Alainachi, I. and Fang, K. (2020) 'Characterisation of fibre-reinforced backfill/rock interface through direct shear tests', *Geotechnical Research*, 7(1)(1), 1-15.

Yilmaz, E., Belem, T., Bussière, B. and Benzaazoua, M. (2011) 'Relationships between microstructural properties and compressive strength of consolidated and unconsolidated cemented paste backfills', *Cement and Concrete Composites*, 33(6), 702-715.

Yilmaz, E., Belem, T., Bussière, B., Mbonimpa, M. and Benzaazoua, M. (2015) 'Curing time effect on consolidation behaviour of cemented paste backfill containing different cement types and contents', *Construction and Building Materials,* 75, 99-111.

Youd, T. L. (1988) *Screening guide for rapid assessment of liquefaction hazard at highway Bridge Sites*, Multidisciplinary Center for Earthquake Engineering Research (US).

Youd, T. L. and Idriss, I. M. (2001) 'Liquefaction resistance of soils: summary report from the 1996 NCEER and 1998 NCEER/NSF workshops on evaluation of liquefaction resistance of soils.' *Journal of Geotechnical and Geoenvironmental Engineering,* 127(4)(4), 297-313.

Yumlu, M. and Guresci, M. (2007) 'Paste backfill bulkhead monitoring: A case study from Inmet's Cayeli Mine, Turkey', in *In Proceedings of the 9th International Symposium in Mining with Backfill*, Montréal, QC, Canada,

Zhan, Y., Jiang, G. and Yao, H. (2014) 'Dynamic Characteristics of Saturated Silty Soil Ground Treated by Stone Column Composite Foundation', *Advances in Materials Science and Engineering*, 2014, 1-7.

CHAPTER 3 Shaking Table Testing of the Behaviour of Fine-Grained Soils Undergoing Cementation (Paper I)

(Submitted)

Imad Alainachi, Mamadou Fall and Muslim Majeed

3.1 Abstract

Cemented paste backfill (CPB), a man-made soil undergoing cementation, is extensively applied for mine support and/or tailings management. Cyclic loading-induced liquefaction potential of CPB structures is a key concern in underground mine backfilling operations. Failures of CPB structures can lead to injuries and/or fatalities and have significant financial ramifications for a mine. However, no studies have addressed the CPB liquefaction by using the shaking table technique. This manuscript presents new findings of assessing the cyclic behaviour of hydrating CPB by using a shaking table. CPB mixtures were prepared and poured into a flexible laminar shear box and cured to different times. Numerous parameters (e.g., pore water pressure, horizontal and vertical displacement, acceleration, temperature, electrical conductivity, etc.) were monitored before, during, and after shaking. Microstructural evolution of CPB was also studied. Cyclic loading was applied using a 1-D shaking table. Obtained results indicate that CPB cured to 2.5 hrs can be prone to liquefaction under the studied conditions. However, CPB samples cured to 4.0 and 10.0 hrs are resistant to liquefaction. These results provide a better comprehension of cyclic behavior of natural or man-made soil undergoing cementation and the design of more cost-effective and safer CPB structures.

Keywords: Cemented paste backfill; Liquefaction; Shaking table; Earthquake; Tailings; Mine

3.2 Introduction

Mining is one of the worldwide industries that has highly influenced the evolution and development of human societies. It has significantly contributed to the economy and effectively impacted the development of several regions and countries around the world. In Ontario (Canada), for instance, mining produces around $10 billion of revenues every year (Dungca et al. 2006, Ontario Mining Association 2017). However, it is known that ore extraction during mining activities may negatively impact the environment because of the production of huge quantities of solid waste (e.g., tailings, which are human-made soils generated by mining activities). The surface disposal or management of these tailings was found to be a potential source of environmental (e.g., generation of acid mine drainage) and geotechnical (e.g., tailings dam failure) hazards. Moreover, mining extraction also creates large underground voids (stopes) that expose the surrounding areas to many geotechnical engineering problems, such as ground subsidence. Furthermore, the

instability of these underground openings can jeopardize the safety of the mining workplace and the surrounding public agglomeration (Kesimal et al. 2005, Jamali 2012).

To enhance the short and long-term stability of these underground mine openings or stopes, and to guarantee the safety of the mine workers and the neighboring areas as well as to manage the aforementioned tailings in more environmental friendly and safer way, a mixture of tailings (predominantly made of silt-size particles), water and binders has been extensively used over the past few decades as the main supporting agent in underground mining operations and as a novel tailings management method around the world. This mixture is named cemented paste backfill (CPB) (Fall et al. 2005, Saebimoghaddam 2010, Abdul-Hussain and Fall 2012). From a geotechnical point of view, CPB is a fine-grained (silt) soil undergoing cementation.

The typical CPB mixture is prepared with a 70% - 85% of tailings, fresh or mine-processed water, and often 3% - 7% (by total weight of solid) of hydraulic binder (usually cement). These ingredients are prepared in paste backfill plant commonly situated on the mine surface and then pumped into the mine stope (Ercikdi et al. 2009b, Yilmaz et al. 2015, Aldhafeeri and Fall 2016). Using CPB in mine stopes backfilling is now a common practice in many mines worldwide, as it can be produced and delivered to the mine stope in a short period. This helps to complete the stope backfilling process (stope cycle) in a matter of days, while it might take weeks or months with older backfilling methods. Besides binder cost saving, decreasing stope cycle time allows additional revenue to be generated (Ercikdi et al. 2009a, Thompson et al. 2009).

However, early aged CPB placed in a mine stope can be susceptible to several geotechnical engineering issues, such as mechanical instability, when it is exposed to static loadings, as well as liquefaction, when it is exposed to dynamic loadings, such as seismic events or blast loadings. Failure of CPB in mine stopes may cause injuries and/or fatalities to mining workers, beside the significant economic consequences for the mine and its related operations (Poulos et al. 1985, Fall and Samb 2008, Abdelaal 2011, Becker et al. 2014). Therefore, understanding and assessing the mechanical stability of CPB structures under static loadings conditions as well as liquefaction potential of CPB under dynamic loading conditions at early ages is critically important for an efficient and safer design of CPB structures.

Most of the previous studies on mechanical stability of early aged CPB focused on static loading conditions (e.g. Thompson et al. 2009, Nasir and Fall 2010, Li and Aubertin 2012, Ghirian and Fall 2016a). There is a paucity of studies (Lu and Fall 2017, Saebimoghaddam 2010) on the behaviour and liquefaction potentials of early aged CPB under dynamic loading conditions, particularly cyclic loadings. There is a need to increase our understanding of the behaviour and liquefaction potential of early age CPB subjected to cyclic loadings since seismicity is common in underground mining activities.

CPB structures in underground mine cavities can be exposed to various sources of seismic loadings. These seismic loadings can originate from natural earthquake or commonly from mining-

induced seismic events. There are numerous sources of mining-induced seismic events, including fault slip (earthquake), rockburst, bump, pillar burst and outburst, pillar punching, disruption of geological features from active longwall mining, failure of overburden strata and phenomena of coal bursts (Hasegawa et al. 1989, Ahn et al. 2017). Moreover, the rate of occurrence and seriousness of mine-induced seismic events tend to rise with a growing rate of volume extraction and depth of mining (Hasegawa et al. 2009). Thus, the gradual reduction of ore available at shallow depths in many underground mines in several regions of the world in combination with a growing rate of volume extraction indicates that underground mining operations are more and more being accomplished at greater depths and with greater volume, and thus at more severe and/or frequent seismic events. This would suggest that CPB structures will be increasingly subjected to more frequent and severe seismic loadings, which could increase liquefaction potential risk of CPB structures at early ages. There is a common consent that earthquake characteristics, such as peak horizontal ground acceleration and shaking duration (number of loading cycles) significantly affect the behavior of liquefiable material (Carter 1988). It was also found that soil might liquefy if it was exposed to an earthquake of peak ground acceleration as low as 0.05g (James et al. 2003).

A shaking table has been commonly used in engineering practice to assess and understand the response of geomaterials and engineering structures to seismic loadings for many decades despite its limitations (e.g., difficulty in reproducing or simulating the in situ stress, high cost) (Moncarz and Krawinkler 1981, Bairro and Vaz 2000, Ngadimon 2006, Ghirian and Fall 2016b). The extensive utilization of shaking table experiments in geotechnical engineering studies is due to its facility to adopt different testing conditions. For instance, a shaking table can function either in one direction or multi directions of loading input, and the user is able to control and measure the cyclic load factors (amplitude and frequency). Also, it can be conducted on many types of soil under different saturation conditions (dry, unsaturated or saturated). Numerous shaking table tests were conducted in the previous decades to evaluate the behaviour and liquefaction potential of natural soils subjected to seismic loadings (Bairro and Vaz 2000, Prasad et al. 2004, Ueng et al. 2006, Mohamed 2014, Guoxing et al. 2015, Wang et al. 2015), whereas only few studies were conducted to assess the seismic or cyclic behaviour of tailings (without cement) by using shaking tables (James et al. 2003, Pépin et al. 2009, 2012a, 2012b, Özgen et al. 2011). These studies have significantly contributed to understanding the behaviour of natural soils and tailings without cement when subjected to cyclic loadings. However, no investigations have been performed to assess the behaviour and liquefaction potential of tailings undergoing cementation under cyclic loadings by using a shaking table. Accordingly, this study aims to use the shaking table technique to assess the geotechnical behavior and response, particularly liquefaction potential, of hydrating CPB at early ages during cyclic loadings.

3.3 Materials and Equipment Used in the Experiment

3.3.1 Materials

Synthetic tailings material (manufactured by the U.S. Silica Co.) made of ground silica, which is known as Silica Tailings (ST), was used in this study as the main component of CPB mixtures. Silica Tailing (ST) is characterized by its grain size distribution, which is comparable to the average grain size distribution of nine mine tailings (9MT) extracted from nine different mines in eastern Canada (Figure 3.1). The minerals of the ST are principally constituted of quartz, which is the predominant mineral in Canadian hard rock mine tailings. The high percentage of silica (99.8% SiO2) makes the ST a chemically inert material. Therefore, ST was selected in this study to reduce the uncertainties associated with the use of natural tailings to a minimum level by minimizing/controlling the potential chemical interactions of the tailings with other ingredients in the CPB mixture (Carraro et al. 2009, Fall et al. 2010, Aldhafeeri and Fall 2016, Haiqiang et al. 2016). The physical properties of the tailings used in this study are illustrated in figure 3.1 and table 3.1.

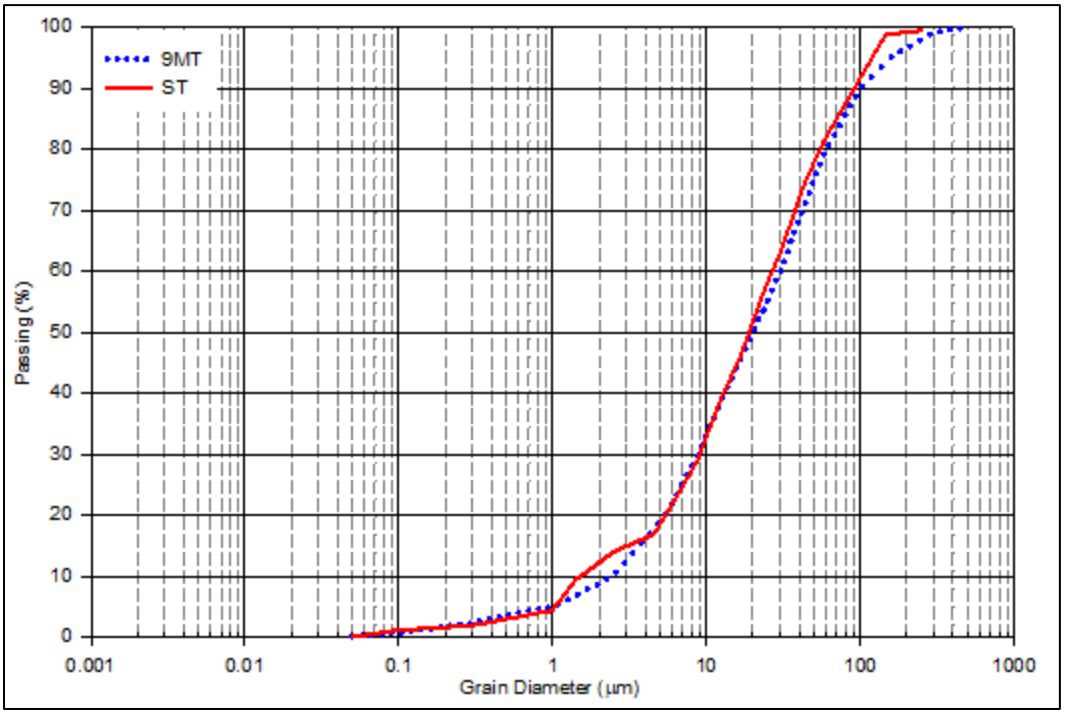

Figure 3.1 Average grain size distribution of tailings extracted from nine Canadian mines (9MT) vs the grain size distribution of the silica tailing (ST).

To improve the mechanical properties of CPB, sufficient amounts of binder, such as Portland cement (PC), are usually added to a mixture of tailings and water. In this study, the binder agent used in the preparation of CPB mixtures is Portland cement type I (PCI) (Table 3.2), which is the most frequent binder used in the preparation of CPB worldwide. Tap water was used as mixing water.

Table 3.1 Primary physical properties of the tailings

Tailings	Gs	D_{10} (μm)	D_{30} (μm)	D_{50} (μm)	D_{60} (μm)
ST	2.7	1.9	9.0	22.5	31.5

Table 3.2 Primary physical and chemical properties of the Portland cement type I (PCI)

Gs	SSA* (m^2/g)	S (wt%)	Ca (wt%)	Si (wt%)	Al (wt%)	Mg (wt%)	Fe (wt%)	Si/Ca
3.15	1.32	1.5	44.9	8.4	2.4	1.6	1.9	0.2

* Specific Surface Area

3.3.2 Preparation of Paste Backfill Mixture

CPB specimens were prepared by mixing tailings with PCI (4.5 wt%) and water, in which the water-cement ratio (w/c) is equal to 7.6. Samples were mixed for 10 min to obtain a homogenous mixture. The slump of the prepared backfill mixture was 18 cm, which is one of the most frequent slump values used in paste backfill operations in Canadian mines. ASTM C143/C143M-15a (2015) was followed for the slump test procedure. The degree of water saturation (S) of the prepared CPB was determined to be equal to 100%.

Afterward, CPB mixtures were poured into the developed laminar shear box (described below). To avoid changes of water content due to evaporation, laminar shear box with CPB mixtures were sealed and kept in a room with stable temperature (~ 20^oc) for curing until reaching the testing ages according to the testing program described in section 3.4.

3.3.3 Shaking Table

To represent the motion of the tested CPB during an earthquake, the shaking table of the University of Ottawa (Figure 3.2) was used in this research. This shaking table consists of a base, a ~1200 mm × ~1060 mm platform, and steel C-channels between them. This table provides a series of one-dimensional (longitudinal) sinusoidal cyclic motions with one degree of freedom of horizontal displacement. This shaking table is driven by a hydraulic actuator and runs in the range of 1 to 17 Hz. The maximum base shear capacity and displacement limit of this table are 27 kN and 120 mm, respectively (Mohamed 2014).

To study the cyclic response of CPB using the shaking table, a Flexible Laminar Shear Box (FLSB) (Figure 3.3) was designed for this research and constructed at the Faculty of Engineering of the University of Ottawa.

The FLSB consists of 30 horizontal laminas made of aluminum alloy box sections of 31.7 mm × 31.7 mm. The inner dimension of each lamina is 750 mm × 750 mm, and the clearance spacing between lamina was arranged to be 2 mm to ensure the independent movement of each

lamina. Accordingly, the total capacity of the assembled FLSB is 750 mm × 750 mm (in plan) and 1,000 mm (in depth).

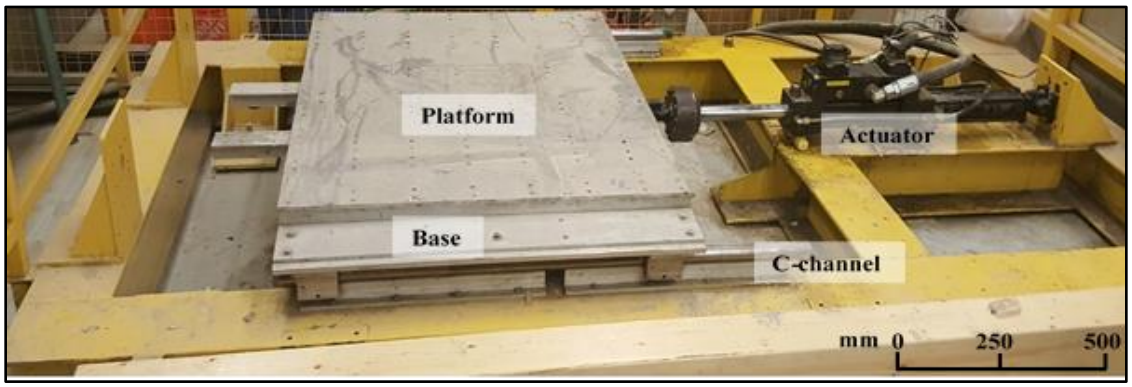

Figure 3.2 Shaking table used in this study

Figure 3.3 Flexible Laminar Shear Box (FLSB) developed and built for this study

A flexible membrane (made of polyethylene) was placed inside the FLSB to contain/hold the CPB mixture. This membrane has a high flexibility with a maximum thickness of 0.5 mm. Thus, the membrane shows no (or negligible) effect on the movement of the FLSB (Mohamed, 2014). The FLSB and the membrane were securely attached to the platform of the shaking table. The prepared CPB mixture was poured inside the FLSB. The final dimension of the CPB sample to be tested was 750 mm × 750 mm × 700 mm.

Various instruments or sensors were installed at different levels in the model (the FLSB and its content) as shown in figure 3.4 (A and B) and described below:

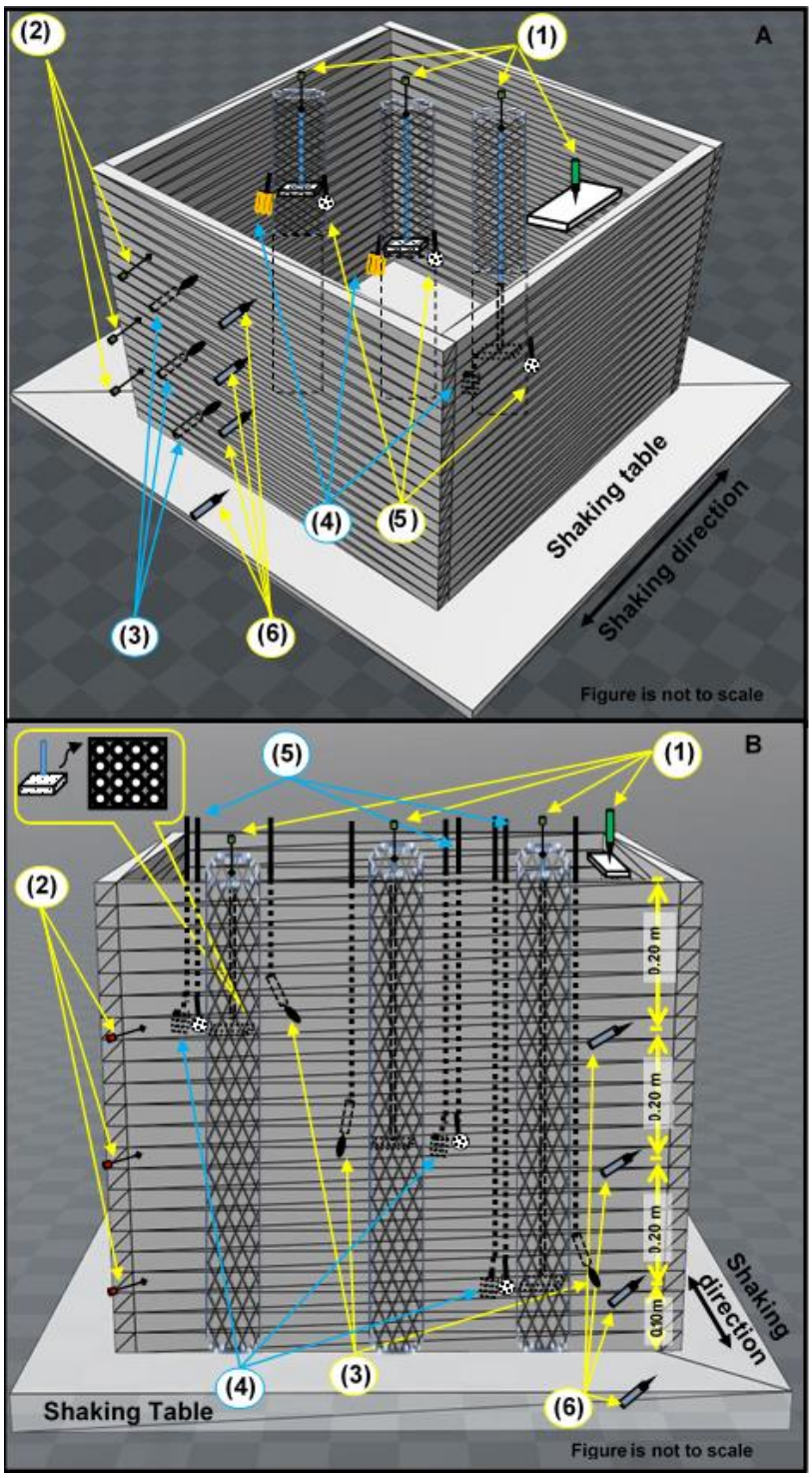

Figure 3.4 Schematic view of the FLSB and instruments locations (A) 3D Sketch, (B) 2D Sketch. (1) Vertical displacement transducers, (2) Horizontal displacement transducers, (3) P.W.P. transducers, (4) VWC/EC/Temp. sensors (5) Suction sensors, and (6) Accelerometers.

- Vertical Displacements Transducers: (**Item 1** in figure 3.4)

a. Linear variable differential transformer (LVDT) to monitor the vertical displacement of the surface of the CPB sample. In this regard, HCD-1000 LVDTs of 25.4 mm range were used.

b. Cable transducers (CTs) to monitor the vertical displacement at various depths of 0.20 m, 0.40 m and 0.60 m from top of the sample (0.5 m, 0.3 m, 0.1 m, respectively from the shaking table). These CTs were attached to thin metal rods connected to 20 mm thick, 20 mm × 20 mm, lightweight, perforated plastic plates that were installed at the three different depths within the sample. These plates were perforated to minimize their displacement due to seepage pressure. These metal rods were installed within cylindrical guidance towers (made of thin metal mesh sheets) to avoid unwanted movement/tilting of these metal tubes during the shaking process. Guidance towers were connected to the shaking table to avoid being a reinforcement factor and to allow the whole system to follow the same motion rhythm (Figure 3.5). The transducers that were used in this regard were Celesco SP2-12 compact string with 317 mm range.

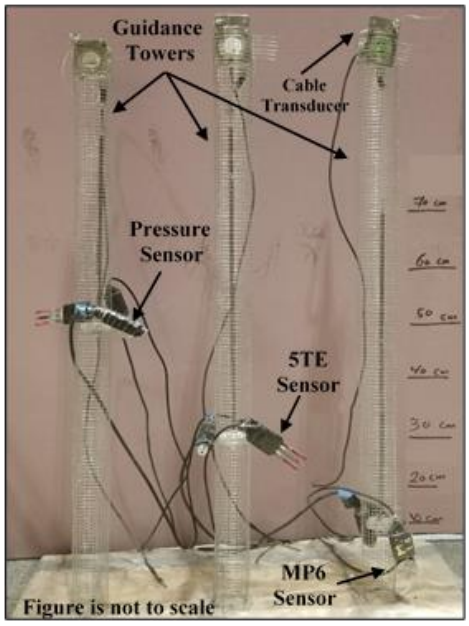

Figure 3.5 Guidance towers and related instrumentation setup

- Horizontal displacement (HD) transducers: Cable transducers (CT) to monitor the horizontal displacement of the CPB sample at different depths (0.20 m, 0.40 m and 0.60 m from top of the sample). These transducers were attached to the outside of the FLSB at the depth-related laminas (**Item 2** in figure 3.4). The same type of transducers as in (a) were used in this regard.

- P.W.P transducers: To monitor the changes in pore-water pressure during the dynamic load, pressure transducers were placed at different depths (0.20 m, 0.40 m and 0.60 m from top of the

sample) of the sample inside the FLSB (**Item 3** in figure 3.4). PX309 series pressure transducers with range of -15 to +15 PSI and ±0.25% static accuracy was used in this regard.

- VWC/EC/Temp. sensors: To monitor the changes in electrical conductivity (EC), the volumetric water content (VWC) and temperature, the ECH2-5TE sensor was used. This sensor determines electrical conductivity (EC) in the range of 0-23 dS/m with the accuracy of ±0.1. It measures volumetric water content (VWC) in the range of 0-80% with the accuracy of ±0.15% from 40-80 (VWC), whereas the temperature measurement accuracy is ±1°C. These sensors were placed at different depths (0.20 m, 0.40 m and 0.60 m from top of the sample) within the sample (**Item 4** in figure 3.4). Changes in EC give information about the rate of ion migration due to the chemical reactions between cement and water. Monitoring EC is a powerful way to assess the cement hydration progress and the related structural changes (Li and Fall 2016). On the other hand, monitoring the VWC enables assessment of the self-desiccation of CPB (capillary water consumed by the cement hydration) as well as the water flow within the CPB mass. Monitoring of the temperature provides valuable information about the progress of the cement hydration.

- Suction Sensors: Dielectric water potential sensors (ECH2-MPS6 sensors) that were designed to measure soil water potential were used to monitor the suction development with time during the CPB curing duration (**Item 5** in figure 3.4). These sensors were placed at different depths (0.20 m, 0.40 m and 0.60 m from top of the sample) within the sample. Measurement range of these sensors are -9 to -100,000 kPa with a resolution of 0.1 kPa, and its accuracy is ±10% of reading + 2 kPa, from -9 to -100 kPa. The monitoring of suction also enables assessment of the self-desiccation of CPB.

- Accelerometers: To measure/maintain the shaking acceleration, four Endevco – 7593A accelerometers of ±2g full-scale range and frequency response of 0 – 50 Hz were used in this regard (**Item 6** in figure 3.4); one was attached to the shaking table to monitor its acceleration. The other three accelerometers were attached to the external side of the box at different depths (0.20 m, 0.40 m and 0.60 m from top of the sample).

The pressure transducers, 5TE and MPS6 sensors were connected to the guidance towers to avoid any changes on their positions. VD transducers, HD transducers, P.W.P. transducers and accelerometers were connected to signal conditioning and Data Acquisition Systems (DAQS). Also, 5TE and MP6 sensors were connected to Decagon Em50 series data loggers. DAQS and Em50 were connected to a computer to record/analyze the required data at almost (1 sec) intervals during shaking and (10 min) intervals before and after shaking. Furthermore, a digital camera was used to record each step of the testing program (mixing, installation and shaking operation).

3.4 Testing Program and Procedure

The main goal of the testing program is to assess the effect of the progress of cement hydration on the behaviour of CPB during shaking or cyclic loading. The experimental testing program carried out in this study is summarized in figure 3.6 and table 3.3 and discussed below.

3.4.1 Shaking Table

3.4.1.1 Cyclic parameters and test conditions

Prior to conducting a shaking table test, the cyclic parameters or test conditions need to be determined in order to simulate a cyclic event. These parameters include Sinusoidal Loading Frequency (SLF), Shaking Peak Horizontal Acceleration (SPHA), Horizontal Displacement Amplitude (HDA), and Shaking Duration (SD).

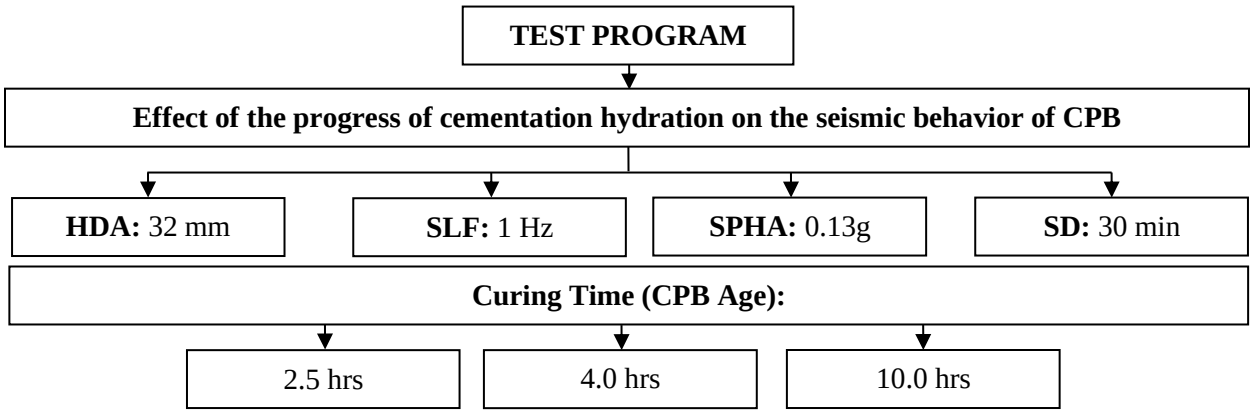

Figure 3.6 Flow chart of the experimental program and testing conditions

Due to experimental limitations (e.g., the maximum capacity of the shaking table, and the sensitivity/limitation of the used monitoring instruments), values of these parameters were modified to accommodate these limitations, although they might not reflect the real situation of a seismic event. However, this type of process is often used in liquefaction research (Ishihara 1996). Thus, shaking table tests were conducted in this study using a dynamic load that was applied in a one-dimensional signal, a uniform amplitude, and at constant frequency.

Table 3.3 Summary of the testing program

Test	Material	Age (hrs)	HDA (mm)	SLF (Hz)	SPHA	SD (min)	PLMD (hrs)
1	CPB	2.5	32	1	0.13g	30	24
2	CPB	4	32	1	0.13g	30	24
3	CPB	10	32	1	0.13g	30	24

HDA : Horizontal Displacement Amplitude **SLF** : Sinusoidal Loading Frequency
SPHA : Shaking Peak Horizontal Acceleration **SD** : Shaking Duration
PLMD : Post Loading Monitoring Duration

Sriskandakumar (2004) found that the value of the loading frequency applied in laboratory seismic tests has a slight influence on the dynamic response of the tested materials. Moreover, Srilatha et al. (2013) concluded that the seismic response of tested material is almost similar at

frequencies less than 7 Hz. Thus, shaking table tests were performed in this study using a sinusoidal loading of 1 Hz frequency. Although the typical frequencies range of many recorded earthquakes in Canada is relatively higher (Nuttli 1973), this selection was made so the models will not be subjected to resonance (Srilatha et al. 2013) and to accommodate the above stated limitations.

On the one hand, the strongest ground motion related to mining events in northeastern Ontario (Canada) was recorded in 2006 with a value of 0.0027g (Atkinson et al. 2008, Saebimoghaddam 2010, Natural Resources Canada 2019). On the other hand, the Saguenay earthquake 1988 in Quebec (Canada) was recorded to have a ground acceleration value of 0.13g (Tuttle et al. 1990). Many studies indicated that tailings may liquefy when they are exposed to a ground motion with peak horizontal ground acceleration that exceeds 0.05g (Carter 1988, James et al. 2003). Hence, the peak ground acceleration in this study was selected to be equal to the acceleration of the Saguenay earthquake 1988 in Quebec.

The maximum displacement of the simulator (deformation amplitude) can be determined using equations (3.1-3.3) (Douglas 2003, Chopra 2005), which are based on the values of loading frequency and peak ground acceleration. Thus, the displacement amplitude used in the tests conducted in this study was calculated to be 32 mm.

$$a = \omega^2 . A \tag{3.1}$$

$$\omega = f . (2\pi) \tag{3.2}$$

$$f = 1/T \tag{3.3}$$

where a and A are the peak ground acceleration and deformation (displacement) amplitude, respectively, ω and f are the radial and circular loading frequency (number of cycles per second), respectively, and T is the loading cycle time (Douglas 2003, Chopra 2005).

Although recorded earthquakes or mine seismic events do not last very long (Natural Resources Canada 2019), the cyclic loading (shaking) in this study is carried out for 30 minutes (1800 seconds) as shown in Table 4. The duration of the dynamic loading in this study is not meant to be representative of the actual duration of earthquakes or mine seismic events. A duration of 30 minutes was used to allow good observation of the dynamic behaviour of the CPB samples and relative comparisons of their response, which is important for the future development of a constitutive model to describe the dynamic response of soils undergoing cementation. Moreover, according to (Pépin et al. 2012b), who investigated the cyclic response of tailings (without cement) using a shaking table approach, the selected shaking duration depends on the material response towards liquefaction (reaching peak excess pore-water pressure). In their study, 1,000 sec. was found to be a suitable shaking duration to reach cyclic peak of liquefaction of tailings without inclusions. They also found that another 1,000 sec of monitoring after shaking is required to obtain the full response of pore-water pressure dissipation. They also concluded that adding inclusions (e.g., blocks of rocks) in tailings would reduce the development of excess pore-water pressure

during shaking (to around 1,700 sec) and accelerate the excess pore-water pressure dissipation after loading. Accordingly, and as the material used in this study is cementing tailings (CPB mix), shaking duration was selected to range from 1 min to 30 min (60 – 1,800 cycles) depending on material response, and the post loading monitoring duration (PLMD) to continue (depending on material response) for additional 24 hr.

3.4.1.2 Effect of the progress of cementation hydration on the cyclic behavior of CPB

To evaluate the cyclic behavior of young CPB under cyclic conditions, and to assess the effect of cementation hydration progress on this behavior, it was important to apply cyclic loadings (dynamic load) on CPB samples of various ages. Thus, CPB mixtures (poured in FLSB) were securely sealed and kept for curing under a stable temperature of 25°C. Then, a series of shaking table tests were conducted on CPB models that were cured at various ages of 2.5 hrs, 4.0 hrs, and 10.0 hrs (see Figure 3.6).

Table 3.4 Selected cyclic parameters used in the present study and previous studies

Parameter	Values used in previous studies [a]	Values used in the present study
Horizontal Displacement Amplitude	10 - 80 (mm)	32 (mm)
Shaking Peak Horizontal Acceleration	0.1g – 1.0g	0.13g
Sinusoidal Loading Frequency	0.1 - 50 (Hz)	1 (Hz)
Shaking Duration [b]	3 – 2,000 (sec)	1,800 (sec.)
Post loading Monitoring Duration	15 (min) – 36 (hr)	24 (hr) [c]

[a] Such as (James et al. 2003, Prasad et al. 2004, Ueng et al. 2006, Pépin et al. 2009, 2012a, 2012b, Özgen et al. 2011, Mohamed 2014, Guoxing et al. 2015).

[b] Depends on the material response

[c] After initial casting

3.4.2 Microstructural Analysis

To understand the effect of microstructural evolution of CPB on its cyclic behavior, microstructural analyses were performed on cement paste samples of CPB cured at different ages. Microstructural analyses include X-ray diffraction (XRD) and thermal analysis (differential thermogravimetry (DTG), thermal gravimetry (TG)). Before conducting microstructural analysis, testing samples were first dried at 45 °C in a vacuum oven up to mass stabilization. Thermal analyses were performed using a TGA Q 5000 IR from TA Instruments. The different (dried) samples (about 20 mg each) were heated in an inert nitrogen atmosphere at the rate of 10°C per minute up to a temperature of 1000°C. The XRD tests were conducted using a Rigaku ultima IV diffractometer that is equipped with cross beam optics.

3.5 Results and Discussion

3.5.1 Acceleration and Lateral Deformation

In this section, the results of acceleration and lateral deformation (horizontal displacement) at different depths within each tested CPB model are presented with respect to curing time (which reflects the degree of cementation). The combined results of these two parameters can give an indication of the shear resistance of the tested material at different depths (Takahashi et al. 2001, Nouri et al. 2006, 2008).

3.5.1.1 Acceleration

Figure 3.7(a-c) shows the peak acceleration histories at different depths during the shaking event for CPB models cured (aged) for 2.5 hrs, 4.0 hrs, and 10.0 hrs, respectively. This figure indicates that the curing time or degree of cementation (progress of the cement hydration) and the depth have an impact on the measured acceleration values. It can be seen that CPB samples cured for a longer time display higher peak acceleration values than CPB samples cured for a shorter time, which is more obvious at shallow depths. The recorded acceleration significantly varied with depth for the models tested at early age (2.5 hrs), while the variation of acceleration with depth was low and insignificant (negligible) for models tested at later ages: 4.0 hrs and 10.0 hrs, respectively. For instance, the peak acceleration of the CPB sample cured to 2.5 hrs (Figure 3.7a) was between 0.10g and 0.125g at 60 cm depth (10 cm above the shaking table), around 0.08g - 0.10g at 40 cm depth (30 cm above the shaking table), as low as 0.04g – 0.08g at 20 cm depth (50 cm above the shaking table). On the other hand, for the CPB model cured to 4.0 hrs, the peak acceleration (Figure 3.7b) at depths 60 cm, 40 cm, and 20 cm was recorded to be around 0.115g – 0.125g, 0.100g – 0.110g, and 0.090g – 0.100g, respectively. For the CPB model cured to 10.0 hrs, the peak acceleration at all depths was around 0.125g – 0.130g. This decrease of the peak acceleration as the age or curing time of CPB decreases can be attributed to the effect of the degree of cementation on the damping ratio. Previous studies (e.g. Acar and El-Tahir 1986, Yang and Woods 2015) have concluded that the (higher) degree of cementation reduces the damping ratio. This means that the CPBs cured for a longer curing time will have a lower damping ratio, since longer curing time is related to greater degree of cementation (cement hydration degree) as evidenced by figures 3.17 and 3.18 and discussed later. The progress of cement hydration increases the bonds between tailings (soil) particles and consequently reduce the deformation level of the material (Mamlouk and Zaniewski 2011). The observed significant alteration (reduction) of the acceleration values with the diminution of the depth in the CPB cured for 2.5 hrs can be attributed to nonlinearity and stiffness degradation of CPB caused by liquefaction as evidenced by the liquefaction analysis results presented in section 3.5.3. Excessive increase of the pore water pressure or liquefaction causes a large deformation of the CPB cured for 2.5 hrs, in which the cementation effect is still weak due to the lower cement hydration degree (see Figures 3.17 and 3.18). The larger the deformation is, the greater the damage of the CPB pore structure. Moreover, the greater the dislocation and slip between the CPB particles (tailings, unreacted cement grains) are, the greater the friction between particles is, and the greater the material damping ratio would be; in other words, the greater would

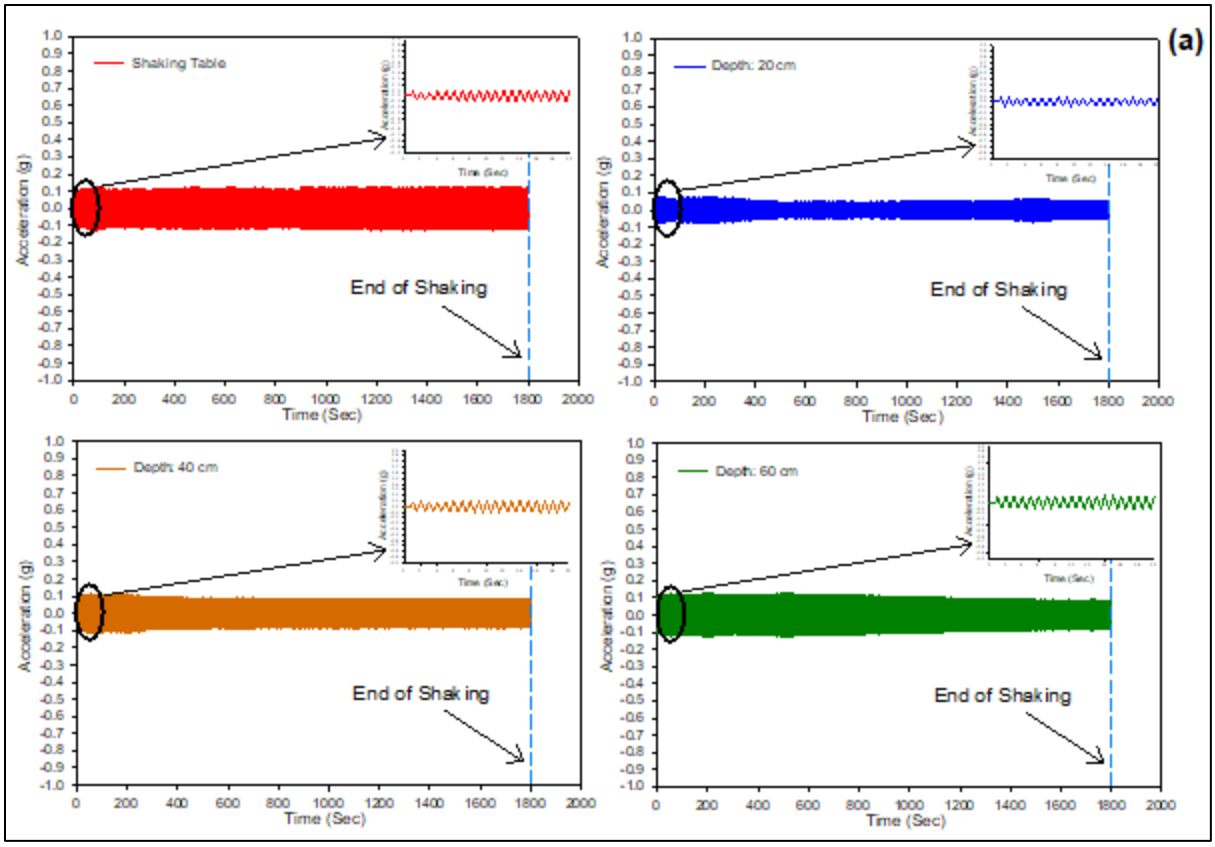
(a)
Shaking Table
Depth: 20 cm
Depth: 40 cm
Depth: 60 cm
End of Shaking
Acceleration (g)
Time (Sec)

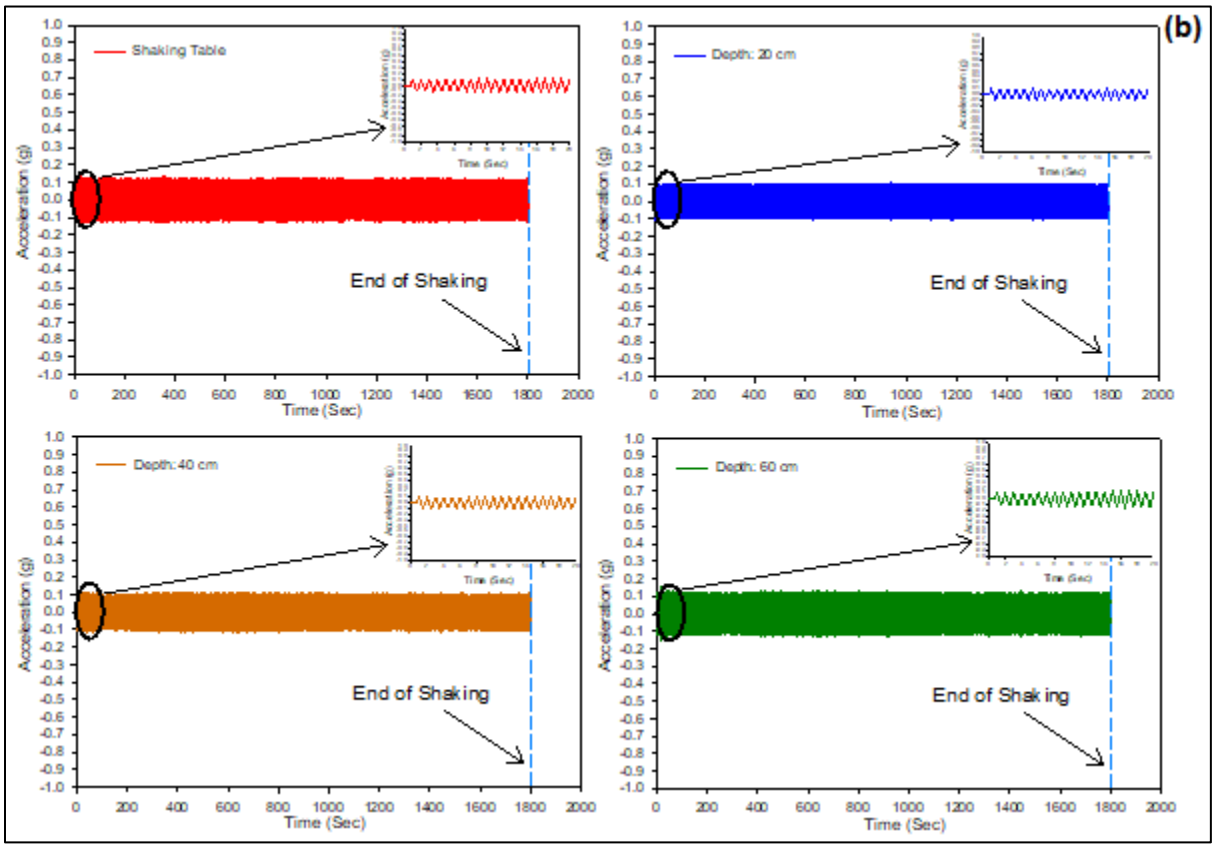
(b)
Shaking Table
Depth: 20 cm
Depth: 40 cm
Depth: 60 cm
End of Shaking
Acceleration (g)
Time (Sec)

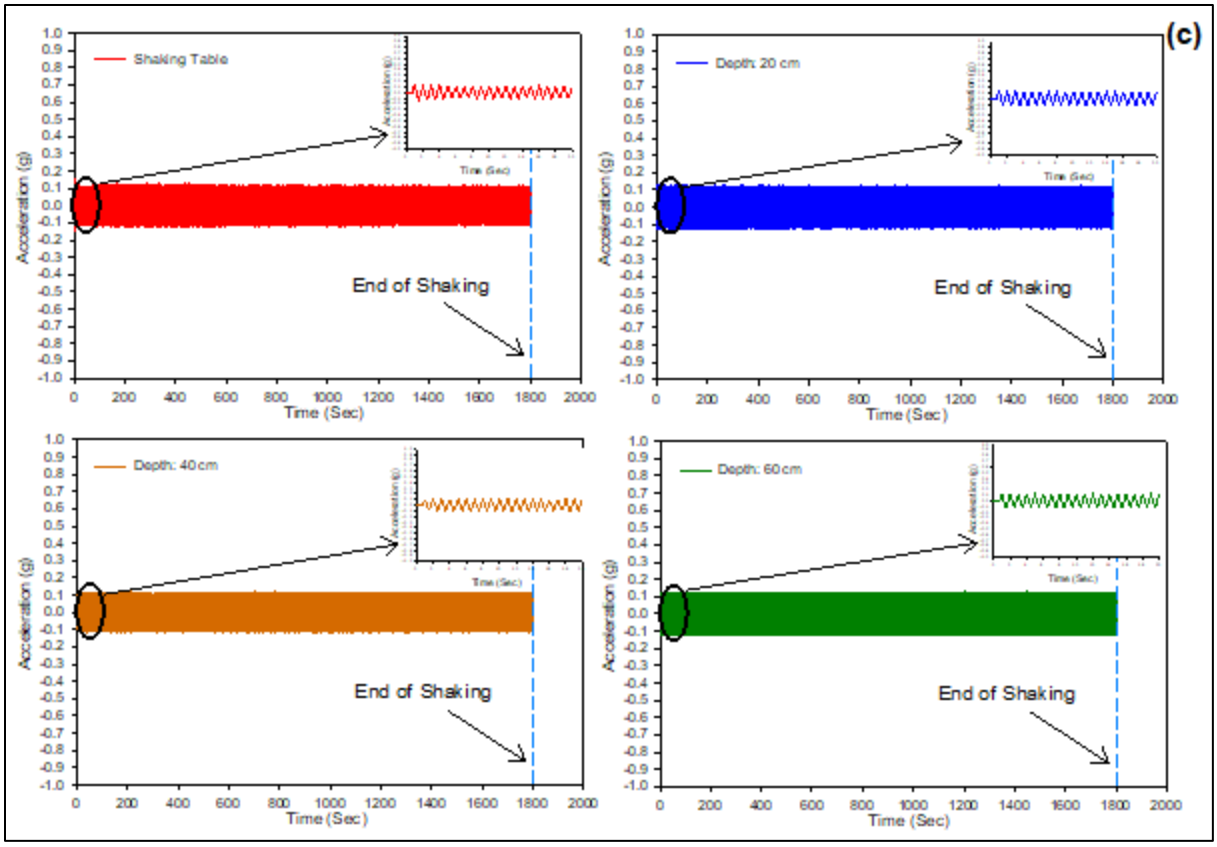

Figure 3.7 Measured peak acceleration histories at different depths vs time for CPB samples cured to different times: (a) 2.5 hrs; (b) 4.0 hrs and (c) 10.0 hrs.

be the decrease of the acceleration value. This assertion and explanation are consistent with the results of displacement monitoring as well as with the determination of effective stress and excess pore-water pressure ratio as discussed later.

3.5.1.2 Lateral (horizontal) displacement

Lateral (horizontal) displacement within liquefiable soils may refer to the deformation of the structure of these soils as a result of shaking-induced liquefaction. This tendency can be attributed to the fact that the ground vibration destabilizes the contact between soil particles, which will lead to a reduction of soil resistance against shaking (Takahashi et al. 2001, Dungca et al. 2006). Figure 3.8(a-c) illustrates the lateral displacement at various depths during the cyclic loading durations for CPB models cured (aged) for 2.5 hrs, 4.0 hrs, and 10.0 hrs, respectively.

Two key behaviors can be observed from these figures:

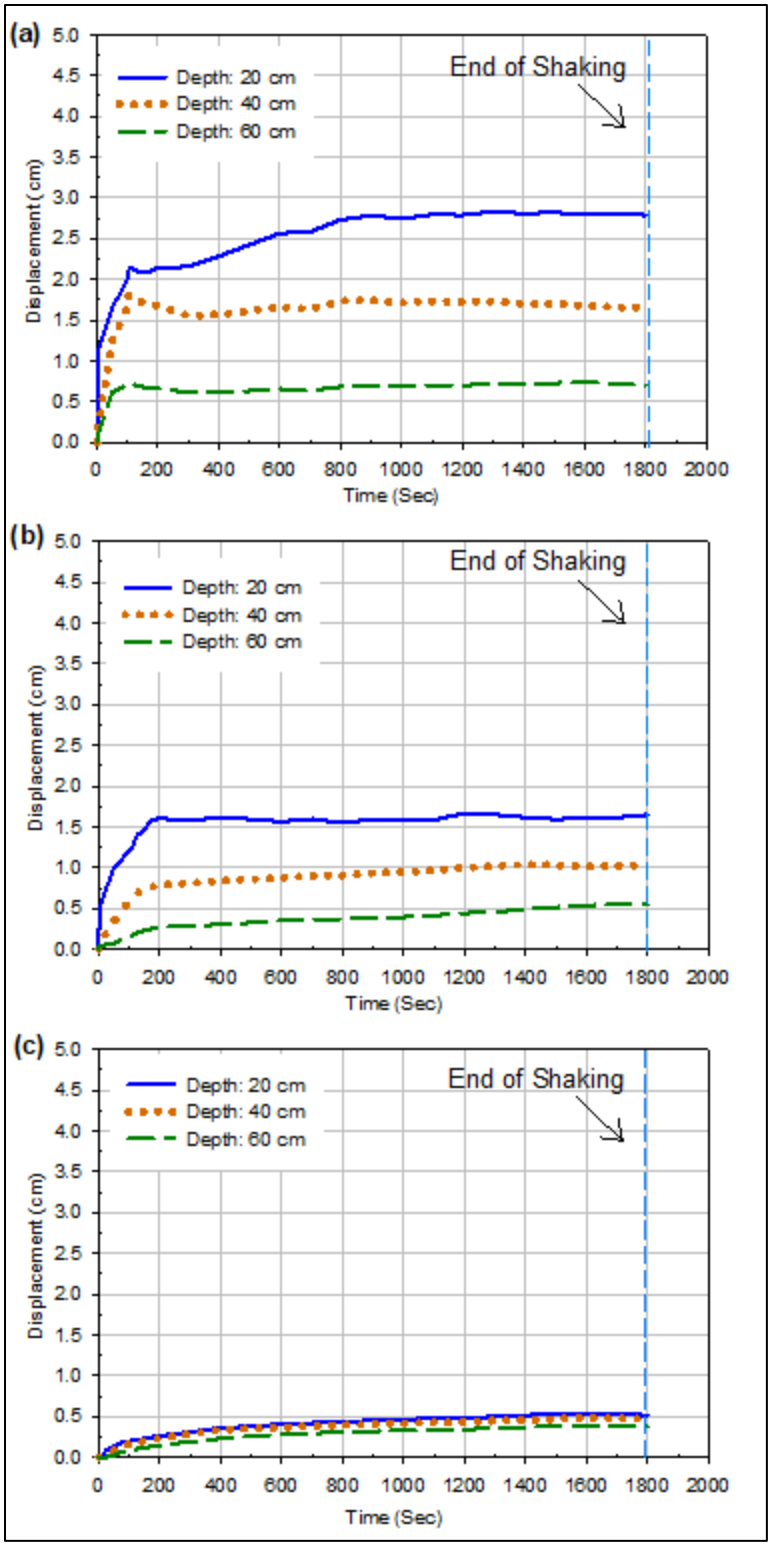

Figure 3.8 Lateral displacement histories at different depths vs times for CPB samples cured to different times: (a) 2.5 hrs; (b) 4.0 hrs and (c) 10.0 hrs.

(a) In all models, the lateral displacement decreased with the increase in depth. This behavior is consistent with the conclusions of several past investigations (e.g. Motamed et al. 2013, Srilatha et al. 2013). This relationship can be attributed to the shaking-induced increase in material density due to the dynamic densification (compaction) of the tailings particles (Zhu and Clark 1994, Anastasopoulos et al. 2010). However, the change in displacement with depth within the CPB model cured to 2.5 hrs was higher than the variation in displacement with depth within the CPB model cured to 4.0 hrs. Moreover, there was a negligible variation in displacement with depth within the CPB model cured to 10.0 hrs. This reduction is related to the CPB solidification due to progress of the cement hydration with time. Longer curing means a generation of a larger amount of cement hydration products (e.g., C-S-H, CH), which in turn enhances the cementation degree or cohesion of the CPB material (Fall et al. 2010; Yilmaz et al. 2015). This argument regarding the increase of cement hydration product with time is experimentally substantiated by the results of TG/DTG on cement pastes of CPB, which are presented (Figures 3.17 and 3.18) and discussed later.

(b) The magnitude of lateral displacement within the CPB model cured to 2.5 hrs was higher in value compared to the CPB model cured to 4.0 hrs, while there was low or insignificant lateral displacement within the CPB model cured to 10.0 hrs. This decrease of lateral displacement with progress of curing time is the consequence of the increase in bonds between the tailings particles with the increase in curing time due to the progress of cement hydration (Mamlouk and Zaniewski 2011) (Figures 3.17 and 3.18).

Comparative analysis of the results presented in Figures 3.7 and 3.8 suggests that the bonds between CPB particles cured to 2.5 hrs were low to resist the cyclic-induced shear stress, while those between the particles of the 4.0 hrs-CPB were stronger and thus had higher shear resistance, which minimizes the acceleration and lateral displacement change. Also, the bonds between the CPB particles cured to 10.0 hrs were high enough to resist the shear stress coming from the laminas and made the FLSB act as a rigid box. These facts strengthen the assumption that the CPB model cured to 2.5 hrs might be susceptible to cyclic loading-induced liquefaction, and the CPB material cured to 4.0 hrs and 10.0 hrs, are more resistant to liquefaction and ground movement.

3.5.2 Evolution of Pore Water Pressure, Effective Stress and Settlement

3.5.2.1 Pore-water pressure

Figure 3.9(a-c) illustrates the changes in pore water pressure (PWP) at various depths with time within the CPB models cured for 2.5 hrs (Figure 3.9a), 4 hrs (Figure 3.9b), and 10 hrs (Figure 3.9c), respectively, before, during and after cyclic loading (i.e., from deposition time to about 24 hours).

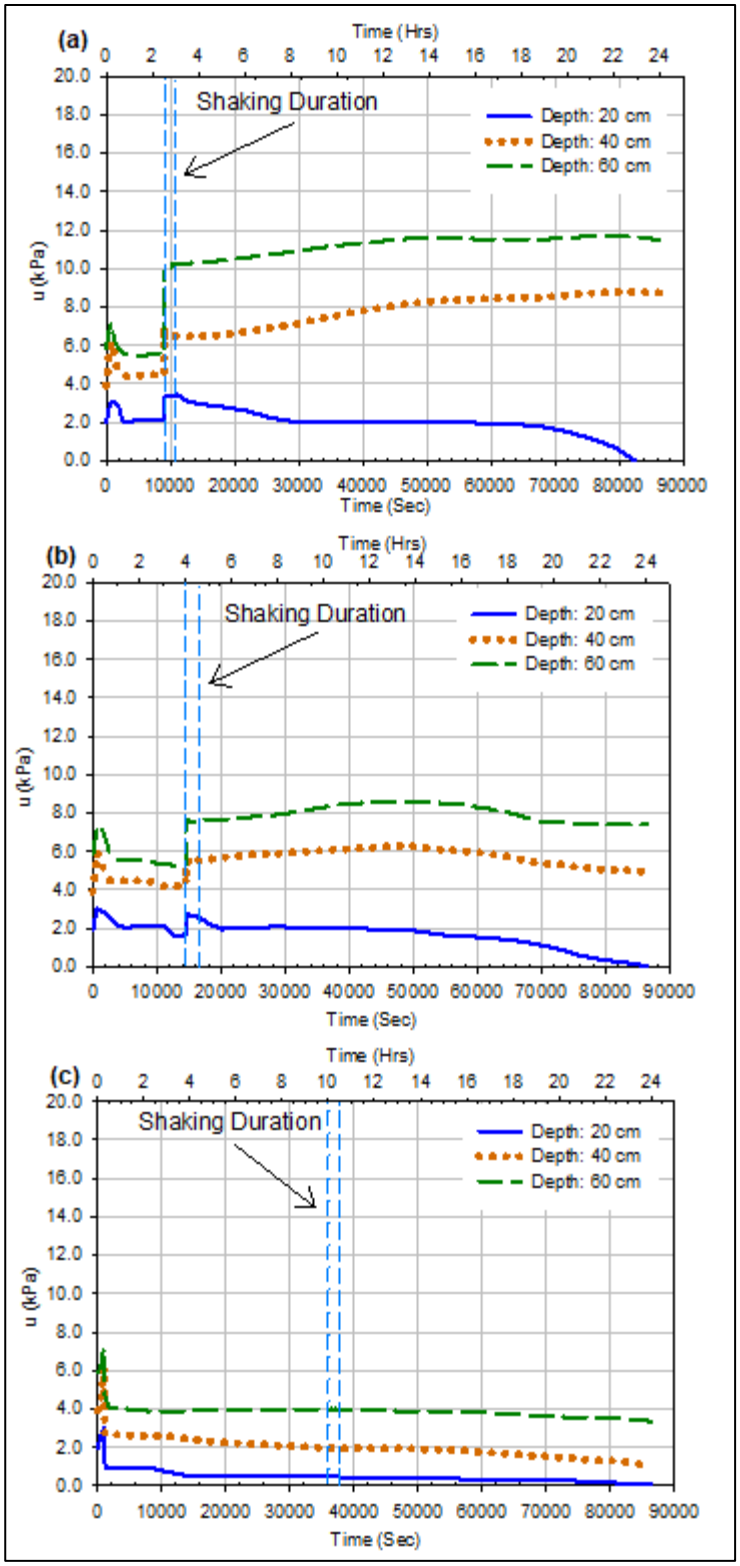

Figure 3.9 Pore water pressure histories at different depths vs times for CPB samples cured to different times: (a) 2.5 hrs; (b) 4.0 hrs and (c) 10.0 hrs.

(i) Before shaking: as can be seen in Figure 3.9a, during the first 1 hour (3600 sec) after the disposal of the fresh CPB, there was first a rapid increase in the PWP in all depths of each CPB model. This increase in PWP is mainly attributed to the self-weight settlement and rearrangement of the tailings particles at the very early age, which decreases the volume of voids (Yilmaz et al. 2012). Subsequently, the PWP rapidly decreases due to the self-desiccation of cement (Helinski et al. 2007, Ghirian and Fall 2014, Scrivener et al. 2015). The latter is experimentally supported by the suction monitoring results presented in Figure 3.10 and discussed later. Moreover, the water evaporation should be considered as an additional factor in decreasing the PWP near the surface of the CPB samples.

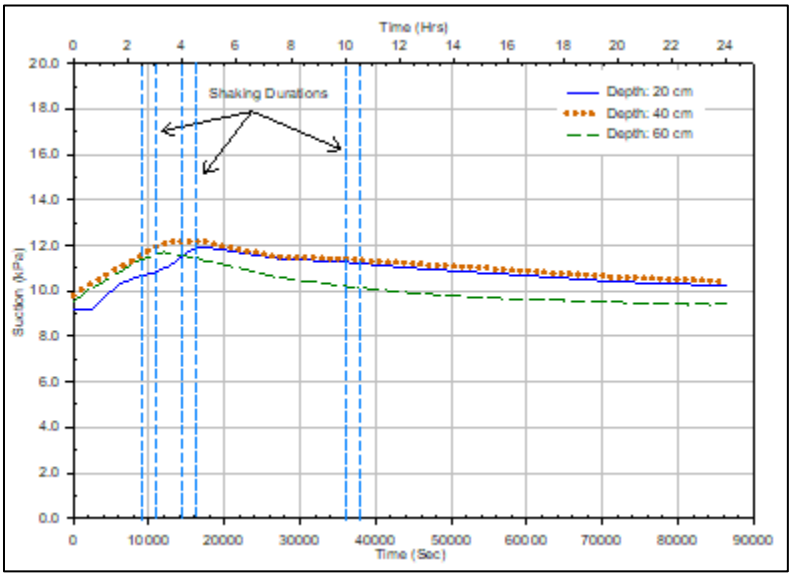

Figure 3.10 Suction evolution at different depths of the CPB sample

(ii) During shaking: prior to applying cyclic loads, initial conditions (hydrostatic conditions) of the CPB material were determined. When shaking began, as expected, there was a quick increase in pore water pressure at all depths within the CPB materials cured to 2.5 hrs and 4.0 hrs until reaching peak values, while there was no rise in pore water pressure in the 10-hrs-old CPB. Moreover, as expected, this increase is bigger at greater depth. This buildup of pore water pressure is related to the generation of excess pore water pressure due to the contractive behaviour of the saturated backfill material or particles (Bouckovalas et al. 2009, Saebimoghaddam 2010, Jefferies and Been 2015, Porcino et al. 2015) (Figure 3.12; will be discussed below). However, the increase in pore water pressure within the CPB sample cured to 2.5 hrs was much higher than the increase in pore water pressure within the CPB sample cured to 4.0 hrs. This can be explained by the joint effect of the following factors: (i) the increase in water consumption by cement hydration (higher self-desiccation) as the curing time increases (i.e., progress of cement hydration) (Scrivener et al. 2015), and (ii) the precipitation of more cement hydration products as the curing time increases (Figure 3.17 and 3.18), which in turn enhances or strengthens the cementing bonds between the

tailings particles (Saebimoghaddam 2010, Ghirian and Fall 2013, Scrivener et al. 2015), and thus reduces the contraction of the CPB materials (Figure 3.12).

(iii) After shaking: after the end of shaking, the pore water pressure first slightly increased with time (i.e., regardless of the progress of cement hydration) at the depths of 20 and 40 cm for the CPB models cured to 2.5 hrs and 4.0 hrs (with different magnitudes). This slight increase in PWP at these depths was then followed by a gradual decrease of the PWP until the end of the monitoring period. However, the PWP gradually decreased at the depth of 60 cm for the CPBs mentioned above after the end of shaking. This observed slight increase in PWP at shallower depths (20 and 40 cm) may be explained by the settlement or contraction of some tailings particles, which might have been partly in suspension at the end of the cycling loading. This contraction generated additional pore water pressure (Pépin et al. 2009). The aforementioned decrease of pore water pressure observed at all depths is mainly due to the self-desiccation (water consumption by cement hydration) (Ghirian and Fall 2013). However, at shallow depths (close to the CPB surface) of each sample, an additional factor contributes to the dissipation of the pore water pressure. This factor is the surface evaporation. Figures 3.9(a-c) show that the pore-water pressure at the shallow depth (20 cm) of each sample declined to less than the hydrostatic pore-water pressure. This phenomena can be explained by the combined effect of (i) self-desiccation due cement hydration (Ghirian and Fall 2013) and (ii) near surface evaporation due to the difference in relative humidity of the CPB surface and the ambient air (Abdul-Hussain and Fall 2012). This argument regarding surface evaporation was experimentally confirmed in this study by determining the evaporation-induced reduction in water content of a CPB material (prepared with the same mix components and conditions as the CPB used in this study) exposed to environmental conditions (relative humidity, temperature) similar to those in which the shaking tests were conducted. It was found that when the CPB sample is exposed to those conditions (temperature of 25°C, and RH of 24%), about 60% of the water loss (reduction in CPB water content) near the surface of the CPB samples was related to evaporation.

3.5.2.2 Effective stress

The evolution of effective vertical stresses at various depths during the shaking durations for CPB models cured (aged) for 2.5 hrs, 4 hrs, and 10 hrs, respectively, are shown in figure 3.11(a-c). During shaking, these stresses decreased from their initial values in the samples cured to 2.5 hrs and 4.0 hrs. This decrease is due to the excess pore pressure development (Figures 3.9a and b) as result of the contraction of CPB particles. However, in samples cured to 10.0 hrs, the effective stresses remain constant during shaking durations because there was no significant excess pore water pressure generation as shown and discussed previously (Figure 3.9c).

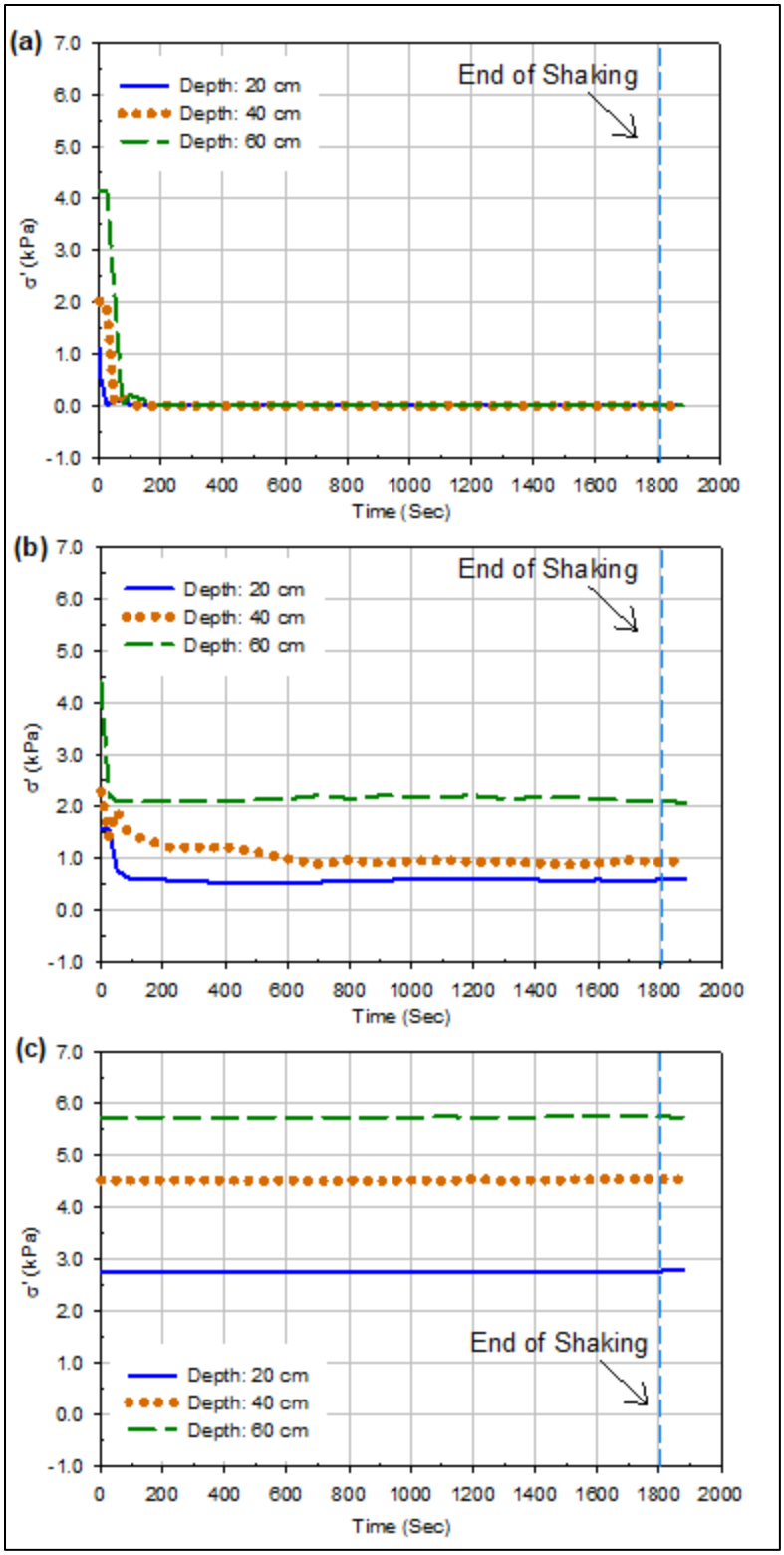

Figure 3.11 Effective stress at different depths vs times for CPB samples cured to different times during shaking: (a) 2.5 hrs; (b) 4.0 hrs and (c) 10.0 hrs.

3.5.2.1 Settlement (vertical displacement)

In this study, downward displacement (settlement) was recorded at different depths within the CPB models during shaking. This can give an indication about the contractive behavior of the CPB particles and the increase in the backfill density (Ueng et al. 2006, Pépin et al. 2012b). Settlement time histories measured during the shaking at different depths within the CPB models cured (aged) for 2.5 hrs, 4.0 hrs, and 10 hrs, respectively, are shown in Figure 3.12(a-c). This figure depicts that the CPBs cured for 2.5 hrs and 4.0 hrs show significant settlement, whereas the CPB cured for 10 hrs shows negligible settlement (< 2 mm). This observed settlement indicates a contractive behaviour of the tailings particles (or volume change of the CPB) induced by the shaking. It can be also seen that the amount of settlement or contraction (volume change) within the CPB cured to 2.5 hrs was higher than its values in the backfill cured to 4.0 hrs and 10 hrs. This observation suggests that the longer the curing time or the higher cement hydration degree, the lesser the settlement induced by the shaking. This behaviour, which is consistent with the results of PWP measurements and liquefaction analysis discussed in sections 3.5.2.1 and 3.5.3, respectively, is due to the fact that a greater cement hydration degree causes the precipitation of more cement hydration products (see Figures 3.17-18), thereby increasing the density and strength of the CPB material (Fall et al. 2010, Scrivener et al. 2015). Consequently, the contracting behaviour or settlement of the CPB becomes smaller (Seed et al. 1975, Tokimatsu and Seed 1987) during shaking. From figure 3.12, it can be also observed that the settlement of CPB cured for 2.5 hrs and 4.0 hrs varied with the measurement depth. The settlement becomes smaller as the depth increases. On Figure 3.12a, the recorded displacement at the depth of 20 cm became higher than expected after 800 seconds because the plastic plate that was installed at this depth was shifted due to the excessive movement.

3.5.3 Liquefaction Analysis

Figure 3.13(a-c) shows a comparison of the excess of PWP development (during shaking) at different depths and curing times for all CPB models. The excess of PWP in the CPBs cured to 2.5 hrs and 4.0 hrs varied with depth and shaking time, while there was no excess pore water pressure development during shaking within the CPB cured to 10.0 hrs. The excess pore-water pressure ratio (R_u), which is the ratio between the excess pore-water pressure (Δu) and the initial effective stress (σ'_o), was used as the evaluation factor of soil liquefaction susceptibility. Liquefaction is generally defined as $R_u \geq 1$, while if $R_u < 1$, there is no liquefaction (Wu et al. 2004).

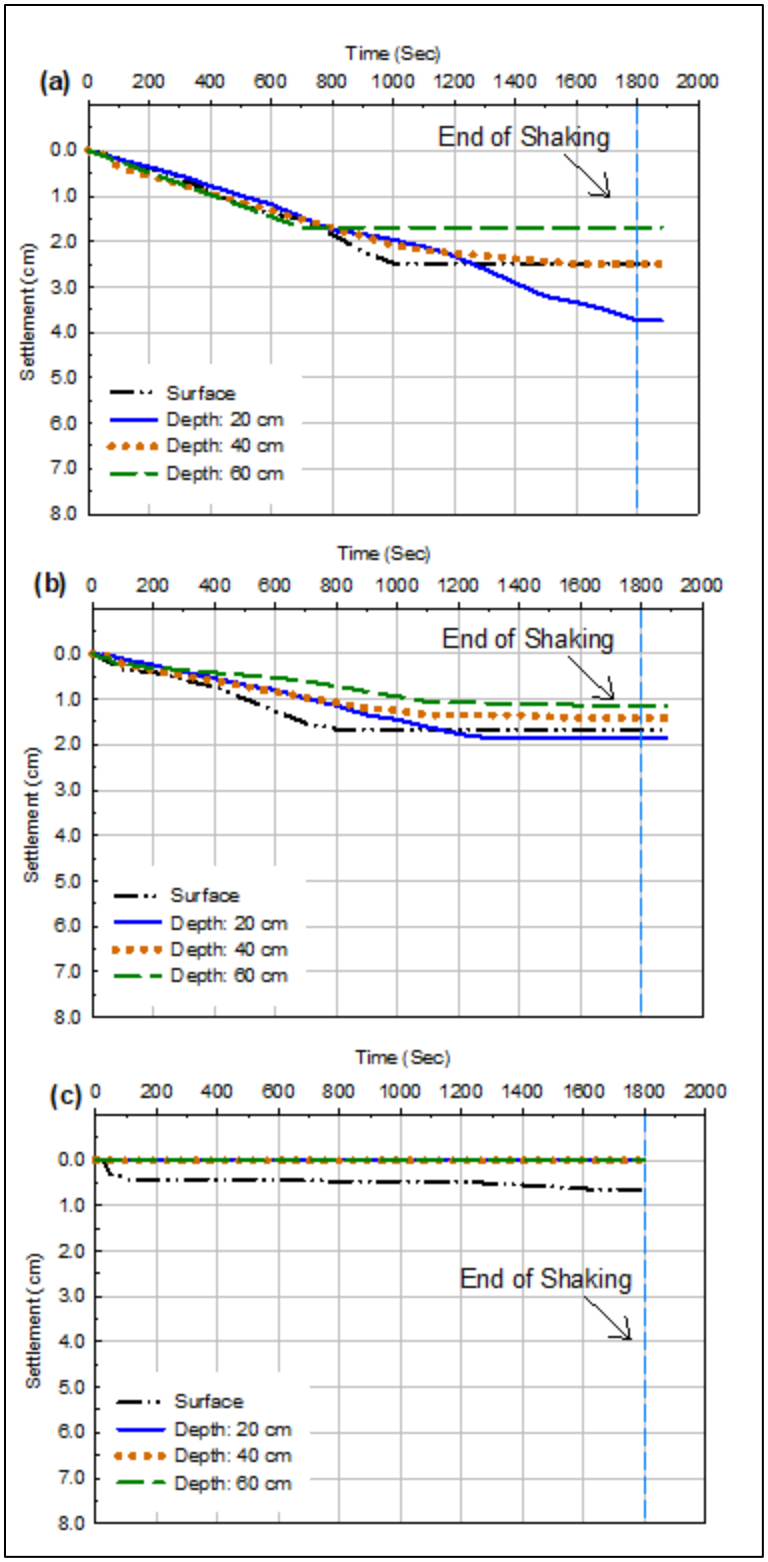

Figure 3.12 Settlement at different depths vs times for CPB samples cured to different times during shaking: (a) 2.5 hrs; (b) 4.0 hrs and (c) 10.0 hrs.

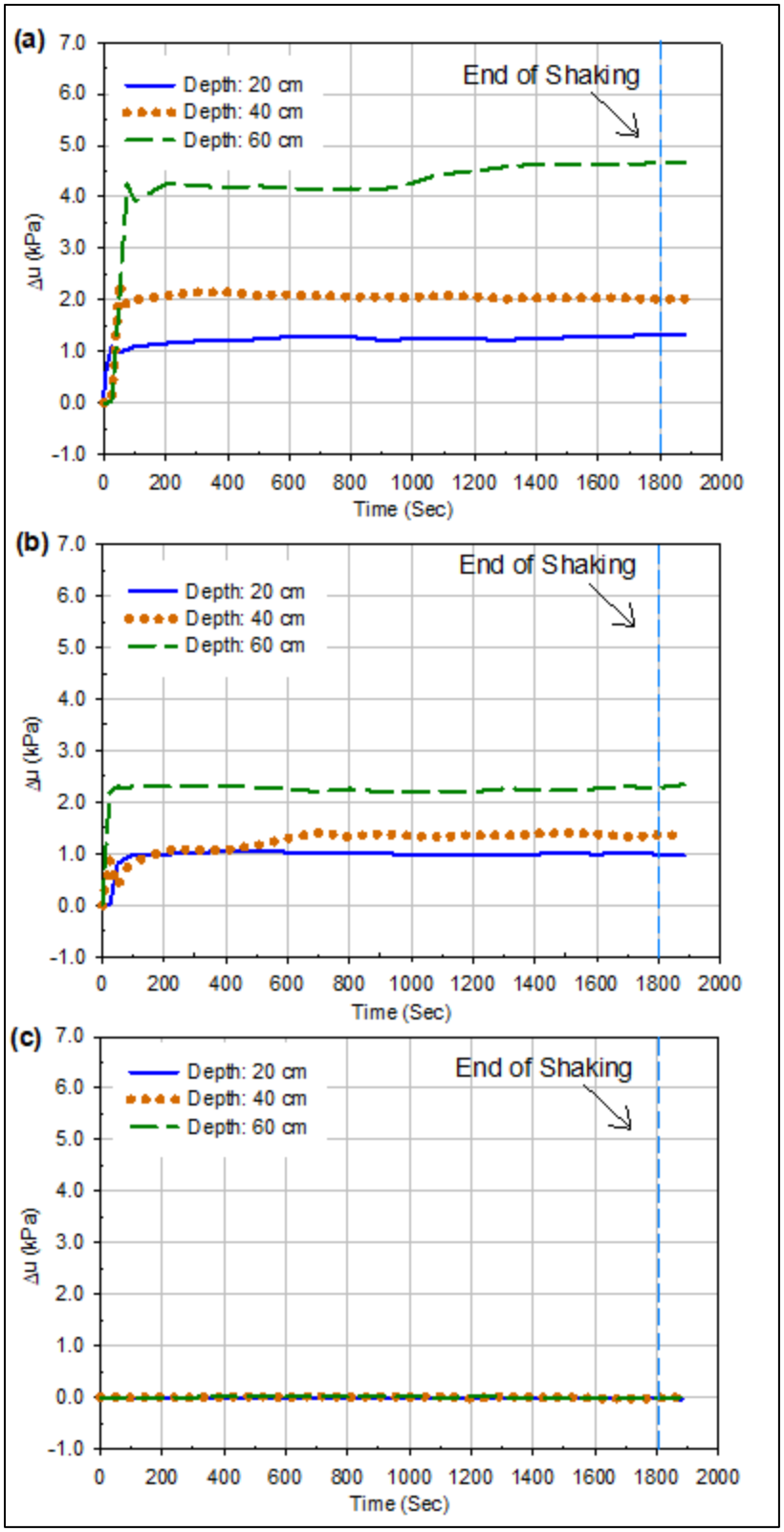

Figure 3.13 Excess pore water pressure (Δu) development at different depths vs times for CPB samples cured to different times: (a) 2.5 hrs; (b) 4.0 hrs and (c) 10.0 hrs.

Figure 3.14(a-c) presents the pore-water pressure ratios determined during shaking of the CPB samples cured to 2.5 hrs, 4.0 hrs, and 10.0 hrs, respectively. It can be seen that CPB samples cured to 2.5 hrs are susceptible to liquefaction ($R_u \geq 1$) under the applied cyclic loading conditions, while samples exposed to shaking after 4.0 and 10.0 hrs of curing were resistant to liquefaction ($R_u < 1$). In other words, the more time that is given to cement to act, the less susceptible to cyclic-induced liquefaction the CPB will be. This increase of liquefaction resistance of CPB as the curing time increases is due to the coupled influence of the following two factors as discussed below: (i) production of more cement hydration products within the CPB pores due to progress of the cement hydration, which enhances the cementation or cohesion between the tailings particles, and thus increasing the shear strength of the CPB material. The latter obviously results in the increase of the liquefaction resistance of the CPB; and (ii) the water consumption by the cement hydration (self-desiccation), and thus decreasing the pore water pressure or excess of pore pressure within the backfill. This is obviously associated with a rise of the effective stress within the CPB, and consequently with an increase of the liquefaction resistance of the cementing backfill.

(i) Production of more cement hydration products

The production of more cement hydration products as the curing time becomes longer is experimentally supported by the results of the microstructural analyses (thermal analysis (TG/DTG) and x-ray diffraction (XRD) analyses) performed on CPBs cured to different ages, 1h and 4hrs, (Figures 3.17 and 3.18), respectively.

From figure 3.17, it can be seen that the first peak (DTG) or modification in weight (TG) is found between 100-200^{o}C, which refers to the decomposition of the cement hydration products, such as ettringite, gypsum and C-S-H (Fall et al. 2010, Wang et al. 2016), while the second peak or weight change occurred at around 400-500^{o}C as a result of the disintegration of CH (Noumowé 1995, Zhou and Glasser 2001). Finally, the third peak or weight change is observed between 600-700^{o}C due to the decomposition of the calcite (Noumowé 1995, Zhou and Glasser 2001, Fall et al. 2010, Haiqiang et al. 2016). Moreover, by comparing the TG/DTG diagrams of the CPB cured to 1.0 hr and 4.0 hrs, it can be clearly noticed that the first and second peaks or weight changes are higher for CPB cured to 4.0 hrs, thus indicating that the amount of hydration products (such as CH and C-S-H) generated increases with a longer curing time. These thermal analysis results are consistent with the results of XRD analysis conducted on CPB samples cured to 1.0 hr and 4.0 hrs, respectively, and presented in figure 3.18 (a, b). This figure shows the types and relative amounts of the cement hydration products (e.g., ettringite, gypsum, CH, C-S-H) formed within the CPB samples. It is observed that some of these products have a higher intensity in the CPB sample cured for 4.0 hrs. In other words, more hydration products were formed in the older than the younger sample. For instance, the intensity of the ettringite at $9^\circ - 2\theta$ is 260 CPS and 300 CPS in the case of CPB samples cured to 1.0 hr and 4.0 hrs, respectively. Similarly, the ettringite intensity at $22^\circ - 2\theta$ is 160 CPS and 200 CPS in the case of CPB samples cured to 1.0 hr and 4.0 hrs, respectively.

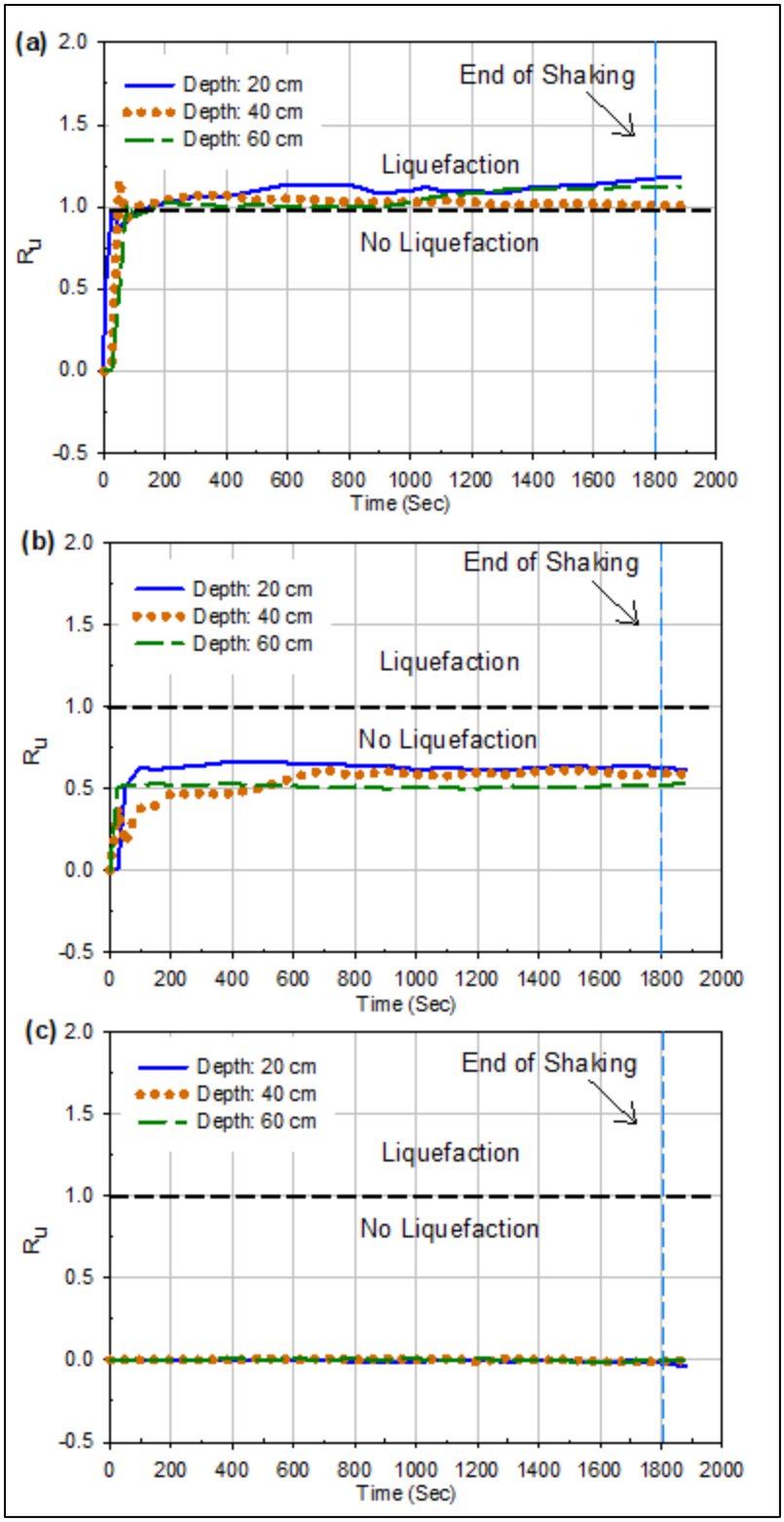

Figure 3.14 Pore -water pressure ratios determined at different depths vs times for CPB samples cured to different times: (a) 2.5 hrs; (b) 4.0 hrs and (c) 10.0 hrs.

Figures 3.15 and 3.16, which present the results of the monitoring of the time-dependent evolution of the temperature and EC at different depths of the CPB models, respectively, show that the rate or progress of the cement hydration, in other words, the amount of cement hydrations formed within the CPB, is relatively similar at all depths of the CPBs. Indeed, from these figures, it can be seen that there is almost an overlap of the time-dependent evolution curves of the temperature and EC at all depths. Moreover, the time required to reach the peak values of EC is similar for all depths. The initial increase of the EC up to the peak value (Figure 3.16) is due to an increase of the concentration of ions in the CPB pore water solution because of the dissolution of cement grains. The observed decrease of the EC after the peak value results from the combined effects of the following factors: (a) start of the development of cement hydration products, (b) decrease of the free water, and (c) refinement and subdivision of the capillary pores (Salem and Ragai 2001, Courard et al. 2014).

(ii) Self-desiccation of CPB

Self-desiccation of cementitious material, a mechanism caused by cement hydration, can be simply described as the reduction of net total volume of water and solid particles or total volume of the material as a result of the process of cement hydration (Li and Fall 2016), leading to a reduction in PWP and/or a generation of negative pore water pressure (suction) (Ghirian and Fall 2013). Accordingly, the effective stress and strength of these materials increase as self-desiccation takes place (Abdul-Hussain and Fall 2012, Fredlund et al. 2012, Ghirian and Fall 2014). Figures 3.19 and 3.10, which show the evolution of the volumetric water content (VWC) and suction in the CPB at different depths, respectively, support the fact that self-desiccation did take place in the CPB. A gradual increase in the volumetric water content (VWC) in the first hours at all depths of the CPB material can be observed in Figure 3.19. The VWC reached its peak value after 6 hrs. Afterward, it experienced a slight decrease and then remained relatively constant till the completion of the monitoring period. This increase in VWC is attributed to the self-desiccation induced decrease of the total volume of the CPB since the VWC expresses the ratio of volume of water to the total volume of the soil. Moreover, the amount of water or water content decreased during this period as evidenced by the suction measurements results presented in Figure 3.10. This figure shows a small suction has developed in the CPB shortly after its disposal into the laminar shear box. Then, the suction value increased until reaching its peak after 6hrs. Afterward, the suction decreased slightly and then remained relatively constant until the end of the monitoring.

This generation of suction and its increase can be explained by the fact that the chemical reactions of the cement hydration result in the consumption of water in the capillary pores of CPB (Wang et al. 2016), which decreases the water content in the hydrating backfill. The reduction of water content in the backfill or soil allows air to enter the pores between tailings or soil particles and thus generate air bubbles. Consequently, this turns the backfill or soil from saturated condition to partially saturated conditions (Fredlund et al. 2012). This effect was experimentally confirmed in this study, as it was noted that the degree of saturation decreased from 100% (immediately after casting) to around 94% - 96% (after about 2 hours). This reduction in water content leads to a

decrease of the pore water pressure, in other words to an increase of the effective stress, and thus to an increase of the liquefaction resistance of the CPB. Moreover, the presence of air bubbles inside the pores of a soil will enhance its liquefaction resistance, because the air can absorb the generated excess PWP by reducing its volume (Okamura and Soga 2006).

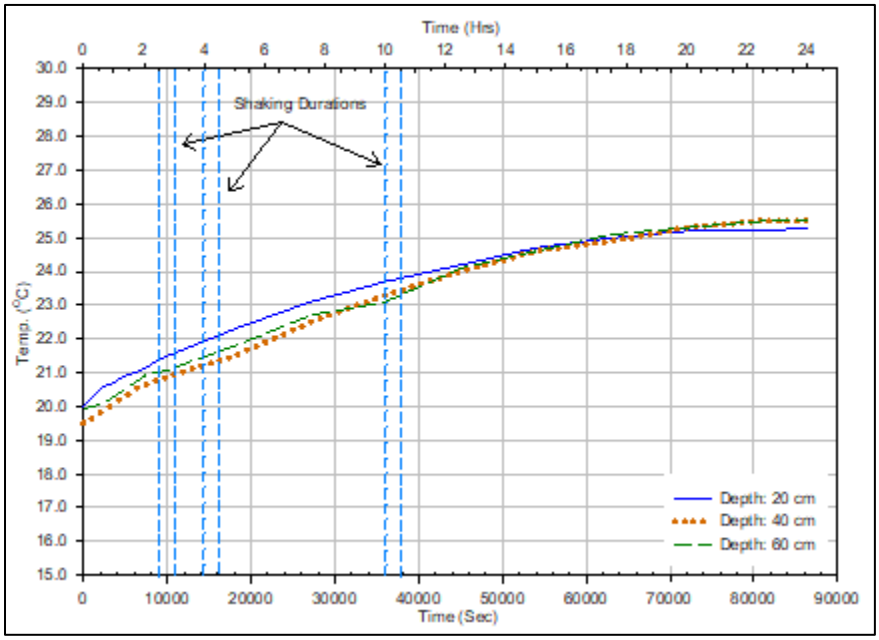

Figure 3.15 Evolution of hydration heat with curing time within CPB samples.

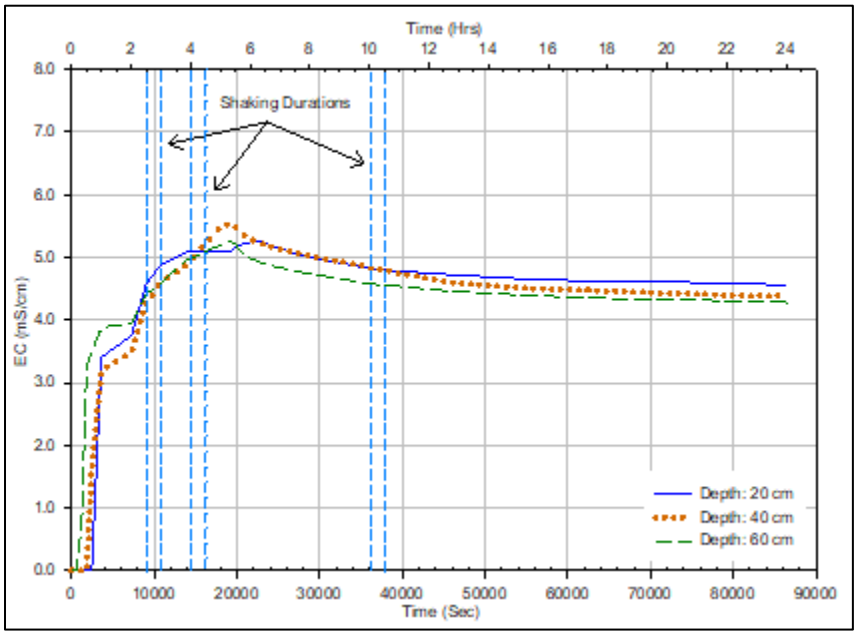

Figure 3.16 Electrical conductivity at different depths of the CPB samples.

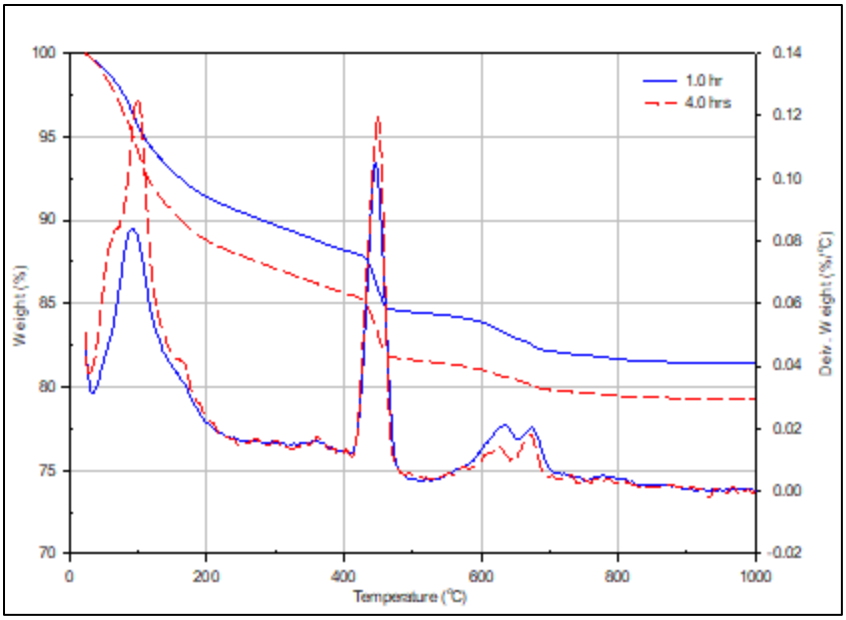

Figure 3.17 Effect of curing time on TG/DTG diagrams for CPB cured to 1.0 hr and 4.0 hrs

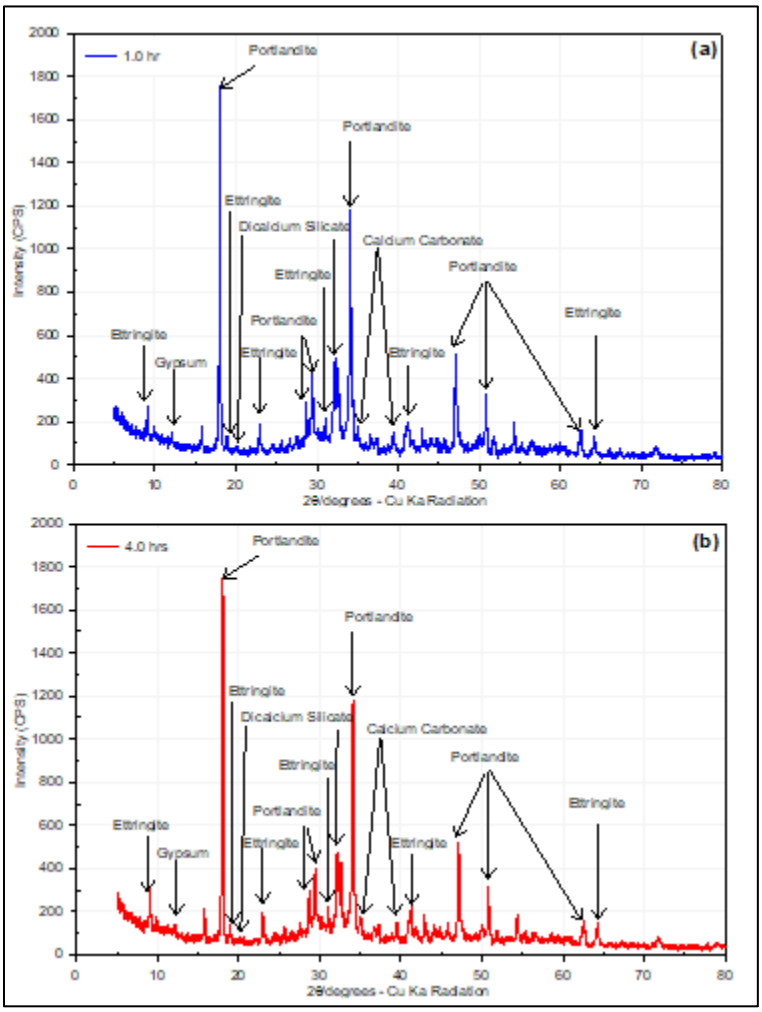

Figure 3.18 Effect of curing time on the XRD result of CPB cured to: (a) 1.0 hr; (b) 4.0 hrs

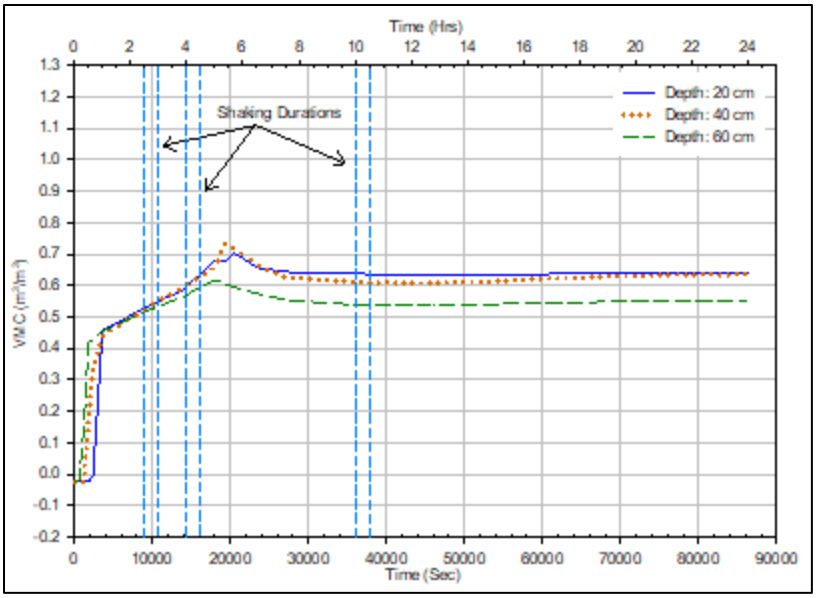

Figure 3.19 Change in volumetric water content at different depths of the CPB samples.

3.6 Summary and Conclusion

This manuscript has evaluated and discussed the geotechnical response (e.g., deformation, excess of pore water pressure, effective stress, liquefaction potential) of paste backfill undergoing cementation to cyclic loadings by using the shaking table testing technique. This assessment was conducted by applying cyclic loading on paste backfill models cured at different times (2.5 hrs, 4.0 hrs and 10.0 hrs), which were casted in a flexible laminar shear box. The paste backfill models were also instrumented with numerous sets of sensors and transducers to monitor the evolution of several parameters (pore water pressure, suction, lateral and horizontal displacement, acceleration, temperature, electrical conductivity) before, during and after shaking. The obtained results show that the acceleration, horizontal and vertical displacement and excess pore water pressure of the CPB under cyclic loading are significantly affected by the curing time or the degree of cement hydration and the depth in the CPB. It is also found that the seismic loading has no significant influence on the progress of the cementation hydration. Moreover, young (2.5 hrs old) CPB material can be susceptible to liquefaction, whereas older CPBs (curing time ≥ 4hrs) are resistant to liquefaction under the studied cyclic conditions. This resistance to liquefaction is due to the combined effect of two factors: (i) the strengthening of the cementation between the soil (tailings) particles, which increases the shear resistance of the CPB material; (ii) the self-desiccation, which decreases the pore water pressure or leads to the development of suction (due to generation of air bulbs) within the backfill, and thus increasing of the effective stress in the CPB. The extent of these effects depends on the curing time, and it increases for a longer curing time. These relatively large-scale 1-g tests on CPB are time consuming and expensive; however, they have facilitated a better understanding of the cyclic behaviour and liquefaction potential of CPB at early ages as well as provided information and data that are useful for liquefaction assessment of CPB structures, and

also for future development of constitutive models to describe and predict the cyclic behaviour of hydrating paste backfill or soil undergoing cementation.

3.7 Acknowledgements

The authors would like to thank the National Natural Sciences and Engineering Research Council of Canada (NSERC) for financially supporting this project. Moreover, the authors would like to thank Dr. Mohammed Al-Umar, Dr. Gamal Elnabelsya, and Mr. Mohamed Salah for their help with the experimental tests.

3.8 References

Abdelaal, A. (2011) *Early age mechanical behavior and stiffness development of cemented paste backfill with sand*, Doctoral dissertation, University of Toronto.

Abdul-Hussain, N. and Fall, M. (2012) 'Thermo-hydro-mechanical behaviour of sodium silicate-cemented paste tailings in column experiments', *Tunnelling and Underground Space Technology*, 29, 85-93.

Acar, Y. B. and El-Tahir, E. T. A. (1986) 'Low strain dynamic properties of artificially cemented sand', *Journal of Geotechnical Engineering*, 112(11), 1001-1015.

Ahn, K. S., Zhang, C. and Canbulat, I. (2017) 'Study of seismic activities associated with Australian underground coal mining', in *Coal Operators' Conference*, University of Wollongong, Australia,

Aldhafeeri, Z. and Fall, M. (2016) 'Time and damage induced changes in the chemical reactivity of cemented paste backfill', *Journal of Environmental Chemical Engineering*, 4(4), 4038-4049.

Anastasopoulos, I., Georgarakos, T., Georgiannou, V., Drosos, V. and Kourkoulis, R. (2010) 'Seismic performance of bar-mat reinforced-soil retaining wall: Shaking table testing versus numerical analysis with modified kinematic hardening constitutive model', *Soil Dynamics and Earthquake Engineering*, 30(10), 1089-1105.

ASTM C143/C143M-15a (2015) 'Standard test method for slump of hydraulic-cement concrete',

Atkinson, G. M., Kaka, S. I., Eaton, D., Bent, A., Peci, V. and Halchuk, S. (2008) 'A very close look at a moderate earthquake near Sudbury, Ontario', *Seismological Research Letters*, 79(1), 119-131.

Bairro, R. and Vaz, C. (2000) *Shaking table testing of civil engineering structures-The LNEC 3D simulator experience,* translated by Auckland, New Zeland.

Becker, D., Cailleau, B., Kaiser, D. and Dahm, T. (2014) 'Macroscopic Failure Processes at Mines Revealed by Acoustic Emission (AE) Monitoring', *Bulletin of the Seismological Society of America,* 104(4), 1785-1801.

Bouckovalas, G. D., Papadimitriou, A. G. and Niarchos, D. (2009) 'Gravel drains for the remediation of liquefiable sites: The Seed & Booker (1977) approach revisited', in *International Conference on Performance-Based Design*, Tokyo, Japan, International Society for Soil Mechanics and Geotechnical Engineering., 61-75.

Carraro, J. A. H., Prezzi, M. and Salgado, R. (2009) 'Shear strength and stiffness of sands containing plastic or nonplastic fines', *Journal of Geotechnical and Geoenvironmental Engineering,* 135(9), 1167-1178.

Carter, D. P. (1988) *Liquefaction potential of sand deposits under low levels of excitation,* California Univ., Berkeley, CA, USA.

Chopra, A. K. (2005) *Earthquake Dynamics of Structures - a Primer,* Earthquake Engineering Research Institute (EERI), USA.

Courard, L., Michel, F., Perkowicz, S. and Garbacz, A. (2014) 'Effects of limestone fillers on surface free energy and electrical conductivity of the interstitial solution of cement mixes', *Cement and Concrete Composites,* 45, 111-116.

Douglas, J. (2003) 'Earthquake ground motion estimation using strong-motion records: a review of equations for the estimation of peak ground acceleration and response spectral ordinates', *Earth-Science Reviews,* 61(1-2), 43-104.

Dungca, J. R., Kuwano, J., Takahashi, A., Saruwatari, T., Izawa, J., Suzuki, H. and Tokimatsu, K. (2006) 'Shaking table tests on the lateral response of a pile buried in liquefied sand', *Soil Dynamics and Earthquake Engineering,* 26(2-4), 287-295.

Ercikdi, B., Cihangir, F., Kesimal, A., Deveci, H. and Alp, I. (2009a) 'Utilization of industrial waste products as pozzolanic material in cemented paste backfill of high sulphide mill tailings', *J Hazard Mater,* 168(2-3), 848-56.

Ercikdi, B., Kesimal, A., Cihangir, F., Deveci, H. and Alp, İ. (2009b) 'Cemented paste backfill of sulphide-rich tailings: Importance of binder type and dosage', *Cement and Concrete Composites,* 31(4), 268-274.

Fall, M., Benzaazoua, M. and Ouellet, S. (2005) 'Experimental characterization of the influence of tailings fineness and density on the quality of cemented paste backfill', *Minerals Engineering,* 18(1), 41-44.

Fall, M., Célestin, J. C., Pokharel, M. and Touré, M. (2010) 'A contribution to understanding the effects of curing temperature on the mechanical properties of mine cemented tailings backfill', *Engineering Geology*, 114(3-4), 397-413.

Fall, M. and Samb, S. S. (2008) 'Pore structure of cemented tailings materials under natural or accidental thermal loads', *Materials Characterization,* 59(5), 598-605.

Fredlund, D. G., Rahardjo, H. and Fredlund, M. D. (2012) *Unsaturated soil mechanics in engineering practice,* Hoboken, New Jersey, USA: John Wiley & Sons.

Ghirian, A. and Fall, M. (2013) 'Coupled thermo-hydro-mechanical–chemical behaviour of cemented paste backfill in column experiments. Part I: Physical, hydraulic and thermal processes and characteristics', *Engineering Geology,* 164, 195-207.

Ghirian, A. and Fall, M. (2014) 'Coupled thermo-hydro-mechanical–chemical behaviour of cemented paste backfill in column experiments', *Engineering Geology*, 170, 11-23.

Ghirian, A. and Fall, M. (2016a) 'Long-term coupled behaviour of cemented paste backfill in load cell experiments', *Geomechanics and Geoengineering*, 11(4), 237-251.

Ghirian, A. and Fall, M. (2016b) 'Strength evolution and deformation behaviour of cemented paste backfill at early ages: Effect of curing stress, filling strategy and drainage', *International Journal of Mining Science and Technology,* 26(5), 809-817.

Guoxing, C., Su, C., Xi, Z., Xiuli, D., Chengzhi, Q. I. and Zhihua, W. (2015) 'Shaking-table tests and numerical simulations on a subway structure in soft soil', *Soil Dynamics and Earthquake Engineering,* 76, 13-28.

Haiqiang, J., Fall, M. and Cui, L. (2016) 'Yield stress of cemented paste backfill in sub-zero environments: Experimental results', *Minerals Engineering,* 92, 141-150.

Hasegawa, A., Nakajima, J., Uchida, N., Okada, T., Zhao, D., Matsuzawa, T. and Umino, N. (2009) 'Plate subduction, and generation of earthquakes and magmas in Japan as inferred from seismic observations: An overview', *Gondwana Research,* 16(3-4), 370-400.

Hasegawa, H. S., Wetmiller, R. J. and Gendzwill, D. J. (1989) 'Induced seismicity in mines in Canada—an overview', *Pure and applied geophysics,* 129(3-4), 423-453.

Helinski, M., Fourie, A., Fahey, M. and Ismail, M. (2007) 'Assessment of the self-desiccation process in cemented mine backfills', *Canadian Geotechnical Journal,* 44(10), 1148-1156.

Ishihara, K. (1996) *Soil Behavior in Earthquake Geotechnics,* NY, USA: Oxford University Press.

Jamali, M. (2012) *Effect of Binder Content and Load History on the One dimensional Compression of Williams Mine Cemented Paste Backfill,* Master of Applied Science dissertation: University of Toronto.

James, M., Jolette, D., Aubertin, M. and Bussière, B. (2003) *An Experimental Set-up to Investigate Tailings liquefaction and control measures,* translated by Montréal, QC, Canada.

Jefferies, M. and Been, K. (2015) *Soil Liquefaction: a critical state approach,* Second ed., Taylor & Francis, London, UK.

Kesimal, A., Yilmaz, E., Ercikdi, B., Alp, I. and Deveci, H. (2005) 'Effect of properties of tailings and binder on the short-and long-term strength and stability of cemented paste backfill', *Materials Letters,* 59(28), 3703-3709.

Li, L. and Aubertin, M. (2012) 'A modified solution to assess the required strength of exposed backfill in mine stopes', *Canadian Geotechnical Journal,* 49(8), 994-1002.

Li, W. and Fall, M. (2016) 'Sulphate effect on the early age strength and self-desiccation of cemented paste backfill', *Construction and Building Materials,* 106, 296-304.

Lu, G. and Fall, M. (2017) 'Simulation of Blast Induced Liquefaction Susceptibility of Subsurface Fill Mass', *Geotechnical and Geological Engineering,* 36(3), 1683-1706.

Mamlouk, M. S. and Zaniewski, J. P. (2011) *Materials for civil and construction engineers,* 3rd ed., Upper Saddle River, New Jersey: Pearson Prentice Hall.

Mohamed, F. M. O. (2014) *Bearing Capacity and Settlement Behaviour of Footings Subjected to Static and Seismic Loading Conditions in Unsaturated Sandy Soils*, Doctoral dissertation: University of Ottawa.

Moncarz, P. D. and Krawinkler, H. (1981) *Theory and application of experimental model analysis in earthquake engineering*, Stanford University.

Motamed, R., Towhata, I., Honda, T., Tabata, K. and Abe, A. (2013) 'Pile group response to liquefaction-induced lateral spreading: E-Defense large shake table test', *Soil Dynamics and Earthquake Engineering*, 51, 35-46.

Nasir, O. and Fall, M. (2010) 'Coupling binder hydration, temperature and compressive strength development of underground cemented paste backfill at early ages', *Tunnelling and Underground Space Technology*, 25(1), 9-20.

Natural Resources Canada (2019) 'Earthquake Reports for 2019', [online], available: http://www.seismescanada.rncan.gc.ca/recent/2019/index-en.php 2019].

Ngadimon, K. (2006) *Design and Simulation of Hydraulic Shaking Table*, Doctoral dissertation: University of Technology.

Noumowé, A. (1995) *Effet des hautes températures (20 °C–600 °C) sur le béton*, Ph.D. Thesis, Institut National des Sciences Appliquèes.

Nouri, H., Fakher, A. and Jones, C. (2006) 'Development of Horizontal Slice Method for seismic stability analysis of reinforced slopes and walls', *Geotextiles and Geomembranes*, 24(3), 175-187.

Nouri, H., Fakher, A. and Jones, C. J. F. P. (2008) 'Evaluating the effects of the magnitude and amplification of pseudo-static acceleration on reinforced soil slopes and walls using the limit equilibrium Horizontal Slices Method', *Geotextiles and Geomembranes*, 26(3)(3), 263-278.

Nuttli, O. W. (1973) 'Seismic wave attenuation and magnitude relations for eastern North America', *Journal of Geophysical Research*, 78(5), 876-885.

Okamura, M. and Soga, Y. (2006) 'Effect of pore fluid compressibility on liquefaction resistance of partially saturated sand', *Soils and Foundations*, 46(5)(5), 695-700.

Ontario Mining Association (2017) *Ontario Miniral Production*.

Özgen, S., Malkoç, Ö., Doğancik, C., Sabah, E. and Şapçi, F. O. (2011) 'Optimization of a Multi Gravity Separator to produce clean coal from Turkish lignite fine coal tailings', *Fuel,* 90(4), 1549-1555.

Pépin, N., Aubertin, M. and James, M. (2009) *An Investigation of the Cyclic Behaviour of tailings using shaking table tests - effect of a drainage inclusion on porewater development,* translated by Halifax, N.S., Canada.

Pépin, N., Aubertin, M. and James, M. (2012a) 'Seismic table investigation of the effect of inclusions on the cyclic behaviour of tailings', *Canadian Geotechnical Journal,* 49(4), 416-426.

Pépin, N., Aubertin, M., James, M. and Leclerc, M. (2012b) 'Seismic Simulator Testing to Investigate the Cyclic Behavior of Tailings in an Instrumented Rigid Box', *Geotechnical Testing Journal,* 35(3), 469-479.

Porcino, D., Marcianò, V. and Granata, R. (2015) 'Cyclic liquefaction behaviour of a moderately cemented grouted sand under repeated loading', *Soil Dynamics and Earthquake Engineering,* 79, 36-46.

Poulos, S. J., Robinsky, E. I. and Keller, T. O. (1985) 'Liquefaction Resistance of Thickened Tailings', *Journal of Geotechnical Engineering,* 111(12), 1380-1394.

Prasad, S. K., Towhata, I., Chandradhara, G. P. and Nanjundaswamy, P. (2004) 'Shaking table tests in earthquake geotechnical engineering', *Current science,* 1398-1404.

Saebimoghaddam, A. (2010) *Liquefaction of Early Age Cemented Paste Backfill,* Doctoral dissertation: University of Toronto.

Salem, T. M. and Ragai, S. M. (2001) 'Electrical conductivity of granulated slag-cement kiln dust-silica fume pastes at different porosities', *Cement and Concrete Research,* 31(5), 781-787.

Scrivener, K. L., Juilland, P. and Monteiro, P. J. M. (2015) 'Advances in understanding hydration of Portland cement', *Cement and Concrete Research,* 78, 38-56.

Seed, H. B., Pyke, R. and Martin, G. R. (1975) *Effect of multi-directional shaking on liquefaction of sands,* Earthquake Engineering Research Center, University of California.

Srilatha, N., Madhavi Latha, G. and Puttappa, C. G. (2013) 'Effect of frequency on seismic response of reinforced soil slopes in shaking table tests', *Geotextiles and Geomembranes,* 36, 27-32.

Sriskandakumar, S. (2004) *Cyclic loading response of Fraser River sand for validation of numerical models simulating centrifuge tests,* University of British Columbia, Canada.

Takahashi, A., Takemura, J., Suzuki, A. and Kusakabe, O. (2001) 'Development and performance of an active type shear box in a centrifuge', *International Journal of Physical Modelling in Geotechnics,* 1(2), 1-17.

Thompson, B. D., Grabinsky, M. W., Bawden, W. F. and Counter, D. B. (2009) *In-situ measurements of cemented paste backfill in long-hole stope,* translated by Toronto, ON, Canada.

Tokimatsu, K. and Seed, H. B. (1987) 'Evaluation of settlements in sands due to earthquake shaking', *Journal of Geotechnical Engineering,* 113(8)(8), 861-878.

Tuttle, M., Law, K. T., Seeber, L. and Jacob, K. (1990) 'Liquefaction and ground failure induced by the 1988 Saguenay, Quebec, qrthquakel', *Canadian Geotechnical Journal,* 27(5), 580-589.

Ueng, T. S., Wang, M. H., Chen, M. H., Chen, C. H. and Peng, L. H. (2006) 'A large biaxial shear box for shaking table test on saturated sand', *Geotechnical Testing Journal,* 29(1), 1-8.

Wang, L., Chen, G. and Chen, S. (2015) 'Experimental study on seismic response of geogrid reinforced rigid retaining walls with saturated backfill sand', *Geotextiles and Geomembranes,* 43(1), 35-45.

Wang, Y., Fall, M. and Wu, A. (2016) 'Initial temperature-dependence of strength development and self-desiccation in cemented paste backfill that contains sodium silicate', *Cement and Concrete Composites,* 67, 101-110.

Wu, J., Kammerer, A. M., Riemer, M. F., Seed, R. B. and Pestana, J. M. (2004) *Laboratory Study of Liquefaction Triggering Criteria,* translated by Vancouver, BC, Canada.

Yang, L. and Woods, R. D. (2015) 'Shear stiffness modeling of cemented clay', *Canadian Geotechnical Journal,* 52(2)(2), 156-166.

Yilmaz, E., Belem, T. and Benzaazoua, M. (2012) 'One-Dimensional Consolidation Parameters Of Cemented Paste Backfills / Parametry Jednowymiarowej Konsolidacji Podsadzki W Postaci Cementowej Pasty', *Gospodarka Surowcami Mineralnymi - Mineral Resources Management,* 28(4)(4), 29-45.

Yilmaz, E., Belem, T., Bussière, B., Mbonimpa, M. and Benzaazoua, M. (2015) 'Curing time effect on consolidation behaviour of cemented paste backfill containing different cement types and contents', *Construction and Building Materials,* 75, 99-111.

Zhou, Q. and Glasser, F. P. (2001) 'Thermal stability and decomposition mechanisms of ettringite at <120°C', *Cement and Concrete Research,* 31(9)(9), 1333-1339.

Zhu, F. and Clark, J. I. (1994) 'The effect of dynamic loading on lateral stress in sand', *Canadian Geotechnical Journal,* 31(2)(2), 308-311.

CHAPTER 4 Chemically Induced Changes in the Behaviour of Cementing Tailings Backfill in Shaking Table Test (Paper II)

Accepted for publication in the Journal of Rock Mechanics and Geotechnical Engineering (in press).

Imad Alainachi, and Mamadou Fall

4.1 Abstract

Cemented paste backfill (CPB) is extensively used for underground mine support and/or tailings management. However, CPB behavior under cyclic loadings might be affected by the chemistry of its pore-water, which often contains sulphate ions. Till today, no studies have addressed the effect of sulphate on the response of CPB to cyclic loadings by using shaking table technique. This manuscript presents new findings of assessing the effect of the sulphate in the pore water of CPB on its geotechnical response to cyclic loading by using shaking table. CPB mixtures were prepared (with and without sulphate), poured into a flexible laminar shear box, cured to 4.0 hours, and then exposed to cyclic loading using 1-D Shaking table. Several parameters (e.g. pore water pressure, settlement, lateral deformation, acceleration, electrical conductivity, effective stress, liquefaction susceptibility etc.) were monitored or determined before, during, and after shaking. Obtained results indicate that the sulphate-bearing CPB cured to 4.0 hours can be prone to liquefaction under the studied conditions. However, sulphate-free CPB samples are resistant to liquefaction. These results are expected to contribute to a better understanding of the effect of water chemistry on the cyclic behavior of CPB, consequently enhancing the cost-effective design of CPB structures.

Keywords: Cemented paste backfill; Liquefaction; Shaking table; Tailings; Mine; Sulphate

4.2 Introduction

Mining is one of the industries that have been significantly influencing the world economy. For instance, in 2017, mining activities produced total revenue of around 20 billion USD in Canada, and around 600 billion USD around the world (Statista 2019). However, these activities may involve several environmental, economic, and safety challenges, such as the production of huge quantities of mining solid wastes like tailings, that become a potential source of environmentally harmful substances or processes (e.g. acid mine drainage, heavy metals) if they are improperly deposed. Also, mining extraction creates large underground openings (stopes) that expose the surrounding areas to several geotechnical hazards, such as ground subsidence. Moreover, the safety of people in the mine workplace and the surrounding area can be endangered owing to the

instability of these underground openings beside the economic damages of the failed mine ground (Ghirian and Fall 2015, Aldhafeeri et al. 2016).

One of the solutions to deal with these challenges was developed by reusing these mine wastes (tailings) and mixing them with certain percentage of water and binder materials (e.g. cement). This mixture is called cemented paste backfill (CPB). This novel method of waste management allows large amount of mining wastes (tailings) to be returned to the mine stope. It can also improve the short and long-term stability of the stopes besides ensuring the safety of the workers in the mine and the neighboring areas (Landriault et al. 1997, Abdul-Hussain and Fall 2012, Thompson et al. 2012, El Mkadmi et al. 2014). CPB is considered as a fine-grained (silt) soil undergoing cementation from a geotechnical point of view.

Typically, CPB mixture consists of 70% - 85% of tailings, fresh or mine processed water, and often 3% - 7% (by total weight of solid) of hydraulic binder (usually cement). These components are generally mixed and prepared in paste backfill plant usually located on the mine surface. Afterwards, the prepared paste is delivered into the mine stope by gravity and/or pumping (Ercikdi et al. 2009b, Aldhafeeri and Fall 2016, Haiqiang et al. 2016, Li and Fall 2016, Walske et al. 2016, Xue et al. 2020). CPB is extensively applied in mine backfilling as it can be produced and delivered to the mine stope in a short period, leading to complete the stope backfilling process in a matter of days, whereas it might take weeks or months with older backfilling methods. This allows additional revenue to be generated (Ercikdi et al. 2009a, Thompson et al. 2009, Yilmaz et al. 2009).

There are several occasions at which the underground mines can be exposed to cyclic loadings. The origins of these cyclic loadings are either natural earthquakes or mining-induced seismic events. Mining-induced seismic events include many sources; fault slip (earthquake), rockburst (violent ejection of rock into mine opening), pillar burst, bump (sudden slip of a quasi-viscous seam, such as coal at great depth or a tremor of unknown origin), and outburst (sudden violent ejection of coal into mine opening). They also include pillar punching, disturbance of geological structures due to active longwall mining, failure of overburden strata, and events of coal bursts (Hasegawa et al. 1989, Ahn et al. 2017). The high rate of volume extraction and the depth of mining increase the frequency and severity of mine-induced seismic events (Hasegawa et al. 2009). Due to the low availability of ores in shallow depths and the increase in the rates of the greater volume extraction, it is noted that underground mining operations around the world have significantly increased with greater volume and at greater depths. Thus, more severe and/or frequent seismic events are expected, so the risk of cyclic-induced liquefaction of CPB structures at the early ages could increase. Liquefaction-induced failure of CPB structures can cause injuries and/or fatalities in the mine workers and the surrounding public besides having negative environmental impacts and economic damages (Poulos et al. 1985, Fall and Samb 2008, Abdelaal 2011, Becker et al. 2014). Therefore, understanding liquefaction potential of CPB under cyclic loading conditions at the early ages is critically important for a cost-effective and safe design of CPB structures.

Nevertheless, only a limited number of experimental studies (e.g. Saebimoghaddam 2010, Abdelaal 2011) have been conducted to assess the behavior and liquefaction potential of early aged CPBs under cyclic loading conditions. Moreover, all these previous studies examined the cyclic behavior of CPB by applying cyclic loading on small-size CPB samples using common small cyclic triaxial test apparatus (Saebimoghaddam 2010, Abdelaal 2011). None of these previous studies have evaluated the effect of sulphate (present in the pore water of CPB) on the response of CPB to cyclic loading.

Previous studies have concluded that they are several sources of sulphate in CPB systems. These sources include, (i) the oxidation of sulphide minerals (such as pyrite) that are commonly present in hard rock tailing materials; (ii) the mine processing water used as the mixing water in CPB preparation; (iii) sulphur dioxide and air method used in the elimination of cyanide in gold mines; and (iv) chemical additives (such as gypsum and anhydrite) that are often added to the clinker to control the cement setting (Ercikdi et al. 2009b, Pokharel and Fall 2013, Ercikdi et al. 2017, Aldhafeeri 2018). Several previous studies (e.g. Fall and Pokharel 2010, Li and Fall 2016) were undertaking on the sulphate-induced changes in the mechanical or geotechnical behavior of CPB under static loading conditions. These studies have revealed that the sulphate ions in the pore water of CPB can significantly deteriorate its static mechanical properties (strength), and thus jeopardize its mechanical stability. However, the fundamental question whether the sulphate ions in the pore water of CPB can deteriorate its liquefaction resistance when subjected to cyclic loadings still remains unanswered. There is a need to address this knowledge gap, since CPB often contains sulphate ions, which are commonly originated from the mine processed water (used as mixing water) and/or the tailings as noted above.

In addition to the facts mentioned above, no study has been conducted to assess the behavior and liquefaction potential of sulphate-bearing CPB by using shaking table testing techniques. Shaking table has become a valuable tool to assess and comprehend the cyclic response of geomaterials and engineering structures since the mid of the past century despite its high cost and the difficulty in reproducing or simulating the in situ stress (Moncarz and Krawinkler 1981, Bairro and Vaz 2000, Ngadimon 2006). Nowadays, shaking tables are being used in numerous researches. For instant, numerous studies, such as (Bairro and Vaz 2000, Prasad et al. 2004, Dungca et al. 2006, Ueng et al. 2006, Chen et al. 2013, Mohamed 2014, Guoxing et al. 2015, Komak Panah et al. 2015), have evaluated the behavior and liquefaction potential of natural soils subjected to cyclic loadings, where only few researches (e.g. Poulos et al. 1985, James et al. 2003, Pépin et al. 2009, Özgen et al. 2011, Pépin et al. 2012a, Pépin et al. 2012b) have used shaking table to assess the cyclic behavior of tailings (without cement). Nevertheless, there are no studies to date that have been conducted to assess the effect of sulphate on behavior and liquefaction potential of early aged tailings undergoing cementation under cyclic loadings by using shaking table.

Accordingly, this study aims at using shaking table technique to understand the effect of the chemistry of the pore water (sulphate content) of hydrating CPB material on its geotechnical behavior and response, particularly liquefaction potential, at the early ages during cyclic loadings.

4.3 Materials and Equipment Used in the Experiment

4.3.1 Materials

Silica Tailings (ST), which is synthetic tailings material (manufactured by the U.S. Silica Co.) made of ground silica, was used in this study as the key component of CPB mixtures. The grain size distribution of ST is similar to the average grain size distribution of nine mine tailings (9MT) extracted from nine different mines in eastern Canada (Figure 4.1). The minerals of the ST are essentially made of quartz, which is the predominant mineral in Canadian hard rock mine tailings. ST was selected in this study thanks to the high percentage of silica (99.8% SiO_2) within ST, which makes ST a chemically inert material and reduces the uncertainties related to the use of natural tailings to a minimum level by minimizing/controlling the potential chemical interactions of the tailings with other ingredients in the CPB mixture (Carraro et al. 2009, Fall et al. 2010, Aldhafeeri and Fall 2016, Haiqiang et al. 2016). Physical properties of the tailings used in this study have been illustrated in Figure 4.1 and Table 4.1.

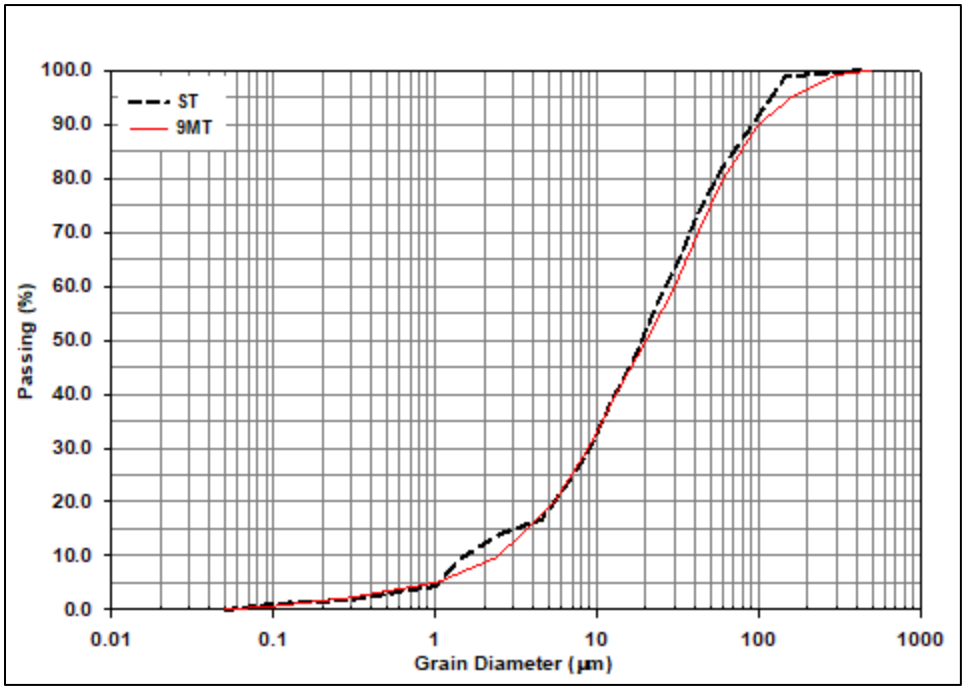

Figure 4.1 Grain size distribution of the silica tailing (ST) vs average grain size distribution of tailings extracted from nine Canadian mines (9MT).

Table 4.1 Primary physical properties of the tailings

Tailings	Gs	D_{10} (μm)	D_{30} (μm)	D_{50} (μm)	D_{60} (μm)
ST	2.7	1.9	9.0	22.5	31.5

To improve the mechanical properties of CPB, sufficient amounts of binder, such as Portland cement (PC), are usually added to a mixture of tailings and water. In this study, the binder agent used in the preparation of CPB mixtures is Portland cement type I (PCI) (Table 4.2), which is the most frequent binder used in the preparation of CPB worldwide. Tap water was used as mixing wat.

Table 4.2 Primary physical and chemical properties of the Portland cement type I (PCI)

Gs	SSA(1) (m^2/g)	Ca (wt%)	Si (wt%)	Al (wt%)	Fe (wt%)	Mg (wt%)	S (wt%)	Si/Ca
3.15	1.32	44.9	8.4	2.4	1.9	1.6	1.5	0.2

* Specific Surface Area

4.3.2 Preparation of Paste Backfill Mixture

In this study, two CPB specimens were prepared. In both specimens, ST was mixed with PCI (4.5 wt%) and water, with water-cement ratio (w/c) of 7.6. CPB specimens were mixed for 10 min in order to obtain homogenous mixture. The degree of water saturation (S) of the prepared CPB was determined to be equal to 100%. Also, the slump of the prepared backfill mixture was tested according to (ASTM C143/C143M-15a 2015), and it was found to be equal to 18 cm, which is one of the most frequent slump values being used in paste backfill operations in Canadian mines. In order to determine the effect of the chemistry of mixing water, sulphate salt (FeSO4 7H2O) was added to one of the CPB specimens. The initial content of the chemical additive was determined to be 5000 ppm. The other CPB specimen was prepared without adding sulphate.

Afterwards, CPB mixtures were poured into the developed laminar shear box (described below). To avoid changes in water content due to evaporation, laminar shear box with CPB mixtures was sealed and kept in a room with stable temperature (~20^o C) for curing until reaching the testing age of 4 hours. It should be underlined that, after its placement, the CPB specimen is expected to undergo some self-weight consolidation. This is because the self-weight pressure of the CPB material can induce consolidation of the pore voids generated due to self-desiccation, as observed in previous studies (e.g. Ghirian and Fall 2014). Detailed testing program is described in Section 4.4.

4.3.3 Shaking Table

Dynamic loading was simulated in this study by applying series of one-dimensional (longitudinal) sinusoidal cyclic motion on the CPB samples. In this regard, the shaking table of the University of Ottawa was used (Figure 4.2).

The platform of this shaking table is around ~1200 mm × ~1060 mm with a maximum base shear capacity and displacement limit of 27 kN and 120 mm, respectively. The shaking ranges from 1 to 17 Hz and is driven by a digitally controlled hydraulic actuator (Mohamed 2014).

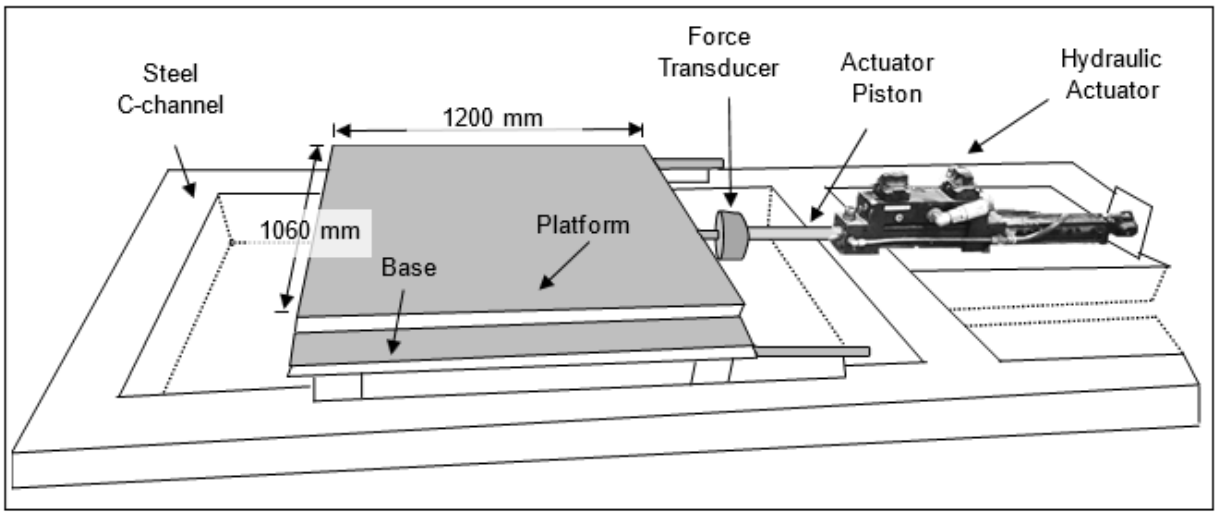

Figure 4.2 Shaking table used in this study

In order to evaluate the cyclic behavior of CPB using the shaking table, a Flexible Laminar Shear Box (FLSB) (Figure 4.3) was used. The FLSB was designed and built at the Faculty of Engineering of the University of Ottawa for this research program.

The FLSB consists of 30 horizontal laminas, made of aluminum alloy box sections of 3.17 cm × 3.17 cm, with inner dimensions of each lamina of 75 cm × 75 cm. In order to ensure the independent movement of each lamina, the FLSB was designed to have a clearance spacing of 0.2 cm between each lamina (2 mm gap between every 2 adjacent laminas). Accordingly, the total capacity of assembled FLSB is 75 cm × 75 cm × 1000 cm.

To contain/hold the CPB mixture, a flexible polyethylene membrane with a maximum thickness of 0.5 mm was placed inside the FLSB. Owing to its high flexibility, the membrane shows no (or negligible) effect on the movement of the FLSB (Mohamed 2014). The FLSB and the membrane were securely attached to the platform of the shaking table. The prepared CPB mixture was poured into the FLSB, with a final dimension of each tested CPB sample of 75 cm × 75 cm × 70 mm.

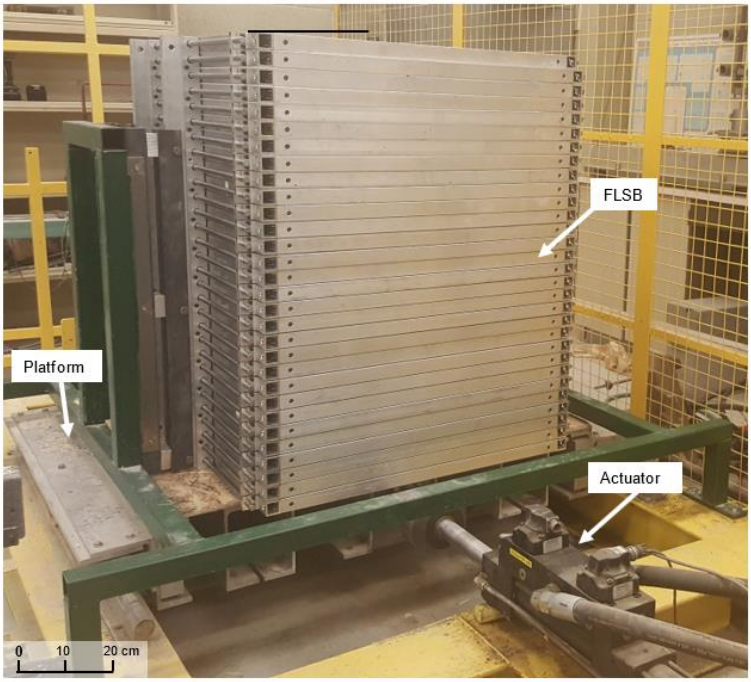

Figure 4.3 Flexible Laminar Shear Box (FLSB) used in this study

Numerous instruments or sensors were placed at different depths within the CPB model (FLSB and its content) as shown in Figures 4.4 & 4.5 and are described below.

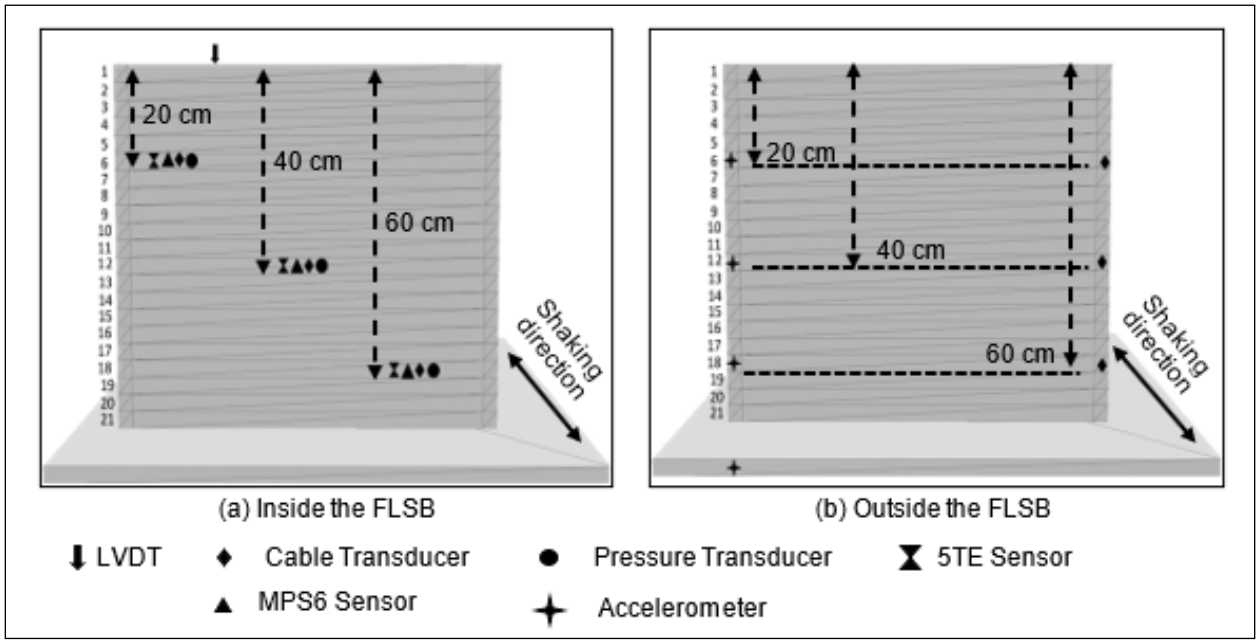

Figure 4.4 Schematic view of the FLSB and instruments locations.

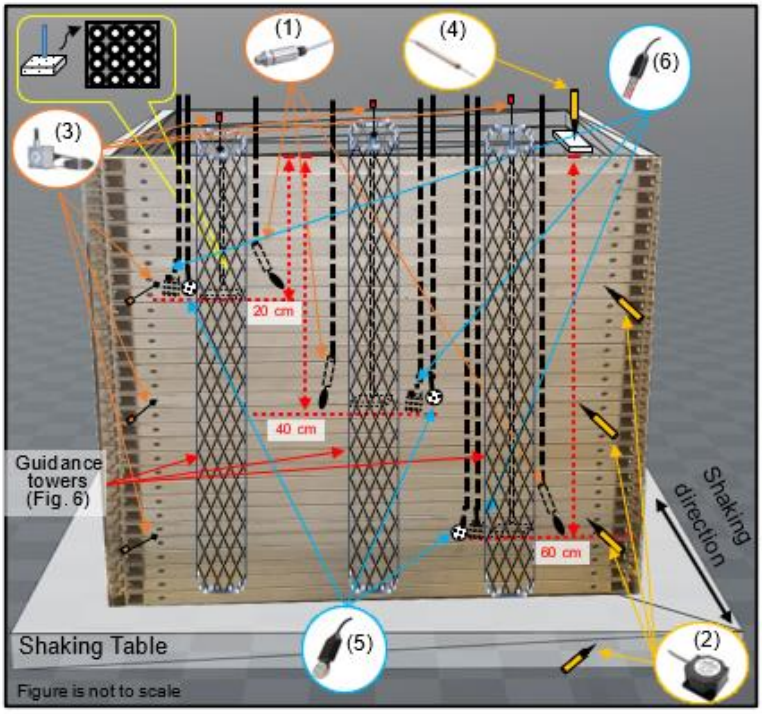

Figure 4.5 Instrumented FLSB: (1) Pressure transducers, (2) Accelerometers, (3) Cable transducers, (4) LVDT, (5) MPS6 sensors, and (6) 5TE sensors.

- Pressure transducers (Item 1 in Figure 4.5) were used to monitor the change in pore-water pressure before, during, and after applying the dynamic load. These transducers were placed at different depths (20 cm, 40 cm, and 60 cm) of the CPB samples inside the FLSB. The pressure transducers of PX309 series (-15 to +15 PSI range and ±0.25% static accuracy) were used in this regard. The dimensions of each transducer was 7.6 cm (length) × 2.2 cm (diameter).

- Accelerometers (Item 2 in Figure 4.5) were used to measure the shaking acceleration. Endevco – 7593A accelerometer with a full-scale range of ±2g and frequency response of 0 – 50 Hz were used and attached to the external side of the FLSB, and screwed with the lamina that is related to each testing depth of (20 cm, 40 cm and 60 cm). In addition, another accelerometer was attached (screwed) to the shaking table to monitor its acceleration. The dimension of each accelerometer was 1.5 cm (length) × 1.5 cm (width) × 1.1 cm (height).

- Cable transducers (Celesco SP2-12 compact string with 317 mm range, and essentially infinite resolution (Item in Figure 4.5) were used to measure:

  a. The horizontal displacement of the CPB sample at different depths (20 cm, 40 cm, and 60 cm). These transducers were attached to the outside of the FLSB at the depth related laminas.

b. The vertical displacement of the CPB sample at different depths of 20 cm, 40 cm, and 60 cm. These transducers were attached to thin metal rods connected to 20 mm thick, 20 mm × 20 mm, lightweight, perforated plastic plates that were installed at the three different depths within the sample. These plates were perforated to minimize its displacement due to seepage pressure. These metal rods were installed within cylindrical guidance towers (Figure 4.6) (made of thin metal mesh sheets) in order to avoid unwanted movement/tilting of these metal tubes during shaking process. Guidance towers were connected to the shaking table in order to avoid being a reinforcement factor and to allow the whole system to follow the same motion rhythm.

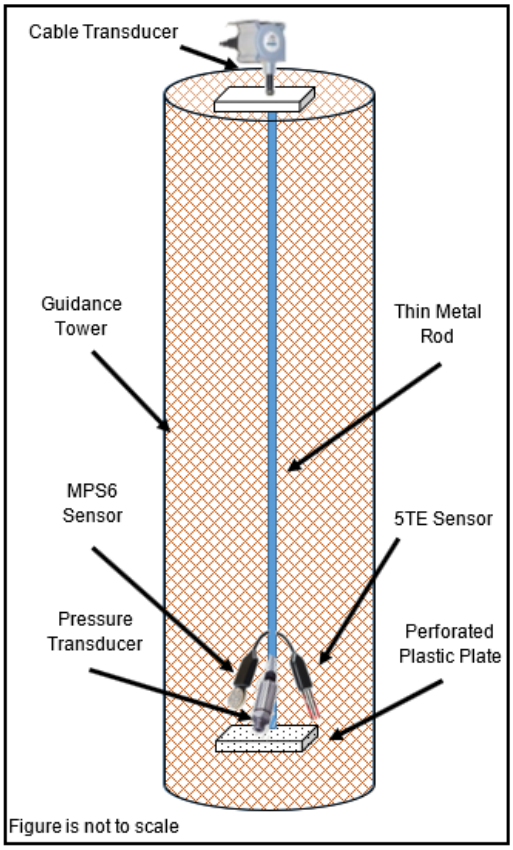

Figure 4.6 Schematic view of the guidance towers and related instrumentation setup.

- Linear variable differential transformer (LVDT) (Item 4 in Figure 5) was used to monitor the vertical displacement of the surface of the CPB sample. In this regard, HCD-1000 LVDTs of 2.5 cm range were used.

- Suction sensors (Item 5 in Figure 4.5) were used to monitor the suction development with time during CPB curing duration. Dielectric water potential sensors (ECH2-MPS6 sensors) that were designed to measure soil water potential were installed at different depths (20 cm, 40 cm, and 60 cm) within the sample. Measurement range of these sensors is -9 to -100,000

kPa with a resolution of 0.1 kPa and its accuracy is ±10% of reading + 2 kPa, from -9 to -100 kPa. The monitoring of suction also enables to assess the self-desiccation of CPB.

- VWC/EC/Temp. sensors (Item 6 in Figure 4.5) were used to monitor the changes in electrical conductivity (EC), the volumetric water content (VWC), and temperature. The ECH2-5TE sensor was used. This sensor measures electrical conductivity (EC) in the range of 0-23 dS/m with the accuracy of ±0.1. It measures volumetric water content (VWC) in the range of 0-80% with the accuracy of ±0.01 from 1 to 40% and the accuracy of ±0.15 from 40 to 80%, whereas the temperature measurement accuracy is ±1°C. These sensors were installed at different depths (0.20 m, 0.40 m, and 0.60 m) within the sample. Changes in EC reflect the rate of ion movement due to the chemical reactions between cement and water. Monitoring EC is an effective way to assess the cement hydration progress and the related structural changes (Li and Fall 2016). On the other hand, monitoring the VWC enables to assess the self-desiccation of CPB (capillary water consumed by the cement hydration) as well as the water flow within the CPB mass. The monitoring of the temperature provides valuable information about the progress of the cement hydration.

The pressure transducers, multi-function sensors, 5TE, and suction sensors, MPS-6, were connected to the guidance towers to avoid any changes in their positions. Transducers, accelerometers and LVDT were connected to signal conditioning and Data Acquisition Systems (DAQS), while 5TE and MP6 sensors were connected to Decagon Em50 series data loggers. DAQS and Em50 were connected to computer in order to record/analyze the required data at almost 1 sec interval during shaking and 10 min interval before and after shaking. Furthermore, digital camera was used to record each step of the testing program (mixing, installation, and shaking operation).

4.4 Testing Program and Procedure

The main goal of the testing program is to assess the influence of the chemistry of mixing water on the behavior of CPB material during shaking. It should be underscored that the objective is not to evaluate the cyclic behaviour of CPB structure, but rather of the CPB material, with sulphate. Indeed, simulating the cyclic response of a CPB structure that can be up to 100-120 m high by using shaking table testing technique needs the use of an extremely large-scale shaking table testing facility to consider a reasonable height or the full size of the CPB structure and/or its complex in situ stress, which is an extremely or unrealistic costly approach, or to properly scale down the parameters of the model experiment based on the similitude laws. However, it is not possible to ensure that all or key factors meet the similitude laws in the 1-g gravity field, if a full field scale prototype model is considered, due to complex field loadings conditions to which a CPB structure may be subjected. Though the CPB material with sulphate was assessed in this research, gaining insight into the response of sulphate-bearing CPB material to cyclic loading will enable to gain an understanding of the effect of sulphate on the cyclic behaviour of CPB structure as well as develop future constitutive samples to describe the cyclic behavior of hydrating CPB.

Experimental testing program carried out in this study has been summarized in Figure 4.7 and Table 4.3 and is discussed below.

4.4.1 Shaking Table

4.4.1.1 Cyclic parameters and test conditions

To better simulate a cyclic event, related cyclic parameters or test conditions have to be determined before conducting a shaking table test. These parameters include Horizontal Displacement Amplitude (HDA), Sinusoidal Loading Frequency (SLF), Shaking Peak Horizontal Acceleration (SPHA), and Shaking Duration (SD). Figure 4.7 shows the experimental program carried out and the testing conditions, whereas Table 4.3 summarizes the testing program.

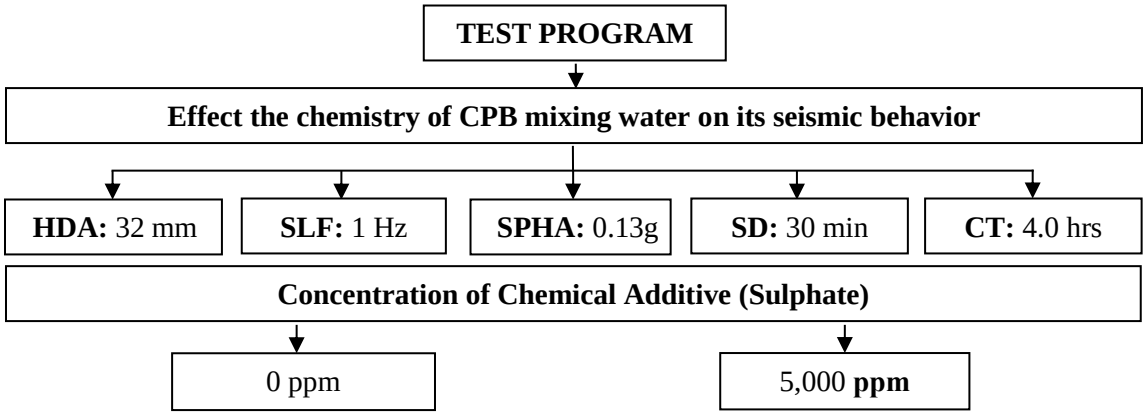

HDA : Horizontal Displacement Amplitude
SLF : Sinusoidal Loading Frequency
SPHA : Shaking Peak Horizontal Acceleration
SD : Shaking Duration
CT : Curing time

Figure 4.7 Flow chart of the experimental program and testing conditions.

Table 4.3 Summary of the testing program

Test	CPB Material	Sulphate (ppm)	HDA (mm)	SLF (Hz)	SPHA	SD (min)	CT (hrs)	PLMD (hrs)
1	CPB without sulphate	0	32	1	0.13g	30	4	24
2	CPB with sulphate	5000	32	1	0.13g	30	4	24

HDA : Horizontal Displacement Amplitude
SLF : Sinusoidal Loading Frequency
SPHA : Shaking Peak Horizontal Acceleration
SD : Shaking Duration
CT : Curing time
PLMD : Post Loading Monitoring Duration

Despite the fact that they might not all reflect the real situation of a seismic event, the values of the testing parameters were modified to accommodate some experimental limitations.

These limitations include the maximum capacity of the shaking table and the sensitivity/limitation of the used monitoring instruments. Hitherto, this modification process is often used in liquefaction research (Ishihara 1996). Thus, shaking table tests were conducted in this study using a dynamic load that was applied in one-dimensional signal, a uniform amplitude, and constant frequency.

The shaking table tests were performed in this study by using a sinusoidal loading frequency of 1 Hz. The selected applied frequency herein was based on previous liquefaction studies (e.g. Ishihara et al. 1981, James et al. 2003, Ueng et al. 2010, Pépin et al. 2012a, 2012b, Geremew and Yanful 2013) and compatible with the capability of the used sensors in terms of the monitoring. Moreover, past studies have concluded (e.g. Sriskandakumar 2004, Srilatha et al. 2013) that the magnitude of loading frequency applied in laboratory seismic tests under undrained conditions has a negligible influence on the response of the tested material. The shaking table tests were conducted in the current study under undrained conditions.

The peak ground acceleration in this study was selected to be 0.13g. This acceleration is equal to the acceleration that was recorded in the Saguenay earthquake 1988 in Quebec (Canada) (Tuttle et al. 1990) (it should be stressed that only the peak acceleration corresponds to the peak of Saguenay Earthquake, not the whole time series). Despite the fact that the strongest mining induced ground motion in north eastern Ontario (Canada) has occurred in 2006 with a ground acceleration of 0.0027 (Atkinson et al. 2008, Natural Resources Canada 2019), the acceleration of 0.13g was selected based on the fact that tailings may liquefy when they are exposed to a ground motion with peak horizontal ground acceleration that exceeds 0.05g (Carter 1988, James et al. 2003).

Table 4.4 Selected cyclic parameters used in the present study and previous studies

Parameter	Values used in previous studies [a]	Values used in the present study
Horizontal Displacement Amplitude	10 - 80 (mm)	32 (mm)
Shaking Peak Horizontal Acceleration	0.1g – 1.0g	0.13g
Sinusoidal Loading Frequency	0.1 - 50 (Hz)	1 (Hz)
Shaking Duration [b]	3 – 2,000 (sec)	1,800 (sec.)
Post loading Monitoring Duration	15 (min) – 36 (hr)	24 (hr) [c]

[a] Such as (James et al. 2003, Prasad et al. 2004, Ueng et al. 2006, Pépin et al. 2009, 2012a, 2012b, Özgen et al. 2011, Mohamed 2014, Guoxing et al. 2015).
[b] Depends on the material response
[c] After initial casting

As shown in Table 4.4, the cyclic loading (shaking) in this study is carried out for 30 minutes (1800 seconds). Although the recorded earthquakes or mine-induced seismic events do not last that much long (Natural Resources Canada 2019), the duration of cyclic loading in this study is not meant to be representative of the actual duration of earthquake. The duration of 30

minutes was selected to allow good observation of the dynamic behavior of the CPB sample and relative comparisons of their response. This will help better develop future constitutive models to describe the dynamic response of soils undergoing cementation and subjected to chemical attacks. Furthermore, similar duration has been used in several previous researches (e.g. James et al. 2003, Pépin et al. 2012b), and it was found that the cyclic peak of the liquefaction of tailings (without inclusions and/or cement) can be reached in shaking for 1000 seconds (James et al. 2003). As the material used in this study is cementing tailings (CPB mix), shaking duration was selected to range from 1 min to 30 min (60 – 1,800 cycles) depending on material response, and the post loading monitoring duration (PLMD) to continue (depending on material response) for additional 24 hours.

4.4.1.2 Effect of the chemistry of mixing water on the cyclic behavior of CPB

To evaluate the cyclic behavior of fresh CPB material under cyclic conditions besides assessing the effect of the presence of sulphate on this behavior, it was important to apply cyclic loadings (dynamic load) on CPB samples with different sulphate contents. Thus, two CPB mixtures were prepared; one mixture did not have sulphate salt added to the mixing water, and the other mixture was prepared with mixing water that contained 5000 ppm of sulphate. Both samples were then poured into FLSB, securely sealed and kept for curing (for the maturity age of 4.0 hrs) under stable temperature of 25^{o}C. Afterwards, series of shaking table tests were performed on both CPB samples (see Figure 4.7).

4.4.2 Microstructural Analysis

Microstructural analysis was conducted on CPB samples that were prepared with and without sulphate to understand the effect of sulphate on its microstructural evolution. In this study, microstructural analysis included thermal analysis (differential thermogravimetry (DTG) and thermal gravimetry (TG)). The TGA Q 5000 IR from TA Instruments were used in this regard. Before conducting these tests, testing samples (4.0 hours old) were first dried at 45 °C in a vacuum oven up to mass stabilization. The various (dried) samples (about 20 mg each) were heated in an inert nitrogen atmosphere at the rate of 10°C per minute up to a temperature of 1000°C.

4.5 Results and Discussion

4.5.1 Acceleration and Lateral Deformation

In this section, the results of acceleration and horizontal displacement (lateral deformation) at different depths within each tested CPB model are presented with respect to initial content of sulphate (which affects the degree of cementation). The combined results of these two parameters can provide an indication about the shear resistance of the tested material at different depths (Takahashi et al. 2001, Nouri et al. 2006, 2008).

4.5.1.1 Acceleration

Figures 4.8(a-b) and 4.9(a-b) shows the peak acceleration histories at different depths during the shaking event for both CPB samples (prepared without and with sulphate) and cured for 4.0 hours.

These figures indicate that the presence of sulphate and the depth have impact on the measured acceleration values. It can be observed that CPB samples prepared without sulphate show higher peak acceleration values than CPB samples prepared with sulphate, which is more obvious at shallow depths. The recorded acceleration significantly varied with depth for the samples prepared with sulphate, while the variation of acceleration with depth was low for samples that do not contain sulphate. For instance, the peak acceleration of CPB sample prepared without sulphate (Figure 4.8a) was between 0.115g and 0.125g at 60 cm depth (10 cm above the shaking table), around 0.100g - 0.110g at 40 cm depth (30 cm above the shaking table), and 0.090g – 0.100g at 20 cm depth (50 cm above the shaking table) (no phase shift was observed in the comparison of the cycles). On the other hand, for the CPB that contains sulphate, the peak acceleration (Figure 4.8b) at 60 cm, 40 cm, and 20 cm depths was recorded to be around 0.100g – 0.110g, 0.080g – 0.100g, and 0.060g – 0.080g, respectively. Moreover, as it can be seen in Figure 4.9(a-b), the shaking acceleration is significantly reduced within the sample with sulphate (Figure 4.9a) compared with the sulfate free sample (Figure 4.9b).

This decrease in the peak acceleration as the sulphate content within CPB increases can be attributed to the effect of sulphate on the degree of cementation and consequently on the damping ratio. It was documented that the damping ratio increases when the degree of cementation is lower (Acar and El-Tahir 1986, Yang and Woods 2015). Furthermore, previous studies (e.g. Fall and Pokharel 2010, Li and Fall 2018) concluded that sulphate ions inhibit the cement hydration. This inhibition is attributed to the production of ettringite as a result of the reaction of sulphate ions in the pore-water with the C_3A grains of the cement. The ettringite creates a thin coating of anhydrated cement grains, which will slow down the reaction between pore-water and C_3A (Li and Fall 2016). Consequently, there will be a reduction in the degree of cementation within CPB that contains sulphate as compared to the sulphate-free CPB that is cured to the same age. It means that the CPBs that contain sulphate will have higher damping ratio, since the presence of sulphate is associated with lower degree of cementation (cement hydration degree) as evidenced by Figure 4.18 (discussed later). The progress of cement hydration increases the bonds between tailings (soil) particles and consequently reduces the deformation level of the material (Mamlouk and Zaniewski 2011); the less cement hydration degree, the less bonds between tailings particles. The observed significant reduction of acceleration with depth in the CPB prepared with sulphate can be attributed to nonlinearity, shear resistance and stiffness degradation of CPB caused by liquefaction as evidenced by the liquefaction analysis presented in Section 4.5.3. Liquefaction causes a large deformation in the CPB that contains sulphate, in which the cementation effect is still weak due to slow progress of cement hydration (see Figures 4.18). This large deformation will cause more damage in the pore structure within CPB material.

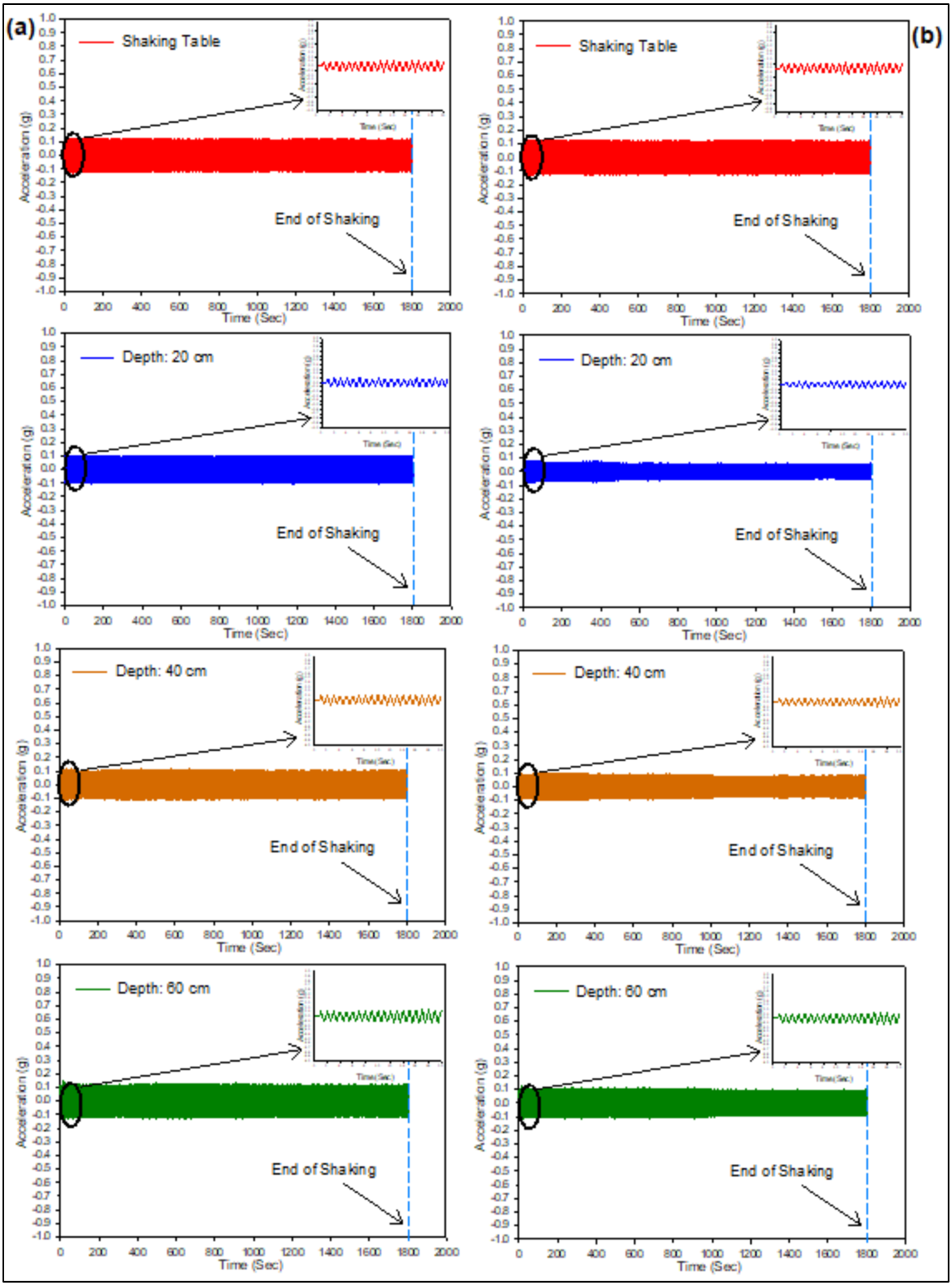

Figure 4.8 Measured peak acceleration histories at different depths vs time for 4.0 hrs-CPB samples prepared: (a) without sulphate; (b) with sulphate.

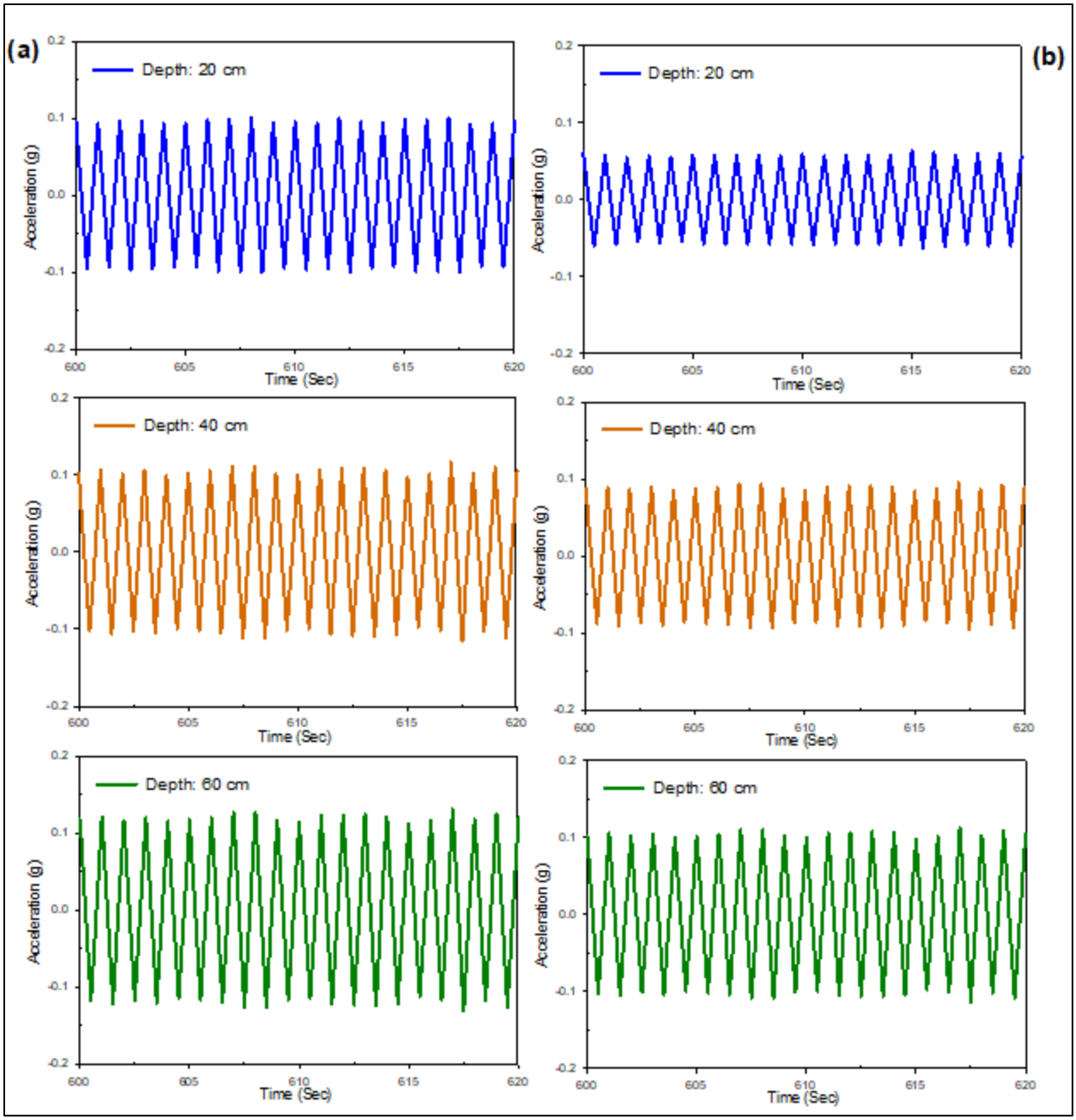

Figure 4.9 Variation in acceleration at different depths after 600 seconds of shaking 4.0 hrs-CPB samples prepared: (a) without sulphate; (b) with sulphate.

4.5.1.2 Lateral (horizontal) displacement

The deformation of liquefiable soils due to shaking-induced liquefaction can be inferred from lateral (horizontal) displacement (Takahashi et al. 2001, Dungca et al. 2006). Indeed, ground shaking will result in a decrease in soil resistance against vibration because of the reduction in effective stress (Takahashi et al. 2001, Dungca et al. 2006).

Figure 4.10(a-b) illustrates the lateral displacement (measured at one side of the laminar shear box) at various depths during the cyclic loading durations for 4 hours aged CPB prepared without sulphate and with sulphate, respectively.

From these figures, two key behaviours can be observed:

(a) In both CPBs, the lateral displacement decreased with the increase in depth. This behavior is consistent with the findings of several previous studies on liquefaction-induced lateral ground displacements in soils (e.g. Motamed et al. 2013, Srilatha et al. 2013) and is related to the increase in material density during shaking as a result of the dynamic densification (compaction) of the tailings particles (Zhu and Clark 1994, Anastasopoulos et al. 2010). However, the change in displacement with depth within the CPB that contains sulphate (Figure 4.10b) was higher than the variation in displacement with depth within the sulphate-free CPB (Figure 4.10a). This increase can be attributed to the effect of sulphate on slowing down the progress of cement hydration, and consequently reducing the CPB solidification. Slower cement hydration means a precipitation of a less amount of cement hydration products (e.g., C-S-H, CH), which plays the main role in increasing the cementation degree or cohesion of the CPB material (Fall et al. 2010, Xue et al. 2020). This argument regarding the decrease in the amount of cement hydration products with sulphate presence is experimentally supported by the results of TG/DTG on cement pastes of CPB, which are presented in Figure 4.18 and will be discussed later.

(b) The magnitude of lateral displacement within sulphate-free CPB was lower in value as compared to the CPB that contains sulphate. This increase in the lateral displacement accompanied by the presence of sulphate is the consequence of the decrease in bonds between the tailings particles with the inhibition of cement hydration progress because of the sulphate ions (Mamlouk and Zaniewski 2011, Li and Fall 2018) (Figure 4.18).

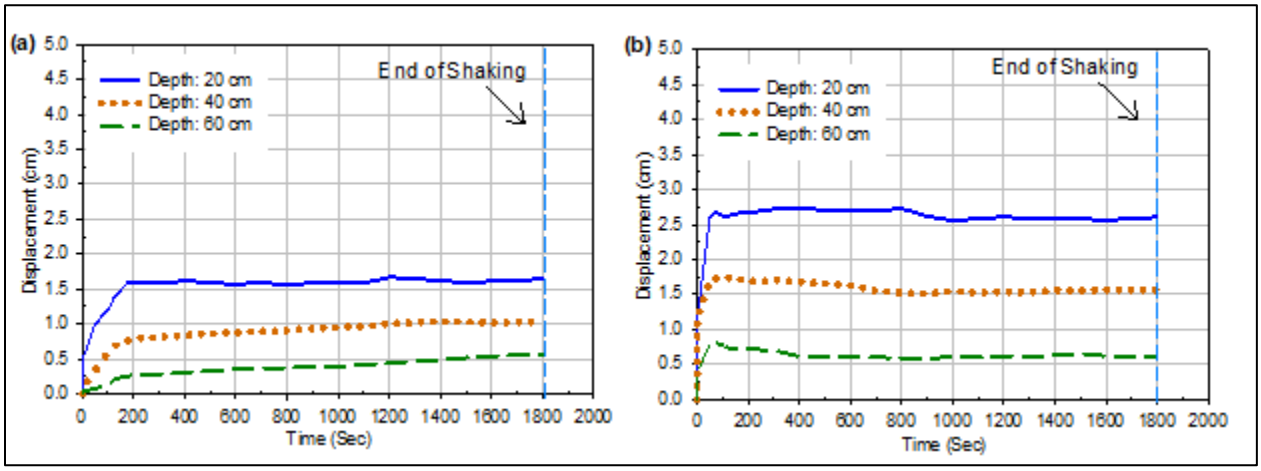

Figure 4.10 Lateral displacement histories at different depths vs times for 4.0 hrs-CPB samples prepared: (a) without sulphate; (b) with sulphate.

Comparative analysis of the results presented in the Figures 8 and 10 suggests that the bonds between particles of 4.0 hours-CPB that contains sulphate were low to resist the cyclic induced shear stress, while those between the particles of the 4.0 hours-CPB without sulphate were stronger and thus had higher shear resistance, which minimizes the acceleration and lateral displacement change. These facts strengthen the assumption that the presence of sulphate within CPB mixture might increase the susceptibility of cyclic loading-induced liquefaction, while the CPB material without sulphate is more resistant to liquefaction during ground movement.

4.5.2 Evolution of Pore Water Pressure, Effective Stress and Settlement

4.5.2.1 Pore-water pressure

Figure 4.11(a-b) illustrates the changes in pore water pressure (PWP) at various depths with time within the sulphate-free CPB (Figure 11a) and CPB that contains sulphate (Figure 4.11b), respectively, before, during, and after shaking (i.e. from the time of casting in the FLSB to about 24 hours).

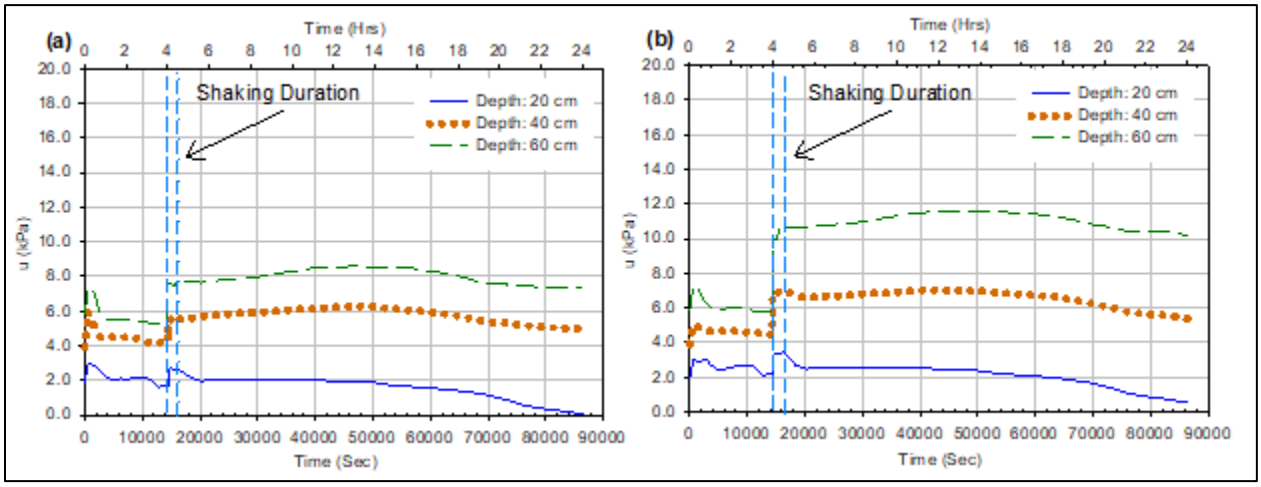

Figure 4.11 Pore water pressure histories at different depths vs times for 4.0 hrs-CPB samples prepared: (a) without sulphate; (b) with sulphate.

(i) Before shaking: during the first 1 hour (3600 sec), after depositing the fresh CPB in the FLSB, PWP rapidly increased in all depths of both 4.0 hours-CPBs. The reason behind this increase is the reduction in the voids volume due to the self-weight settlement, which might reach more than 2% in 4.0 hours after the end of filling process, and the rearrangement of the tailings particles at the very early age (Belem et al. 2016, Yilmaz 2018). Afterwards, PWP decreased in both samples as a result of the water consumption during cement hydration (Helinski et al. 2007, Ghirian and Fall 2014, Scrivener et al. 2015). However, the decrease in PWP within the CPB sample that contains sulphate was lower than the decrease in PWP within the sulphate-free CPB. For instant, after 4.0 hours of curing, there was approximately 27-45% of reduction in PWP within the sulphate free CPB sample, while the reduction in PWP within the CPB sample that contains sulphate ions was about 10.7-28.5%. This observation is consistent with the results of suction monitoring presented

in Figure 4.12(a-b) (discussed later). In addition, the PWP near the surface of the CPB might also be subjected to water evaporation.

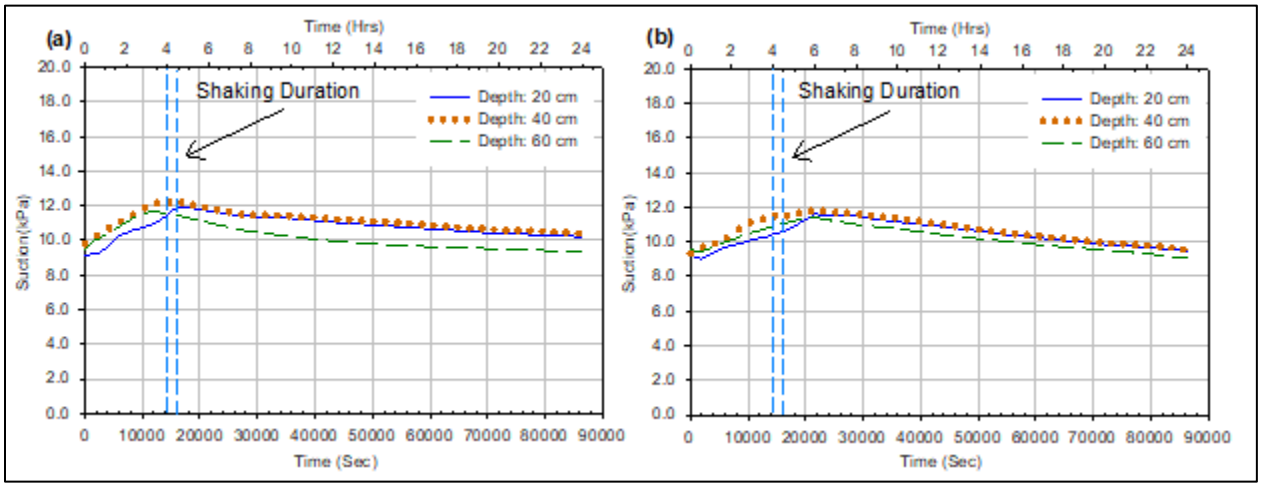

Figure 4.12 Suction evolution at different depths vs times for 4.0 hrs-CPB samples prepared: (a) without sulphate; (b) with sulphate.

(ii) During shaking: when shaking began, as expected, there was a rapid buildup of pore water pressure at all depths within both 4.0 hours-CPB materials until reaching peak values. Also, as expected, the greater depths showed bigger buildup in PWP. This increase in pore water pressure can be attributed to the contractive behavior of the saturated backfill material or particles causing rapid generation of excess pore water (Bouckovalas et al. 2009, Saebimoghaddam 2010, Jefferies and Been 2015, Porcino et al. 2015) (Figure 4.15; will be discussed below). However, the increase in pore water pressure within the CPB sample that contains sulphate was much higher than the increase in pore water pressure within the CPB that does not contain sulphate. This can be attributed to the coupled effect of: (i) the positive impact of curing time on cement hydration, at which the cement hydration consumes more water (self-desiccation), and more cement hydration products will be precipitated as the curing time increases. This strengthens the cementing bonds between the tailings particles, thereby reducing the contraction of the CPB materials (Saebimoghaddam 2010, Ghirian and Fall 2013, Scrivener et al. 2015), and (ii) the negative impact of sulphate ions on the cement hydration processes, which inhibits the progress of cement hydration and reduces the water consumption by the cement hydration (as mentioned above in section 4.5.1.1) (Fall and Benzaazoua 2005, Fall and Pokharel 2010, Li and Fall 2016).

(iii) After shaking: after the shaking, both 4 hours-CPBs exhibited a slight increase in pore water pressure with time at all depths (with different magnitudes) regardless of the progress of cement hydration. This observed slight increase in PWP at these depths may be caused by the settlement or contraction of some tailings particles, which might have been partly in suspension at the end of the cycling loading. This contraction generated additional pore water pressure (Pépin et al. 2009). This slight increase in PWP at these depths was then followed by a gradually decrease in the PWP until the end of the monitoring period. The decrease in pore water pressure observed at all depths

is mainly due to the water consumption by cement hydration (i.e. self-desiccation) (Ghirian and Fall 2013). However, surface evaporation at shallow depths (close to CPB surface) of both samples caused additional dissipation of the pore water pressure to less than the hydrostatic pore-water pressure. This phenomena can be explained by the coupled effect of self-desiccation due to cement hydration and the near surface evaporation as a result of the difference of relative humidity (RH) between the ambient air and the surface of the CPB (Abdul-Hussain and Fall 2012, Ghirian and Fall 2013). To confirm this explanation, the evaporation-induced reduction in water content of a CPB material was experimentally determined in this study by exposing CPB samples (prepared with the same mix components and conditions as the CPB used in this study) to environmental conditions (RH and temperature) similar to those, in which the shaking tests were conducted. It was found that around 60% of the near surface reduction in CPB water content (water loss) was related to evaporation when the CPB sample is placed under the conditions of 20°C temperature and 24% of RH. Moreover, the contribution of the evaporation to the dissipation of the PWP decreases as the depth of the CPB increases. This is in agreement with the lower rate of dissipation of PWP observed at the depths of 40 cm and 60 cm compared to the depth of 20 cm. It should be also underlined, since the CPB is a low permeability soil ($k \sim 10^{-7}$ cm/s), the fluid (water) transport process is slow. Thus, long time will be required to withdraw water from deeper layers (i.e. 40 cm, 60 cm) through evaporation.

4.5.2.2 Effective stress

Figure 4.13 (a-b) presents the vertical effective stress evolution during shaking at different depths of 4 hours-CPBs that were prepared with and without sulphate. During shaking, there was a reduction in these stresses from their initial values in both samples due to the contraction of CPB particles leading to development of excess pore pressure. However, the 4 hours-CPB sample that contains sulphate experienced higher reduction in effective stress as compared to the sulphate-free 4 hours-CPB sample due to the aforementioned effects of sulphate on cement hydration.

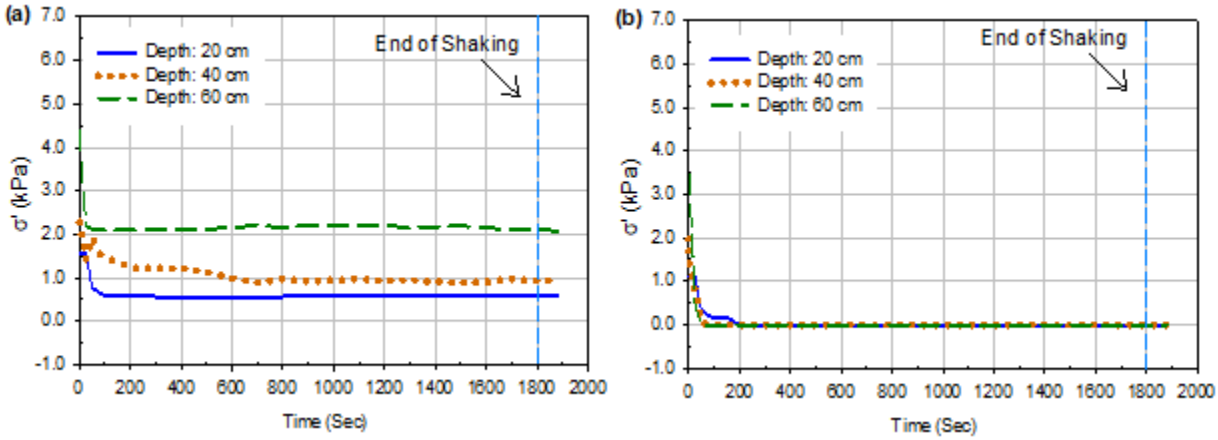

Figure 4.13 Effective stress at different depths vs times for 4.0 hrs-CPB samples prepared:

(a) without sulphate; (b) with sulphate.

4.5.2.3 Vertical displacement (settlement)

The downward displacement (settlement) in soil due to ground shaking gives an indication of the contractive behavior of the particles of liquefiable soil and the increases in the soil density (Ueng et al. 2006, Pépin et al. 2012b). In this study, shaking-induced settlement was recorded in both 4.0 hours-CPB samples, as shown in Figure 4.14(a-b). However, this figure shows that the CPB that does not contain sulphate (Figure 4.14a) shows less significant settlement as compared to the CPB sample that contains sulphate (Figure 4.14b). This observation suggests that the presence of sulphate will reduce the degree of cement hydration, causing higher settlement or contraction (volume change) during shaking. This behavior, which is consistent with the results of PWP measurements and liquefaction analysis discussed in Sections 4.5.2.1 and 4.5.3, respectively, is due to the fact that less cement hydration degree (due to cement hydration inhibition by the sulphate ions) leads to the precipitation of less cement hydration products (see Figure 4.18), thereby decreasing the strength of the CPB material (Fall et al. 2010, Scrivener et al. 2015). Consequently, the dynamic loading-induced contracting behavior or settlement of the CPB becomes higher (Saebimoghaddam 2010, Jafari 2020). From Figure 4.14, it can also be observed that the settlement of 4.0 hours-CPB varied with the measurement depth. The settlement becomes higher in shallow depths. This could be explained by the fact that the CPB material may be slightly less dense at shallower depth due to tailings particles self-weight settlement.

On Figure 4.14b, the recorded displacement at the depth of 20 cm became higher than expected after 1200 seconds because the plastic plate that was installed at this depth was shifted due to the excessive movement.

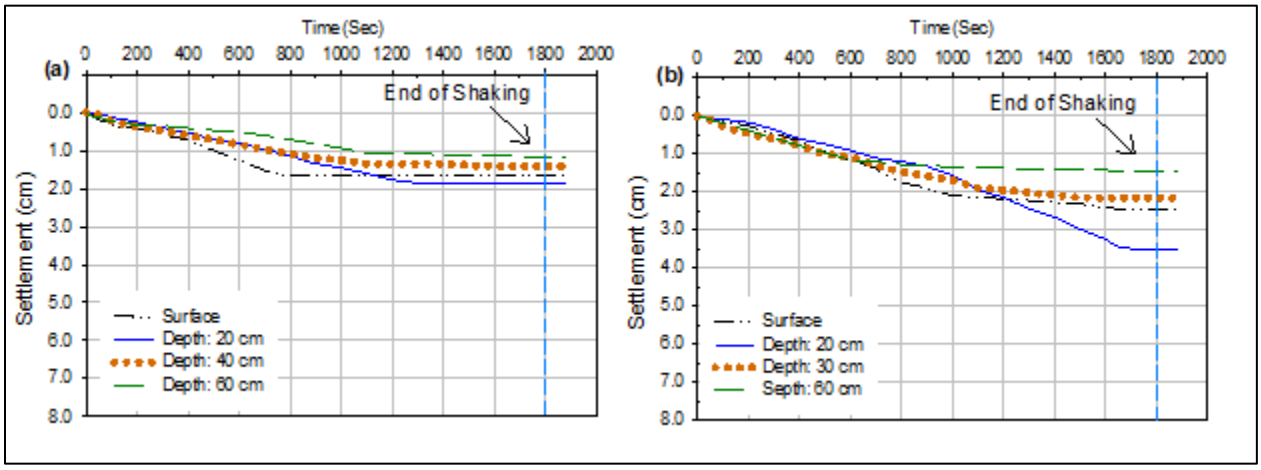

Figure 4.14 Settlement at different depths vs times for 4.0 hrs-CPB samples prepared:

(a) without sulphate; (b) with sulphate.

4.5.3 Liquefaction Analysis

Various liquefaction triggering criteria have been suggested and used to describe or determine soil liquefaction. These criteria comprise strength-based criteria, strain/deformation-based liquefaction

criteria, energy-based liquefaction criteria, and (excess) pore ratio-based criteria. Each of these methods has advantages, but also limitations, as explained in various past studies (e.g. Wu et al. 2004). Moreover, the liquefaction assessment based on the evaluation of the stress-strain relationship, which can be interpreted from the accelerometer measurements, was conducted in previous shaking table tests (Turan et al. 2009). On the other hand, the excess pore-water pressure ratio criteria have been extensively used in assessing the liquefaction potential of soils or tailings, specially in shaking table tests (e.g. Adalier et al. 2003, Shahir and Pak 2010, Cetin et al. 2012, Pépin et al. 2012a, Wang et al. 2019, Bahadori et al. 2020). In this study, the excess pore-water pressure ratio was used as the evaluation factor of soil liquefaction susceptibility. The excess pore-water pressure ratio (R_u) represents the ratio between the excess PWP (Δu) and the initial effective stress (σ'_o). Liquefaction is generally defined if $R_u \geq 1$. However, if $R_u < 1$, there is no liquefaction (Wu et al. 2004).

Excess PWPs developed during shaking at different depths within 4.0 hours-CPB sample prepared without sulphate and 4.0 hours-CPB sample prepared with sulphate are illustrated in Figure 4.15 (a & b), respectively. This figure depicts that the excess PWP developed within both samples varied with depth and shaking time. The pore-water pressure ratios determined during shaking of the sulphate-free 4.0 hours-CPB sample and sulphate-rich 4.0 hours-CPB have been depicted in Figure 4.16 (a & b), respectively.

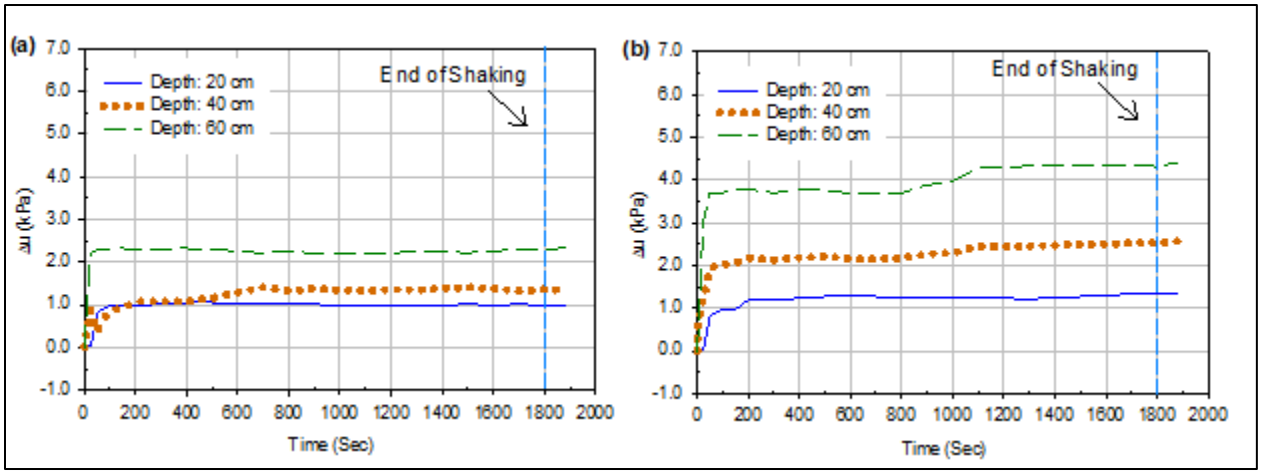

Figure 4.15 Excess pore water pressure (Δu) development at different depths vs times for CPB samples prepared: (a) without sulphate; (b) with sulphate.

It can be seen that 4.0 hours-CPB sample that contains sulphate is susceptible to liquefaction ($R_u \geq 1$) when exposed to cyclic loading, while the sulphate-free 4.0 hours-CPB sample was resistant to shaking-induced liquefaction ($R_u < 1$). In other words, the presence of sulphate in CPB mixing water increases the susceptibility of CPB liquefaction under cyclic conditions. This reduction in liquefaction resistance of CPB prepared with sulphate can be attributed to the combined effects of the following two factors as discussed below: (i) the inhibition of cement hydration process because of the effect of sulphate leading to enfeeblement of self-

desiccation of CPB; and (ii) production of less cement hydration products within the CPB pores due to the inhibition of the cement hydration, which diminishes the cementation or cohesion between the tailings particles, thus reducing the shear strength of the CPB material. These factors obviously result in the increase in the liquefaction susceptibility of the CPB. The aforementioned arguments are supported by the experimental evidence discussed below.

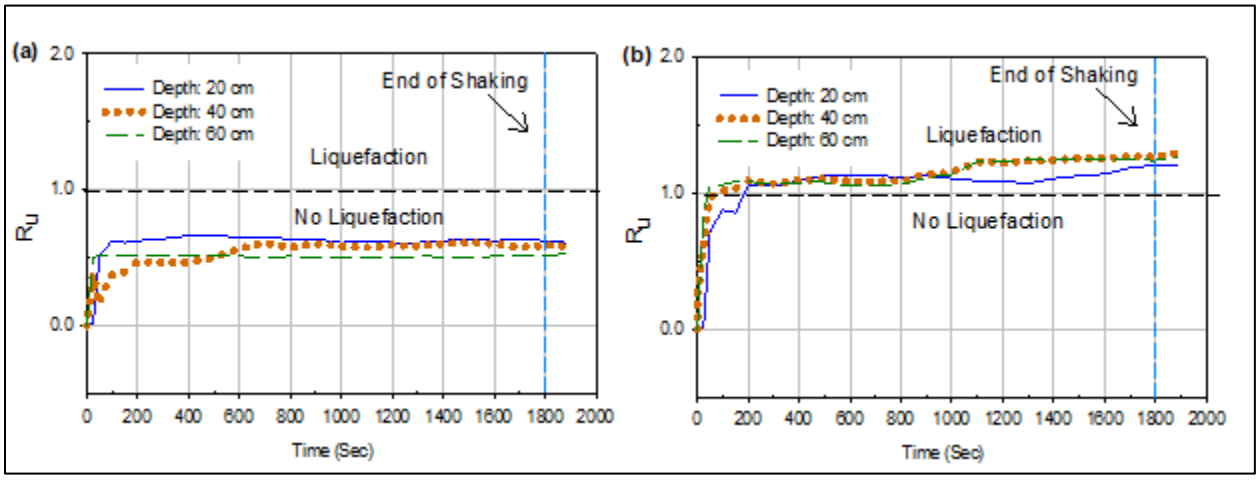

Figure 4.16 Pore-water pressure ratios determined at different depths vs times for CPB samples prepared: (a) without sulphate; (b) with sulphate.

(i) Cement hydration rate

The negative effect of sulphate ions on cement hydration rate is attributed to the reaction of the sulphate anions in the CPB pore-liquid with the C_3A grains of the cement to form ettringite. The ettringite forms a thin coating of anhydrated cement particles, thus prevents the quick C_3A - water reaction (Li and Fall 2016). This will consequently reduce the intensity of the cement self-desiccation within CPB particles, which plays a significant role in the strength of materials undergoing cementation (Persson 1997).

Self-desiccation is the process of shrinkage in pores; consequently, the reduction in the volumetric water content of cemented-based materials, which are seal cured under saturated conditions (Bentz 2008). This will consequently decrease the PWP and/or generate negative pore water pressure (suction) (Ghirian and Fall 2013). Hence, self-desiccation improves the effective stress and strength of these materials (Abdul-Hussain and Fall 2012, Fredlund et al. 2012, Ghirian and Fall 2014). Figures 4.17 (a, b) and 4.12 (a, b), which show the evolution of the volumetric water content (VWC) and suction in the CPB at different depths respectively, support the fact that self-desiccation did take place in both 4.0 hours-CPB samples. It was observed from Figure 4.17 that there was a gradual increase in the VWC in the first hours at all depths of both CPB materials, which reached its peak value after 6 hrs. However, it is evident that the sulphate free CPB material experienced more increase in VWC as compared to CPB material that contains sulphate. For example, between 0.5 hour (the end of filling process) and 6 hours of curing (when VWC reached

its peak), the VWC within the sulphate free CPB sample increased from around 0.3 m^3/m^3 to around 0.7 m^3/m^3, while the VWC within the sulphated CPB sample increased (in the same time period) from around 0.3 m^3/m^3 to around 0.6 m^3/m^3. Accordingly, the less increase in VWC within the CPB material with sulphate indicates the effect of sulphate in inhibiting the self-desiccation process. Afterwards, the VWC slightly decreased and then remained relatively constant until the end of the monitoring period. This increase in VWC is attributed to the self-desiccation induced decrease in the total volume of the CPB since the VWC expresses the ratio of volume of water to the total volume of the soil. Also, the decrease in the amount of water or water content during this period was confirmed by the suction measurements results presented in Figure 4.12, at which a small suction has been recorded in both CPB samples shortly after its disposal into the laminar shear box. Afterwards, there was a gradual increase in suction until reaching its peak after 6hrs. After that, the suction decreased slightly and then remained relatively constant until the end of the monitoring. The evolution of suction in both samples can be attributed to the chemical reactions of the cement hydration, which causes the consumption of water in the capillary pores of CPB (Wang et al. 2016) and reduces the water content in the hydrating backfill or any other cemented soils. This reduction in water content will allow air to enter the pores between tailings or soil particles, generating the air bubbles. As a result, the backfill or soil will turn from saturated condition to partially saturated conditions (Fredlund et al. 2012). The reduction in saturation leads to a decrease in the pore water pressure, in other words to an increase in the effective stress, and thus to an increase in the liquefaction resistance of the CPB. Moreover, the air bubbles that enter inside the pores of a soil will reduce the pores volume, so it will absorb the generated excess PWP and enhance liquefaction resistance (Okamura and Soga 2006). It was also noted that the suction values in the CPB material that contains sulphate were lower than those in CPB material that does not contain sulphate, which provides a strong indication of the negative effect of sulphate on the performance of cement hydration. In other words, this negative effect results in the higher water content and less air bubbles in the CPB that contains sulphate. Thus, the effective stress and effect of air bubbles in absorbing the excess PWP will be reduced in the CPB that contains sulphate, and liquefaction resistant will consequently decrease. It should be pointed out that, as mentioned in the Section 2.3, the suction sensor (ECH2-MPS6) used has a measurement accuracy of ±10% of reading + 2 kPa, from 9 to 100 kPa. Thus, considering the low values of suction obtained (Figure 4.12) and these suction sensor measurement limitations, the evolution of the suction presented in Figure 4.12 should be considered as qualitative.

(ii) Production of less cement hydration products

The production of less cement hydration products in the 4.0 hours-CPB with sulphate as compared to the same sample without sulphate is experimentally supported by the results of the thermal analyses (TG/DTG), as shown in Figure 4.18. In this figure, a comparison of the TG/DTG diagrams between the CPB samples with and without sulphate is shown. The CPB with sulphate results in lower weight loss (TG) and the peaks (DTG) in the 400-500^oC temperature, that means less amount of hydration products in CPB sample due to sulphate (Wang et al. 2016, Xu et al.

2020). The first peak (sudden change in weight) is due to the destruction of the C-S-H, ettringite, and gypsum (Taylor 1990, Fall et al. 2010), while the second peak is associated with the degradation of CH (Li and Fall 2016) and is much lower for the CPB sample that is prepared with sulphate compared to the sulphate free CPB sample. The third peak represents the decomposition of the calcite in the cement (Bian et al. 2019).

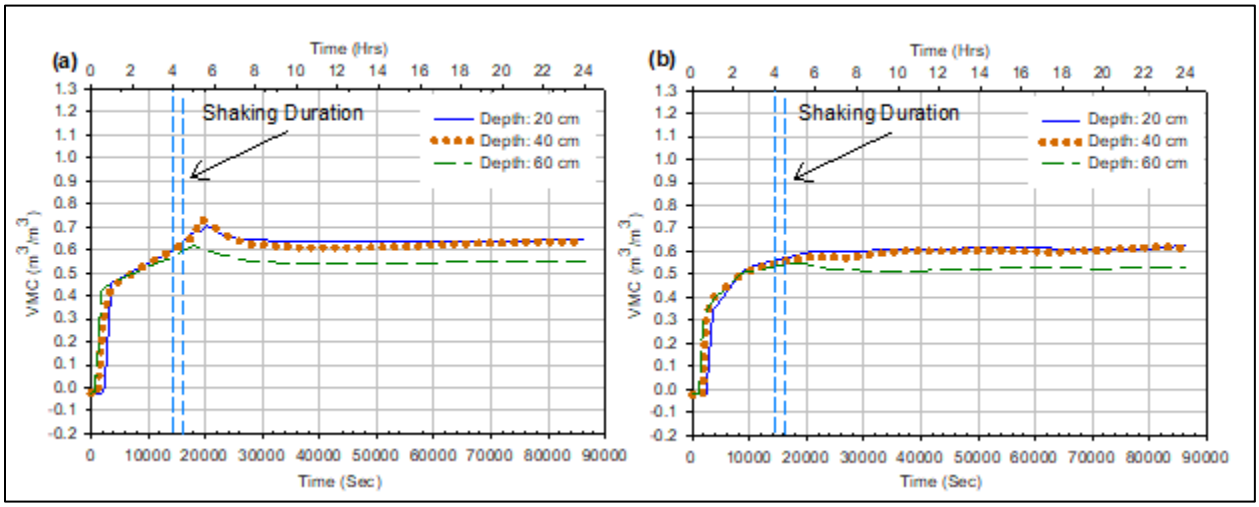

Figure 4.17 Change in volumetric water content at different depths vs times for 4.0 hrs-CPB samples prepared: (a) without sulphate; (b) with sulphate.

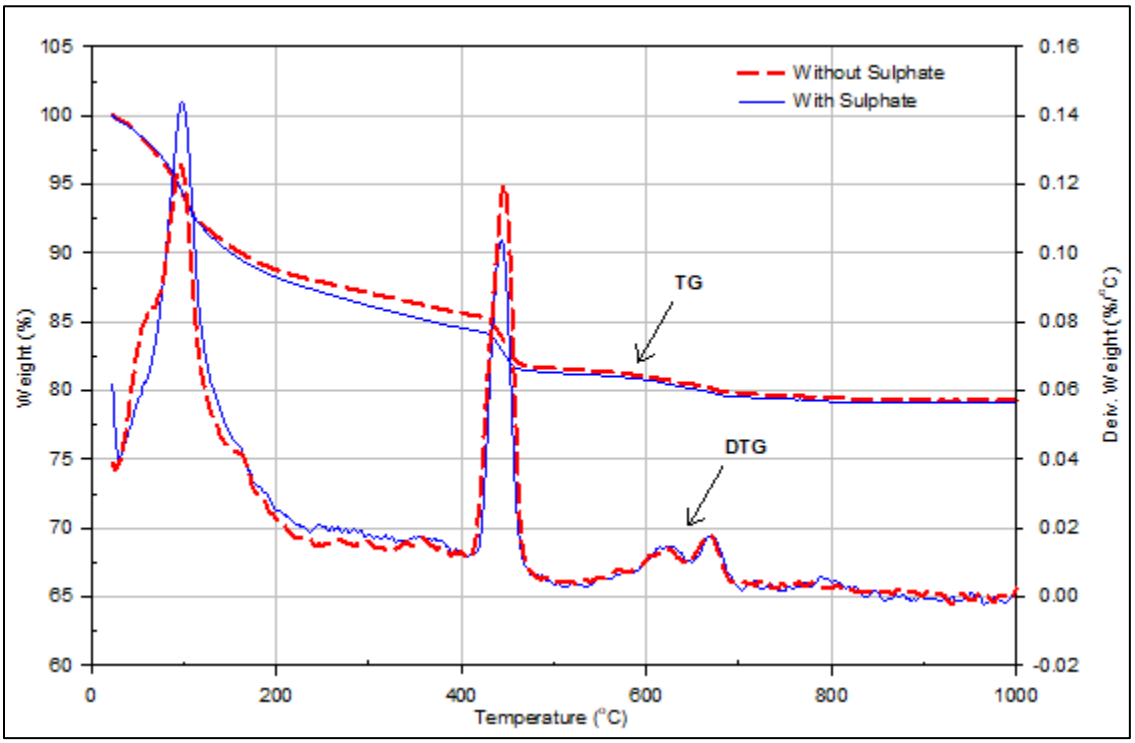

Figure 4.18 Effect of sulphate content on TG/DTG diagrams for 4.0 hrs-CPB samples prepared: (a) without sulphate; (b) with sulphate.

Moreover, Figures 4.19 and 4.20 present the results of the monitoring of the evolution of EC and temperature with curing time progress at different depths of both CPBs, respectively. From these figures, it can be seen that the rate or progress of the cement hydration, in other words the amount of cement hydrations formed within the CPB, is relatively similar at all depths of each CPB sample. However, the presence of sulphate has affected these rates.

For instance, the EC reaches the peak value in the CPB without sulphate (Figure 4.19a) faster than in the CPB with sulphate (Figure 4.19b). Moreover, it was noted that the EC peak value of CPB with sulphate is lower than the EC peak value of CPB without sulphate. According to the working principles of EC sensors, the initial increase in EC refers to the increase in the concentration of ions in the CPB pore water solution due to the dissolution of cement particles. So, the delay in EC to reach the peak value with the presence of sulphate indicates the retardation of cement hydration process, and the lower EC values indicate a reduction in cement hydration intensity (Li and Fall 2016).

On the other hand, by comparing the generation of hydration heat of sulphate-free CPB sample (Figure 4.20a) and CPB sample that contains sulphate (Figure 4.20b), it can be seen that the presence of sulphate reduced the amount of generated hydration heat. It is agreed that the generated heat of hydration is a result of the exothermic reaction of aluminate (C_3A), gypsum, and tricalcium silicate (C_3S) with water to form ettringite and the Calcium silicate hydrate (C-S-H) (Bullard et al. 2011, Ghirian and Fall 2015). Thus, the reduction in the hydration heat generated within CPB samples that contain sulphate may confirm the above stated assumption of the effect of sulphate on the production of less cement hydration products.

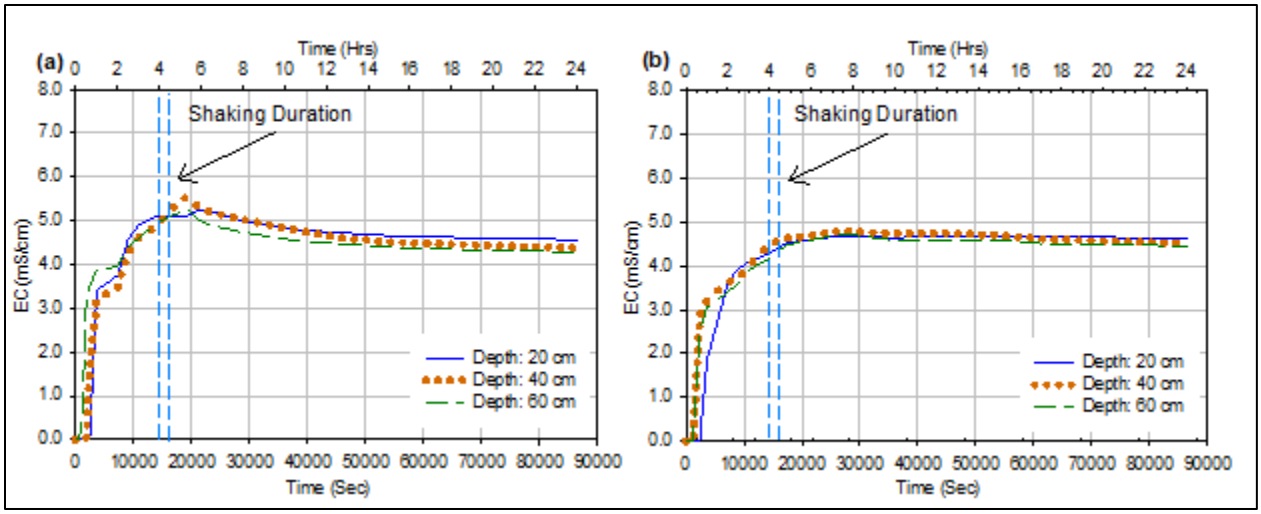

Figure 4.19 Electrical conductivity at different depths of 4.0 hrs-CPB samples prepared: (a) without sulphate; (b) with sulphate.

Thus, this production of less amount of hydration products due the sulphate ions, as demonstrated above, will reduce the cohesion between the tailings particles, thus decreasing the

shear strength of the CPB material as well as increasing the CPB damping ratio. Indeed, the movement (due to shaking) of tailings particles, which did not react with cement (within the sulphate-bearing CPB), will cause high friction between particles and increase the material damping ratio. This assertion and the explanation are consistent with the above discussed results of acceleration and displacement monitoring, such as the evident decrease in the acceleration values within sulphate-free sample. It should be underlined that the impact of the volume of cement hydration products generated or progress of cement hydration on the consolidation behavior of the CPB samples were not assessed in this study. Future study should address it

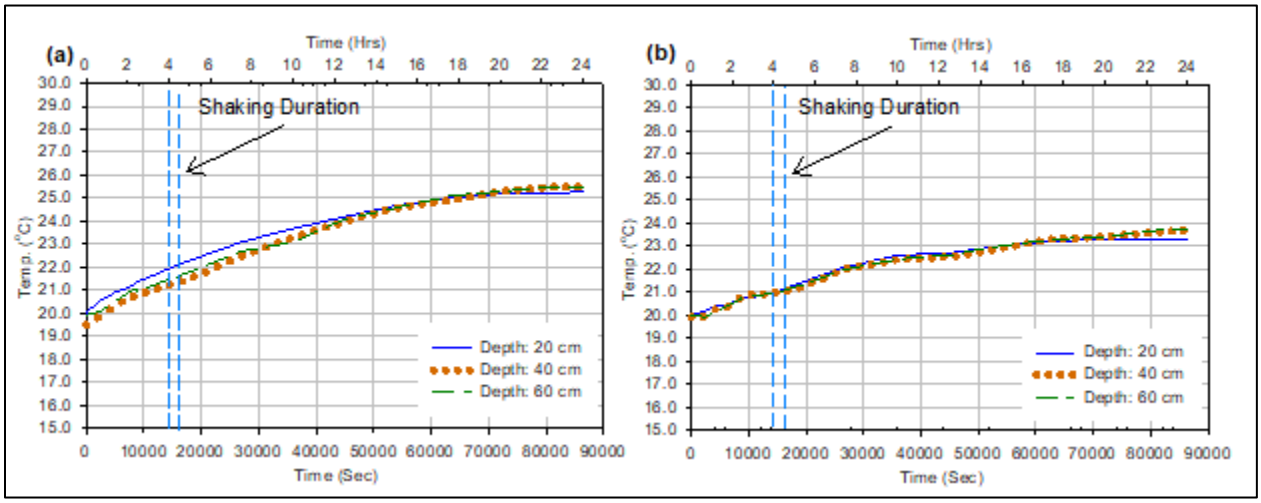

Figure 4.20 Evolution of hydration heat with curing time at different depths vs times for 4.0 hrs-CPB samples prepared: (a) without sulphate; (b) with sulphate.

4.6 Summary and Conclusion

This manuscript has assessed and discussed the effect of the chemistry of CPB pore water (initial sulphate content) on the geotechnical response (e.g. deformation, excess of pore water pressure, effective stress, and liquefaction potential) of paste backfill undergoing cementation to cyclic loadings by using the shaking table testing technique. This assessment was conducted by applying cyclic loading on paste backfills prepared by adding sulphate to the mixing water and without adding sulphate to the mixing water. Both samples were casted in a flexible laminar shear box and securely cured to 4.0 hours. The paste backfills were also instrumented with numerous sets of sensors and transducers to monitor the evolution of several parameters (pore water pressure, suction, lateral and horizontal displacement, acceleration, temperature, and electrical conductivity) before, during, and after shaking. The obtained results show that the presence of sulphate significantly affects the cyclic response of the CPB in terms of acceleration, horizontal and vertical displacement, and excess pore water pressure. Moreover, 4.0 hours old CPB material that contains sulphate can be susceptible to liquefaction, whereas the sulphate-free 4.0 hours old CPB is resistant to liquefaction under the studied cyclic conditions. This liquefaction susceptibility is due to the combined effect of two factors: (i) the sulphate induced decrease in cement hydration intensity that

leads to a less self-desiccation within the CPB with sulphate. It results in lower effective stress in the sulphate-bearing CPB, and consequently increases the liquefaction susceptibility; (ii) the sulphate-induced inhibition of cement hydration process that leads to the formation of less cement hydration products (C-S-H and CH) within the CPB that contains sulphate. It reduces and weakens the cementation between the tailings particles, and thus increases the liquefaction susceptibility of CPB with sulphate. These 1-g shaking table tests on CPB are time consuming, however they have allowed to acquire a better understanding of the effect of the pore water chemistry or chemistry of mixing water on the cyclic behavior and liquefaction potential of CPB at early ages besides acquiring information and data that are useful for liquefaction assessment of CPB structures, and also for future development of constitutive samples to describe and predict the cyclic behavior of hydrating paste backfill or soil undergoing cementation.

4.7 Acknowledgements

The authors would like to thank the National Natural Sciences and Engineering Research Council of Canada (NSERC) for financially supporting this project. Moreover, the authors would like to thank Dr. Mohammed Al-Umar, and Dr. Muslim Majeed for their help with the experimental tests.

4.8 References

Abdelaal, A. (2011) *Early age mechanical behavior and stiffness development of cemented paste backfill with sand*, Doctoral dissertation, University of Toronto.

Abdul-Hussain, N. and Fall, M. (2012) 'Thermo-hydro-mechanical behaviour of sodium silicate-cemented paste tailings in column experiments', *Tunnelling and Underground Space Technology*, 29, 85-93.

Acar, Y. B. and El-Tahir, E. T. A. (1986) 'Low strain dynamic properties of artificially cemented sand', *Journal of Geotechnical Engineering*, 112(11), 1001-1015.

Adalier, K., Elgamal, A., Meneses, J. and Baez, J. I. (2003) 'Stone columns as liquefaction countermeasure in non-plastic silty soils', *Soil Dynamics and Earthquake Engineering*, 23(7), 571-584.

Ahn, K. S., Zhang, C. and Canbulat, I. (2017) 'Study of seismic activities associated with Australian underground coal mining', in *Coal Operators' Conference*, University of Wollongong, Australia,

Aldhafeeri, Z. (2018) *Reactivity of Cemented Paste Backfill*, University of Ottawa.

Aldhafeeri, Z. and Fall, M. (2016) 'Time and damage induced changes in the chemical reactivity of cemented paste backfill', *Journal of Environmental Chemical Engineering*, 4(4), 4038-4049.

Aldhafeeri, Z., Fall, M., Pokharel, M. and Pouramini, Z. (2016) 'Temperature dependence of the reactivity of cemented paste backfill', *Applied Geochemistry*, 72, 10-19.

Anastasopoulos, I., Georgarakos, T., Georgiannou, V., Drosos, V. and Kourkoulis, R. (2010) 'Seismic performance of bar-mat reinforced-soil retaining wall: Shaking table testing versus numerical analysis with modified kinematic hardening constitutive model', *Soil Dynamics and Earthquake Engineering*, 30(10), 1089-1105.

ASTM C143/C143M-15a (2015) 'Standard test method for slump of hydraulic-cement concrete',

Atkinson, G. M., Kaka, S. I., Eaton, D., Bent, A., Peci, V. and Halchuk, S. (2008) 'A very close look at a moderate earthquake near Sudbury, Ontario', *Seismological Research Letters*, 79(1), 119-131.

Bahadori, H., Motamedi, H., Hasheminezhad, A. and Motamed, R. (2020) 'Shaking table tests on shallow foundations over geocomposite and geogrid-reinforced liquefiable soils', *Soil Dynamics and Earthquake Engineering*, 128.

Bairro, R. and Vaz, C. (2000) *Shaking table testing of civil engineering structures-The LNEC 3D simulator experience*, translated by Auckland, New Zeland.

Becker, D., Cailleau, B., Kaiser, D. and Dahm, T. (2014) 'Macroscopic Failure Processes at Mines Revealed by Acoustic Emission (AE) Monitoring', *Bulletin of the Seismological Society of America*, 104(4), 1785-1801.

Belem, T., El Aatar, O., Bussière, B. and Benzaazoua, M. (2016) 'Gravity-driven 1-D consolidation of cemented paste backfill in 3-m-high columns', *Innovative Infrastructure Solutions*, 1(1).

Bentz, D. P. (2008) 'A review of early-age properties of cement-based materials', *Cement and Concrete Research*, 38(2), 196-204.

Bian, J., Fall, M. and Haruna, S. (2019) 'Sulphate induced changes in rheological properties of fibre-reinforced cemented paste backfill', *Magazine of Concrete Research*, 1-35.

Bouckovalas, G. D., Papadimitriou, A. G. and Niarchos, D. (2009) 'Gravel drains for the remediation of liquefiable sites: The Seed & Booker (1977) approach revisited', in *International Conference on Performance-Based Design*, Tokyo, Japan, International Society for Soil Mechanics and Geotechnical Engineering., 61-75.

Bullard, J. W., Jennings, H. M., Livingston, R. A., Nonat, A., Scherer, G. W., Schweitzer, J. S., Scrivener, K. L. and Thomas, J. J. (2011) 'Mechanisms of cement hydration', *Cement and Concrete Research*, 41(12), 1208-1223.

Carraro, J. A. H., Prezzi, M. and Salgado, R. (2009) 'Shear strength and stiffness of sands containing plastic or nonplastic fines', *Journal of Geotechnical and Geoenvironmental Engineering*, 135(9), 1167-1178.

Carter, D. P. (1988) *Liquefaction potential of sand deposits under low levels of excitation*, California Univ., Berkeley, CA, USA.

Cetin, K. O., Unutmaz, B. and Jeremic, B. (2012) 'Assessment of seismic soil liquefaction triggering beneath building foundation systems', *Soil Dynamics and Earthquake Engineering*, 43, 160-173.

Chen, G., Wang, Z., Zuo, X., Du, X. and Gao, H. (2013) 'Shaking table test on the seismic failure characteristics of a subway station structure on liquefiable ground', *Earthquake Engineering & Structural Dynamics*, 42(10), 1489-1507.

Dungca, J. R., Kuwano, J., Takahashi, A., Saruwatari, T., Izawa, J., Suzuki, H. and Tokimatsu, K. (2006) 'Shaking table tests on the lateral response of a pile buried in liquefied sand', *Soil Dynamics and Earthquake Engineering*, 26(2-4), 287-295.

El Mkadmi, N., Aubertin, M. and Li, L. (2014) 'Effect of drainage and sequential filling on the behavior of backfill in mine stopes', *Canadian Geotechnical Journal*, 51(1), 1-15.

Ercikdi, B., Cihangir, F., Kesimal, A. and Deveci, H. (2017) 'Practical Importance of Tailings for Cemented Paste Backfill' in Yilmaz, E. and Fall, M., eds., *Paste Tailings Management*, Cham: Springer International Publishing, 7-32.

Ercikdi, B., Cihangir, F., Kesimal, A., Deveci, H. and Alp, I. (2009a) 'Utilization of industrial waste products as pozzolanic material in cemented paste backfill of high sulphide mill tailings', *J Hazard Mater*, 168(2-3), 848-56.

Ercikdi, B., Kesimal, A., Cihangir, F., Deveci, H. and Alp, İ. (2009b) 'Cemented paste backfill of sulphide-rich tailings: Importance of binder type and dosage', *Cement and Concrete Composites,* 31(4), 268-274.

Fall, M. and Benzaazoua, M. (2005) 'Modeling the effect of sulphate on strength development of paste backfill and binder mixture optimization', *Cement and Concrete Research,* 35(2), 301-314.

Fall, M., Célestin, J. C., Pokharel, M. and Touré, M. (2010) 'A contribution to understanding the effects of curing temperature on the mechanical properties of mine cemented tailings backfill', *Engineering Geology*, 114(3-4), 397-413.

Fall, M. and Pokharel, M. (2010) 'Coupled effects of sulphate and temperature on the strength development of cemented tailings backfills: Portland cement-paste backfill', *Cement and Concrete Composites,* 32(10), 819-828.

Fall, M. and Samb, S. S. (2008) 'Pore structure of cemented tailings materials under natural or accidental thermal loads', *Materials Characterization,* 59(5), 598-605.

Fredlund, D. G., Rahardjo, H. and Fredlund, M. D. (2012) *Unsaturated soil mechanics in engineering practice,* Hoboken, New Jersey, USA: John Wiley & Sons.

Geremew, A. M. and Yanful, E. K. (2013) 'Dynamic properties and influence of clay mineralogy types on the cyclic strength of mine tailings', *International Journal of Geomechanics,* 13(4), 441-453.

Ghirian, A. and Fall, M. (2013) 'Coupled thermo-hydro-mechanical–chemical behaviour of cemented paste backfill in column experiments. Part I: Physical, hydraulic and thermal processes and characteristics', *Engineering Geology,* 164, 195-207.

Ghirian, A. and Fall, M. (2014) 'Coupled thermo-hydro-mechanical–chemical behaviour of cemented paste backfill in column experiments', *Engineering Geology*, 170, 11-23.

Ghirian, A. and Fall, M. (2015) 'Coupled Behavior of Cemented Paste Backfill at Early Ages', *Geotechnical and Geological Engineering,* 33(5), 1141-1166.

Guoxing, C., Su, C., Xi, Z., Xiuli, D., Chengzhi, Q. I. and Zhihua, W. (2015) 'Shaking-table tests and numerical simulations on a subway structure in soft soil', *Soil Dynamics and Earthquake Engineering,* 76, 13-28.

Haiqiang, J., Fall, M. and Cui, L. (2016) 'Yield stress of cemented paste backfill in sub-zero environments: Experimental results', *Minerals Engineering*, 92, 141-150.

Hasegawa, A., Nakajima, J., Uchida, N., Okada, T., Zhao, D., Matsuzawa, T. and Umino, N. (2009) 'Plate subduction, and generation of earthquakes and magmas in Japan as inferred from seismic observations: An overview', *Gondwana Research*, 16(3-4), 370-400.

Hasegawa, H. S., Wetmiller, R. J. and Gendzwill, D. J. (1989) 'Induced seismicity in mines in Canada—an overview', *Pure and applied geophysics*, 129(3-4), 423-453.

Helinski, M., Fourie, A., Fahey, M. and Ismail, M. (2007) 'Assessment of the self-desiccation process in cemented mine backfills', *Canadian Geotechnical Journal*, 44(10), 1148-1156.

Ishihara, K. (1996) *Soil Behavior in Earthquake Geotechnics*, NY, USA: Oxford University Press.

Ishihara, K., Yasuda, S. and Yokota, K. (1981) *Cyclic strength of undisturbed mine tailings*, translated by University of Missouri-Rolla, St. Louis, USA: 53-58.

Jafari, M. (2020) *Experimental study of physical and mechanical properties of a cemented mine tailings*, Ph. D. Thesis: University of Toronto.

James, M., Jolette, D., Aubertin, M. and Bussière, B. (2003) *An Experimental Set-up to Investigate Tailings liquefaction and control measures*, translated by Montréal, QC, Canada.

Jefferies, M. and Been, K. (2015) *Soil Liquefaction: a critical state approach*, Second ed., Taylor & Francis, London, UK.

Komak Panah, A., Yazdi, M. and Ghalandarzadeh, A. (2015) 'Shaking table tests on soil retaining walls reinforced by polymeric strips', *Geotextiles and Geomembranes*, 43(2), 148-161.

Landriault, D., Verburg, R., Cincilla, W. and Welch, D. (1997) *Paste technology for underground backfill and surface tailings disposal applications.*, Short Course notes—Technical Workshop, Vancouver, British Columbia: unpublished.

Li, W. and Fall, M. (2016) 'Sulphate effect on the early age strength and self-desiccation of cemented paste backfill', *Construction and Building Materials*, 106, 296-304.

Li, W. and Fall, M. (2018) 'Strength and self-desiccation of slag-cemented paste backfill at early ages: Link to initial sulphate concentration', *Cement and Concrete Composites,* 89, 160-168.

Mamlouk, M. S. and Zaniewski, J. P. (2011) *Materials for civil and construction engineers,* 3rd ed., Upper Saddle River, New Jersey: Pearson Prentice Hall.

Mohamed, F. M. O. (2014) *Bearing Capacity and Settlement Behaviour of Footings Subjected to Static and Seismic Loading Conditions in Unsaturated Sandy Soils*, Doctoral dissertation: University of Ottawa.

Moncarz, P. D. and Krawinkler, H. (1981) *Theory and application of experimental model analysis in earthquake engineering,* Stanford University.

Motamed, R., Towhata, I., Honda, T., Tabata, K. and Abe, A. (2013) 'Pile group response to liquefaction-induced lateral spreading: E-Defense large shake table test', *Soil Dynamics and Earthquake Engineering,* 51, 35-46.

Natural Resources Canada (2019) 'Earthquake Reports for 2019', [online], available: http://www.seismescanada.rncan.gc.ca/recent/2019/index-en.php 2019].

Ngadimon, K. (2006) *Design and Simulation of Hydraulic Shaking Table,* Doctoral dissertation: University of Technology.

Nouri, H., Fakher, A. and Jones, C. (2006) 'Development of Horizontal Slice Method for seismic stability analysis of reinforced slopes and walls', *Geotextiles and Geomembranes,* 24(3), 175-187.

Nouri, H., Fakher, A. and Jones, C. J. F. P. (2008) 'Evaluating the effects of the magnitude and amplification of pseudo-static acceleration on reinforced soil slopes and walls using the limit equilibrium Horizontal Slices Method', *Geotextiles and Geomembranes,* 26(3)(3), 263-278.

Okamura, M. and Soga, Y. (2006) 'Effect of pore fluid compressibility on liquefaction resistance of partially saturated sand', *Soils and Foundations,* 46(5)(5), 695-700.

Özgen, S., Malkoç, Ö., Doğancik, C., Sabah, E. and Şapçi, F. O. (2011) 'Optimization of a Multi Gravity Separator to produce clean coal from Turkish lignite fine coal tailings', *Fuel,* 90(4), 1549-1555.

Pépin, N., Aubertin, M. and James, M. (2009) *An Investigation of the Cyclic Behaviour of tailings using shaking table tests - effect of a drainage inclusion on porewater development,* translated by Halifax, N.S., Canada.

Pépin, N., Aubertin, M. and James, M. (2012a) 'Seismic table investigation of the effect of inclusions on the cyclic behaviour of tailings', *Canadian Geotechnical Journal,* 49(4), 416-426.

Pépin, N., Aubertin, M., James, M. and Leclerc, M. (2012b) 'Seismic Simulator Testing to Investigate the Cyclic Behavior of Tailings in an Instrumented Rigid Box', *Geotechnical Testing Journal,* 35(3), 469-479.

Persson, B. (1997) 'Self-desiccation and its importance in concrete technology', *Materials and Structures,* 30(5), 293-305.

Pokharel, M. and Fall, M. (2013) 'Combined influence of sulphate and temperature on the saturated hydraulic conductivity of hardened cemented paste backfill', *Cement and Concrete Composites,* 38, 21-28.

Porcino, D., Marcianò, V. and Granata, R. (2015) 'Cyclic liquefaction behaviour of a moderately cemented grouted sand under repeated loading', *Soil Dynamics and Earthquake Engineering,* 79, 36-46.

Poulos, S. J., Robinsky, E. I. and Keller, T. O. (1985) 'Liquefaction Resistance of Thickened Tailings', *Journal of Geotechnical Engineering,* 111(12), 1380-1394.

Prasad, S. K., Towhata, I., Chandradhara, G. P. and Nanjundaswamy, P. (2004) 'Shaking table tests in earthquake geotechnical engineering', *Current science,* 1398-1404.

Saebimoghaddam, A. (2010) *Liquefaction of Early Age Cemented Paste Backfill,* Doctoral dissertation: University of Toronto.

Scrivener, K. L., Juilland, P. and Monteiro, P. J. M. (2015) 'Advances in understanding hydration of Portland cement', *Cement and Concrete Research,* 78, 38-56.

Shahir, H. and Pak, A. (2010) 'Estimating liquefaction-induced settlement of shallow foundations by numerical approach', *Computers and Geotechnics,* 37(3), 267-279.

Srilatha, N., Madhavi Latha, G. and Puttappa, C. G. (2013) 'Effect of frequency on seismic response of reinforced soil slopes in shaking table tests', *Geotextiles and Geomembranes,* 36, 27-32.

Sriskandakumar, S. (2004) *Cyclic loading response of Fraser River sand for validation of numerical models simulating centrifuge tests,* University of British Columbia, Canada.

Statista (2019) 'Total revenue of the top mining companies worldwide from 2002 to 2017', [online], available: https://www.statista.com/statistics/208715/total-revenue-of-the-top-mining-companies/ 2019].

Takahashi, A., Takemura, J., Suzuki, A. and Kusakabe, O. (2001) 'Development and performance of an active type shear box in a centrifuge', *International Journal of Physical Modelling in Geotechnics,* 1(2), 1-17.

Taylor, H. F. (1990) *Cement Chemistry,* 2nd ed., London: Academic press.

Thompson, B. D., Bawden, W. F. and Grabinsky, M. (2012) 'In situ measurements of cemented paste backfill at the Cayeli Mine', *Canadian Geotechnical Journal,* 49(7), 755-772.

Thompson, B. D., Grabinsky, M. W., Bawden, W. F. and Counter, D. B. (2009) *In-situ measurements of cemented paste backfill in long-hole stope,* translated by Toronto, ON, Canada.

Turan, A., Hinchberger, S. D. and El Naggar, H. (2009) 'Design and commissioning of a laminar soil container for use on small shaking tables', *Soil Dynamics and Earthquake Engineering,* 29(2), 404-414.

Tuttle, M., Law, K. T., Seeber, L. and Jacob, K. (1990) 'Liquefaction and ground failure induced by the 1988 Saguenay, Quebec, qrthquakel', *Canadian Geotechnical Journal,* 27(5), 580-589.

Ueng, T. S., Wang, M. H., Chen, M. H., Chen, C. H. and Peng, L. H. (2006) 'A large biaxial shear box for shaking table test on saturated sand', *Geotechnical Testing Journal,* 29(1), 1-8.

Ueng, T. S., Wu, C. W., Cheng, H. W. and Chen, C. H. (2010) 'Settlements of saturated clean sand deposits in shaking table tests', *Soil Dynamics and Earthquake Engineering,* 30(1-2), 50-60.

Walske, M. L., McWilliam, H., Doherty, J. and Fourie, A. (2016) 'Influence of curing temperature and stress conditions on mechanical properties of cementing paste backfill', *Canadian Geotechnical Journal,* 53(1), 148-161.

Wang, J., Salam, S. and Xiao, M. (2019) 'The Effect of Shaking History on Liquefaction Resistance of Sand Deposit Using Shake Table Testing', in *Geo-Congress 2019: Earthquake Engineering and Soil Dynamics*, Reston, VA, USA, American Society of Civil Engineers, 285-293.

Wang, Y., Fall, M. and Wu, A. (2016) 'Initial temperature-dependence of strength development and self-desiccation in cemented paste backfill that contains sodium silicate', *Cement and Concrete Composites,* 67, 101-110.

Wu, J., Kammerer, A. M., Riemer, M. F., Seed, R. B. and Pestana, J. M. (2004) *Laboratory Study of Liquefaction Triggering Criteria,* translated by Vancouver, BC, Canada.

Xu, X., Fall, M., Alainachi, I. and Fang, K. (2020) 'Characterisation of fibre-reinforced backfill/rock interface through direct shear tests', *Geotechnical Research,* 7(1)(1), 1-15.

Xue, G., Yilmaz, E., Song, W. and Cao, S. (2020) 'Fiber length effect on strength properties of polypropylene fiber reinforced cemented tailings backfill specimens with different sizes', *Construction and Building Materials,* 241.

Yang, L. and Woods, R. D. (2015) 'Shear stiffness modeling of cemented clay', *Canadian Geotechnical Journal,* 52(2)(2), 156-166.

Yilmaz, E. (2018) 'Stope depth effect on field behaviour and performance of cemented paste backfills', *International Journal of Mining, Reclamation and Environment,* 32(4)(4), 273-296.

Yilmaz, E., Benzaazoua, M., Belem, T. and Bussière, B. (2009) 'Effect of curing under pressure on compressive strength development of cemented paste backfill', *Minerals Engineering,* 22(9-10), 772-785.

Zhu, F. and Clark, J. I. (1994) 'The effect of dynamic loading on lateral stress in sand', *Canadian Geotechnical Journal,* 31(2)(2), 308-311.

CHAPTER 5 Temperature Induced Changes in the Behaviour of Cementing Fine-Grained Soils under Dynamic Loadings (Paper III)

(Submitted)

Imad Alainachi, and Mamadou Fall

5.1 Abstract

Cemented paste backfill (CPB), which consists of a fine-grained soil undergoing cementation, has been extensively used in the mine industry to backfill underground mine cavities for ground support and/or tailings management. Generally, CPB consists of tailings (mostly silt particles) mixed with water and binders cement. Once placed in mine underground cavities, the geotechnical and liquefaction response of the CPB under dynamic (cyclic) loadings is a key design concern in mine backfilling. Moreover, fresh CPB might be exposed to several sources of heat that might affect its cyclic behavior and liquefaction potential. However, up to date, no studies have addressed the effect of temperature on the geotechnical and liquefaction response of CPB under cyclic loadings by using shaking table technique. This manuscript presents findings of assessing the effect of backfill temperature on its geotechnical and liquefaction response to cyclic loading by using shaking table. CPB mixtures were prepared under different temperatures (20^{o}C and 35^{o}C), poured into a flexible laminar shear box, cured (under the same mixing temperature) for 2.5 hours, and then exposed to cyclic loading using 1-D Shaking table. Numerous parameters (pore water pressure, lateral deformation, settlement, acceleration, suction, electrical conductivity, effective stress, liquefaction susceptibility etc.) were monitored or determined before, during, and after shaking. Obtained results illustrate that CPB prepared and cured under the temperature of 20^{o}C can be prone to liquefaction under the studied loadings conditions. However, CPB prepared and cured under the temperature of 35^{o}C is resistant to liquefaction. These results are expected to provide better comprehension of the effect of backfill temperature on the cyclic behavior of CPB, and thus assist in designing more efficient CPB structures.

Keywords: Cemented paste backfill; Liquefaction; Shaking table; Earthquake; Tailings; Mine

5.2 Introduction

World economy is known to be significantly affected by the development of mine industry. For example, in 2018, mining activities produced around 700 billion USD to the world economy (Statista 2020). However, the process of ore extraction creates large underground openings (stopes) that might be susceptible to several geotechnical issues, such as ground subsidence and the instability of the mine. This might endanger the safety of the people in the mine workplace and the neighboring area along with the economic damages of the failed mine ground. Also, various

environmental challenges were found to be associated with mining activities, such as the generation of huge quantities of harmful mining wastes (tailings; tailings are the soil material that are generated in a mine processing plant), which were found to be a potential source of environmentally hazardous materials, such as acid mine drainage (Ghirian and Fall 2015, Aldhafeeri et al. 2016, Xiangqian Xu et al. 2020).

An innovative solution of tailings management method was developed in past decades in order to deal with these challenges, by allowing large amount tailings to be returned to the mine cavity or stope. This method is named cemented paste backfilling. Cement paste backfill (CPB) can also improve the short and long-term stability of the stopes besides ensuring the safety of the workers in the mine and the surrounding areas. CPB involves the reuse of around up to 60% of the total amount of tailings produced by the mine, and mixing them with certain percentage of water and hydraulic binder (cement), to fill the voids created by mining activities (Landriault et al. 1997, Benzaazoua et al. 2004, Haruna and Fall 2020). From a geotechnical point of view, CPB is considered as a fine-grained (silt) soil undergoing cementation.

The CPB is prepared in the paste backfill plant usually located on the mine surface. Freshly prepared CPB is then delivered into the mine stope by gravity and/or pumping (Landriault et al. 1997, Benzaazoua et al. 2004, Aldhafeeri et al. 2016, Yilmaz and Fall 2017). CPB can shorten the completion of the stope backfilling process to several days, whereas with traditional backfilling methods, it might take weeks or months. This characteristic makes CPB a globally common practice as it improves the generated revenue (Ercikdi et al. 2009, Thompson et al. 2009).

Underground mines were found to be exposed to cyclic loadings at several occasions. These cyclic loadings are either naturally generated (natural earthquakes) or produced owing to mining activities (e.g. due to fault slip, pillar punching, pillar burst, rockburst, outburst, failure of overburden strata and bump) (Hasegawa et al. 1989, Ahn et al. 2017). Due to the low availability of ores in the shallow depths and the increase in the rates of the greater volume extraction, underground mining operations around the world have significantly increased with greater volume and at greater depths. The frequency and severity of mining-induced seismicity have been found to increase with the high rate of volume extraction and the increase in the extraction depth (Hasegawa et al. 1989, Becker et al. 2014). Hence, the risk of cyclic-induced liquefaction of CPB structures at the early ages could increase because more severe and/or frequent cyclic events are expected. Liquefaction-induced failure of CPB structures can cause injuries and/or fatalities in the mine workers and the surrounding public besides having negative environmental impacts and economic damages (Poulos et al. 1985, Abdelaal 2011). Therefore, understanding liquefaction potential of CPB material under cyclic loading conditions at the early ages is critically important for an efficient and safe design of CPB structures.

Moreover, there are several heat sources that might affect the temperature of fresh CPB placed in mine stopes. These sources include the internal heat produced during cement hydration, and external heat that is related to geothermal gradient (i.e. temperature variation with depth,

geological conditions, and geographic location of the mine) (Fall et al. 2010, Aldhafeeri et al. 2016, Ali et al. 2021). Thus, with the increase in the depths of the underground mine stopes and the associated mine and rock temperature increase, it is essential to understand the cyclic performance of CPB under diverse temperature conditions.

Up to date, only few studies (e.g. Saebimoghaddam 2010, Abdelaal 2011) have experimentally examined the behavior and liquefaction potential of early aged CPBs under cyclic loading conditions. However, all these previous studies assessed the liquefaction response of CPB by applying cyclic loading on small-size CPB samples using common small cyclic triaxial test apparatus (Saebimoghaddam 2010, Abdelaal 2011). Moreover, none of these previous studies has evaluated the effect of temperature (initial and curing) on the response of CPB to cyclic loading. All the previous studies (e.g. Fall and Samb 2008, Fall et al. 2010, Fall and Pokharel 2010, Cui and Fall 2016) on the temperature-induced changes in the mechanical or geotechnical behavior of CPB were conducted under static loading conditions. These studies have revealed that high initial temperature of CPB can significantly improve its static mechanical properties (strength), and thus enhances its mechanical stability. However, the question whether the initial temperature of CPB can enhance its liquefaction resistance when subjected to cyclic loadings still remains ambiguous and unanswered. There is a need to address this information dearth, since CPB is often subjected to internal and/or external heat, which is commonly originated from cement hydration of the CPB itself or from the adjacent circumference.

In addition to the facts mentioned above, no study has been conducted to assess the behavior and liquefaction potential of CPB under different temperatures by using shaking table testing techniques. Despite its high cost and the difficulty in reproducing or simulating the in-situ stress, shaking tables have been frequently used for assessing the cyclic response of geo-materials and engineering structures in the past decades (Moncarz and Krawinkler 1981, Bairro and Vaz 2000, Ngadimon 2006). Since the beginning of the current century, numerous researches (e.g. Bairro and Vaz 2000, Prasad et al. 2004, Dungca et al. 2006, Ueng et al. 2006, Chen et al. 2013, Mohamed 2014, Guoxing et al. 2015, Ghorbani et al. 2020) have applied the shaking table test to evaluate the cyclic-induced liquefaction response of natural soils. On the other hand, only few studies (James et al. 2003, Pépin et al. 2009, 2012a, 2012b, Özgen et al. 2011, Salam et al. 2020) have used shaking table to assess the cyclic behavior of tailings (without cement). Nevertheless, there are no studies to date that have been conducted to assess the effect of initial temperature on behavior and liquefaction potential of early aged tailings undergoing cementation or CPB under cyclic loadings by using shaking table.

Accordingly, this study aims at using shaking table technique to understand the effect of the temperature (mixing and curing) of hydrating CPB material on its geotechnical behavior and liquefaction response at the early ages during cyclic loadings.

5.3 Materials and Equipment Used in the Experiment

5.3.1 Materials

The materials used in this study for the preparation of the CPB mixtures were silica tailings (ST) as the main component of CPB, Portland cement type I (PCI) as hydraulic binder, and tap water as mixing water. ST is synthetic tailings material that contains ground silica. It is essentially made of quartz, which is the predominant mineral in Canadian hard rock mine tailings. The grain size distribution of ST is similar to that of numerous natural tailings (NT) from Canadian hard rock mines. Figure 5.1 shows a comparison between the grain size distribution of ST and the average grain size distribution of nine mine tailings (9MT) extracted from nine different mines in eastern Canada. The use of ST can eliminate uncertainties that are otherwise found with the use of natural tailings, because ST contains high percentage of silica (99.8% SiO_2), which makes it a chemically inert material. The NT may contain reactive minerals that can potentially have chemical interactions with other ingredients in the CPB mixture (Carraro et al. 2009, Fall et al. 2010, Aldhafeeri and Fall 2016). Table 5.1 illustrates the physical properties of the tailings used in this study.

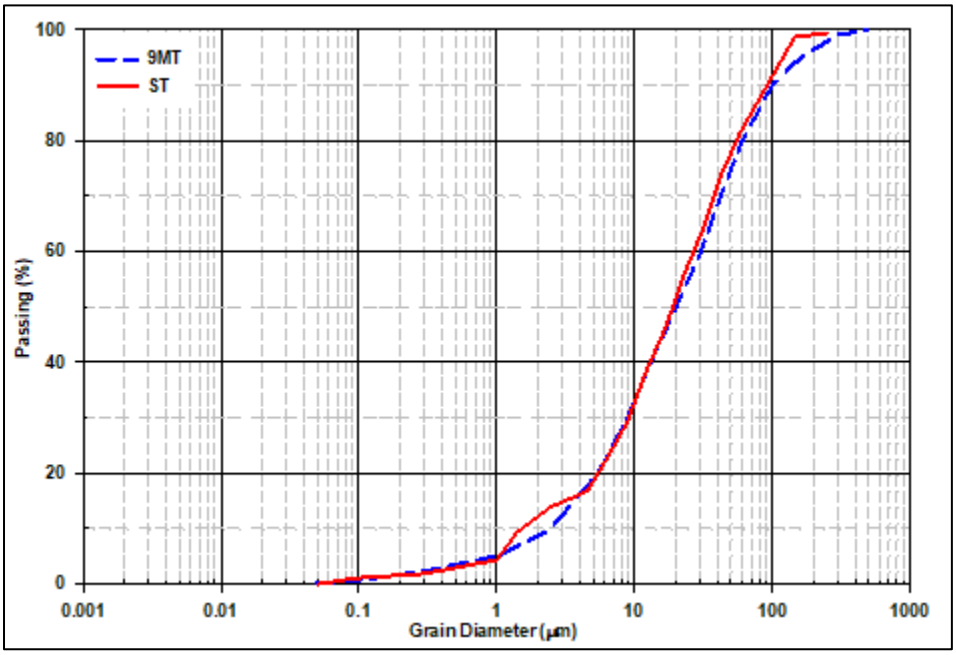

Figure 5.1 Grain size distribution of the silica tailing (ST) vs average grain size distribution of tailings extracted from nine Canadian mines (9MT).

5.3.2 Preparation of Paste Backfill Mixture

In this study, two CPB specimens were prepared. In both specimens, ST was mixed with PCI (4.5 wt %) and water, with water-cement ratio (w/c) of 7.6. CPB specimens were mixed for 10 min in order to obtain homogenous mixture. The degree of water saturation (S) of the prepared CPB was determined to be equal to 100%. Also, the slump of the prepared backfill mixture was tested

according to (ASTM C143/C143M-15a 2015), and it was found to be equal to 18 cm, which is one of the most frequent slump values being used in paste backfill operations in Canadian mines.

Table 5.1 Primary physical properties of the tailings

Tailings	Gs	D_{10} (μm)	D_{30} (μm)	D_{50} (μm)	D_{60} (μm)
ST	2.7	1.9	9.0	22.5	31.5

Table 5.2 Primary physical and chemical properties of the Portland cement type I (PCI)

Gs	SSA[(1)] (m^2/g)	Ca (wt%)	Si (wt%)	Al (wt%)	Fe (wt%)	Mg (wt%)	S (wt%)	Si/Ca
3.15	1.32	44.9	8.4	2.4	1.9	1.6	1.5	0.2

[(1)] Specific Surface Area

In order to determine the effect of the initial (mixing and curing) temperature of CPB on its cyclic response, the CPB components (ST, PCI, and water) were first stored in a temperature controlled chamber for a minimum duration of 24 hours or until they reach the desired temperature (20oC and 35oC). Afterwards, the two CPB samples were prepared and mixed as described above, and then CPB mixtures were poured into the developed laminar shear box (described below). In order to maintain the desired curing temperature and to avoid changes in water content due to evaporation, laminar shear box with CPB mixtures was sealed and kept for curing under the same temperatures (~20^{o}C and ~23^{o}C) until it reached the testing age of 2.5 hours. Detailed testing program is described in Section 5.4.

5.3.3 Shaking Table

The shaking table of the University of Ottawa (Figure 2) was used in this research to simulate dynamic loading. Series of one-dimensional (longitudinal) sinusoidal cyclic motion was applied in this regard.

This shaking table consists of around ~1200 mm × ~1060 mm platform with a maximum base displacement and shear capacity limit of 12 cm and 27 kN respectively. The shaking ranges from 1 to 17 Hz and is driven by a digitally controlled hydraulic actuator (Mohamed 2014).

In order to evaluate the cyclic behavior of CPB using the shaking table, a Flexible Laminar Shear Box (FLSB) (Figure. 5.2) was used. The FLSB was designed and built at the Faculty of Engineering of the University of Ottawa for this research program.

The FLSB consists of 30 horizontal laminas, made of aluminum alloy box sections of 31.7 mm × 31.7 mm, with inner dimensions of each lamina of 750 mm × 750 mm. In order to ensure the independent movement of each lamina, the FLSB was designed to have a clearance spacing of 2 mm between each lamina. Accordingly, the total capacity of assembled FLSB becomes 750 mm × 750 mm × 10000 mm.

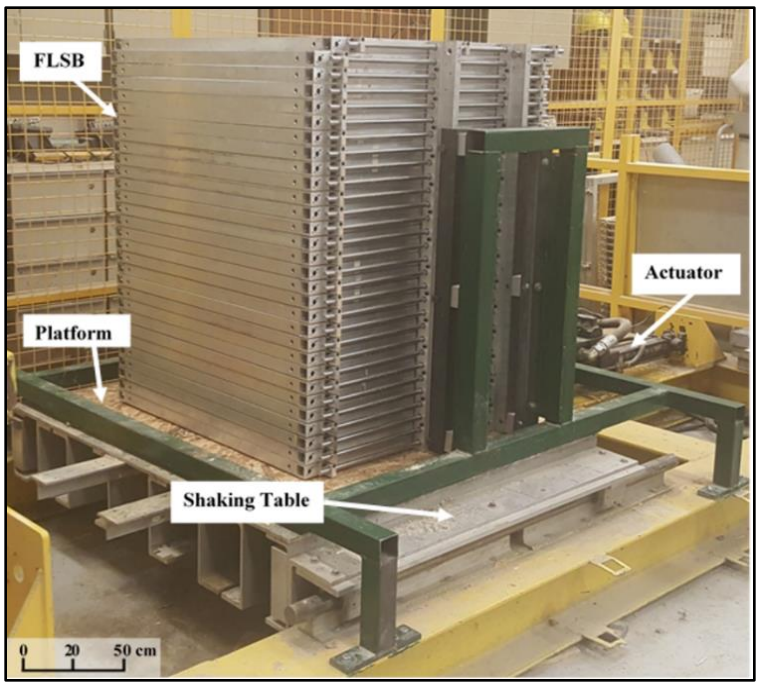

Figure 5.2 Shaking table and Flexible Laminar Shear Box (FLSB) used in this study

A 0.5 mm thick flexible polyethylene membrane was placed in the FLSB to contain/hold the CPB mixture before and during the tests. The high flexibility of the membrane shows no (or negligible) effect on the movement of the FLSB (Mohamed 2014). The FLSB and the membrane were securely attached to the platform of the shaking table.

The prepared CPB mixture was poured into the FLSB, with a final dimension of each tested CPB sample of 750 mm × 750 mm × 700 mm. Several sensors and transducers were placed at different levels within the CPB model (FLSB and its content) as shown in Figure 5.3. They are described below:

- Linear variable differential transformer (LVDT) (Item 1 in Figure 5.3) was used to monitor the vertical displacement (settlement) of the surface of the CPB sample. In this regard, HCD-1000 LVDTs of 25 mm range were used.

- Cable transducers (Celesco SP2-12 compact string with 317 mm range) (Item 2 in Figure 5.3) were used to measure:

  a. The vertical displacement (settlement) within the CPB sample at different depths of 20 cm, 40 cm, and 60 cm. These transducers were attached to a measuring supporting system that consists of thin metal rods, lightweight plastic plates, and cylindrical guidance towers (Figure 5.4). The thin metal rods were connected to the plastic plates. These plates have dimensions of 20 mm (length) × 20 mm (width) × 20 mm (thick) and were perforated to minimize their displacement due to seepage pressure. The plastic plates were installed at the three different depths within the sample. In order to avoid unwanted movement/tilting

during shaking process, the metal rods and the perforated plastic plates were installed within the cylindrical guidance towers that are made of thin metal mesh sheets. The measuring supporting system was then securely connected to the shaking table to follow the same motion rhythm and to avoid being a reinforcement factor.

- The horizontal displacement of the CPB sample at different depths (20 cm, 40 cm, and 60 cm). These transducers were attached to the outside of the FLSB at the depth related laminas.

- Pressure transducers (Item 3 in Figure 5.3) were used to monitor the change in pore-water pressure before, during, and after applying the dynamic load. PX309 series pressure transducers, with a measuring range and static accuracy of -15 to +15 PSI and ±0.25%, respectively, were used and installed at different depths (20 cm, 40 cm, and 60 cm) of the CPB models inside the FLSB.

- Accelerometers (Item 4 in Figure 5.3) were used to measure the shaking acceleration. These accelerometers were attached to the external side of the FLSB at different depths (20 cm, 40 cm and 60 cm). In addition, another accelerometer was attached to the shaking table to monitor its acceleration. Endevco – 7593A accelerometer with a full-scale range of ±2g and frequency response of 0 – 50 Hz was used in this regard.

- Suction Sensors (Item 5 in Figure 5.3) were used and installed at different depths (20 cm, 40 cm, and 60 cm) within the sample to monitor the suction potential with time during CPB curing duration. The monitoring of suction also enables to assess the self-desiccation of CPB. In this regard, dielectric water potential sensors (ECH2-MPS6 sensors) that were designed to measure soil water potential were used. These sensors are characterized with a measurement range of -9 to -100,000 kPa, a resolution of 0.1 kPa. The accuracy of these sensors is ±10% of reading + 2 kPa, from -9 to -100 kPa.

- EC/VWC/Temp. sensors (ECH2-5TE sensor) (Item 6 in Figure 5.3) were used and installed at different depths (20 cm, 40 cm, and 60 cm) within the sample to monitor the changes in electrical conductivity (EC), the volumetric water content (VWC), and temperature. The changes in EC reflect the rate of ion movement due to the chemical reactions between cement and water. Monitoring EC is an effective way to assess the cement hydration progress and the related structural changes (Li and Fall 2016). This sensor measures electrical conductivity (EC) in the range of 0-23 dS/m with the accuracy of ±0.1. On the other hand, monitoring the VWC enables to assess the self-desiccation of CPB (capillary water consumed by the cement hydration) as well as the water flow within the CPB mass. This sensor measures volumetric water content (VWC) in the range of 0-80% with the accuracy of ±0.01 from 1 to 40% and the accuracy of ±0.15 from 40 to 80%. Furthermore, the monitoring of the temperature provides valuable information about the progress of the cement hydration. The temperature measurement accuracy of this sensor is ±1°C.

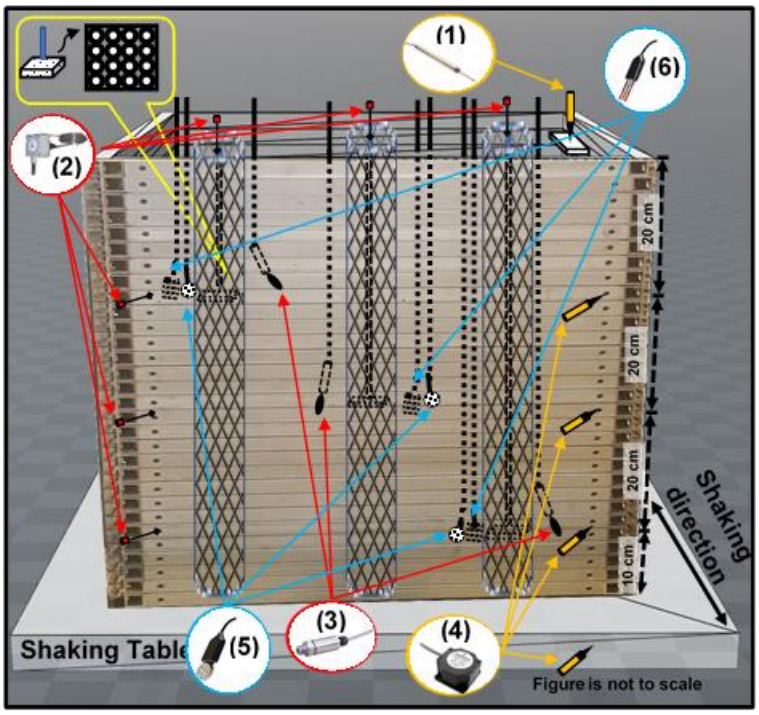

Figure 5.3 Schematic view of the FLSB and instruments locations: (1) LVDT, (2) Cable transducers, (3) Pressure transducers, (4) Accelerometers, (5) MPS6 sensors, and (6) 5TE sensors.

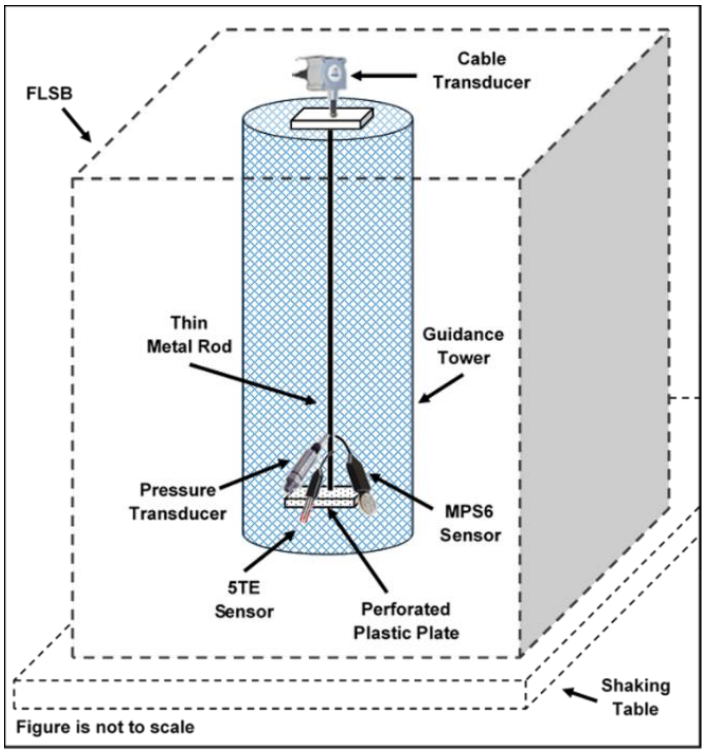

Figure 5.4 Schematic view of one the guidance towers and related instrumentation setup.

In order to maintain its positions during shaking, the pressure transducers, MPS6 and 5TE sensors were connected to the guidance towers. Transducers, accelerometers and LVDT were connected to signal conditioning and Data Acquisition Systems (DAQS), while 5TE and MP6 sensors were connected to Decagon Em50 series data loggers. DAQS and Em50 were connected to computer in order to record/analyze the required data at an interval of almost 1 sec during shaking and an interval of 10 min before and after shaking. Furthermore, digital camera was used to record each step of the testing program (mixing, installation, and shaking operation).

5.4 Testing Program and Procedure

5.4.1 Shaking Table

5.4.1.1 Cyclic parameters and test conditions

Figure 5.5 shows the experimental program carried out and the testing conditions, whereas Table 5.3 summarizes the testing program.

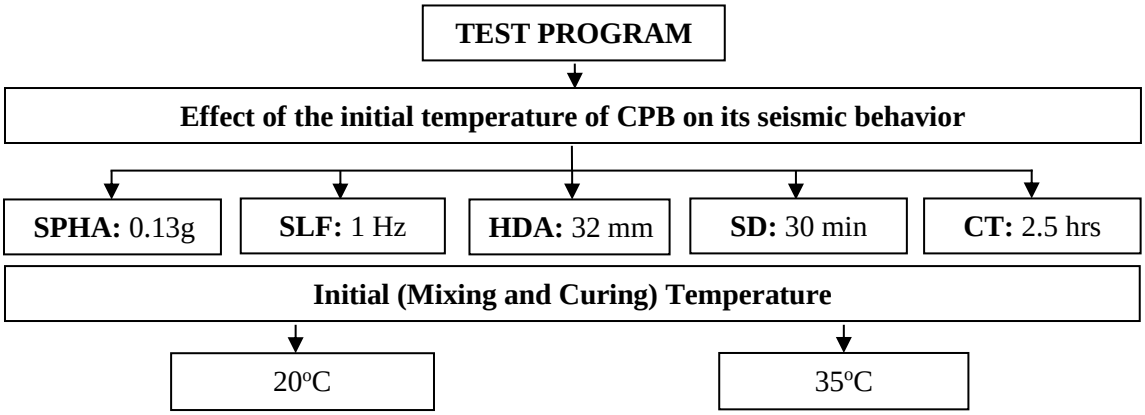

SPHA : Shaking Peak Horizontal Acceleration
SLF : Sinusoidal Loading Frequency
HDA : Horizontal Displacement Amplitude
SD : Shaking Duration
CT : Curing time

Figure 5.5 Flow chart of the experimental program and testing conditions

Table 5.3 Summary of the testing program

Test	Material	Initial Temp. (°C)	SPHA	SLF (Hz)	HDA (mm)	SD (min)	CT (hrs)	PLMD (hrs)
1	CPB	20	0.13g	1	32	30	2.5	24
2	CPB	35	0.13g	1	32	30	2.5	24

SPHA : Shaking Peak Horizontal Acceleration
SLF : Sinusoidal Loading Frequency
HDA : Horizontal Displacement Amplitude
SD : Shaking Duration
CT : Curing time
PLMD : Post Loading Monitoring Duration

The values of the testing parameters applied in this research (Table 5.4) were based on parameters used in previous shaking table studies (e.g. Carter 1988, Ishihara 1996, James et al. 2003, Pépin et al. 2012a, Salam et al. 2020) as well as adapted to accommodate the experimental (shaking table) limitations though they might not reflect the real situation of a seismic event. Thus, shaking table tests were conducted in this study using a dynamic load that was applied in one-dimensional signal, a uniform amplitude, and constant frequency. Comparable types of loading have often been used in other cyclic behaviour and/or liquefaction studies (e.g. Finn et al. 1971, DeAlba et al. 1975, James et al. 2003, James 2009, Pépin et al. 2012a,b, Ferdosi et al. 2014). It should be underlined that in natural earthquakes, the number of cycles is a function of the earthquake magnitude (and is commonly of the order of 5 to 20), and the motion amplitudes have a gradual increase, and a gradual decrease. The shaking table tests were performed in this study using a sinusoidal loading of 1 Hz frequency, under undrained conditions. As shown in table 4, a similar loading frequency has been used in previous shaking table studies, such as (Pépin et al. 2012a, Salam et al. 2020). Also, previous studies (e.g. Sriskandakumar 2004, Srilatha et al. 2013) have mentioned that the seismic response of the tested soil materials is insignificantly affected by the values of loading frequency applied in laboratory seismic tests under undrained loading, and the response of these materials is almost similar at frequencies less than 7 Hz. The peak ground acceleration applied in this study was 0.13g, which is equal to the acceleration that was recorded in the Saguenay earthquake 1988 in Quebec (Canada) (Tuttle et al. 1990) (it is important to mention that only the peak acceleration corresponds to the peak of Saguenay Earthquake, not the whole time series). Also, this selection was made based on the fact that tailings may liquefy when they are exposed to a ground motion with peak horizontal ground acceleration that exceeds 0.05g, as concluded in previous studies (e.g. James et al. 2003, Pépin et al. 2012a). Although the recorded earthquakes or mine-induced seismic events do not last that much long (Natural Resources Canada 2019), the cyclic loading (shaking) in this study (Table 4) has been carried out for 30 minutes (1800 seconds). The duration of cyclic loading in this study is not meant to be representative of the actual duration of earthquake, but it was selected to allow good observation of the dynamic behavior of the CPB sample and relative comparisons of their response. This will help better develop future constitutive models to describe the effect of initial temperature on the dynamic response of soils undergoing cementation. Moreover, several previous researches (e.g. James et al. 2003, Pépin et al. 2012b) have used similar durations in their studies. Also, it was found that the cyclic peak of the liquefaction of tailings (without inclusions and/or cement) can be reached in shaking for 1000 seconds (James et al. 2003). As the material used in this study is cementing tailings (CPB mix), shaking duration was selected in the range of 1 min to 30 min (60 – 1,800 cycles) depending on the material response and the post loading monitoring duration (PLMD) to continue (depending on material response) for additional 24 hours.

Table 5.4 Selected cyclic parameters used in the present study and previous studies

Parameter	Values used in previous studies [a]	Values used in the present study
Shaking Peak Horizontal Acceleration	0.1g – 1.0g	0.13g
Sinusoidal Loading Frequency	0.1 - 50 (Hz)	1 (Hz)
Horizontal Displacement Amplitude	10 - 80 (mm)	32 (mm)
Shaking Duration [b]	3 – 2,000 (sec)	1,800 (sec)
Post loading Monitoring Duration	15 (min) – 36 (hr)	24 (hr) [c]

[a]Such as (James et al. 2003, Prasad et al. 2004, Ueng et al. 2006, Pépin et al. 2009, 2012a, 2012b, Özgen et al. 2011, Mohamed 2014, Guoxing et al. 2015, Salam et al. 2020, Peng Xu et al. 2020); [b]Depends on the material response; [c]After initial casting.

5.4.1.2 Effect of initial temperature on the cyclic behavior of CPB

To evaluate the cyclic behavior of fresh CPB under cyclic conditions and different initial temperatures, two CPB mixtures were prepared; one mixture was prepared at room temperature (20^{o}C), while the other mixture was prepared at 35^{o}C. Both samples were then poured into FLSB, securely sealed and kept for curing (for the maturity age of 2.5 hrs) under same temperature of 20^{o}C and 35^{o}C, respectively. Afterwards, series of shaking table tests were performed on both CPB samples (see Figure 5.5).

5.4.2 Microstructural Analysis

Microstructural analysis was conducted on CPB samples that were prepared and cured at temperatures of 20^{o}C and 35^{o}C. The microstructural analysis enabled to assess the temperature-induced changes in the microstructure of the CPB material, which may impact its response to cyclic loadings. In this study, microstructural analysis included thermal analysis (differential thermogravimetry (DTG) and thermal gravimetry (TG)). The TGA Q 5000 IR from TA Instruments was used in this regard. Before conducting these tests, testing samples were first dried at 45 °C in a vacuum oven up to mass stabilization. The various (dried) samples (about 20 mg each) were heated in an inert nitrogen atmosphere at the rate of 10°C per minute up to a temperature of 1000°C.

5.5 Results and Discussion

5.5.1 Acceleration and lateral deformation

5.5.1.1 Acceleration

The peak acceleration histories at different depths during the shaking event for both CPB samples (with different temperatures) and cured for 2.5 hours are illustrated in Figure 5.6(a-b). This figure illustrates that the change in initial temperature and the depth have impact on the measured acceleration values. It can be observed that CPB samples mixed and cured at 20^{o}C show lower

peak acceleration values than CPB samples mixed and cured at 35^{o}C, especially at shallow depths. The recorded acceleration significantly varied with depth for the models prepared and cured at 20^{o}C, while the variation of acceleration with depth was low for models with initial temperature of 35^{o}C. For instance, the peak acceleration of CPB sample prepared at 20^{o}C (Figure 5.6a) was between 0.100g and 0.125g at 60 cm depth (10 cm above the shaking table), around 0.080g - 0.100g at 40 cm depth (30 cm above the shaking table), and 0.040g – 0.080g at 20 cm depth (50 cm above the shaking table). On the other hand, for the CPB sample that was prepared at 35^{o}C, the peak acceleration (Figure 5.6b) at 60 cm, 40 cm, and 20 cm depths was recorded to be around 0.125g – 0.130g, 0.105g – 0.118g, and 0.107g – 0.115g respectively. This increase in the peak acceleration as the initial temperature of CPB rises can be attributed to the effect of the high initial temperature on increasing the rate of cementation and consequently decreasing the damping ratio. It was mentioned in the literature that the damping ratio decreases when the degree of cementation is higher (Acar and El-Tahir 1986, Yang and Woods 2015). Furthermore, previous studies (e.g. Fall et al. 2010, Cui and Fall 2016) concluded that high initial temperature increases the curing temperature and consequently accelerates the cement hydration process. The acceleration of cement hydration process leads to more precipitation of cement hydration products, such as CH and C-S-H), and intensifies the cement self-desiccation (Nasir and Fall 2010). Consequently, there will be an increase in the degree of cementation within CPB that was prepared and cured at high temperature as compared to those CPBs that were prepared and cured (to the same age) at low temperature. It means that the CPBs that were prepared at high temperature will have lower damping ratio, since the high initial temperature is associated with higher degree of cementation (cement hydration rate) as evidenced by Figure 5.15 (discussed later). The higher the degree of cement hydration, the more the bonds between tailings (soil) particles; consequently, less deformation level of the material (Mamlouk and Zaniewski 2011). However, the decrease in cement hydration degree reduces the bonds between tailings particles. The significant reduction in acceleration values that was observed at lower depths in the CPB prepared at 20^{o}C can be attributed to nonlinearity and stiffness degradation of CPB caused by liquefaction as evidenced by the liquefaction analysis results presented in Section 5.5.3. The significant development of excess pore-water pressure (i.e. liquefaction) causes a large deformation in the CPB that was prepared and cured at lower temperature, wherein the cementation effect is still weak due to slow progress of cement hydration (see Figures 5.15). This large deformation will cause more damage in the pore structure within CPB material. Moreover, the shaking-induced slip and dislocation of tailings particles, which did not react with cement (within the CPB of low initial temperature), will cause high friction between particles and increase the material damping ratio. Thus, there will be decrease in the acceleration values. This finding and the explanation are coherent with the other results of this research, such as displacement monitoring, the determination of effective stress, and liquefaction analysis, which will be discussed later.

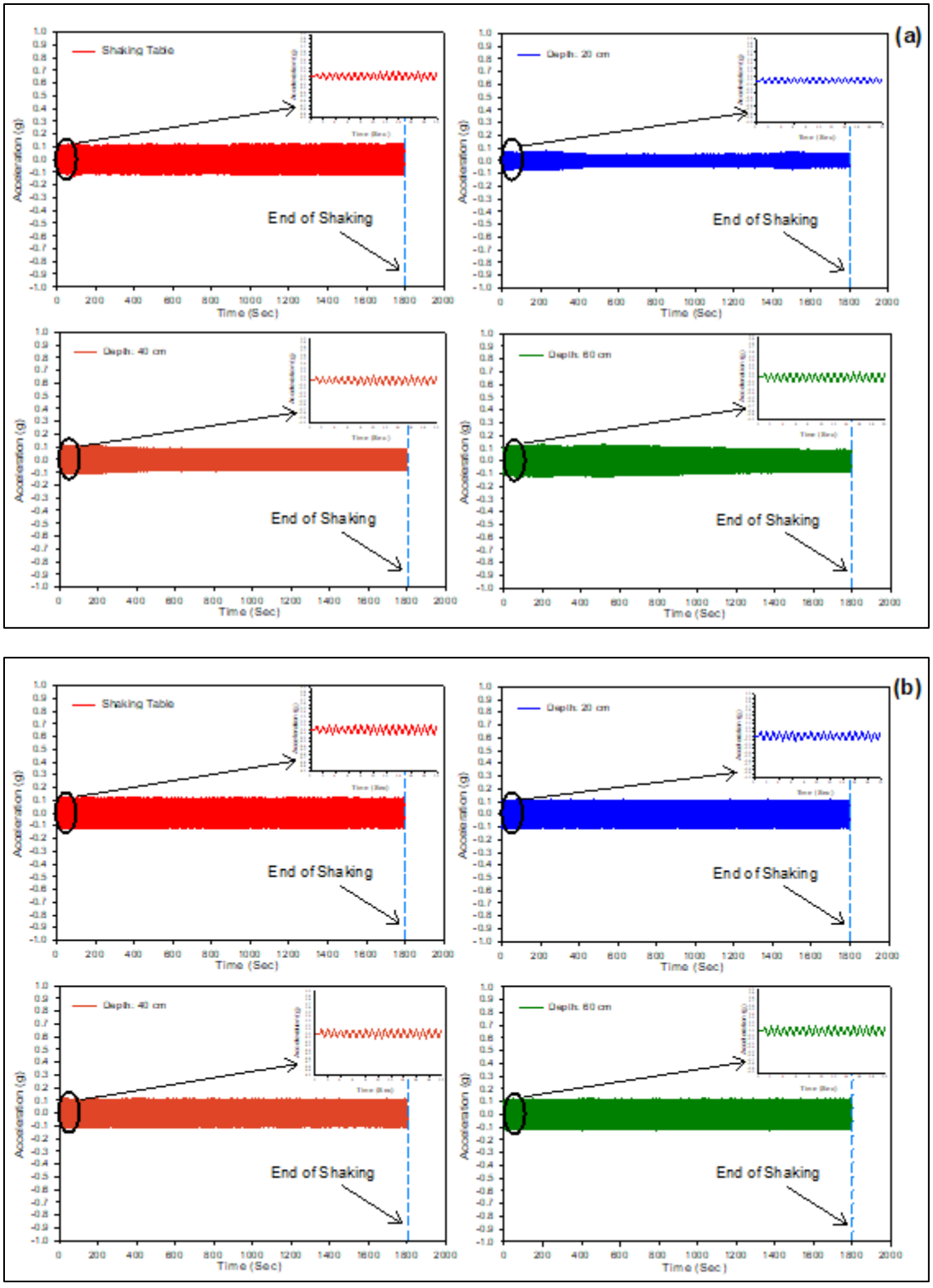

Figure 5.6 Measured peak acceleration histories at different depths vs time for 2.5 hrs-CPB samples prepared at different temperatures: (a) 20ºC; (b) 35ºC.

5.5.1.2 Lateral (horizontal) displacement

Shaking-induced liquefaction causes deformation of liquefiable soils, which can be inferred from lateral (horizontal) displacement. Indeed, ground vibration destabilizes the contact between solid particles, which will diminish the soil resistance against shaking (Takahashi et al. 2001, Dungca et al. 2006). Figure 5.7(a-b) illustrates the lateral displacement at various depths during the cyclic loading durations for 2.5 hours aged CPB models mixed and cured at temperatures of 20°C and 35°C, respectively.

Two key behaviors can be observed, as shown in Figure 5.7(a-b):

(a) In both samples, the lateral displacement decreased in higher depths. This behavior is coherent with the findings of several past researches (e.g. Motamed et al. 2013, Srilatha et al. 2013) and can be attributed to the shaking-induced densification (compaction) of the tailings particles that leads to the increase in material density during shaking (Zhu and Clark 1994, Anastasopoulos et al. 2010). However, the displacement variation with depth was lower within the CPB sample that was prepared at 35°C (Figure 5.7b) as compared to the specimen prepared at 20°C (Figure 5.7a). This reduction can be attributed to the effect of high initial temperature on accelerating the progress of cement hydration, and consequently increasing the CPB solidification. Faster cement hydration means the precipitation of a more amount of cement hydration products (e.g., C-S-H, CH), which plays the main role in increasing the cementation degree or cohesion of the CPB material (Ercikdi et al. 2009, Fall et al. 2010, Fang and Fall 2018, Yilmaz 2018). This argument regarding the increase in the amount of cement hydration products with the increase in temperature is experimentally supported by the results of thermal analysis (TG/DTG) on cement pastes of CPB, which are presented in Figure 5.15 and will be discussed later.

(b) The magnitude of lateral displacement within CPB sample of initial temperature of 35°C was lower in value as compared to the CPB specimen of initial temperature of 20°C. This reduction in the lateral displacement at high temperature is the consequence of the increase in bonds between the tailings particles with the acceleration of cement hydration progress because of the high temperature (Yilmaz et al. 2004, Fall et al. 2007, Ercikdi et al. 2009) (Figure 5.16). Comparative analysis of the results presented in the Figures 6 and 7 suggests that the bonds between particles of 2.5 hours-CPB mixed and cured at high temperature were strong enough to resist the cyclic induced shear stress, while the bonds between the particles of the 2.5 hours-CPB mixed and cured at low temperature were weaker and thus had lower shear resistance, which minimizes the acceleration and increases the lateral displacement. These facts strengthen the assumption that the high initial temperature of CPB mixture might enhance the CPB resistance against liquefaction during ground movement, while the CPB material of low initial temperature is more susceptible to the cyclic loading-induced liquefaction.

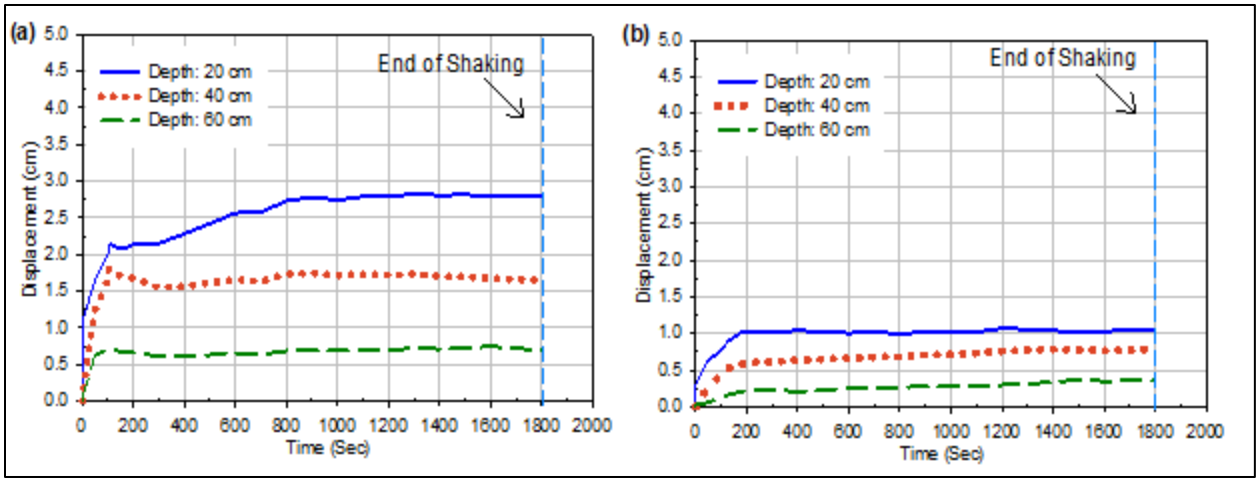

Figure 5.7 Lateral displacement histories at different depths vs times for 2.5 hrs-CPB samples prepared at different temperatures: (a) 20ºC; (b) 35ºC.

5.5.2 Evolution of Pore Water Pressure, Effective Stress and Settlement

5.5.2.1 Pore-water pressure

The pore water pressure (PWP) variation with depths before, during, and after shaking (from the time of casting in the FLSB to about 24 hours) within the CPB samples mixed and cured at 20ºC and 35ºC has been illustrated in Figure (5.8a) and (5.8b), respectively.

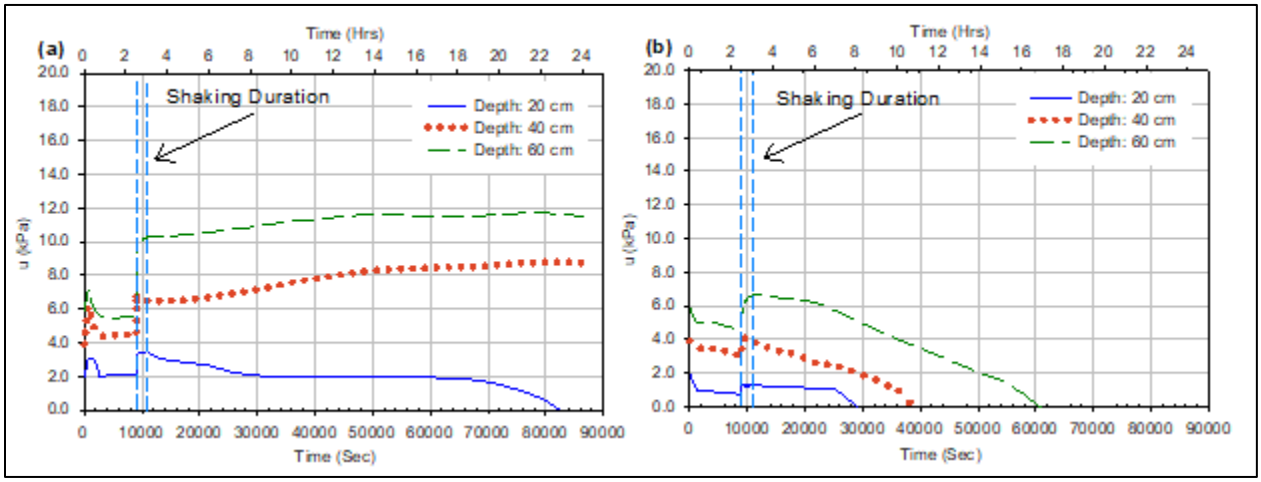

Figure 5.8 Pore water pressure histories at different depths vs times for 2.5 hrs-CPB samples prepared at different temperatures: (a) 20ºC; (b) 35ºC.

(i) Before shaking: during the first 1 hour (3600 sec), after depositing the fresh CPB in the FLSB, there was a rapid increase in PWP in all depths of both 2.5 hours-CPB samples. This is related to the reduction in the voids volume due to the self-weight settlement and rearrangement of the tailings particles at the very early age (Yilmaz 2018). Afterwards, there was a clear reduction

in PWP in both samples as a result of the water consumption during cement hydration (Helinski et al. 2007, Ghirian and Fall 2014, Scrivener et al. 2015). However, it was evident that the decrease in PWP within the CPB sample prepared at 35^{o}C was more significant than the decrease in PWP within CPB sample that was prepared at 20^{o}C. This observation is consistent with the results of suction monitoring presented in Figure 5.9(a-b) (discussed later). Moreover, it is worth noting that the PWP near the surface of the CPB might also be subjected to water evaporation.

(ii) During shaking: when shaking began, as expected, there was a rapid increase in pore water pressure at all depths within both 2.5 hours-CPB materials until reaching peak values. Also, as expected, the greater depths showed higher increase in PWP. This shaking-induced buildup in pore water pressure can be attributed to the contractive behavior of the saturated backfill material or particles causing rapid evolution of excess pore water (Bouckovalas et al. 2009, Saebimoghaddam 2010, Jefferies and Been 2015, Porcino et al. 2015) (Figure 5.12; it will be discussed later). However, the increase in pore water pressure within the CPB sample mixed and cured at 35^{o}C was insignificant as compared to the increase in pore water pressure within the CPB that was mixed and cured at 20^{o}C. This can be attributed to the coupled effect of curing time and the influence of high initial temperature on the cement hydration processes. Regarding the curing time, as the cement hydration progresses with time, cement hydration products will be precipitated within the CPB pores (Bullard et al. 2011, Scrivener et al. 2015). Also, the progress of cement hydration with time leads to the consumption of pore-water (self-desiccation), which strengthens the cementing bonds between the tailings particles, and thus reduces the contraction of the CPB materials (Saebimoghaddam 2010, Jamali 2012, Ghirian and Fall 2013). As far as the effect of high initial temperature on the cement hydration processes is concerned, it accelerates the progress of cement hydration, leading to more production of cement hydration products (as mentioned above in section 5.5.1.1). This will increase the consumption of the pore-water and thereby intensify the self-desiccation (Fall et al. 2010, Aldhafeeri et al. 2016).

(iii) After shaking: after the end of shaking, the 2.5 hours-CPB specimen prepared at 20^{o}C exhibited a slight increase in pore water pressure with time at all depths (with different magnitudes) regardless of the progress of cement hydration. This observed slight increase in PWP can be explained by the settlement or contraction of some tailings particles, which might have been partly in suspension due to the termination of the cycling loading. This contraction generated additional pore water pressure (Pépin et al. 2009). This slight increase in PWP within the CPB sample prepared at 20^{o}C was then followed by relative stabilization of the PWP at each depth until the end of the monitoring period. However, after around 16 hours of curing (around 13.5 hours after the end of shaking), the near surface depth experienced dissipation of PWP, which is attributed to the combined effect of self-desiccation due to cement hydration and the near surface evaporation as a result of the difference of relative humidity (RH) between the ambient air and the surface of the CPB model (Abdul-Hussain and Fall 2012). This explanation was confirmed by determining the evaporation-induced reduction in water content of a CPB material. This was experimentally conducted by exposing CPB samples (prepared with the same mix components and conditions as

the CPB used in this study) to environmental conditions (RH and temperature) similar to those in which the shaking tests were conducted. It was found that around 60% of the near surface reduction in CPB water content (water loss) was associated to evaporation when the CPB sample is placed under the conditions of 20°C temperature and 24% of RH.

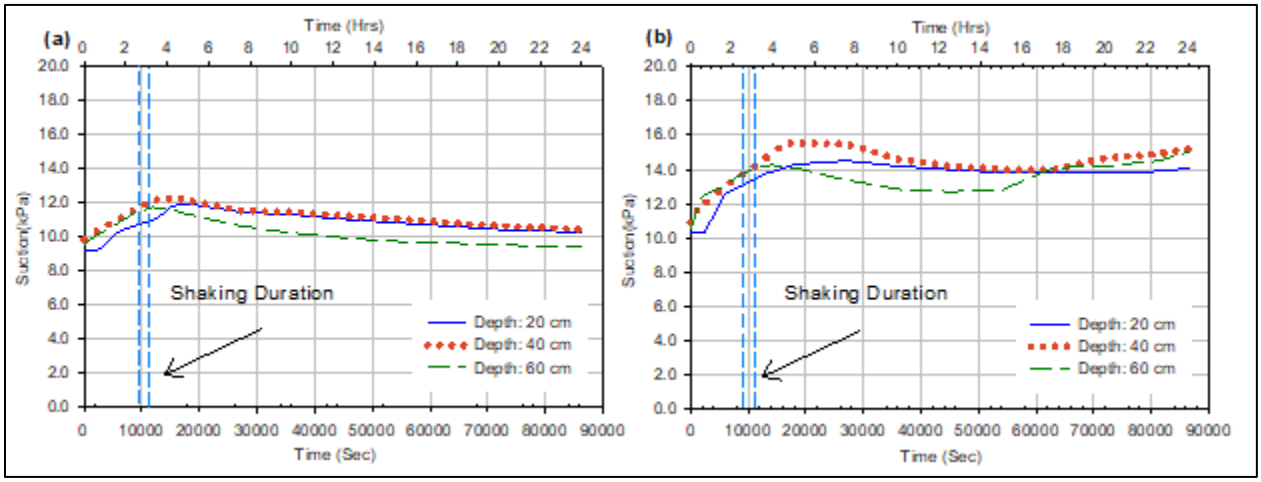

Figure 5.9 Suction evolution at different depths vs times for 2.5 hrs-CPB samples prepared at different temperatures: (a) 20°C; (b) 35°C.

On the other hand, there was no noticeable change in PWP (for around three hours) after shaking the 2.5 hours-CPB model prepared at 35°C. Afterwards, this sample exhibited a significant and rapid reduction in PWP and reached full dissipation at all depths of the sample. This can also be attributed to the acceleration of cement hydration process due to the high initial temperature (Aldhafeeri et al. 2016).

5.5.2.2 Effective stress

Figure 5.10 (a-b) presents the vertical effective stress evolution during shaking at different depths of 2.5 hours-CPB samples that were prepared at temperatures of 20°C and 35°C. During shaking, there was a reduction in these stresses from their initial values in both samples due to the contraction of CPB particles leading to development of excess pore pressure. However, the 2.5 hours-CPB sample prepared at 35°C experienced less reduction in effective stress as compared to the 2.5 hours-CPB sample prepared at 20°C due to the aforementioned effects of temperature on accelerating the cement hydration.

5.5.2.1 Vertical displacement (Settlement)

The downward movement (settlement) in soil particles during ground shaking can provide an indication of the contractive behavior of the particles of liquefiable soil and the increase in the soil density (Ueng et al. 2006, Pépin et al. 2012b). In this study, shaking-induced vertical displacement was recorded in both 2.5 hours-CPB samples that were prepared at different temperatures, as shown in Figure 5.11(a-b). However, it was evident that the CPB prepared at higher temperature (Figure 5.11b) shows less significant settlement as compared to the CPB sample prepared at lower temperature (Figure 5.11a).

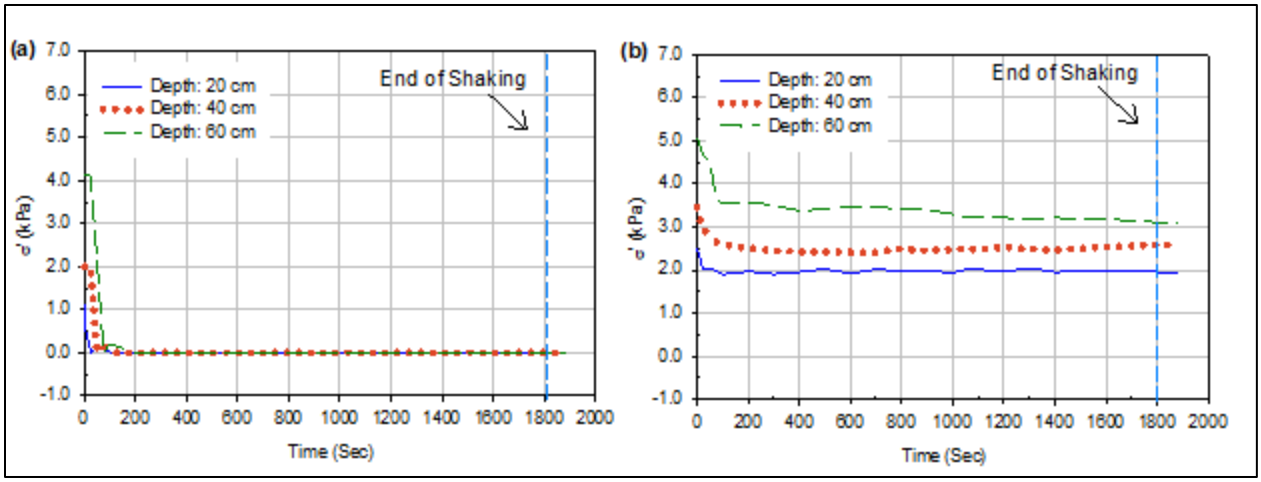

Figure 5.10 Effective stress at different depths vs times for 2.5 hrs-CPB specimens prepared at different temperatures: (a) 20ºC; (b) 35ºC.

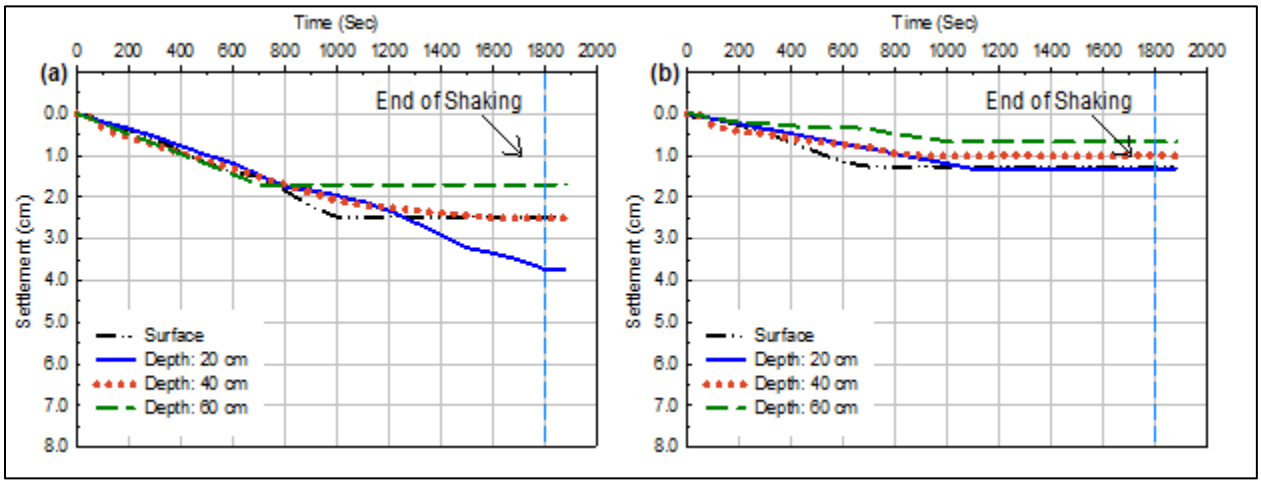

Figure 5.11 Settlement at different depths vs times for 2.5 hrs-CPB samples prepared at different temperatures: (a) 20ºC; (b) 35ºC.

This observation suggests that high temperature will increase the degree of cement hydration, causing less settlement or contraction (volume change) during shaking. This behavior, which is consistent with the results of PWP measurements and liquefaction analysis discussed in Sections 4.2.1 and 4.3 respectively, is owing to the fact that higher cement hydration degree (due to high temperature-induced acceleration in cement hydration) leads to the precipitation of more cement hydration products (see Figure 5.15), thus increasing the strength of the CPB material (Fall et al. 2010, Yilmaz 2018). Therefore, the contracting behavior or settlement of the CPB of higher initial temperature becomes lower (Seed et al. 1975, Tokimatsu and Seed 1987) during shaking. It is also evident from Figure 5.11 that the settlement of 2.5 hours-CPB varied with the measurement depth. The settlement becomes higher in shallow depths. This could be explained by the fact that the CPB material may be slightly less dense at shallower depth due to tailings particles self-weight settlement. However, as expected and coherently with the above-mentioned explanation, the

settlement variation with depth was more significant within the CPB samples prepared at 20oC. On Figure 5.11a, the recorded displacement at the depth of 20 cm became higher than expected after 600 seconds because the plastic plate that was installed at this depth was shifted due to the excessive movement.

5.5.3 Liquefaction Analysis

There are several triggering criteria for assessing soil liquefaction in the laboratory. These criteria encompass strength-based criteria, strain/deformation-based liquefaction criteria, energy-based liquefaction criteria, and (excess) pore ratio-based criteria. However, previous studies (e.g. Wu et al. 2004) have indicated that each of these criteria has its advantages and limitations. This study has assessed the liquefaction of CPB using the criteria that determine the excess pore-water pressure ratio (R_u), which represents the ratio between the excess PWP (Δu) and the initial effective stress (σ_o'). This criterion was extensively used in the shaking table assessment of liquefaction potential of natural soils and/or tailings, as it defines liquefaction when $R_u \geq 1$. However, if $R_u < 1$, there is no liquefaction (Wu et al. 2004, Ueng et al. 2010, Pépin et al. 2012a).

Figure 5.12 (a-b) illustrates the excess PWPs developed during shaking at different depths within 2.5 hours-CPB samples prepared at the temperatures of 20°C and 35°C, respectively. This figure depicts that the excess PWP developed within both samples varied with depth and shaking time. The pore-water pressure ratios determined during shaking of the 2.5 hours-CPB samples mixed and cured at 20°C and 35°C have been depicted in Figure 5.13 a & b, respectively.

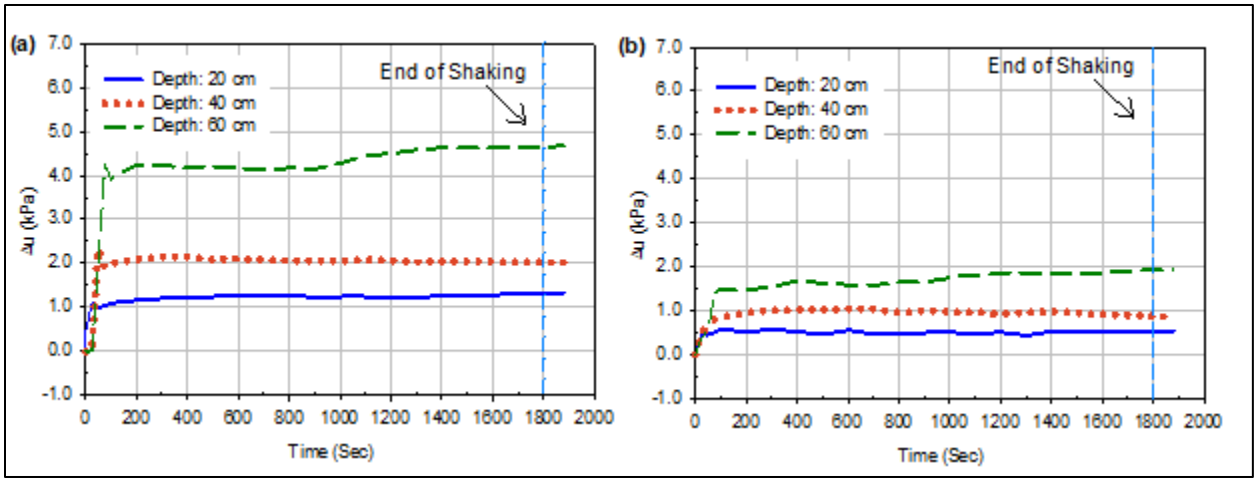

Figure 5.12 Excess pore water pressure (Δu) development at different depths vs times for 2.5 hrs-CPB samples prepared at different temperatures: (a) 20°C; (b) 35°C.

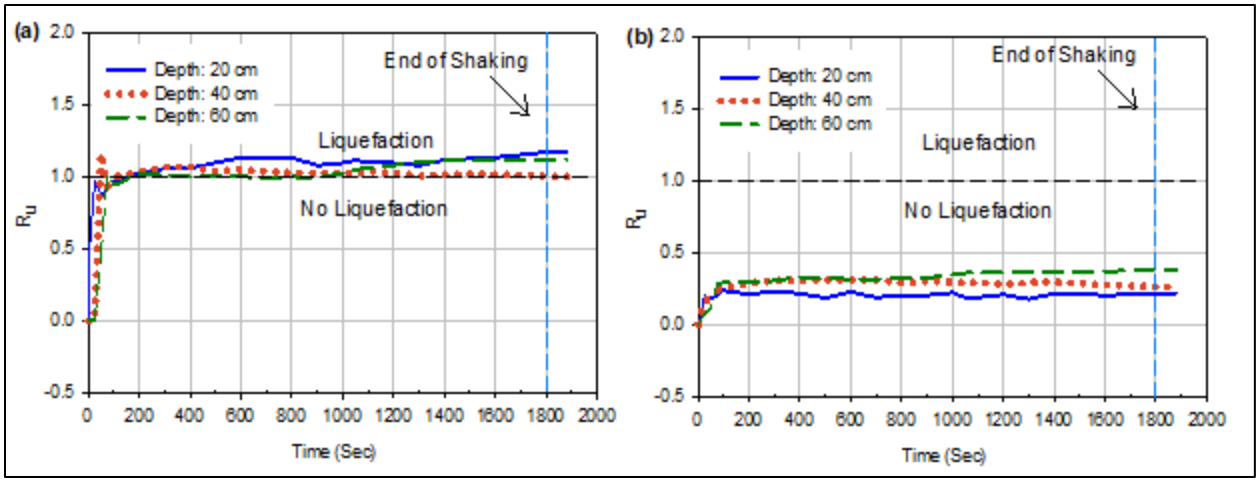

Figure 5.13 Pore-water pressure ratios determined at different depths vs times for 2.5 hrs-CPB samples prepared at different temperatures: (a) 20°C; (b) 35°C.

It is evident that 2.5 hours-CPB sample prepared at 20°C is susceptible to liquefaction ($R_u \geq 1$) when exposed to these cyclic loading conditions, while the 2.5 hours-CPB sample prepared at 35°C was resistant to shaking-induced liquefaction ($R_u < 1$). In other words, the higher initial temperature of CPB reduces the susceptibility of CPB liquefaction under cyclic conditions. This enhancement in liquefaction resistance of CPB with higher initial temperature can be attributed to the combined effects of the following two factors as discussed below: (i) the acceleration of cement hydration process because of the effect of high temperature leading to intensification of self-desiccation of CPB; and (ii) production of more cement hydration products within the CPB pores due to the acceleration of the cement hydration, which strengthen the cementation or cohesion between the tailings particles, thus corroborates the shear strength of the CPB material. These factors obviously result in the enhancement in the liquefaction resistance of the CPB. The aforementioned arguments are supported by the experimental evidence discussed below.

(i) Cement hydration rates

It is generally agreed that the primary goal of using cement (or other hydraulic binders) in cementitious soils is to bind the soil particles, which increases the strength of the mixture as the cement hydration progresses with time (Bullard et al. 2011, Jamali 2012). It is also known that cement hydration progress leads to a net reduction in the total volume of water and solids (self-desiccation), which plays a significant role in the strength of materials undergoing cementation (Persson 1997, Bentz 2008).

The effect of temperature on boosting the cement hydration rate is attributed to the role of the high temperature in accelerating the cement hydration process leading to fast consumption of the pore-fluid, and consequently increases the intensity of self-desiccation. This will consequently decrease the PWP and/or generate negative pore water pressure (suction) (Helinski et al. 2007, Ghirian and Fall 2013). Therefore, the intense self-desiccation improves the effective stress and

strength of these materials (Helinski et al. 2007, Ghirian and Fall 2014). Figures 5.14 (a, b) and 5.9 (a, b), which show the evolution of the volumetric water content (VWC) and suction in the CPB at different depths respectively, support the fact that self-desiccation was insignificant or less intense in both 2.5 hours-CPB samples. However, it is evident that the increase in VWC within the CPB material prepared at 35^{o}C was much faster and significantly higher as compared to CPB material prepared at 20^{o}C. Hence, it can be said that the faster and higher increase in VWC within the CPB material prepared at higher temperature indicates the effect high temperature in accelerating and intensifying the self-desiccation process. Afterwards, the VWC exhibited reduction within the CPB samples of initial temperature of 35^{o}C and remained relatively constant within the CPB samples of initial temperature of 20^{o}C until the end of the monitoring period. Since the VWC expresses the ratio of volume of water to the total volume of the soil, so the increase in VWC can be related to the self-desiccation-induced decrease in the total volume of the CPB. Also, the decrease in the amount of water or water content during this period was confirmed by the suction measurements results presented in Figure 5.9, at which a gradual increase in suction was evident in both samples until reaching its peak after around 6 hours. However, it was clearly observed that the suction potential was much higher within the CPB sample prepared at higher temperature, while it was less within the CPB sample prepared at low temperature. After that, the suction slightly decreased and then remained relatively constant within both CPB samples with respect to the difference in values between the two samples. The evolution of suction in both samples can be attributed to the chemical reactions of the cement hydration, which causes the consumption of water in the capillary pores of CPB (Wang et al. 2016) and reduces the water content in the hydrating backfill or any other cemented soils. This reduction in water content will allow air to enter the pores between tailings or soil particles, generating the air bubbles. As a result, the backfill or soil will turn from saturated condition to partially saturated conditions (Fredlund et al. 2012). The reduction in water content leads to a decrease in the pore water pressure, in other words to an increase in the effective stress, and thus to an increase in the liquefaction resistance of the CPB. Furthermore, the presence of air bubbles inside the pores of a soil will enhance its liquefaction resistance, because the air can absorb the generated excess PWP, and consequently enhances liquefaction resistance (Okamura and Soga 2006). It was also noted that the suction values in the CPB material prepared at higher temperature were higher than those in CPB material prepared at lower temperature, which strongly support the argument of the effect of high temperature on boosting the performance of cement hydration. In other words, this positive effect of high temperature results in the higher water consumption and more air bubbles in the CPB model that was prepared at high temperature. Thus, the effective stress and effect of air bubbles in absorbing the excess PWP will increase in the CPB prepared at 35^{o}C, and liquefaction resistant will consequently improve.

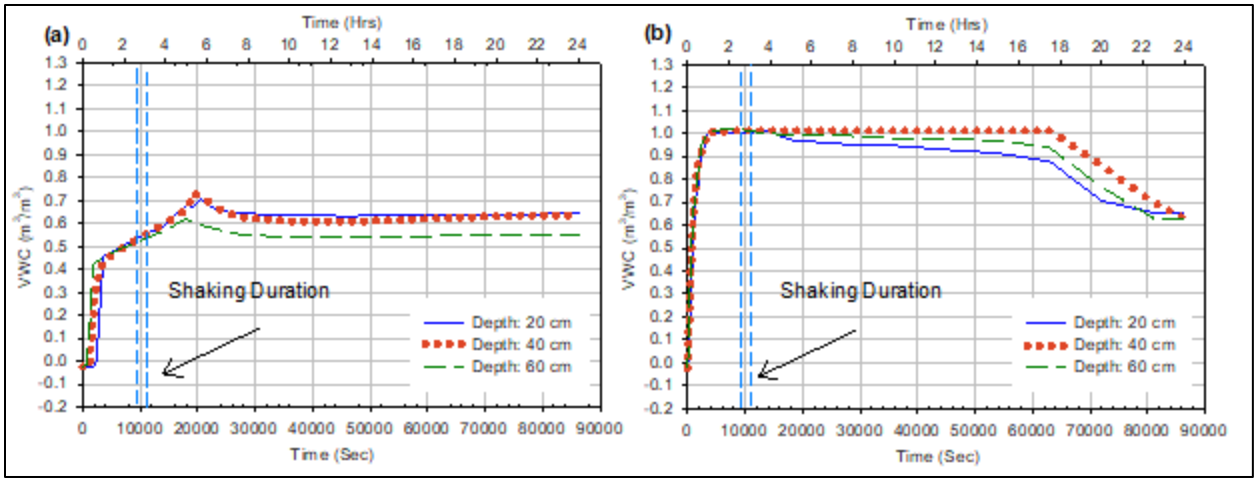

Figure 5.14 Change in volumetric water content at different depths vs times for 2.5 hrs-CPB samples prepared at different temperatures of 20ºC and 35ºC.

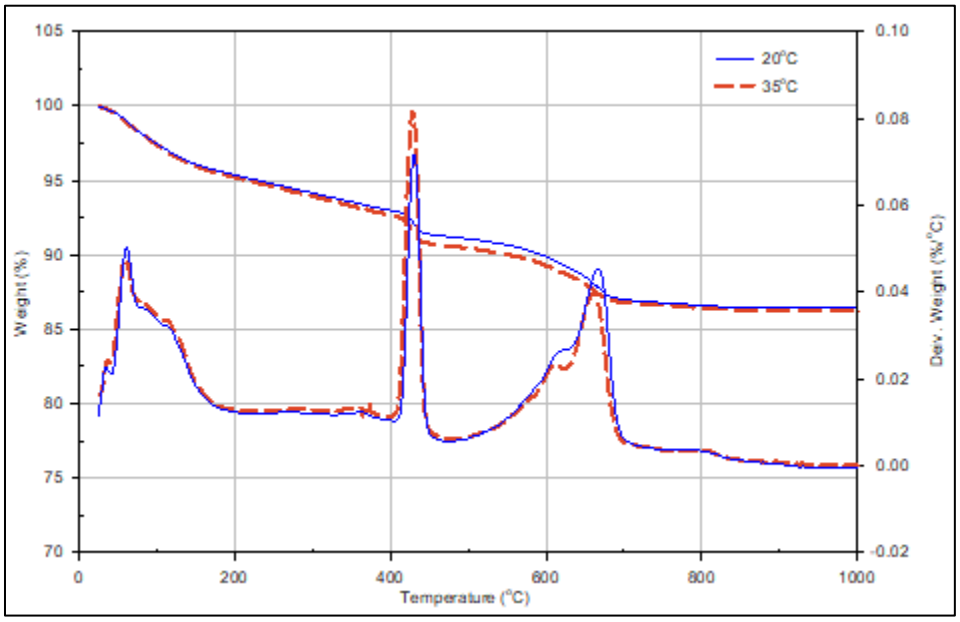

Figure 5.15 Effect of initial temperature on TG/DTG diagrams for 2.5 hrs-CPB samples prepared at different temperatures of 20ºC and 35ºC.

(ii) Production of more cement hydration products

The production of more cement hydration products in the 2.5 hours-CPB prepared at higher temperature as compared to the 2.5 hours-CPB sample prepared at lower temperature is experimentally supported by the results of the thermal analyses (TG/DTG) performed on 2.5 hours-CPBs mixed and cured at temperatures of 20ºC and 35ºC (Figure 15). In this figure, a comparison of the TG/DTG diagrams of the two 2.5 hours-CPB samples (of higher and lower initial temperature) shows that the weight loss (TG) and the peaks (DTG) in the 400-500ºC

temperature range are higher for the CPB prepared at 35ºC, which refers to more amount of hydration products that were formed in CPB sample of high initial (Wang et al. 2016, Fang and Fall 2018).

Moreover, Figures 16 and 17 present the results of the monitoring of the evolution of EC and temperature with curing time progress at different depths of both CPB samples respectively. From these figures, it can be seen that the rate or progress of the cement hydration, in other words the amount of cement hydrations formed within the CPB, is relatively similar at all depths of each CPB sample. However, the difference in initial temperature has affected these rates.

For instance, the EC reaches the peak value in the CPB prepared at 35ºC (Figure 16b) faster than in the CPB prepared at 20ºC (Figure 16a). Moreover, it was noted that the EC peak value of CPB of higher initial temperature is higher than the EC peak value of CPB of lower initial temperature. According to the working principles of EC sensors, the initial increase in EC refers to the increase in the concentration of ions in the CPB pore water solution owing to the dissolution of cement particles. So, the quick increase in EC to reach the peak value in high initial temperatures indicates the acceleration of cement hydration process, and the higher EC values indicate a boosting in cement hydration intensity (Fang and Fall 2018).

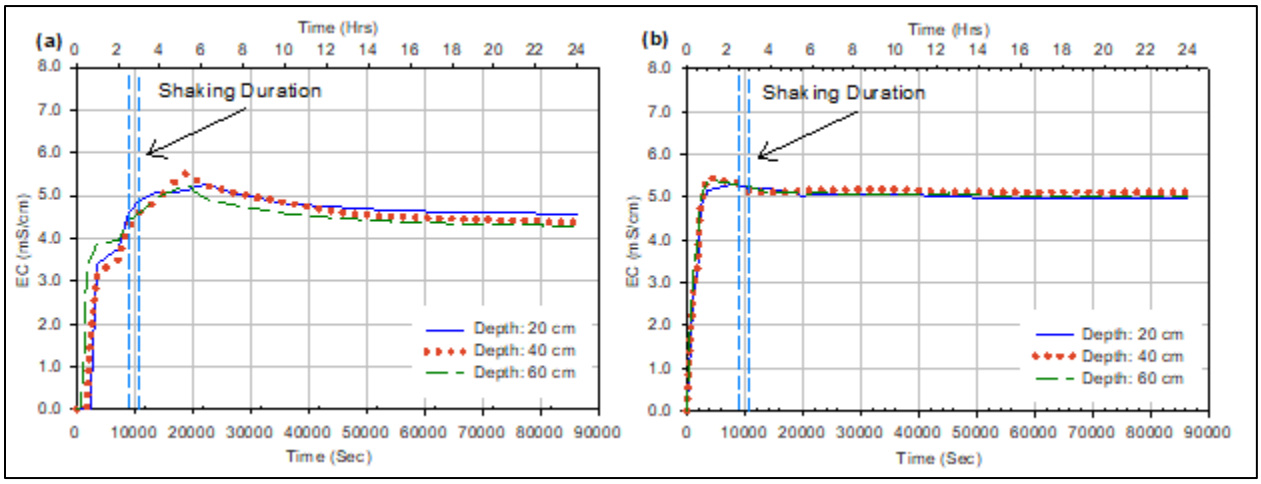

Figure 5.16 Electrical conductivity at different depths for 2.5 hrs-CPB samples prepared at different temperatures: (a) 20ºC; (b) 35ºC.

On the other hand, by comparing the generation of hydration heat of CPB sample prepared at 20ºC (Figure 17 a) and CPB sample prepared at 35ºC (Figure 17 b), it can be seen that the generation of hydration heat was faster and higher within the CPB sample prepared at 35ºC. It is agreed that the generated heat of hydration is a result of the exothermic reaction of aluminate (C_3A), gypsum, and tricalcium silicate (C_3S) with water to form ettringite and the Calcium silicate hydrate (C-S-H) (Bullard et al. 2011, Ghirian and Fall 2015). Thus, the quick and higher generation of hydration heat within CPB of high initial temperature may confirm the above stated assumption of the effect of high temperature on the production of more cement hydration products.

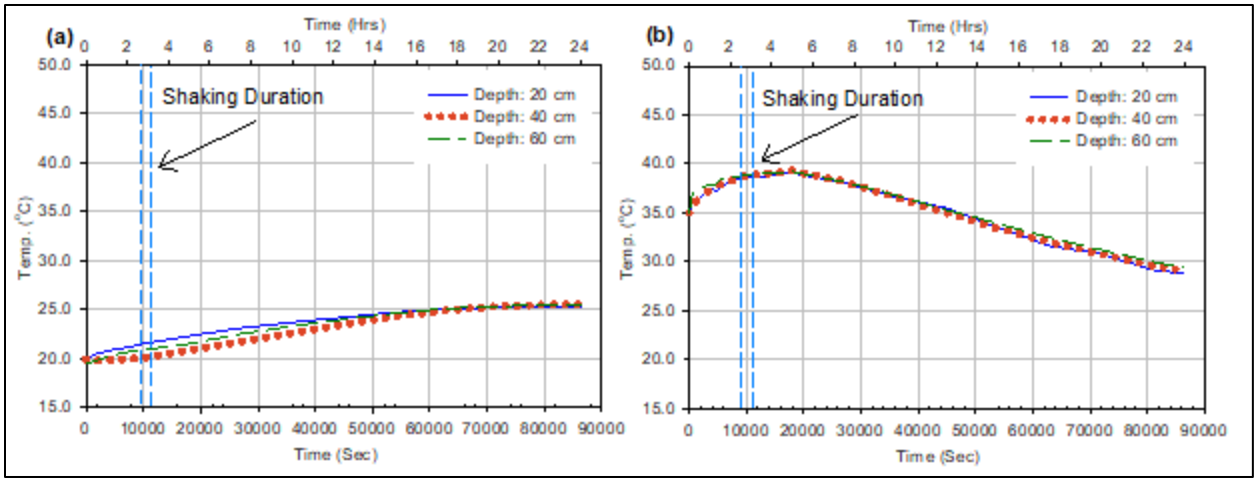

Figure 5.17 Evolution of hydration heat with curing time at different depths vs times for 2.5 hrs-CPB samples prepared at different temperatures: (a) 20°C; (b) 35°C.

5.6 Summary and Conclusion

This manuscript has assessed and discussed the effect of the initial temperature of CPB on the geotechnical response (e.g. liquefaction potential, deformation, excess of pore water pressure, and effective stress) of paste backfill undergoing cementation to cyclic loadings by using the shaking table testing technique. This assessment was conducted by applying cyclic loading on paste backfill samples prepared at different mixing and curing temperatures of 20°C and 35°C. Both samples were casted in a flexible laminar shear box and securely cured to 2.5 hours. The paste backfill samples were also instrumented with numerous sets of sensors and transducers in order to monitor the evolution of several parameters (vertical and horizontal displacement, pore water pressure, acceleration, suction, and electrical conductivity etc.) before, during, and after shaking. The obtained results show that high initial temperature significantly affects the cyclic response of the CPB in terms of acceleration, horizontal and vertical displacement, and excess pore water pressure. Moreover, 2.5 hours old CPB material prepared at high temperature is resistant to liquefaction, whereas the 2.5 hours old CPB prepared at lower temperature can be susceptible to liquefaction under the studied cyclic conditions. This liquefaction resistance can be attributed to the combined effect of two factors: (i) the high temperature-induced increase in cement hydration rate and increase in the self-desiccation intensity within the CPB of high initial temperature. It results in higher effective stress in the CPB prepared at high temperature, and consequently enhances the liquefaction resistance; (ii) the high temperature-induced acceleration of cement hydration process that leads to the formation of more cement hydration products (C-S-H and CH) within the CPB prepared at high temperature. It increases and strengthens the cementation between the tailings particles, and thus improves the liquefaction resistant of CPB mixed and cured at 35°C. These 1-g shaking table tests on CPB are time consuming and expensive, however they have allowed to acquire a better understanding of the effect of the initial (mixing and curing) temperature on the cyclic behavior and liquefaction potential of CPB at early ages besides acquiring information and data that are useful for liquefaction assessment of CPB structures, and

also for future development of constitutive samples to describe and predict the cyclic behavior of hydrating paste backfill or soil undergoing cementation.

5.7 Acknowledgements

The authors would like to thank the National Natural Sciences and Engineering Research Council of Canada (NSERC) for financially supporting this project. Moreover, the authors would like to thank Dr. Mohammed Al-Umar, Dr. Muslim Majeed and Mrs. Ghada Ali for their help with the experimental tests.

5.8 References

Abdelaal, A. (2011) *Early age mechanical behavior and stiffness development of cemented paste backfill with sand*, Doctoral dissertation, University of Toronto.

Abdul-Hussain, N. and Fall, M. (2012) 'Thermo-hydro-mechanical behaviour of sodium silicate-cemented paste tailings in column experiments', *Tunnelling and Underground Space Technology*, 29, 85-93.

Acar, Y. B. and El-Tahir, E. T. A. (1986) 'Low strain dynamic properties of artificially cemented sand', *Journal of Geotechnical Engineering*, 112(11), 1001-1015.

Ahn, K. S., Zhang, C. and Canbulat, I. (2017) 'Study of seismic activities associated with Australian underground coal mining', in *Coal Operators' Conference*, University of Wollongong, Australia,

Aldhafeeri, Z. and Fall, M. (2016) 'Time and damage induced changes in the chemical reactivity of cemented paste backfill', *Journal of Environmental Chemical Engineering*, 4(4), 4038-4049.

Aldhafeeri, Z., Fall, M., Pokharel, M. and Pouramini, Z. (2016) 'Temperature dependence of the reactivity of cemented paste backfill', *Applied Geochemistry*, 72, 10-19.

Ali, G., Fall, M. and Alainachi, I. (2021) 'Time- and temperature-dependence of rheological properties of cemented tailings backfill with sodium silicate', *ASCE's Journal of Materials in Civil Engineering*, DOI: 10.1061/(ASCE)MT.1943-5533.0003605.

Anastasopoulos, I., Georgarakos, T., Georgiannou, V., Drosos, V. and Kourkoulis, R. (2010) 'Seismic performance of bar-mat reinforced-soil retaining wall: Shaking table testing versus numerical analysis with modified kinematic hardening constitutive model', *Soil Dynamics and Earthquake Engineering*, 30(10), 1089-1105.

ASTM C143/C143M-15a (2015) 'Standard test method for slump of hydraulic-cement concrete',

Bairro, R. and Vaz, C. (2000) *Shaking table testing of civil engineering structures-The LNEC 3D simulator experience*, translated by Auckland, New Zeland.

Becker, D., Cailleau, B., Kaiser, D. and Dahm, T. (2014) 'Macroscopic Failure Processes at Mines Revealed by Acoustic Emission (AE) Monitoring', *Bulletin of the Seismological Society of America*, 104(4), 1785-1801.

Bentz, D. P. (2008) 'A review of early-age properties of cement-based materials', *Cement and Concrete Research*, 38(2), 196-204.

Benzaazoua, M., Fall, M. and Belem, T. (2004) 'A contribution to understanding the hardening process of cemented pastefill', *Minerals Engineering*, 17(2), 141-152.

Bouckovalas, G. D., Papadimitriou, A. G. and Niarchos, D. (2009) 'Gravel drains for the remediation of liquefiable sites: The Seed & Booker (1977) approach revisited', in *International Conference on Performance-Based Design*, Tokyo, Japan, International Society for Soil Mechanics and Geotechnical Engineering., 61-75.

Bullard, J. W., Jennings, H. M., Livingston, R. A., Nonat, A., Scherer, G. W., Schweitzer, J. S., Scrivener, K. L. and Thomas, J. J. (2011) 'Mechanisms of cement hydration', *Cement and Concrete Research*, 41(12), 1208-1223.

Carraro, J. A. H., Prezzi, M. and Salgado, R. (2009) 'Shear strength and stiffness of sands containing plastic or nonplastic fines', *Journal of Geotechnical and Geoenvironmental Engineering*, 135(9), 1167-1178.

Carter, D. P. (1988) *Liquefaction potential of sand deposits under low levels of excitation*, California Univ., Berkeley, CA, USA.

Chen, G., Wang, Z., Zuo, X., Du, X. and Gao, H. (2013) 'Shaking table test on the seismic failure characteristics of a subway station structure on liquefiable ground', *Earthquake Engineering & Structural Dynamics*, 42(10), 1489-1507.

Cui, L. and Fall, M. (2016) 'Mechanical and thermal properties of cemented tailings materials at early ages: Influence of initial temperature, curing stress and drainage conditions', *Construction and Building Materials*, 125, 553-563.

DeAlba, P., Chan, C. and Seed, H. (1975) 'Determination of soil liquefaction characteristics by large-scale laboratory tests (EERC 75-14)', *Berkeley, CA: Berkeley University-Earthquake Engineering Research Center*.

Dungca, J. R., Kuwano, J., Takahashi, A., Saruwatari, T., Izawa, J., Suzuki, H. and Tokimatsu, K. (2006) 'Shaking table tests on the lateral response of a pile buried in liquefied sand', *Soil Dynamics and Earthquake Engineering*, 26(2-4), 287-295.

Ercikdi, B., Cihangir, F., Kesimal, A., Deveci, H. and Alp, I. (2009) 'Utilization of industrial waste products as pozzolanic material in cemented paste backfill of high sulphide mill tailings', *J Hazard Mater*, 168(2-3), 848-56.

Fall, M., Célestin, J. C., Pokharel, M. and Touré, M. (2010) 'A contribution to understanding the effects of curing temperature on the mechanical properties of mine cemented tailings backfill', *Engineering Geology*, 114(3-4), 397-413.

Fall, M., Nasir, O. and Celestine, J. (2007) 'Paste backfill responses in deep mine temperature conditions', in Symposium minefill, Montreal, Canada, CD-Room,

Fall, M. and Pokharel, M. (2010) 'Coupled effects of sulphate and temperature on the strength development of cemented tailings backfills: Portland cement-paste backfill', *Cement and Concrete Composites*, 32(10), 819-828.

Fall, M. and Samb, S. S. (2008) 'Pore structure of cemented tailings materials under natural or accidental thermal loads', *Materials Characterization*, 59(5), 598-605.

Fang, K. and Fall, M. (2018) 'Effects of curing temperature on shear behaviour of cemented paste backfill-rock interface', *International Journal of Rock Mechanics and Mining Sciences*, 112, 184-192.

Ferdosi, B., James, M. and Aubertin, M. (2014) 'Numerical modeling of seismic table testing of tailings with and without inclusion', *Proceedings of GeoRegina*.

Finn, W., Pickering, D. J. and Bransby, P. L. (1971) 'Sand liquefaction in triaxial and simple shear tests', *Journal of Soil Mechanics & Foundations Div*.

Fredlund, D. G., Rahardjo, H. and Fredlund, M. D. (2012) *Unsaturated soil mechanics in engineering practice*, Hoboken, New Jersey, USA: John Wiley & Sons.

Ghirian, A. and Fall, M. (2013) 'Coupled thermo-hydro-mechanical–chemical behaviour of cemented paste backfill in column experiments. Part I: Physical, hydraulic and thermal processes and characteristics', *Engineering Geology*, 164, 195-207.

Ghirian, A. and Fall, M. (2014) 'Coupled thermo-hydro-mechanical–chemical behaviour of cemented paste backfill in column experiments', *Engineering Geology*, 170, 11-23.

Ghirian, A. and Fall, M. (2015) 'Coupled Behavior of Cemented Paste Backfill at Early Ages', *Geotechnical and Geological Engineering*, 33(5), 1141-1166.

Ghorbani, A., Eslami, A. and Nezhad Moghadam, M. (2020) 'Effect of non-plastic silt on liquefaction susceptibility of marine sand by transparent laminar shear box in shaking table', *International Journal of Geotechnical Engineering*, 1-13.

Guoxing, C., Su, C., Xi, Z., Xiuli, D., Chengzhi, Q. I. and Zhihua, W. (2015) 'Shaking-table tests and numerical simulations on a subway structure in soft soil', *Soil Dynamics and Earthquake Engineering*, 76, 13-28.

Haruna, S. and Fall, M. (2020) 'Strength Development of Cemented Tailings Materials Containing Polycarboxylate ether-based Superplasticizer: Experimental Results on the Effect of Time and Temperature', *Canadian Journal of Civil Engineering*.

Hasegawa, H. S., Wetmiller, R. J. and Gendzwill, D. J. (1989) 'Induced seismicity in mines in Canada—an overview', *Pure and applied geophysics*, 129(3-4), 423-453.

Helinski, M., Fourie, A., Fahey, M. and Ismail, M. (2007) 'Assessment of the self-desiccation process in cemented mine backfills', *Canadian Geotechnical Journal*, 44(10), 1148-1156.

Ishihara, K. (1996) *Soil Behavior in Earthquake Geotechnics*, NY, USA: Oxford University Press.

Jamali, M. (2012) *Effect of Binder Content and Load History on the One dimensional Compression of Williams Mine Cemented Paste Backfill*, Master of Applied Science dissertation: University of Toronto.

James, M. (2009) *The use of waste rock inclusions to control the effect of liquefaction in tailings impoundments.*, Ph.D. thesis: Department of Civil, Geological, and Mining Engineering, École Polytechnique de Montréal, Montréal, Québic.

James, M., Jolette, D., Aubertin, M. and Bussière, B. (2003) *An Experimental Set-up to Investigate Tailings liquefaction and control measures,* translated by Montréal, QC, Canada.

Jefferies, M. and Been, K. (2015) *Soil Liquefaction: a critical state approach,* Second ed., Taylor & Francis, London, UK.

Landriault, D., Verburg, R., Cincilla, W. and Welch, D. (1997) *Paste technology for underground backfill and surface tailings disposal applications.*, Short Course notes—Technical Workshop, Vancouver, British Columbia: unpublished.

Li, W. and Fall, M. (2016) 'Sulphate effect on the early age strength and self-desiccation of cemented paste backfill', *Construction and Building Materials,* 106, 296-304.

Mamlouk, M. S. and Zaniewski, J. P. (2011) *Materials for civil and construction engineers,* 3rd ed., Upper Saddle River, New Jersey: Pearson Prentice Hall.

Mohamed, F. M. O. (2014) *Bearing Capacity and Settlement Behaviour of Footings Subjected to Static and Seismic Loading Conditions in Unsaturated Sandy Soils*, Doctoral dissertation: University of Ottawa.

Moncarz, P. D. and Krawinkler, H. (1981) *Theory and application of experimental model analysis in earthquake engineering,* Stanford University.

Motamed, R., Towhata, I., Honda, T., Tabata, K. and Abe, A. (2013) 'Pile group response to liquefaction-induced lateral spreading: E-Defense large shake table test', *Soil Dynamics and Earthquake Engineering,* 51, 35-46.

Nasir, O. and Fall, M. (2010) 'Coupling binder hydration, temperature and compressive strength development of underground cemented paste backfill at early ages', *Tunnelling and Underground Space Technology,* 25(1), 9-20.

Natural Resources Canada (2019) 'Earthquake Reports for 2019', [online], available: http://www.seismescanada.rncan.gc.ca/recent/2019/index-en.php 2019].

Ngadimon, K. (2006) *Design and Simulation of Hydraulic Shaking Table*, Doctoral dissertation: University of Technology.

Okamura, M. and Soga, Y. (2006) 'Effect of pore fluid compressibility on liquefaction resistance of partially saturated sand', *Soils and Foundations*, 46(5)(5), 695-700.

Özgen, S., Malkoç, Ö., Doğancik, C., Sabah, E. and Şapçi, F. O. (2011) 'Optimization of a Multi Gravity Separator to produce clean coal from Turkish lignite fine coal tailings', *Fuel*, 90(4), 1549-1555.

Pépin, N., Aubertin, M. and James, M. (2009) *An Investigation of the Cyclic Behaviour of tailings using shaking table tests - effect of a drainage inclusion on porewater development*, translated by Halifax, N.S., Canada.

Pépin, N., Aubertin, M. and James, M. (2012a) 'Seismic table investigation of the effect of inclusions on the cyclic behaviour of tailings', *Canadian Geotechnical Journal*, 49(4), 416-426.

Pépin, N., Aubertin, M., James, M. and Leclerc, M. (2012b) 'Seismic Simulator Testing to Investigate the Cyclic Behavior of Tailings in an Instrumented Rigid Box', *Geotechnical Testing Journal*, 35(3), 469-479.

Persson, B. (1997) 'Self-desiccation and its importance in concrete technology', *Materials and Structures*, 30(5), 293-305.

Porcino, D., Marcianò, V. and Granata, R. (2015) 'Cyclic liquefaction behaviour of a moderately cemented grouted sand under repeated loading', *Soil Dynamics and Earthquake Engineering*, 79, 36-46.

Poulos, S. J., Robinsky, E. I. and Keller, T. O. (1985) 'Liquefaction Resistance of Thickened Tailings', *Journal of Geotechnical Engineering*, 111(12), 1380-1394.

Prasad, S. K., Towhata, I., Chandradhara, G. P. and Nanjundaswamy, P. (2004) 'Shaking table tests in earthquake geotechnical engineering', *Current science*, 1398-1404.

Saebimoghaddam, A. (2010) *Liquefaction of Early Age Cemented Paste Backfill*, Doctoral dissertation: University of Toronto.

Salam, S., Xiao, M. and Wang, J. (2020) 'Physical Modeling of Fine Coal Refuse Using Shake Table Testing', in *Geo-Congress 2020: Geotechnical Earthquake Engineering and Special Topics*, Reston, VA, American Society of Civil Engineers., 114-122.

Scrivener, K. L., Juilland, P. and Monteiro, P. J. M. (2015) 'Advances in understanding hydration of Portland cement', *Cement and Concrete Research,* 78, 38-56.

Seed, H. B., Pyke, R. and Martin, G. R. (1975) *Effect of multi-directional shaking on liquefaction of sands,* Earthquake Engineering Research Center, University of California.

Srilatha, N., Madhavi Latha, G. and Puttappa, C. G. (2013) 'Effect of frequency on seismic response of reinforced soil slopes in shaking table tests', *Geotextiles and Geomembranes,* 36, 27-32.

Sriskandakumar, S. (2004) *Cyclic loading response of Fraser River sand for validation of numerical models simulating centrifuge tests,* University of British Columbia, Canada.

Statista (2020) 'Total revenue of the top mining companies worldwide from 2002 to 2018', [online], available: 2020].

Takahashi, A., Takemura, J., Suzuki, A. and Kusakabe, O. (2001) 'Development and performance of an active type shear box in a centrifuge', *International Journal of Physical Modelling in Geotechnics,* 1(2), 1-17.

Thompson, B. D., Grabinsky, M. W., Bawden, W. F. and Counter, D. B. (2009) *In-situ measurements of cemented paste backfill in long-hole stope,* translated by Toronto, ON, Canada.

Tokimatsu, K. and Seed, H. B. (1987) 'Evaluation of settlements in sands due to earthquake shaking', *Journal of Geotechnical Engineering,* 113(8)(8), 861-878.

Tuttle, M., Law, K. T., Seeber, L. and Jacob, K. (1990) 'Liquefaction and ground failure induced by the 1988 Saguenay, Quebec, qrthquakel', *Canadian Geotechnical Journal,* 27(5), 580-589.

Ueng, T. S., Wang, M. H., Chen, M. H., Chen, C. H. and Peng, L. H. (2006) 'A large biaxial shear box for shaking table test on saturated sand', *Geotechnical Testing Journal,* 29(1), 1-8.

Ueng, T. S., Wu, C. W., Cheng, H. W. and Chen, C. H. (2010) 'Settlements of saturated clean sand deposits in shaking table tests', *Soil Dynamics and Earthquake Engineering,* 30(1-2), 50-60.

Wang, Y., Fall, M. and Wu, A. (2016) 'Initial temperature-dependence of strength development and self-desiccation in cemented paste backfill that contains sodium silicate', *Cement and Concrete Composites,* 67, 101-110.

Wu, J., Kammerer, A. M., Riemer, M. F., Seed, R. B. and Pestana, J. M. (2004) *Laboratory Study of Liquefaction Triggering Criteria,* translated by Vancouver, BC, Canada.

Xu, P., Hatami, K. and Jiang, G. (2020) 'Study on seismic stability and performance of reinforced soil walls using shaking table tests', *Geotextiles and Geomembranes,* 48(1), 82-97.

Xu, X., Fall, M., Alainachi, I. and Fang, K. (2020) 'Characterisation of fibre-reinforced backfill/rock interface through direct shear tests', *Geotechnical Research,* 7(1)(1), 1-15.

Yang, L. and Woods, R. D. (2015) 'Shear stiffness modeling of cemented clay', *Canadian Geotechnical Journal,* 52(2)(2), 156-166.

Yilmaz, E. (2018) 'Stope depth effect on field behaviour and performance of cemented paste backfills', *International Journal of Mining, Reclamation and Environment,* 32(4)(4), 273-296.

Yilmaz, E. and Fall, M. (2017) *PasteTailings Management,* Cham, Switzerland: Springer International Publishing.

Yilmaz, E., Kesimal, A. and Ercidi, B. (2004) *Strength development of paste backfill simples at Long term using different binders,* translated by China: 281-285.

Zhu, F. and Clark, J. I. (1994) 'The effect of dynamic loading on lateral stress in sand', *Canadian Geotechnical Journal,* 31(2)(2), 308-311.

CHAPTER 6 Pore Water Pressure and Liquefaction Response of Layered Fine-Grained Soils Undergoing Cementation to Dynamic Loadings (Paper IV)

(Submitted)

Imad Alainachi, and Mamadou Fall

6.1 Abstract

Cemented paste backfill (CPB) is widely used in underground mining operations as it provides support for the underground opening (mine stope) and allows the reuse of the mining wastes (tailings) that might cause environmental damage if improperly disposed. In general, CPB may be placed in the mine stope in different filling methods. It may be placed in one layer (continuous filing), or by multiple layers (discontinuous or sequential filling). However, it was previously noted that CPB are prone to liquefaction when subjected to cyclic loading at the early age. Till today, no studies have addressed the effect of the different filling strategies on the response of CPB during cyclic events by using the new findings of investigating the effect of the different filling strategies of CPB on its geotechnical response to dynamic loading by using shaking table. CPB samples were prepared with different scenarios, including one Layered-CPB (discontinuous filling) sample at which each layer was cured to different curing time, and two unlayered-CPB (continuous filling) that were cured to 2.5 hrs and 4.0 hrs, respectively. All samples were exposed to same cyclic loading using 1-D Shaking table. Geotechnical parameters, including pore-water pressure, settlement, volumetric water content and liquefaction susceptibility were monitored or determined before, during, and after shaking. Obtained results indicate that Layered-CPB samples are resistant to liquefaction, while the unlayered-CPB samples are prone to liquefaction when are cured to less than 4.0 hrs of curing time. These results are expected to contribute significantly to enhancing the efficient designs of CPB structures.

Keywords: Cemented paste backfill; Liquefaction; Shaking table; Tailings; Mine; Sulphate

6.2 Introduction

The mining industry has been contributing significantly to the economies of numerous countries and regions in the world. However, mining activities generate a large volume of potentially harmful wastes, such as tailings. The tailings are man-made soils with high water content that result from the hydrometallurgical processing during the mineral extraction/liberation process (Fall et al. 2009). The solid particles of the tailings mainly consist of fine-grained soil particles (typically silt-sized), whereas the water results from the water used in the aforementioned recovery process. Traditionally, the tailings have been stored on the ground surface in a variety of ways. However, the surface tailings disposal methods are associated with major environmental (e.g., acid mine drainage, ecosystem pollution) and geotechnical (e.g., tailings dam failures) hazards with severe social and economic consequences

One of the most novel technologies developed in the past decades to reduce the aforementioned issues related to surface tailings disposal methods is the technology of cemented paste backfilling. Cemented paste backfill (CPB) also enables to increase the mine productivity and stability of the underground mine cavities (Yilmaz et al. 2004, Ghirian and Fall 2013). CPB is a mixture of tailings (mostly silt-sized soil particles; 70% - 85% solids), 3% - 7% (by total weight of solid; often) of hydraulic binder (usually cement), and a large volume of fresh and/or mine processed water. In other words, CPB is a fine-grained soil undergoing cementation. The CPB components are mixed and prepared in the paste backfill plant usually located on the mine surface, and delivered into the mine cavity or stope (Figure 6.1) by gravity and/or pumping (Fall and Benzaazoua 2005, Aldhafeeri et al. 2016). To prevent the initially fluid CPB from flowing into the active mining area during the stope filling process, a barricade (retaining structure) is commonly built at the drawpoint, which represents the access points at the base of the stope (Ghirian and Fall 2016, Cui 2017). The barricade blocks the drawpoint until the CPB mass gains sufficient strength.

The mechanical stability of the barricade represents a vital part of a successfully application of cemented paste backfilling. Barricade failures often result in fatalities and are associated with severe financial and social consequences for the mine. Numerous barricade failures have been reported in the literature (e.g. Grice 1998, Yumlu and Guresci 2007, Nasir and Fall 2010, Mozaffaridana 2011, Abdul-Hussain and Fall 2012, Li and Yang 2015, Cihangir and Akyol 2016, Cui and Fall 2017). Excessive pressure applied by the CPB mass (at early ages) to the barricade is one of the main causes of barricade failures. Therefore, in the practice, it is imperative to ensure that the pressure applied by the fresh CPB does not exceed the barricade strength or capacity (Ghirian and Fall 2016, Fang and Fall 2019). To achieve this goal, the sequential or two-stage backfilling strategy, which leads to formation of layered CPB, has been adopted in many mines. This backfilling strategy begins with filling the stope to a height just above the barricade to form a first layer of CPB or a plug. Then, the plug is cured for few hours or days to allow cementation and consolidation to take place. Subsequently, the remainder of the stope is backfilled (residual fill) (Yumlu and Guresci 2007, Abdul-Hussain and Fall 2012). Adopting this discontinuous filling strategy helps to maintain reasonable (not excessive) stress on the barricade (Ghirian and Fall

2016). Moreover, the discontinuous backfilling of a stope, in other words, the formation of layered CPB mass, can also result from backfilling interruptions due to technical issues related to the backfilling operations and/or mining activities (Ghirian and Fall 2013).

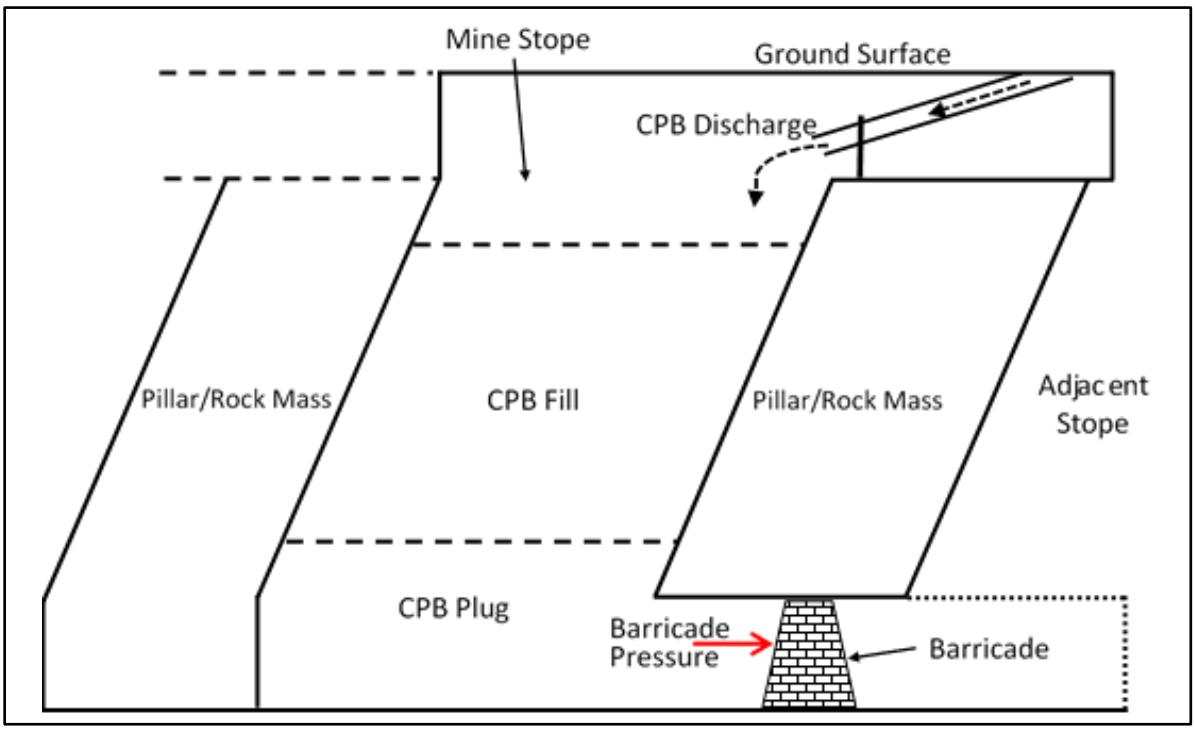

Figure 6.1 Underground mine stope and sequential (two-stage) filling strategy.

The resistance or susceptibility of the freshly placed layered CPB to liquefaction induced by seismic events is a concern in backfilling operations because CPB can be exposed in underground mines to various types of seismic events, including natural earthquakes and seismic events induced by mining activities (e.g., outburst, pillar burst, pillar punching, rockburst, failure of overburden strata) (Hasegawa et al. 1989, Ahn et al. 2017). Moreover, due to the progressive depletion of ore available at shallow depths in many underground mines in the world, mining activities are more and more taking place at greater depths, which is obviously associated with more severe and/or frequent seismic events (Hasegawa et al. 1989, Becker et al. 2014). However, the liquefaction resistance of layered CPB during its curing at the early age is not understood or well-known.

This lack of understanding leads to the fact that, in the practice, the judgment of the liquefaction resistance of CPB is often based on unconfirmed “rule of thumbs” or anecdotal evidences, which may be unreliable, conservative and not supported by scientific evidences. The evaluation of the liquefaction resistance of the CPB by the aforementioned approaches can lead to the design of unsafe and/or uneconomical CPB structures as well as to a significant delay in the opening of the barricades. Delayed opening of barricades has a significant impact on the mining cycle, thus on the productivity of the mine. Therefore, in order to better judge the liquefaction

susceptibility or resistance of CPB, and thus achieve an efficient and safe design of barricades and CPB structures, it is critically important to understand the geotechnical behavior (e.g., pore water pressure response, liquefaction potential) of layered CPB material subjected to cyclic loading at the early ages. At the time of writing however, no studies have addressed the geotechnical behavior of layered and hydrating CPB at early ages under cyclic loadings. This research gap has motivated the authors of this paper to assess the geotechnical behavior of layered CPB during its hydration at the early age by using the shaking table technique. This manuscript presents new findings of pore water pressure and liquefaction responses of layered and hydrating CPB material under cyclic loading conditions by using a shaking table. The behaviour of the layered CPB materials is compared to those of unlayered CPB materials of different ages. This paper emphasizes the evaluation of the behaviour of the CPB material under cyclic loadings rather than that of the CPB structure. The assessment of the behaviour of freshly placed and hydrating CPB structure under cyclic loadings is out of the scope of this paper.

6.3 Materials and Equipment Used in the Experiment

6.3.1 CPB Material and Mix Design

The ingredients of the CPB material used in this study include synthetic silica tailings (ST), hydraulic binder, and water. ST is essentially made of quartz, which is the predominant mineral in Canadian hard rock mine tailings, and its grain size distribution is similar to the average grain size distribution of nine mine tailings (9MT) extracted from nine different mines in eastern Canada (Figure 6.2). Natural tailings usually contain reactive minerals that can potentially have chemical interactions with other ingredients in the CPB mixture. This may influence the interpretation of the obtained results. Thus, the use of ST can eliminate uncertainties that are found with the use of natural tailings, because ST contains high percentage of silica (99.8% SiO_2), which makes it a chemically inert material in CPB systems (Carraro et al. 2009, Fall et al. 2010, Aldhafeeri and Fall 2016). Portland cement type I (PCI) was used as the hydraulic binder, as PCI is most popular type of cement used in backfill operations. Tap water was used as the mixing water.

ST, PCI and water were mixed and homogenized for about 10 min. The cement proportion was 4.5%, and the water-to-cement ratio (w/c) was 7.6 in all mixtures prepared in this study. The degree of water saturation (S) of the prepared CPB was determined to be equal to 100%. The slump (according to ASTM C143/C143M-15a) value of the prepared CPB material was 18 cm, which enables the transportability of the CPB in the field (Ghirian and Fall 2013, Aldhafeeri and Fall 2016). The prepared fresh CPB mixtures were then poured into the developed laminar shear box (Figure 6.3) with a final dimension of each tested CPB sample of 75 cm × 75 cm × 70 cm (length × width × height). In order to avoid changes in water content due to evaporation, the laminar shear box with CPB mixtures was sealed and kept for curing under the room temperature (~20^{o} C) until it reached the desired testing age.

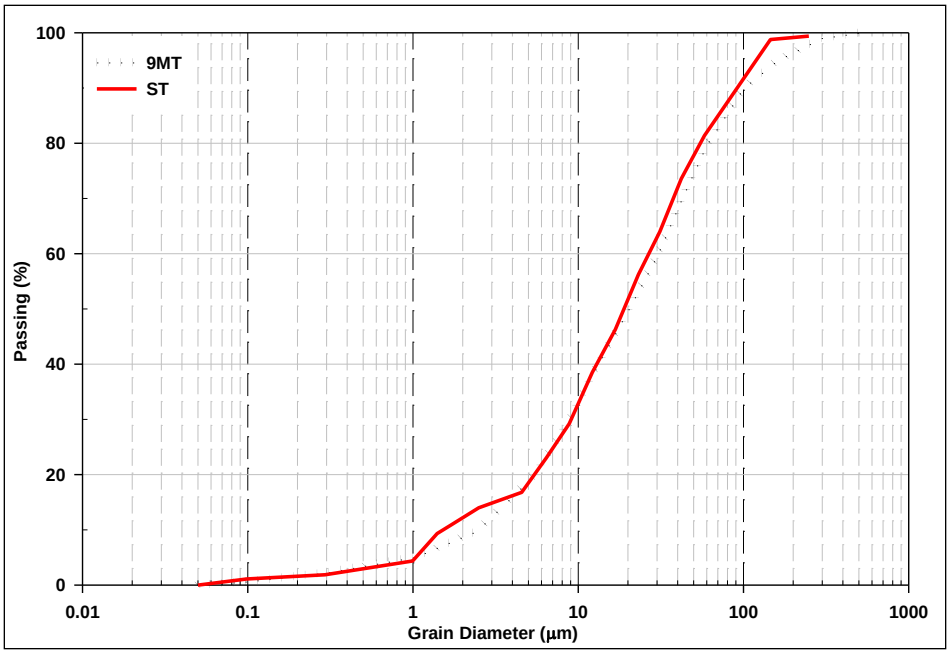

Figure 6.2 Grain size distribution of the silica tailing (ST) vs average grain size distribution of tailings extracted from nine Canadian mines (9MT).

6.3.2 Test Setup and Instrumentation

The Flexible Laminar Shear Box (FLSB) shown in Figure 6.3 was designed and built at the Faculty of Engineering of the University of Ottawa for this research program. The FLSB was securely attached to the platform of the shaking table of the University of Ottawa (Figure 6.3) to simulate the behaviour of the CPB samples under cyclic loadings.

The platform of this shaking table is around ~120 cm × ~106 cm. The table is driven by a digitally controlled hydraulic actuator with a shaking range from 1 to 17 Hz. The maximum base displacement and shear capacity limit in this shaking table are 12 cm and 27 kN respectively (Mohamed 2014). The FLSB was made of 30 horizontal aluminum laminas. The inner dimensions of each lamina are 75 cm × 75 cm. To ensure the independent movement of each lamina, the FLSB was designed to have a clearance spacing of 0.2 cm between each lamina. Accordingly, the total capacity of assembled FLSB becomes 75 cm × 75 cm × 100 cm. In order to contain/hold the CPB mixture in the FLSB before and during the tests, a high flexible polyethylene membrane of 0.5 mm thickness was placed in the FLSB before pouring the CPB mixtures. The high flexibility of the membrane shows insignificant effect on the movement of the FLSB (Mohamed 2014).

Various types of instruments or sensors were placed at different depths in the FLSB to monitor the properties and response of the CPB sample before, during and after shaking, as shown in Figure 6.4. These instruments or sensors include:

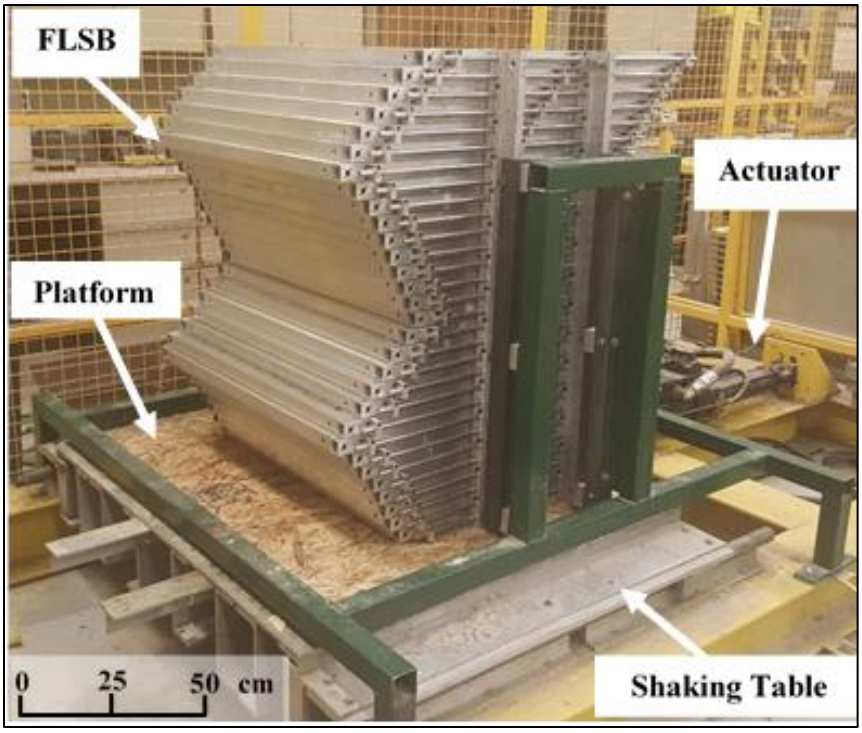

Figure 6.3 Shaking table and Flexible Laminar Shear Box (FLSB) used in this study.

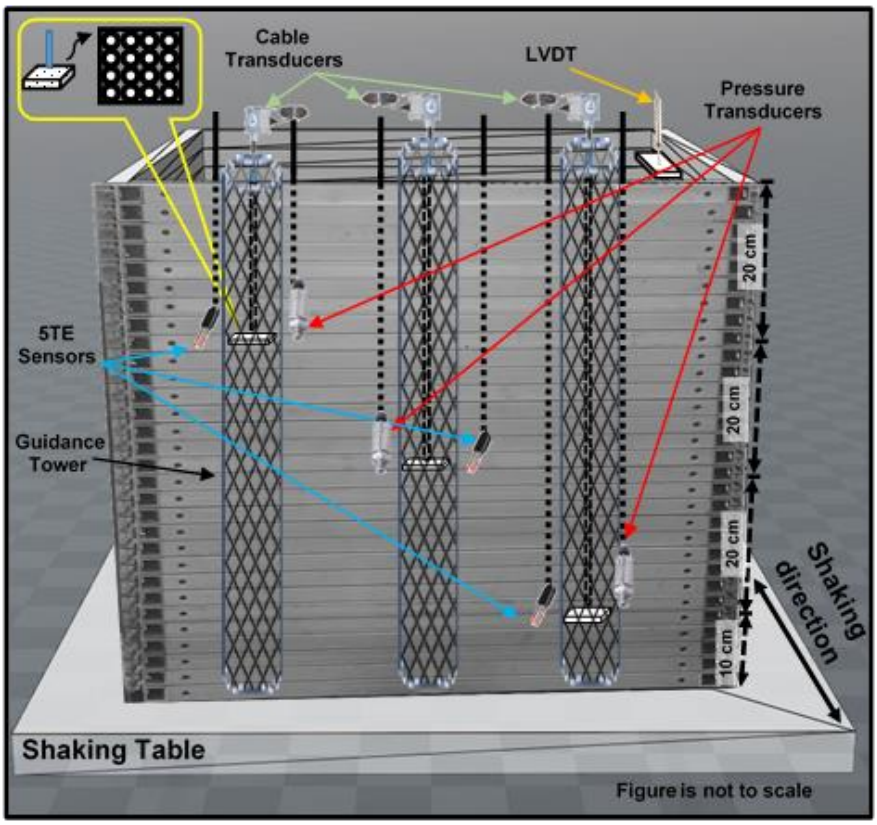

Figure 6.4 Schematic view of the physical model showing the instrumented FLSB.

1. Linear variable differential transformer (LVDT), which was used to monitor the vertical displacement (settlement) of the surface of the CPB sample. HCD-1000 LVDT of 2.5 cm range was used in this regard.

2. Cable transducers (Celesco SP2-12 compact string with 31.7 cm range) were used to measure the settlement (vertical displacement) within the CPB sample during shaking at different depths of 20 cm, 40 cm, and 60 cm. These transducers were attached to thin metal rods connected to 0.2 cm thick, 0.2 cm × 0.2 cm, lightweight, perforated plastic plates that were installed at three different depths within the sample. These plates were perforated to minimize their displacement due to seepage pressure. These metal rods were installed within cylindrical guidance towers (made of thin metal mesh sheets) in order to avoid unwanted movement/tilting of these metal tubes during the shaking process. Guidance towers were connected to the shaking table in order to avoid being a reinforcement factor and to allow the whole system to follow the same motion rhythm.

3. Pressure transducers were used to monitor the change in pore-water pressure before, during, and after shaking. PX309 series pressure transducers, with a measuring range and static accuracy of -15 to +15 PSI and ±0.25% respectively, were used and installed at different depths (20 cm, 40 cm, and 60 cm) of the CPB models inside the FLSB. These transducers were also connected to the above-mentioned guidance towers in order to maintain its positions during shaking.

4. Volumetric Water Content (VWC) sensors were installed at different depths (20 cm, 40 cm, and 60 cm) within the sample to monitor the changes in the volumetric water content (VWC), and were also connected to the guidance towers to maintain their positions during shaking. The sensor used in this regard was ECH2-5TE sensor, which measures volumetric water content (VWC) in the range of 0-80% with the accuracy of ±0.01 from 1-40% and the accuracy of ±0.15 from 40-80%. Monitoring the VWC enables assessment of the self-desiccation of CPB (capillary water consumed by the cement hydration) as well as the water flow within the CPB mass

The LVDT, transducers and accelerometers were all connected to signal conditioning and Data Acquisition Systems (DAQS). The 5TE sensors, on the other hand, were connected to Decagon Em50 series data loggers. DAQS and Em50 were connected to computer to record/analyze the required data at an interval of almost 1 sec during applying the cyclic loading and an interval of 10 min before and after applying the cyclic loading. Furthermore, digital camera was used to record each step of the testing program (mixing, installation, and shaking operation).

6.3.3 Description of the Tested CPB Specimens

As described earlier, the main objective of the study is to investigate the pore water pressure and liquefaction responses of layered CPB materials of early age to dynamic (cyclic) loading. To do so, shaking table tests were conducted on three CPBs that were prepared with different filling

scenarios (discontinuous vs continuous) to create layered and unlayered (serve as a control) CPB specimens as well as cured at different ages:

(i) Layered CPB sample was constructed by filling the FLSB with the prepared CPB mixture in two stages (discontinuous filling) to create two layers of CPB. The first layer was poured into the FLSB and kept for curing for 1.5 hrs before pouring the second layer. Then, the second layer was cured for 2.5 hrs before applying the cyclic loading. This means that at the time of applying cyclic loadings, the first layer was 4 hrs old. For simplicity, this sample will be called in the following sections, Layered-CPB.

(ii) 2.5-hr-old unlayered CPB specimen was constructed by continuously filling the FLSB (continuous filling) with the CPB mixtures until reaching the target sample height (70 cm) to create one layer of CPB. The freshly deposited CPB mixture was then cured for 2.5 hrs before the cyclic loads were applied. Thus, the curing time of this unlayered CPB corresponds to that of the second layer of the Layered-CPB specimen described above. This sample will be called 2.5hrs&Continuous filling-CPB in the rest of the manuscript.

(iii) 4.0-hr-old unlayered CPB sample was constructed in the same manner (continuous filling) as the 2.5-hr-old unlayered CPB specimen. However, in this case, the CPB mixture was cured for 4.0 hrs before applying the cyclic loading. The curing time of the 4.0-hr-old unlayered CPB corresponds to that of the first layer of the layered CPB specimen described previously. This sample will be called 4.0hrs&Continuous filling-CPB in the sections below.

In practice, continuous backfilling has been suggested to enable early opening of the barricades, and thus speed up the mining cycle. However, there is a significant concern and uncertainties with respect to liquefaction susceptibility of CPB structures placed by using continuous backfilling.

6.3.4 Shaking Table Test Conditions

The shaking table testing program carried out and the related testing conditions are illustrated in Figure 6.5 and discussed below.

The cyclic loading conditions applied in this study are similar to those adopted in previous studies on cyclic behaviour of slurry tailings (e.g. James et al. 2003, Pépin et al. 2009, 2012a, 2012b). The shaking table testing program and conditions (Tables 6.1-6.2) consisted of applying in one-dimensional signal, a uniform amplitude, constant frequency (1 Hz) and peak horizontal acceleration of 0.13g on the CPB sample. Moreover, the CPB was shaken for about 1,800s. In should be underlined that the loading conditions applied in this study were not meant to be representative of the same conditions that happen during a natural or real earthquake, since these conditions had a one-dimensional signal, uniform amplitude, constant frequency and long duration. In natural earthquakes, the number of cycles depends on the earthquake magnitude (and

is typically of the order of 5 to 20), and the motion amplitudes have a gradual increase, and a gradual decrease.

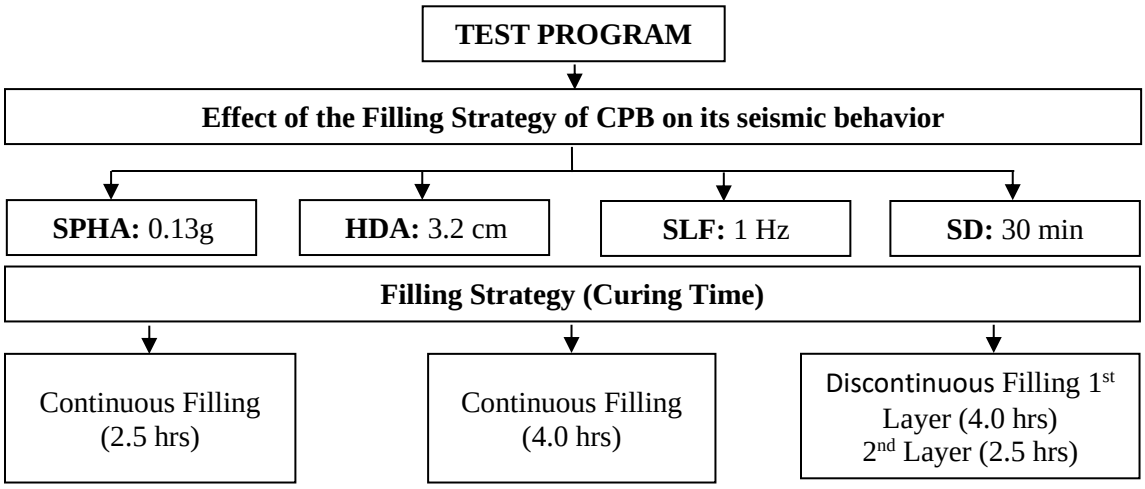

SPHA : Shaking Peak Horizontal Acceleration **SLF** : Sinusoidal Loading Frequency
HDA : Horizontal Displacement Amplitude **SD** : Shaking Duration

Figure 6.5 Flow chart of the testing program and conditions.

Table 6.1 Summary of the testing program

Test	Material	Filling Strategy	CT (hrs)	SPHA	SLF (Hz)	HDA (cm)	SD (min)	PLMD (hrs)
1	CPB	Continuous	2.5	0.13g	1	3.2	30	24
2	CBP	Continuous	4.0	0.13g	1	3.2	30	24
3	CPB	Discontinuous	1st Layer: 4.0 2nd Layer: 2.5	0.13g	1	3.2	30	24

SPHA : Shaking Peak Horizontal Acceleration **SD** : Shaking Duration
SLF : Sinusoidal Loading Frequency **CT** : Curing time
HDA : Horizontal Displacement Amplitude **PLMD** : Post Loading Monitoring Duration

Table 6.2 Selected cyclic parameters used in the present study and previous studies

Parameter	Values used in previous studies [a]	Values used in the present study
Shaking Peak Horizontal Acceleration	0.1g – 1.0g	0.13g
Sinusoidal Loading Frequency	0.1 - 50 (Hz)	1 (Hz)
Horizontal Displacement Amplitude	1.0 – 8.0 (cm)	3.2 (cm)
Shaking Duration [b]	3 – 2,000 (sec)	1,800 (sec)
Post Loading Monitoring Duration	15 (min) – 36 (hr)	24 (hr) [c]

[a] Such as (James et al. 2003, Prasad et al. 2004, Ueng et al. 2006, Pépin et al. 2009, 2012a, 2012b, Özgen et al. 2011, Mohamed 2014, Guoxing et al. 2015, Salam et al. 2020, Xu et al. 2020).
[b] Depends on the material response
[c] After initial casting

The selected applied frequency (sinusoidal loading of 1 Hz frequency) herein was based on previous liquefaction studies (e.g. Ishihara et al. 1981, Ishihara 1996, James et al. 2003, Pépin et al. 2009, 2012a, 2012b, Ueng et al. 2010, Geremew and Yanful 2012) and compatible with the capability of the used sensors in terms of the monitoring as well as with the capacity of the used shaking table. Previous studies (e.g. Sriskandakumar 2004) concluded that the value of the loading frequency adopted in laboratory seismic tests under undrained loading has only a minor effect or negligible effect on the dynamic response of the tested porous media (undrained conditions were applied in this study). Moreover, Srilatha et al. (2013) found that the cyclic responses of the tested soils are virtually comparable at frequencies less than 7 Hz. The applied peak horizontal acceleration (0.13g) corresponded to the peak ground acceleration recorded in the Saguenay earthquake in 1988 in Québec (Tuttle et al. 1990). It should be indicated that only the peak acceleration correlates with the peak of Saguenay Earthquake, not the whole time series. Previous researches (e.g. Carter 1988, James et al. 2003) have found that tailings may liquefy under ground shaking with peak horizontal ground acceleration of 0.05g or more. Furthermore, the cyclic loading in this study was applied to CPB samples for 1,800 seconds. Although recorded earthquakes do not last that much long (Natural Resources Canada 2019), the purpose of applying this long shaking duration is to allow good observation of the dynamic behavior of the CPB samples and relative comparisons of their responses. This will help to develop future constitutive models to compare the dynamic response of CPBs that are placed in different filling methods. Moreover, similar durations were used in several previous investigations on dynamic behavior of tailings materials (e.g. James et al. 2003, Pépin et al. 2012b). Furthermore, it has been reported that the cyclic peak of the liquefaction of tailings (without inclusions and/or cement) can be reached in shaking for 1000 seconds (James et al. 2003). As the material used in this study is cementing tailings (CPB mix), shaking duration was selected in the range of 1 min to 30 min (60 – 1,800 cycles) depending on the material response and the post loading monitoring duration (PLMD) to continue (depending on material response) for additional 24 hours.

6.4 Results and Discussion

6.4.1 Evolution of Pore Water Pressure

Figure 6.6(a-c) illustrates the changes in pore water pressure (PWP) at various depths with time within the Layered-CPB (Figure 6.6a), 2.5 hrs&Continuous filling-CPB (Figure 6.6b), and 4.0 hrs&Continuous filling-CPB (Figure 6.6c) samples, respectively, before, during and after cyclic loading (i.e. from deposition time to about 24 hours).

(i) Before shaking: Figure 6.6a shows that during the first 15 minutes (900 sec) of the disposal of the first layer of the Layered-CPB sample, the pore water pressure (PWP) within the CPB gradually increased to reach the peak values of 3.0 kPa at the end of the first filling. This initial increase in PWP is resultant of the increase of the CPB height (total stress increase), the reduction in the volume of the voids between tailing particles due to the self-weight settlement and rearrangement of the tailings particles at the very early age (Yilmaz et al. 2012, Ghirian and Fall 2013, Muir Wood et al. 2016). Afterwards, the PWP values progressively decreased down to 2.0 kPa before the start of second filling. This decrease in PWP before the start of second filling is attributed to the dissipation of the PWP due to the cement hydration-induced self-desiccation (Helinski et al. 2007, Ghirian and Fall 2014, Scrivener et al. 2015). At the end of the second filling, the PWP in the first (bottom) layer increased up to 4.5 kPa. This second increase in PWP within the first layer (depth: 60 cm) following the addition of the second layer is mainly related to the increase in total stress at this depth due to weight of the CPB material added. Also, the second CPB fill (upper layer) gives additional hydrostatic load and drain its water (gravity-drainage) through the interface to the first CPB fill (lower layer) (El Mkadmi et al. 2014, Ghirian and Fall 2014, Karaoglu and Yilmaz 2017). This can also contribute to this increase in PWP because of the water accumulation in the lower layer. Indeed, the reduction of water content in the (older) lower layer allows unsaturated voids to be generated between tailings particles. In turn, these voids will be filled up with water that comes from the upper layer. . In addition, there was an increase in PWP within the second layer (depth: 20 cm) and at the interface between the two layers (depth: 40 cm). This increase can also be attributed to the self-weight settlement and the rearrangement of tailings particles within the second layer. Subsequently, the PWP decreased slightly at all depths just after the end of the second filling (due to self-desiccation) and then remained relatively stable within all depths of the Layered-CPB until the start of the shaking. From Figures 6.6b and 6.6c, it can be noted that the PWP behavior or evolution in the unlayered CPB samples (2.5 hrs&Continuous and 4.0 hrs&Continuous filling CPBs) during the filling of the FLSB is qualitatively similar to that observed during the disposal of the first layer of the Layered-CPB. Indeed, both unlayered CPB samples experienced the initial increase in PWP in all depths (due to aforementioned causes). This increase was followed by a self-desiccation-induced decrease in PWP in all depths. However, the unlayered samples did not experience the second increase in PWP that was noted in the Layered-CPB sample.

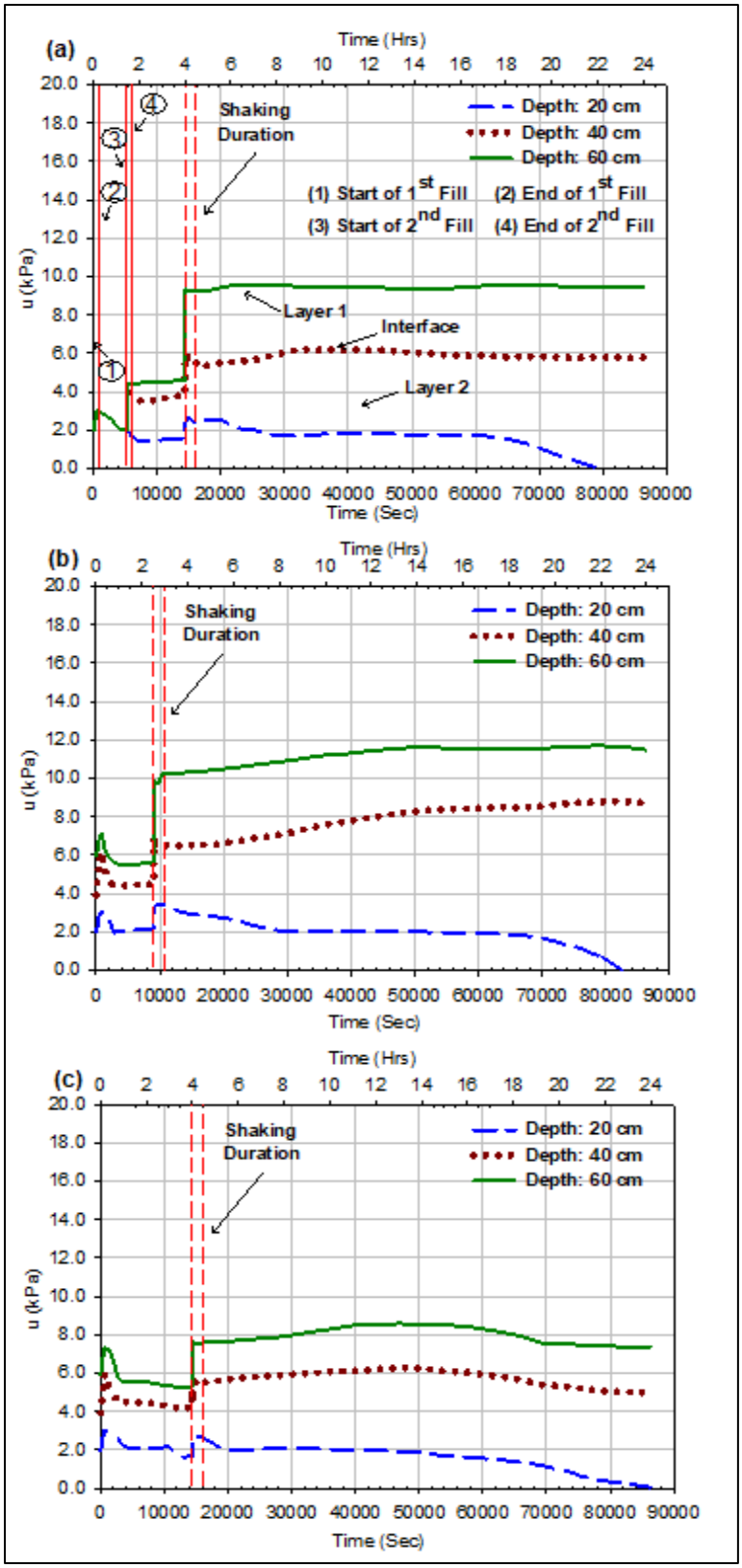

Figure 6.6 histories at different depths vs times for the CPB samples:

(a) Layered CPB; (b) 2.5 hrs&continuous filling-CPB (c) 4.0 hrs&continuous filling-CPB fill.

(ii) During shaking: prior to applying cyclic loads, initial conditions (hydrostatic conditions) of each CPB sample were determined. When shaking began, as expected, there was a quick increase in pore water pressure at all depths within all CPB samples until reaching peak values due to the generation of excess pore water because of the contractive behavior of the saturated backfill material or particles (Bouckovalas et al. 2009, Saebimoghaddam 2010, Jefferies and Been 2015, Porcino et al. 2015) (as supported by Figure 6.8; will be discussed below). Moreover, as expected, greater depths experienced more increase in PWP. However, the increase in pore water pressure within the Layered-CPB sample was less than that within the unlayered CPB samples for comparable depths and curing times. This can be explained by the downward water drainage from the upper layer towards the bottom layer (during shaking) because the lower layer, which was cured for 4.0 hrs and thereby experienced higher progress of cement hydration (Figure 6.10), have acted as a preferential path for excess PWP from the upper layer. This will allow the excess pore-water to flow downward instead of the upward buildup, and thus cause less increase (dissipation) in the PWP comparing with the unlayered samples (Pépin et al. 2009, El Mkadmi et al. 2014).

(iii) After shaking: after the end of shaking, the pore water pressure first slightly increased (with different magnitudes) with time (i.e. regardless of the progress of cement hydration) at the depths of 60 and 40 cm for all CPB samples. This slight increase in PWP at these depths was then followed by a gradual decrease in the PWP until the end of the monitoring period. This observed slight increase in PWP may be related to the end of the cyclic loading, which allowed the settlement or contraction of some tailings particles that might have been partly in suspension at the end of shaking, thereby generating additional PWP (Pépin et al. 2009). Similar behaviours were observed by Pépin et al. (2012a,b), who assessed the liquefaction susceptibility of uncemented hard rock slurry tailings using the shaking table technique. The aforementioned decrease in PWP observed in all samples is mainly attributed to the self-desiccation (Ghirian and Fall 2013). On the other hand, the PWP at the shallow depth (20 cm) for all CPB samples declined to less than the hydrostatic PWP as shown in figure 6.6(a-c). This can be attributed to the combined effect of (i) self-desiccation process (Ghirian and Fall 2013) and (ii) near surface evaporation due to the difference in relative humidity of the CPB surface and the ambient air (Abdul-Hussain and Fall 2012).

6.4.2 Settlement (vertical displacement)

In shaking table tests, the cyclic-induced settlement of soil particles usually provides an indication of the contractive behavior of these particles and the increase in its density (Ueng et al. 2006, Pépin et al. 2012b). The measured vertical (downward) movement induced by shaking of CPB in this study are presented in Figure 6.7(a-c). Figure 6.7a presents the settlement time histories measured during the cyclic loading within the Discontinuous filling-CPB sample, while Figures 6.7b and 6.7c illustrates the settlement within the unlayered CPB samples cured for 2.5 hrs and 4 hrs, respectively. It is clearly observed from Figure 6.7(a-c) that Layered-CPB sample shows less settlement (0.6 cm – 2.0 cm) as compared to 2.5 hrs&Continuous filling-CPB sample (2.5 cm –

3.8 cm) and the 4.0 hrs&Continuous filling CPB-sample (1.2 cm – 1.9 cm). The variation in settlement between these samples can be related to two factors.

(i) The effect of the cement hydration progress with time: the longer curing time leads to less shaking-induced settlement. This is evident from the 4.0 hrs-continuous filling sample and the first layer (depth 60 cm) within the discontinuous filling sample as compared to the 2.5 hrs-continuous sample. This is attributed to the fact that a greater cement hydration degree causes the precipitation of more cement hydration products (see Figure 6.10), thereby increasing the density and strength of the CPB material (Fall et al. 2010, Scrivener et al. 2015). Consequently, the contracting behavior or settlement of the CPB becomes smaller (Seed et al. 1975, Tokimatsu and Seed 1987) during shaking.

(ii) The effect of the filling discontinuity (multiple layer): it leads to less settlement within the second layer (depth 20 cm) and the interface (40 cm) that were cured for 2.5 hrs as compared to the CPB material that was prepared with continuous filling and was cured for the same curing time. This can be attributed to the fact that the bottom layer (first layer that was cured for 4.0 hrs) acted as a preferential path for the excess PWP generated within the upper layer during shaking. Hence, the excess PWP development was inhibited, and the contraction behavior or the settlement within this layer becomes smaller (Pépin et al. 2009, El Mkadmi et al. 2014) (Pépin et al. 2009, El Mkadmi et al. 2014, Rollins et al. 2019). While the continuous filling sample remained in undrained condition at each depth, so only path for the PWP buildup is upward, thereby the contracting behavior became higher and more settlement encountered (Seed et al. 1975, Tokimatsu and Seed 1987).

The above-mentioned explanations are consistent with the results of PWP measurements and liquefaction analysis discussed in Sections 6.4.3. On Figure 6.7(a&b), the recorded displacement at the depth of 20 cm became higher than expected after 1200 seconds because the plastic plate that was installed at this depth was shifted due to the excessive movement.

6.4.3 Liquefaction Analysis

Soil liquefaction is often assessed by different methods, such as strength-based method, stain/deformation-based method, energy-based method, and excess pore-water pressure-based method. However, selecting any of these criteria has its advantages and limitations (Wu et al. 2004). Shaking-induced liquefaction of CPB was investigated in this study by using the excess pore-water pressure-based method. This method has been extensively used to evaluate the liquefaction potential of soils and/or tailings in shaking table tests by several previous researches (e.g. Ueng et al. 2010, Pépin et al. 2012a, Dinh et al. 2020, Sudevan et al. 2020). In this method, the liquefaction is assessed by determining the excess PWP ratio (R_u), which represents the ratio between the excess PWP (Δu) and the initial effective stress (σ'_o). When $R_u \geq 1$, the liquefaction is generally defined, while if $R_u < 1$, there is no liquefaction (Wu et al. 2004).

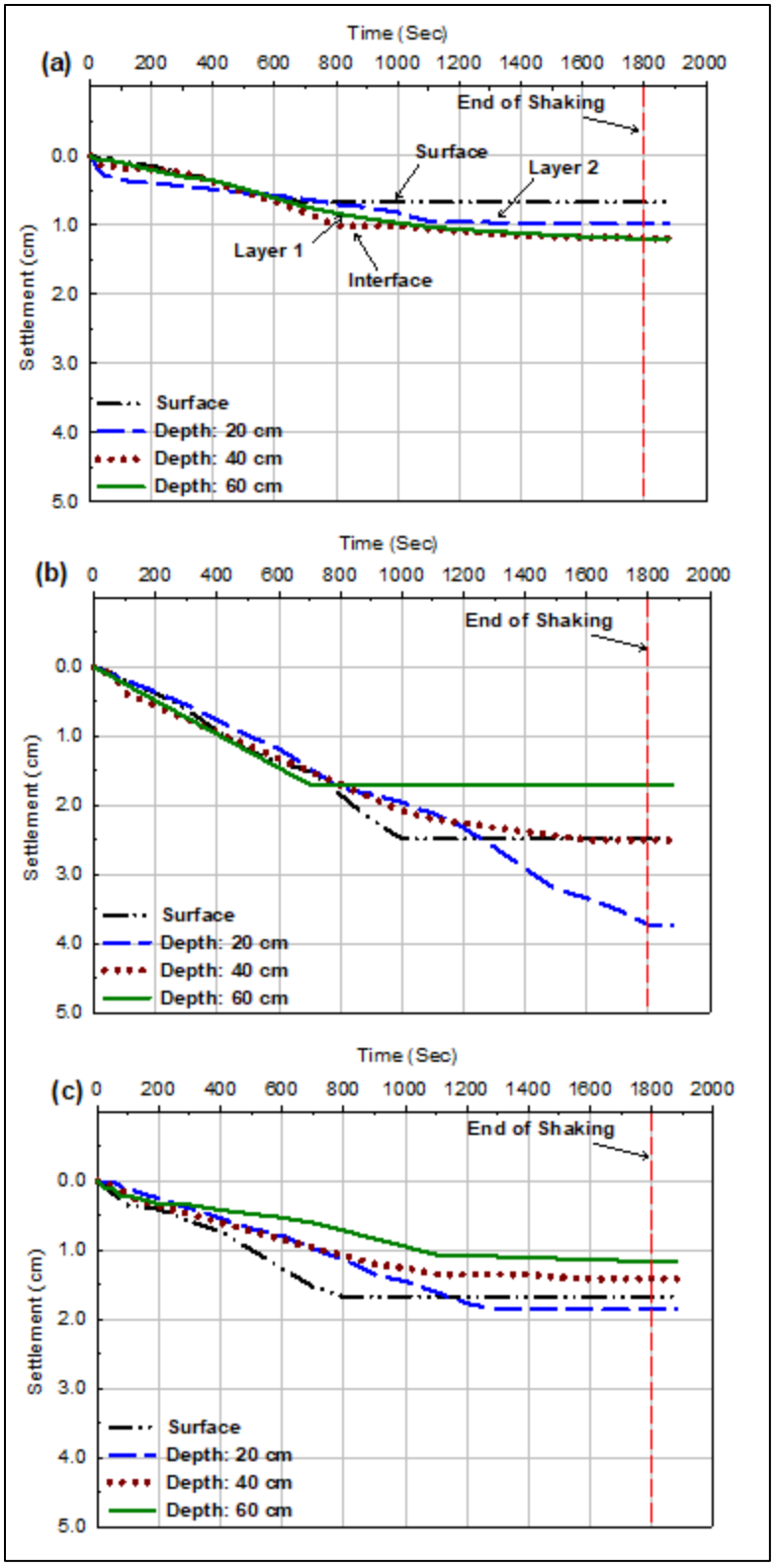

Figure 6.7 Settlement at different depths vs times for CPB models prepared with: (a) Discontinuous fill; (b) 2.5 hrs&continuous fill (c) 4.0 hrs&continuous fill.

Figure 6.8(a-c) shows a comparison of the excess PWP developed, during shaking, at different layers/depths for the Layered-CPB and unlayered CPB samples. As expected and in line with previous studies (e.g. Saebimoghaddam 2010), the excess PWP developed during shaking of the 2.5 hrs&Continuous filling CPB sample (Figure 6.8b) was significantly higher than that developed during the shaking the 4.0 hrs&Continuous filling CPB specimen (Figure 6.8c). However, it was clearly observed that the excess PWP developed within the bottom layer (depth: 60 cm) of the Layered-CPB (Figure 6.8a) was higher than that observed in the same depth of the 4.0 hrs&Continuous filling CPB, regardless of the fact that they were both cured for the same time (4.0 hrs). Moreover, it was also observed that the excess PWP developed within the upper layer (depth: 20 cm) and the interface between the two layers (depth: 40 cm) of the discontinuous filling CPB was lower than that observed in the same depth of the 2.5 hrs&Continuous filling CPB, although they were both cured for the same time (2.5 hrs). This can be attributed to the fact that the lower layer became a partial drainage pathway for the excess PWP generated within the upper layer during shaking, which causes a reduction in excess PWP at the upper layer and the interface and an increase in the excess PWP in the lower layer.

Figure 6.9(a-c) presents the pore-water pressure ratios determined during shaking of the – Layered-CPB samples, 2.5 hrs&Continuous filling and 4.0 hrs&Continuous filling CPB samples, respectively. The 2.5 hrs&Continuous filling CPB sample (Figure 6.9b) was susceptible to liquefaction ($R_u \geq 1$) under the applied cyclic loading conditions, while the 4.0 hrs&Continuous filling CPB sample (Figure 6.9c) was resistant to liquefaction ($R_u < 1$). In other words, the longer curing time reduces the susceptibility to cyclic-induced liquefaction of the CPB, which is consistent with the conclusion of Saebimoghaddam (2010).

On the other hand, it is evident that the sequential (discontinuous) filling strategy enhanced the liquefaction resistant of CPB, as both layers (lower layer that was cured for 4.0 hrs and upper layer that was cured for 2.5 hrs) as well as the interface between these layers were resistant to liquefaction ($R_u < 1$).

Analogous to the settlement behavior, which is explained in section 6.4.2, the variation in liquefaction resistance between the Layered-CPB sample and the two unlayered-CPB samples can be attributed to the coupled influence of two factors:

(i) Progress of cement hydration process

The progress of cement hydration will lead to more precipitation of cement hydration products, such as ettringite, gypsum C-S-H, and CH as shown in the thermal analysis (TG/DTG) diagrams presented in Figure 6.10. These hydration products will progressively bond the tailings particles together (generation of cohesion) and reduce the pore spaces between these particles (Fall et al. 2010, Wang et al. 2016). Also, the progress of cement hydration will lead to a net reduction in total volume of water and solid particles or total volume of the material, which is called

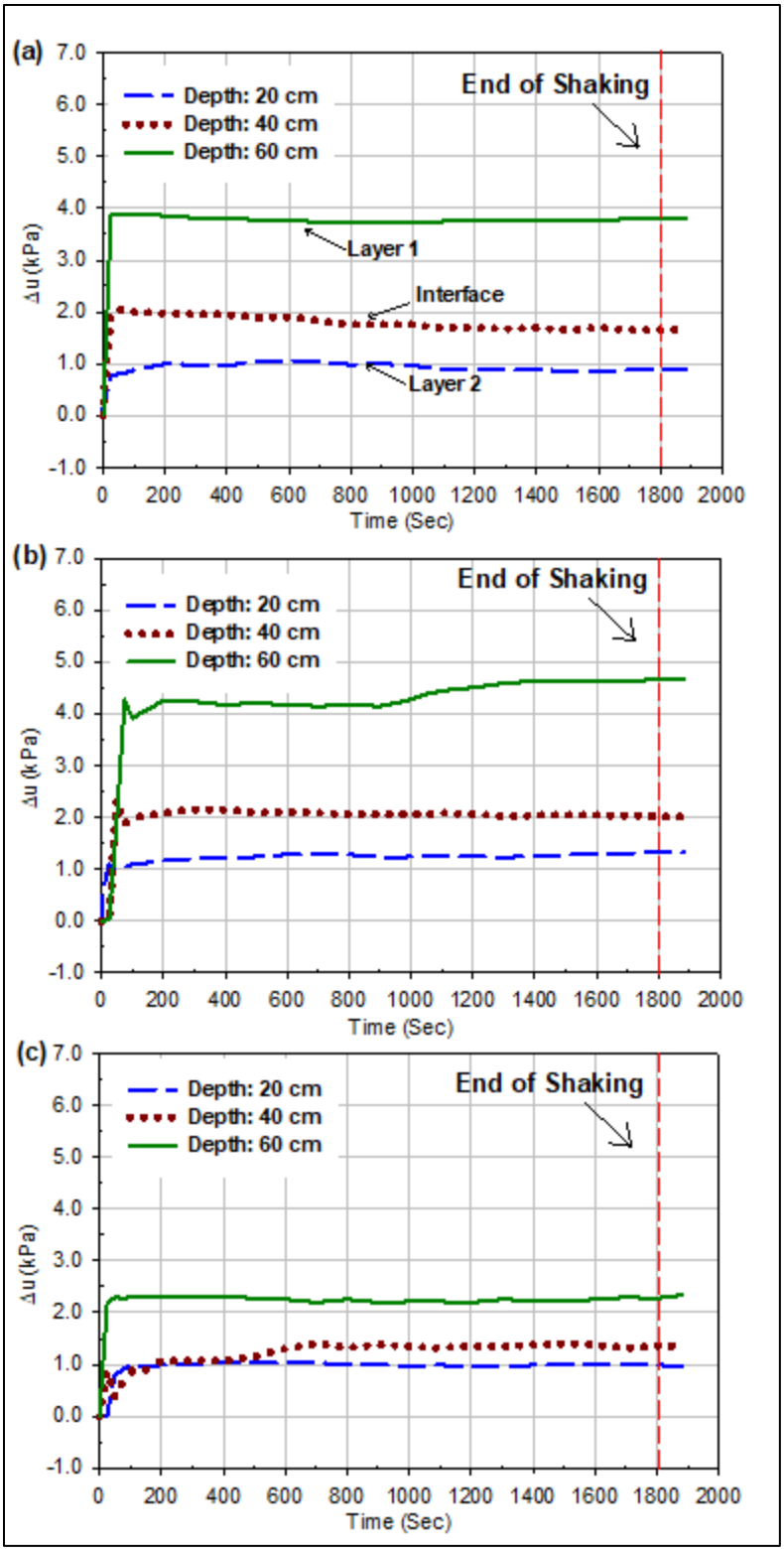

Figure 6.8 Excess pore-water pressure (Δu) development at different depths vs times for CPB models prepared with: (a) Discontinuous fill; (b) 2.5 hrs&continuous fill (c) 4.0 hrs&continuous fill.

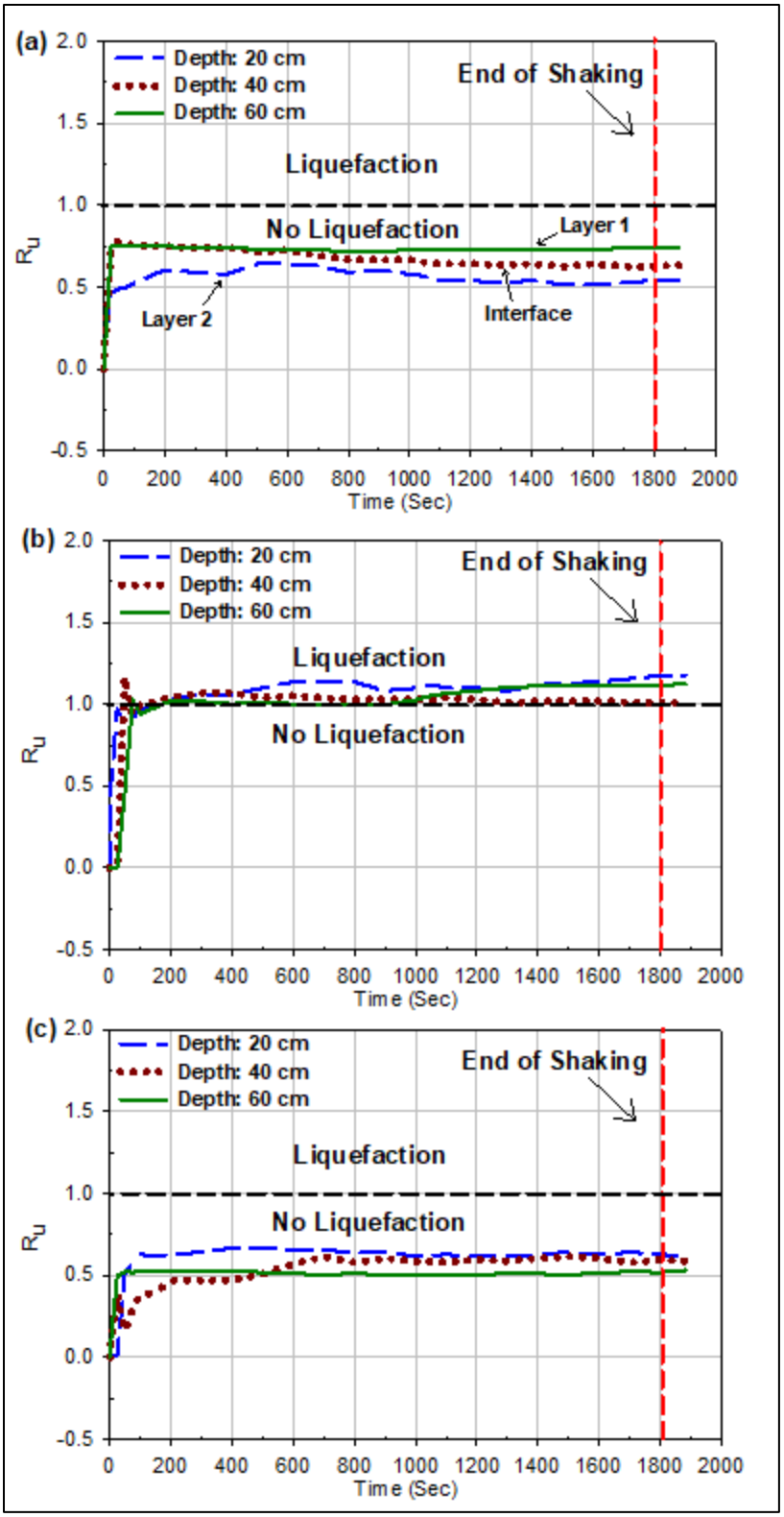

Figure 6.9 Pore -water pressure ratios determined at different depths vs times for CPB models prepared with: (a) Discontinuous fill; (b) 2.5 hrs&continuous fill (c) 4.0 hrs&continuous fill.

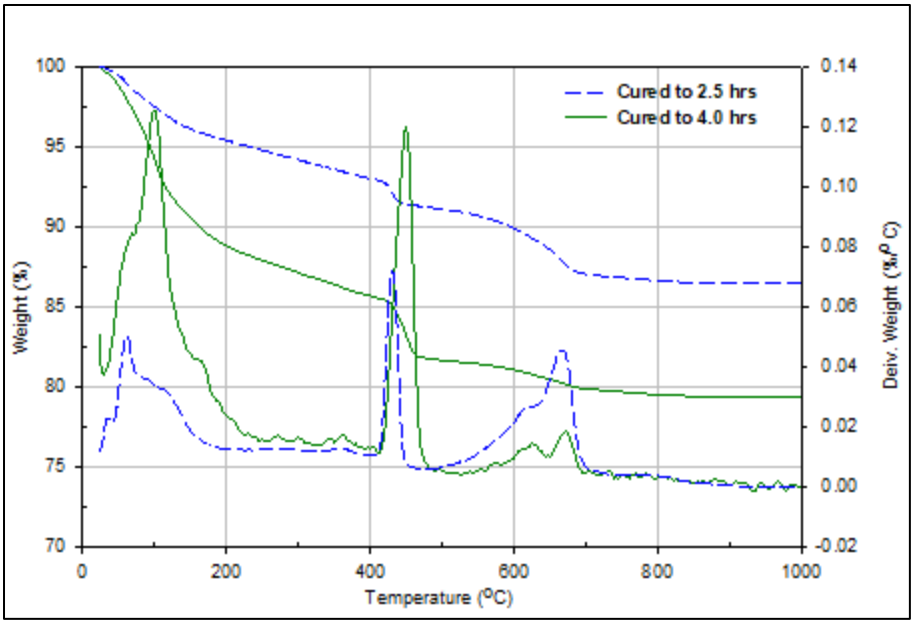

Figure 6.10 Effect of curing time on TG/DT diagrams of CPB cured to 2.5 hrs and 4.0 hrs.

self-desiccation (Li and Fall 2016). This causes a reduction in PWP and moisture content in the hydrating backfill. The reduction in water content in the backfill or soil allows air to enter the pores between tailings or soil particles and generates air bubbles. Consequently, this turns the backfill or soil from saturated condition to partially saturated conditions (Fredlund et al. 2012, Ghirian and Fall 2013). The presence of air bubbles inside the pores of a soil will enhance its liquefaction resistance, because the air can absorb the generated excess PWP by reducing its volume (Okamura and Soga 2006).

(ii) Influence of created drainage condition

As mentioned above, letting the CPB material of the lower layer (layer 1) to cure up to 4.0 hrs before applying the cyclic load allowed the cement self-desiccation to progress and reduces the PWP and water content of the CPB material. Hence, the material of this layer has turned to unsaturated condition. Accordingly, the excess PWP generated (during shaking) within the upper layer (layer 2 that was cured for 2.5 hrs) have found a preferential path to evacuate through the unsaturated lower layer, instead of building upward and causing liquefaction. In other words, applying discontinuous (sequential) filling strategy allows the shaking to be applied in drained condition. Previous researches (Marinucci et al. 2008, Pépin et al. 2009, Hasan et al. 2013, Rollins et al. 2019) have stated that the presence of vertical drains is effective in reducing the PWP ratios, and thus reduces the liquefaction susceptibility of this material. Moreover, it was previously found that CPB material cured in drained conditions have shown higher shear strength than those cured in undrained conditions (Helinski et al. 2007, El Mkadmi et al. 2014, Ghirian and Fall 2016, Fang and Fall 2019).

Figure 6.11(a-b), which shows the evolution of the volumetric water content (VWC) at different layers/depths within the CPB models that were prepared with discontinuous (sequential) filling and continuous filling strategies respectively, supports the fact that self-desiccation did take place in the CPB. A gradual increase in the volumetric water content (VWC) in the initial hours at all depths of each CPB model can be observed in Figure 6.11(a-b). The VWC reached its peak value after around 5-6 hrs. Afterwards, it experienced a slight decrease and then remained relatively constant till the completion of the monitoring period. This increase in VWC is attributed to the self-desiccation induced decrease in the total volume of the CPB since the VWC expresses the ratio of volume of water to the total volume of the soil. Furthermore, it was clearly observed in Figure 6.11a that the VWC within the lower layer (layer 1) of the discontinuous filling CPB model has experienced two rapid increases. The first rapid increase, which occurred after around 1.5 hrs (between stages 3 and 4 in figure 6.11a) is mainly due to the rapid filling of the second fill (layer 2). This argument is consistent with the PWP development at this depth (60 cm) that was observed in this same period of figure 6.6a. The second rapid development of VWC in the lower layer has encountered during shaking period. This increase is attributed to the shaking induced-development of the excess PWP within this layer, in addition to the excess PWP evacuated from the upper layer downwards. Thus, the VWC within the upper layer (20 cm) was less than in the lower layer. On the other hand, the VWC development within CPB sample prepared with continuous filling (Figure 6.11b) showed different behavior. Firstly, there was no rapid increase in VWC after around 1.5 hrs as the hole CPB material was filled once at the same time. Secondly, the values of VWC during shaking periods in the shallow depth (20 cm) were higher than those in the deep depth (60 cm), because the shaking was applied in undrained condition and the developed excess PWP (at all depths) had only on pathway to move, which is the upward buildup.

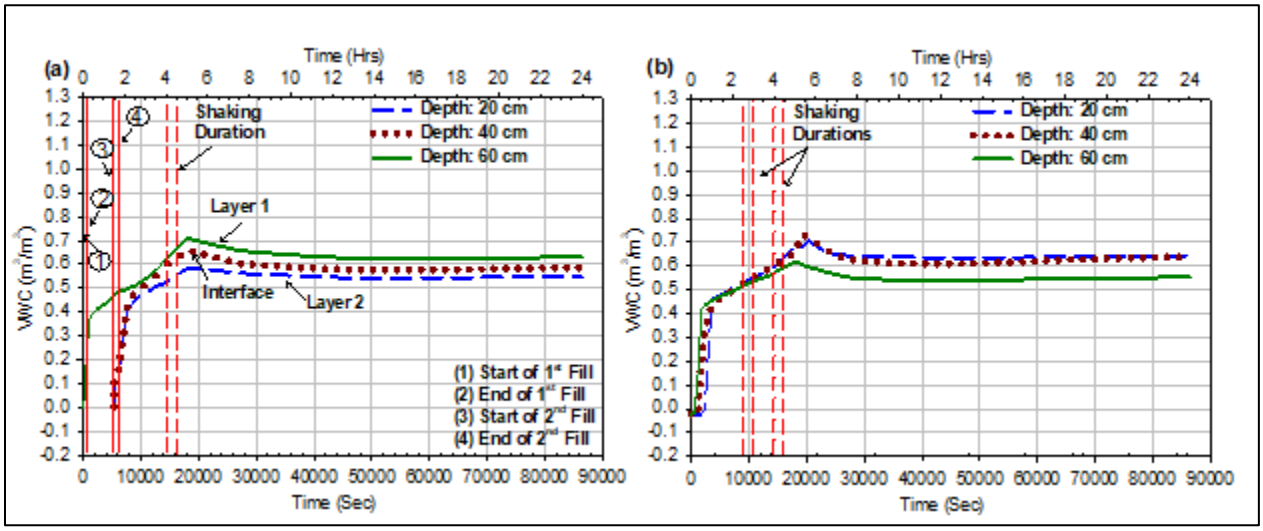

Figure 6.11 Change in volumetric water content at different depths of the CPB models prepared with: (a) Layered-CPB; (b) Continuous fill.

Accordingly, the findings of Figure 6.11(a-b) confirm the aforementioned argument that the effect of filling the fresh CPB material in sequential or discontinuous (layered) filling strategy may reduce the susceptibility of shaking-induced liquefaction of fresh CPB during seismic events.

6.5 Summary and Conclusion

This study has used the shaking table testing technique to investigate the geotechnical response (e.g. settlement, excess pore-water pressure, and liquefaction analysis) of fresh cemented paste backfill to cyclic loadings, with respect to the effect of different filling strategies. This assessment was conducted by applying cyclic loading on paste backfill samples prepared with different filling strategies of discontinuous (layered) filling, 2.5 hrs&Continuous filling, and 4.0 hrs&Continuous filling, which were casted in a flexible laminar shear box. The paste backfill samples were instrumented with numerous sets of sensors and transducers to monitor the evolution of several parameters (pore water pressure, vertical displacement, and volumetric water content) before, during, and after shaking. The obtained results show that adopting different filling strategies leads to significant variation in settlement and the development of excess pore water pressure of the CPB when subjected to cyclic loading. It is also found that discontinuous (layered) CPB material is resistant to liquefaction, whereas continuous filling CPB material can liquefy under the studied cyclic conditions if it was exposed to cyclic loading before achieving 4.0 hrs of curing time. The enhanced liquefaction resistance of Layered-CPB sample is attributed to the combined effect of two factors: (i) strengthening of the cementation between the soil (tailings) particles of the lower (first) layer, which increases the shear resistance of the CPB material in this layer; (ii) the influence of the created drainage conditions within the lower layer, which creates a preferential path for the excess pore water pressure to escape from the upper layer and minimizes the upward buildup of excess PWP and downward movement (settlement) of the soils particles within the backfill. These 1-g tests on CPB are time consuming and expensive. However, they have facilitated a better understanding of the cyclic behavior and liquefaction potential of layered and unlayered CPB at early ages as well as provided information and data that are useful for liquefaction assessment of CPB structures and also for future development of constitutive models to describe and predict the cyclic behavior of hydrating paste backfill or soil undergoing cementation.

6.6 Acknowledgements

The authors would like to thank the National Natural Sciences and Engineering Research Council of Canada (NSERC) for financially supporting this project. Moreover, the authors would like to thank Dr. Mohammed Al-Umar, Dr. Muslim Majeed, Mr. Othman Benamrane and Mr. Fawwaz Ibrahim for their help with the experimental tests.

6.7 References

Abdul-Hussain, N. and Fall, M. (2012) 'Thermo-hydro-mechanical behaviour of sodium silicate-cemented paste tailings in column experiments', *Tunnelling and Underground Space Technology*, 29, 85-93.

Ahn, K. S., Zhang, C. and Canbulat, I. (2017) 'Study of seismic activities associated with Australian underground coal mining', in *Coal Operators' Conference*, University of Wollongong, Australia,

Aldhafeeri, Z. and Fall, M. (2016) 'Time and damage induced changes in the chemical reactivity of cemented paste backfill', *Journal of Environmental Chemical Engineering*, 4(4), 4038-4049.

Aldhafeeri, Z., Fall, M., Pokharel, M. and Pouramini, Z. (2016) 'Temperature dependence of the reactivity of cemented paste backfill', *Applied Geochemistry*, 72, 10-19.

ASTM C143/C143M-15a (2015) 'Standard test method for slump of hydraulic-cement concrete',

Becker, D., Cailleau, B., Kaiser, D. and Dahm, T. (2014) 'Macroscopic Failure Processes at Mines Revealed by Acoustic Emission (AE) Monitoring', *Bulletin of the Seismological Society of America*, 104(4), 1785-1801.

Bouckovalas, G. D., Papadimitriou, A. G. and Niarchos, D. (2009) 'Gravel drains for the remediation of liquefiable sites: The Seed & Booker (1977) approach revisited', in *International Conference on Performance-Based Design*, Tokyo, Japan, International Society for Soil Mechanics and Geotechnical Engineering., 61-75.

Carraro, J. A. H., Prezzi, M. and Salgado, R. (2009) 'Shear strength and stiffness of sands containing plastic or nonplastic fines', *Journal of Geotechnical and Geoenvironmental Engineering*, 135(9), 1167-1178.

Carter, D. P. (1988) *Liquefaction potential of sand deposits under low levels of excitation*, California Univ., Berkeley, CA, USA.

Cihangir, F. and Akyol, Y. (2016) 'Mechanical, hydrological and microstructural assessment of the durability of cemented paste backfill containing alkali-activated slag', *International Journal of Mining, Reclamation and Environment*, 32(2), 123-143.

Cui, L. (2017) *Multiphysics Modeling and Simulation of the Behavior of Cemented Tailings Backfill*, Doctoral dissertation: University of Ottawa.

Cui, L. and Fall, M. (2017) 'Multiphysics modeling of arching effects in fill mass', *Computers and Geotechnics*, 83, 114-131.

Dinh, D. N., Kobayashi, K., Murakami, S. and Yasuhara, K. (2020) *1G laboratory-scale shaking table tests on reduction of liquefaction damage in sand using short gravel compaction piles*, translated by Singapore: Springer Singapore, 635-639.

El Mkadmi, N., Aubertin, M. and Li, L. (2014) 'Effect of drainage and sequential filling on the behavior of backfill in mine stopes', *Canadian Geotechnical Journal,* 51(1), 1-15.

Fall, M., Adrien, D., Célestin, J. C., Pokharel, M. and Touré, M. (2009) 'Saturated hydraulic conductivity of cemented paste backfill', *Minerals Engineering,* 22(15), 1307-1317.

Fall, M. and Benzaazoua, M. (2005) 'Modeling the effect of sulphate on strength development of paste backfill and binder mixture optimization', *Cement and Concrete Research,* 35(2), 301-314.

Fall, M., Célestin, J. C., Pokharel, M. and Touré, M. (2010) 'A contribution to understanding the effects of curing temperature on the mechanical properties of mine cemented tailings backfill', *Engineering Geology,* 114(3-4), 397-413.

Fang, K. and Fall, M. (2019) 'Shear Behavior of the Interface Between Rock and Cemented Backfill: Effect of Curing Stress, Drainage Condition and Backfilling Rate', *Rock Mechanics and Rock Engineering,* 53(1), 325-336.

Fredlund, D. G., Rahardjo, H. and Fredlund, M. D. (2012) *Unsaturated soil mechanics in engineering practice,* Hoboken, New Jersey, USA: John Wiley & Sons.

Geremew, A. M. and Yanful, E. K. (2012) 'Laboratory investigation of the resistance of tailings and natural sediments to cyclic loading', *Geotechnical and Geological Engineering,* 30(2), 431-447.

Ghirian, A. and Fall, M. (2013) 'Coupled thermo-hydro-mechanical–chemical behaviour of cemented paste backfill in column experiments. Part I: Physical, hydraulic and thermal processes and characteristics', *Engineering Geology,* 164, 195-207.

Ghirian, A. and Fall, M. (2014) 'Coupled thermo-hydro-mechanical–chemical behaviour of cemented paste backfill in column experiments', *Engineering Geology,* 170, 11-23.

Ghirian, A. and Fall, M. (2016) 'Strength evolution and deformation behaviour of cemented paste backfill at early ages: Effect of curing stress, filling strategy and drainage', *International Journal of Mining Science and Technology*, 26(5), 809-817.

Grice, T. (1998) *Stability of hydraulic backfill barricades*, translated by 117-120.

Guoxing, C., Su, C., Xi, Z., Xiuli, D., Chengzhi, Q. I. and Zhihua, W. (2015) 'Shaking-table tests and numerical simulations on a subway structure in soft soil', *Soil Dynamics and Earthquake Engineering*, 76, 13-28.

Hasan, A., Suazo, G. and Fourie, A. B. (2013) 'Full scale experiments on the effectiveness of a drainage system for cemented paste backfill', in *Proceedings of the 16th International Seminar on Paste and Thickened Tailings*, Australian Centre for Geomechanics, 379-392.

Hasegawa, H. S., Wetmiller, R. J. and Gendzwill, D. J. (1989) 'Induced seismicity in mines in Canada—an overview', *Pure and applied geophysics*, 129(3-4), 423-453.

Helinski, M., Fourie, A., Fahey, M. and Ismail, M. (2007) 'Assessment of the self-desiccation process in cemented mine backfills', *Canadian Geotechnical Journal*, 44(10), 1148-1156.

Ishihara, K. (1996) *Soil Behavior in Earthquake Geotechnics*, NY, USA: Oxford University Press.

Ishihara, K., Yasuda, S. and Yokota, K. (1981) *Cyclic strength of undisturbed mine tailings*, translated by University of Missouri-Rolla, St. Louis, USA: 53-58.

James, M., Jolette, D., Aubertin, M. and Bussière, B. (2003) *An Experimental Set-up to Investigate Tailings liquefaction and control measures*, translated by Montréal, QC, Canada.

Jefferies, M. and Been, K. (2015) *Soil Liquefaction: a critical state approach*, Second ed., Taylor & Francis, London, UK.

Karaoglu, K. and Yilmaz, E. (2017) 'Cemented paste backfill pressure monitoring and field testing' in *Paste tailings management*, Springer, 195-214.

Li, L. and Yang, P. (2015) 'A numerical evaluation of continuous backfilling in cemented paste backfilled stope through an application of wick drains', *International Journal of Mining Science and Technology*, 25(6), 897-904.

Li, W. and Fall, M. (2016) 'Sulphate effect on the early age strength and self-desiccation of cemented paste backfill', *Construction and Building Materials*, 106, 296-304.

Marinucci, A., Rathje, E., Kano, S., Kamai, R., Conlee, C., Howell, R., Boulanger, R. W. and Gallagher, P. (2008) 'Centrifuge Testing of Prefabricated Vertical Drains for Liquefaction Remediation' in *Geotechnical Earthquake Engineering and Soil Dynamics IV*, 1-10.

Mohamed, F. M. O. (2014) *Bearing Capacity and Settlement Behaviour of Footings Subjected to Static and Seismic Loading Conditions in Unsaturated Sandy Soils*, Doctoral dissertation: University of Ottawa.

Mozaffaridana, M. (2011) *Using thermal profiles of cemented paste backfill to predict strength*, M.A.Sc. dissertation University of Toronto.

Muir Wood, D., Doherty, J. and Walske, M. (2016) 'Deposition and self-weight consolidation of a shrinking fill', *Géotechnique Letters*, 6(1), 72-76.

Nasir, O. and Fall, M. (2010) 'Coupling binder hydration, temperature and compressive strength development of underground cemented paste backfill at early ages', *Tunnelling and Underground Space Technology*, 25(1), 9-20.

Natural Resources Canada (2019) 'Earthquake Reports for 2019', [online], available: http://www.seismescanada.rncan.gc.ca/recent/2019/index-en.php 2019].

Okamura, M. and Soga, Y. (2006) 'Effect of pore fluid compressibility on liquefaction resistance of partially saturated sand', *Soils and Foundations*, 46(5)(5), 695-700.

Özgen, S., Malkoç, Ö., Doğancik, C., Sabah, E. and Şapçi, F. O. (2011) 'Optimization of a Multi Gravity Separator to produce clean coal from Turkish lignite fine coal tailings', *Fuel*, 90(4), 1549-1555.

Pépin, N., Aubertin, M. and James, M. (2009) *An Investigation of the Cyclic Behaviour of tailings using shaking table tests - effect of a drainage inclusion on porewater development*, translated by Halifax, N.S., Canada.

Pépin, N., Aubertin, M. and James, M. (2012a) 'Seismic table investigation of the effect of inclusions on the cyclic behaviour of tailings', *Canadian Geotechnical Journal*, 49(4), 416-426.

Pépin, N., Aubertin, M., James, M. and Leclerc, M. (2012b) 'Seismic Simulator Testing to Investigate the Cyclic Behavior of Tailings in an Instrumented Rigid Box', *Geotechnical Testing Journal*, 35(3), 469-479.

Porcino, D., Marcianò, V. and Granata, R. (2015) 'Cyclic liquefaction behaviour of a moderately cemented grouted sand under repeated loading', *Soil Dynamics and Earthquake Engineering*, 79, 36-46.

Prasad, S. K., Towhata, I., Chandradhara, G. P. and Nanjundaswamy, P. (2004) 'Shaking table tests in earthquake geotechnical engineering', *Current science*, 1398-1404.

Rollins, K. M., Oakes, C. and Meservy, T. (2019) 'Liquefaction Mitigation Potential of Prefabricated Vertical Drains from Large-Scale Laminar Shear Box Testing', in *Proceedings of 16th Panamerican conference on soil mechanics and geotechnical engineering*, Cancun, Mexico, IOS Press, 2104-2115.

Saebimoghaddam, A. (2010) *Liquefaction of Early Age Cemented Paste Backfill*, Doctoral dissertation: University of Toronto.

Salam, S., Xiao, M. and Wang, J. (2020) 'Physical Modeling of Fine Coal Refuse Using Shake Table Testing', in *Geo-Congress 2020: Geotechnical Earthquake Engineering and Special Topics*, Reston, VA, American Society of Civil Engineers., 114-122.

Scrivener, K. L., Juilland, P. and Monteiro, P. J. M. (2015) 'Advances in understanding hydration of Portland cement', *Cement and Concrete Research*, 78, 38-56.

Seed, H. B., Pyke, R. and Martin, G. R. (1975) *Effect of multi-directional shaking on liquefaction of sands*, Earthquake Engineering Research Center, University of California.

Srilatha, N., Madhavi Latha, G. and Puttappa, C. G. (2013) 'Effect of frequency on seismic response of reinforced soil slopes in shaking table tests', *Geotextiles and Geomembranes*, 36, 27-32.

Sriskandakumar, S. (2004) *Cyclic loading response of Fraser River sand for validation of numerical models simulating centrifuge tests*, University of British Columbia, Canada.

Sudevan, P. B., Boominathan, A. and Banerjee, S. (2020) 'Numerical Study of Liquefaction-Induced Uplift of Underground Structure', *International Journal of Geomechanics*, 20(2).

Tokimatsu, K. and Seed, H. B. (1987) 'Evaluation of settlements in sands due to earthquake shaking', *Journal of Geotechnical Engineering,* 113(8)(8), 861-878.

Tuttle, M., Law, K. T., Seeber, L. and Jacob, K. (1990) 'Liquefaction and ground failure induced by the 1988 Saguenay, Quebec, qrthquakel', *Canadian Geotechnical Journal,* 27(5), 580-589.

Ueng, T. S., Wang, M. H., Chen, M. H., Chen, C. H. and Peng, L. H. (2006) 'A large biaxial shear box for shaking table test on saturated sand', *Geotechnical Testing Journal,* 29(1), 1-8.

Ueng, T. S., Wu, C. W., Cheng, H. W. and Chen, C. H. (2010) 'Settlements of saturated clean sand deposits in shaking table tests', *Soil Dynamics and Earthquake Engineering,* 30(1-2), 50-60.

Wang, Y., Fall, M. and Wu, A. (2016) 'Initial temperature-dependence of strength development and self-desiccation in cemented paste backfill that contains sodium silicate', *Cement and Concrete Composites,* 67, 101-110.

Wu, J., Kammerer, A. M., Riemer, M. F., Seed, R. B. and Pestana, J. M. (2004) *Laboratory Study of Liquefaction Triggering Criteria,* translated by Vancouver, BC, Canada.

Xu, P., Hatami, K. and Jiang, G. (2020) 'Study on seismic stability and performance of reinforced soil walls using shaking table tests', *Geotextiles and Geomembranes*, 48(1), 82-97.

Yilmaz, E., Belem, T. and Benzaazoua, M. (2012) 'One-Dimensional Consolidation Parameters Of Cemented Paste Backfills / Parametry Jednowymiarowej Konsolidacji Podsadzki W Postaci Cementowej Pasty', *Gospodarka Surowcami Mineralnymi - Mineral Resources Management,* 28(4)(4), 29-45.

Yilmaz, E., Kesimal, A. and Ercidi, B. (2004) *Strength development of paste backfill simples at Long term using different binders*, translated by China: 281-285.

Yumlu, M. and Guresci, M. (2007) 'Paste backfill bulkhead monitoring: A case study from Inmet's Cayeli Mine, Turkey', in *In Proceedings of the 9th International Symposium in Mining with Backfill*, Montréal, QC, Canada,

CHAPTER 7 Synthesis and Integration of Results

7.1 Introduction

In order to better understand the cyclic behavior of fresh CPB material subjected to cyclic conditions at the early age, the results obtained from the four technical papers presented in Chapters 3, 4, 5, and 6 of this dissertation have been synthesized in this chapter. Each of these papers has investigated one or more factors affecting the behavior of fresh CPB material subjected to cyclic conditions at the early age by using the shaking table testing technique as shown in Table 7.1. Although these chapters (technical papers) did not explain the development and design of the experimental setup in detail, the detailed explanation and presentation of the development and design of the setup can be found in the appendix of this thesis.

Table 7.1 Summary of influential factors investigated in this dissertation

Technical Paper	Chapter	Curing Time (hrs)			Sulphate Content (ppm)		Initial Temperature (^oC)		Filling Strategy	
		2.5	4.0	10	0	5000	20	35	CF	DF
1	3	×	×	×	×		×		×	
2	4		×		×	×	×		×	
3	5	×			×		×	×	×	
4	6	×	×		×		×		×	×

CF: Continuous Filling; DF: Discontinuous Filling

Section 7.2 of this chapter presents the synthesis of representative results from Chapter 3 in order to illustrate the effect of the progress of cement hydration on the cyclic behavior of CPB samples that were cured for different curing time (2.5 hrs, 4.0 hrs, and 10.0 hrs). Afterwards, Section 7.2 presents the main results obtained from Chapter 5, which discusses the effect of the chemistry of the mixing water of CPB on its cyclic behavior by conducting the shaking table testing on CPB samples that were prepared with different content of sulphate (0 ppm and 5000 ppm). Next, the representative results of Chapter 5, which studies the effect of the initial (mixing and curing) temperature on the cyclic behavior of CPB samples that were prepared and cured under different temperatures (20^{o}C and 35^{o}C), are presented in Section 7.3. In addition, the cyclic behavior of CPB prepared with different filling strategies (continuous filling and discontinuous filling) are compared in Section 7.4, which illustrates the main results of Chapter 6.

7.2 Effect of Cement Hydration Progress with Time

In Chapter 3, the effect of cement hydration progress (curing time) on the liquefaction potential of fresh CPB under cyclic loadings has been studied by conducting shaking table testing on three CPB specimens that were poured into FLSB and cured for different maturity age (curing time). All CPB samples were filled inside the FLSB in one layer (continuous filling), and the three CPB samples were cured under stable room temperature of 20^{o}C for 2.5, 4.0, and 10.0 hours respectively.

It has been observed that the progress of cement hydration process with time has a significant effect on the cyclic behavior of CPB, as the young (2.5 hrs old) CPB material was found to be susceptible to liquefaction under the considered cyclic loading conditions, while the older CPB materials (cured for 4.0 hrs or 10 hrs) were resistant to liquefaction. Moreover, cyclic loading has negligible effect on CPB materials that were cured for 10.0 hrs. The enhancement in the liquefaction resistance of CPB with the progress of curing time is due to the combined effect of two factors: (i) the increase in the shear resistance of the CPB material due to the improvement in the cementation between soil (tailings) particles; and (ii) the reduction in PWP and the development of suction (negative PWP) within the backfill due to the progress of cement self-desiccation with time, consequently increasing the effective stress in the CPB. This will enhance the liquefaction resistance of CPB under seismic conditions.

In addition to the above stated findings, it is possible to expand the implication of the results obtained from this study in backfill practice by connecting the seismic behavior of early age CPB material with the values of the compressive strength of CPB material that is freshly placed in mine stopes. Several researches have used this approach and connected the cyclic failure or liquefaction of CPB to the minimum required strength values (UCS_{min}). The "role of thumb" suggested by le Roux (2004) considers that the UCS of CPB material must be ≥100 kPa to be judged as resistant to liquefaction. Belem and Mbonimpa (2016), on the other hand, found that the value of UCS_{min} of non-liquefiable CPB was 32 kPa. However, none of these recommendations or values was based on the cyclic response of CPB in shaking table test. Accordingly, it is worth to analyze the results obtained in the current study with respect to the UCS values of CPB that were determined based on vane shear tests performed on fresh CPB material at very early ages (less than 24 hours) by Fall and Haruna (2020) (Figure 7.1). The CPB tested has the same mix composition as the CPB material considered in this PhD study. It is widely agreed that the unconfined (uniaxial) compression test of a soil represents a special case of the undrained shear test of that soil at which the confining pressure (σ_3) is equal to zero, and the relation between the shear strength (τ) and the unconfined compression strength (or the axial pressure, σ_1) can be defined as $\tau = 0.5\sigma_1$ (Das and Sobhan 2013).

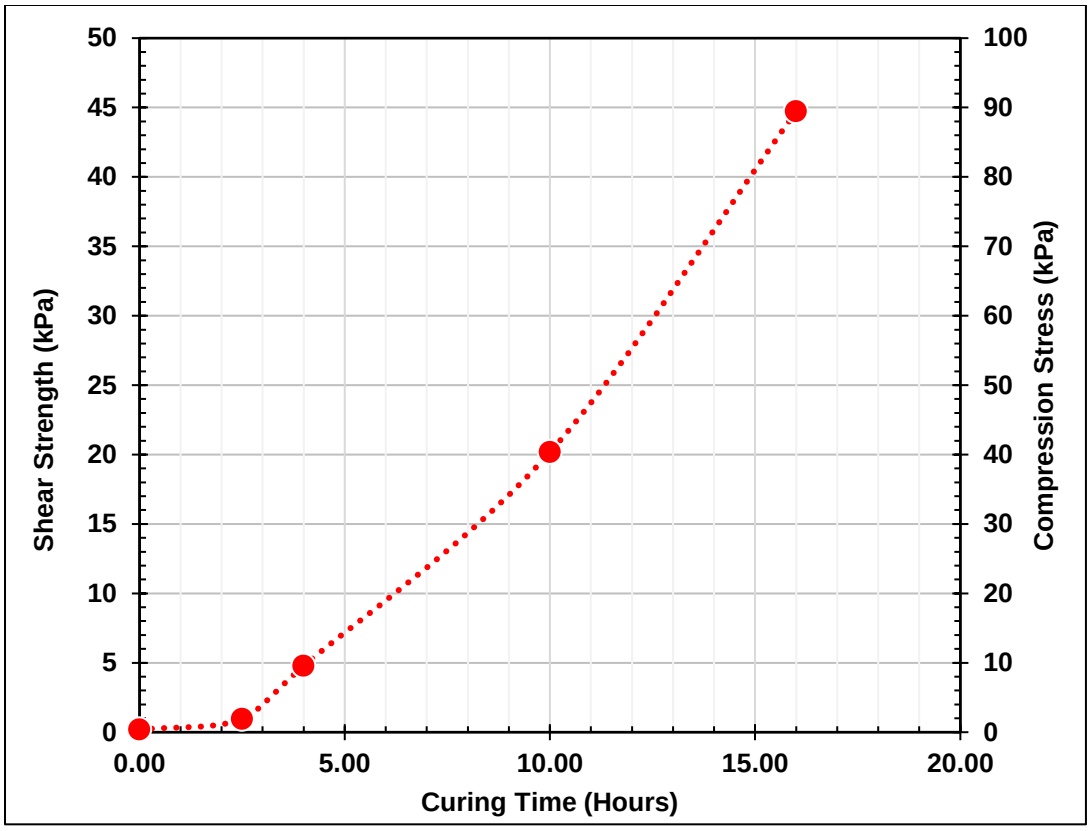

Figure 7.1 Strength development of CPB sample made with 4.5%PCI (w/c: 7.6; Silica tailings used) (experimental data from Fall and Haruna 2020)

From figure 7.1, the UCS values of CPB are determined to be around 2.0 kPa, 10.0 kPa, and 40 kPa at 2.5 hours (curing time), 4.0 hours (curing time), and 10.0 hours (curing time), respectively. By comparing these values with the results of the current study, wherein it is found that the CPB material cured for 4.0 hours is resistant to liquefaction under the tested cyclic conditions, it can be assumed that the minimum compressive strength (UCS_{min}) of CPB material (composed of 4.5% PCI and w/c of 7.6) is 10.0 kPa. It is also found from this analysis that under earthquake-induced stresses caused by ground acceleration of 0.13g, the risk of the liquefaction failure becomes negligible when the UCS value reaches 10.0 kPa (i.e. after 4.0 hours of curing). Owing to these estimations, the aforementioned "role of thumb" for this condition was found to be too conservative. Adopting UCS_{min} values that are less conservative in backfilling practices instances may have significant implications with respect to the mining cycle and productivity, as the lower UCS_{min} values allow more CPB material to be backfilled in the mine stopes in shorter time. In other words, instead of waiting the CPB material to have a strength of 100 kPa, which might need around 35 hours (as per Figure 7.1), the cyclic time could be reduced to 4.0 hours (UCS_{min}:10.0 kPa) or (conservatively) 10.0 hours (UCS_{min}:40.0 kPa). However, it is important to know that this conclusion is subjected to several uncertainties, because there is a large number of (internal and external) variables that can command the seismic response of CPB at a particular age. The internal variables include the origin of tailings and their grain size, mineralogy, binder type, and content,

water content (w/c ratio) of CPB mix, and the presence of chemical elements etc. The external variables include the magnitude of seismic events (such as the acceleration, frequency, and amplitude), temperature variation of CPB, and the surrounding environment, backfilling method, and the condition of water drainage during backfilling and curing period. Accordingly, further interpretation with respect to these variables is always required.

7.3 Effect of the Chemistry of Mixing Water

Previous studies (e.g. Ercikdi et al. 2009, Fall and Pokharel 2010, Pokharel and Fall 2013, Ercikdi et al. 2017, Aldhafeeri 2018) have found several (internal and external) sources of sulphate in CPB. Internal sources include the oxidation of sulphide minerals (such as pyrite) that are commonly found in hard rock tailings, and the mine processing water used as the mixing water in CPB preparation that might contain sulphate ions. The external sources include the usage of sulphur dioxide and air method in the remediation of cyanide in gold mines as well as the chemical additives (such as gypsum and anhydrite) that are often added to the clinker to control the cement setting.

In Chapter 4, the effect of chemistry of the mixing water (initial sulphate content) on the liquefaction potential of 4.0 hours aged CPB under cyclic loadings has been studied by conducting shaking table testing on two CPB samples that were prepared with different sulphate contents of 0 and 5000 ppm. Both CPB samples were prepared and cured under stable room temperature of 20^{o}C for 4.0 hrs and were poured into the FLSB in one layer (continuous filling).

It has been found that the presence of sulphate has a considerable effect on the cyclic behavior of CPB. The 4.0 hours old CPB materials containing sulphate are susceptible to liquefaction, while the sulphate-free 4.0 hours old CPB materials were resistant to liquefaction. The sulphate-induced reduction in liquefaction resistance of CPB is related to the effect of two factors: (i) the reduction in the intensity of cement hydration, and the consequent reduction in self-desiccation, which weakens the effective stress of CPB containing sulphate; and (ii) the inhibition of cement hydration process due to the presence of sulphate, which reduced the production of cement hydration products, thereby resulting in weakening of the bonds between CPB particles. This will consequently increase the liquefaction susceptibility of sulphate-rich-CPB when subjected to seismic conditions.

Based on the findings of this chapter, it can be concluded that the decrease in the liquefaction resistance of CPB due to the presence of sulphate ions may have practical consequences with respect to the mining cycle and productivity. The decrease in CPB liquefaction resistance because of the sulphate-induced inhibition of cement hydration process will slow down the filling cycles, as more time will be required for each fill of CPB material to reach the minimum required strength before allowing more CPB material to be backfilled. Hence, the productivity of the mine will be reduced. However, there are several solutions that can be adopted to address this challenge. Indeed, the use of binders (e.g. Portland cement type V and blast furnace slag), which are resistant to sulphate attack, will improve the strength and strength gain rate of the CPB, and

consequently enhance its liquefaction resistance. Moreover, adopting or allowing proper drainage conditions during the backfilling process will help in reducing the seismic-induced development of excess pore-water pressure.

7.4 Effect of the Initial Temperature of CPB

Previous studies (e.g. Fall et al. 2010, Aldhafeeri et al. 2016) have found that several heat sources can influence the temperature of CPB in the field. These sources include internal heat that is generated during cement hydration process and/or produced by CPB transportation through pipelines, and external heat sources that are related to the temperature variation with depth, geological conditions, geographic location of the mine, and human-induced temperature variations.

In Chapter 5, the effect of the initial mixing and curing of CPB on its cyclic response was studied subjecting shaking conditions on two CPB samples that were prepared and cured at different temperatures of 20^{o}C and 35^{o}C, by using the shaking table test. Both CPB samples were poured into the FLSB in one layer (continuous filling), and were prepared and cured for 2.5 hrs.

The results of this part of the study show that high initial temperature reduces the liquefaction susceptibility of CPB material subjected to dynamic loading. The 2.5 hours old CPB samples prepared and cured at 35^{o}C temperature can be resistant to liquefaction, whereas the 2.5 hours old CPB samples prepared and cured at 20^{o}C temperature are prone to liquefaction. The improvement in the liquefaction resistance of CPB samples when prepared and cured at high temperature is attributed to the coupled effect of two factors: (i) the increase in cement hydration rate in CPB of high initial temperature, which intensifies the self-desiccation and consequently increases the effective stress in the CPB; and (ii) the acceleration of cement hydration process due to the high initial temperature, which leads to the formation of more cement hydration products and strengthens the cementation between tailings particles. Accordingly, the resistance of CPB towards the cyclic-induced liquefaction will enhance when prepared and cured at high temperature.

Based on the findings of this chapter, it can be concluded that backfill operations carried out under conditions (e.g. deep mines, and CPB prepared with a binder that generates large amount of heat (Portland cement), long transportation of CPB through the pipelines, mining operations near geothermal sources, and use of warm mixing water that favors an increase in the temperature of the backfill will result in CPB structures that are more resistant to liquefaction. This has practical implications with respect to the mining cycle and productivity. The enhancement in liquefaction resistance because of the high initial temperature-induced acceleration in cement hydration process will speed up the filling cycles, as less time will be required for each fill of CPB material to reach the minimum required strength, consequently allowing more CPB material to be backfilled in shorter time. Hence, the productivity of the mine will be improved. On the other hand, when backfilling conditions result in CPB with low or lower temperature (e.g. mine in permafrost or cold region, use of cold mixing water, and use of binders with low hydration heat), CPB structures' higher liquefaction susceptibility will be expected. In other words, the mining cycle will increase,

which will, in turn, decrease the productivity of the mine, because low or lower initial temperature will diminish the liquefaction resistance of CPB. For instance, by reducing the initial temperature to near zero degree, the cement hydration process will significantly slow down and thereby increase the time required for CPB material to reach the desired strength. This will definitely cause delay in the backfilling process as more time will be required for each CPB fill before allowing the next fill to be placed. Thus, the backfilling cycle will require more time. This issue can be fixed by using chemical additives (such as sodium silicate) that accelerate cement hydration process, altering the mixing temperature, and/or using some additional artificial heat sources that can help in balancing the reduction in the temperature of the surrounding environment. Further assessment is suggested in this regard.

7.5 Effect of CPB Backfilling Strategy

In most modern underground mines, it is common practice to sequentially place the CPB in the mine stope in two (or more) layers or stages (Plug + residual or main fill). The first layer often consists of high binder content (7% wt) and is usually kept for curing for several (2-7) days. The second layer consists of lower binder content (typically 3-4.5% wt) and is usually left for curing for longer period. On the other hand, some mines adopt continuous filling, where the CPB material is placed within the mined-out stope continuously (in one layer). However, in some cases, the continuous filling operation might be interrupted due to technical issues (such as plant breakdown, and operational factors), causing the CPB to be filled in multiple layers (Yilmaz et al. 2015, Abdul-Hussain and Fall 2012).

In Chapter 6, the effect of backfilling strategy of CPB on its cyclic response has been investigated by conducting shaking table testing on three CPB samples (layered, unlayered) that were prepared with different filling strategies. The first CPB sample was prepared and filled inside the FLSB in one layer (continuous filling) and kept for curing for 2.5 hrs. The second CPB sample was prepared and filled inside the FLSB in one layer (continuous filling) and kept for curing for 4.0 hrs, while the third CPB sample was prepared and filled inside the FLSB in two layers (sequential or discontinuous filling), where the first layer was kept for curing for 4.0 hrs, and the second layer (consisting of the components exactly same as that of the first layer) was cured for 2.5 hrs. All CPB samples were prepared and cured under stable room temperature of 20^{o}C.

It was found from the results obtained from this part of the study that the discontinuous (layered) filling of CPB material will reduce the liquefaction susceptibility or increase the liquefaction resistance of CPB, while the CPB material prepared in continuous (one layer) filling can liquefy under the studied cyclic conditions before achieving 4.0 hrs of curing. The liquefaction resistance in the layered CPB sample is related to the combined effect of two factors: (i) strengthening of the cementation between soil particles of the lower layer, which increases the shear resistance of the material of this layer; and (ii) the influence of the created drainage conditions within the lower layer, which creates a preferential path for the excess PWP to escape from the upper layer, and consequently reduces the shaking-induced buildup of PWP within the

backfill. Hence, the CPB material prepared in discontinuous (sequential or layered) filling will be less prone to liquefaction when subjected to the studied cyclic loadings.

The results presented and discussed in the Chapter 6 suggest that discontinuous filling strategy enhances the liquefaction resistance of CPB. However, unlike the common sequential filling, where the plug has to contain high binder content (e.g., 7%) and has to be first cured for 1-3 days before pouring the residual fill of lower binder content (e.g., 3-4.5%) to minimize the liquefaction risk of the CPB structure, the results obtained indicate that a much shorter curing time of the plug with lower binder content may be possible without jeopardizing the liquefaction resistance of the backfill structure, which means that the backfilling cycle can be significantly accelerated, thus the mine productivity will be potentially improved. Indeed, the liquefaction susceptibility of the layered CPB samples, where the first layer is cured for 4.0 hours and the second layer is cured for 2.5 hours, has been found to be potentially low.

7.6 References

Abdul-Hussain, N. and Fall, M. (2012) 'Thermo-hydro-mechanical behaviour of sodium silicate-cemented paste tailings in column experiments', *Tunnelling and Underground Space Technology*, 29, 85-93.

Aldhafeeri, Z. (2018) *Reactivity of Cemented Paste Backfill*, University of Ottawa.

Aldhafeeri, Z., Fall, M., Pokharel, M. and Pouramini, Z. (2016) 'Temperature dependence of the reactivity of cemented paste backfill', *Applied Geochemistry*, 72, 10-19.

Belem, T. and Mbonimpa, M. (2016) *Minimum strength required for resisting cyclic softening/failure of cemented paste backfill at early age*, translated by 102-107.

Das, B. M. and Sobhan, K. (2013) *Principles of geotechnical engineering*, Cengage learning.

Ercikdi, B., Cihangir, F., Kesimal, A. and Deveci, H. (2017) 'Practical Importance of Tailings for Cemented Paste Backfill' in Yilmaz, E. and Fall, M., eds., *Paste Tailings Management*, Cham: Springer International Publishing, 7-32.

Ercikdi, B., Kesimal, A., Cihangir, F., Deveci, H. and Alp, İ. (2009) 'Cemented paste backfill of sulphide-rich tailings: Importance of binder type and dosage', *Cement and Concrete Composites*, 31(4), 268-274.

Fall, M., Célestin, J. C., Pokharel, M. and Touré, M. (2010) 'A contribution to understanding the effects of curing temperature on the mechanical properties of mine cemented tailings backfill', *Engineering Geology*, 114(3-4), 397-413.

Fall, M. and Haruna, S. (2020) *Vane shear tests on hydrating cemented paste backfills to their undrained shear strength*, University of Ottawa, Canada.

Fall, M. and Pokharel, M. (2010) 'Coupled effects of sulphate and temperature on the strength development of cemented tailings backfills: Portland cement-paste backfill', *Cement and Concrete Composites*, 32(10), 819-828.

le Roux, K. (2004) *In situ properties and liquefaction potential of cemented paste backfill*, Doctoral dissertation: University of Toronto, Ontario, Canada.

Pokharel, M. and Fall, M. (2013) 'Combined influence of sulphate and temperature on the saturated hydraulic conductivity of hardened cemented paste backfill', *Cement and Concrete Composites*, 38, 21-28.

Yilmaz, E., Belem, T., Bussière, B., Mbonimpa, M. and Benzaazoua, M. (2015) 'Curing time effect on consolidation behaviour of cemented paste backfill containing different cement types and contents', *Construction and Building Materials*, 75, 99-111.

CHAPTER 8 Conclusions and Recommendations

8.1 Conclusions

Following findings have been drawn from the results obtained in this study: -

- There was a significant increase in PWP (development of excess PWP) when shaking CPB samples were cured for 2.5 hours.
- Less excess PWP was developed under cyclic conditions for CPB samples cured for 4.0 hours.
- No excess PWP was developed under cyclic conditions for CPB samples cured for 10.0 hours.
- Cyclic-induced liquefaction was achieved for CPB samples cured for 2.5 hours.
- CPB samples cured for 4.0 hours were resistant to liquefaction under dynamic loadings.
- CPB samples cured for 10.0 hours were highly resistant to cyclic loadings.
- Excess PWP was significantly developed by shaking sulphate-rich 4.0 hours-aged CPB samples.
- Less development of excess PWP was observed owing to shaking sulphate-free 4.0 hours aged CPB sample.
- The presence of sulphate within the CPB mixture will increase the susceptibility of cyclic-induced liquefaction of CPB material at an early age.
- Development of excess PWP was significantly reduced in shaking 2.5 hours-aged CPB samples that were prepared and mixed in high initial temperature.
- Higher development of excess PWP was observed in shaking 2.5 hours-aged CPB samples that were prepared and mixed in low initial temperature.
- The high initial (mixing and curing) temperature of CPB mixture will decrease the susceptibility of cyclic-induced liquefaction of CPB material at an early age.

- Using discontinuous or sequential (layered) backfilling strategy while placing the fresh CPB material in underground mine stopes will reduce the susceptibility of this material to liquefy.

- Using continuous (one layer) backfilling strategy while placing the young CPB material will increase its liquefaction susceptibility when subjected to cyclic conditions at an early age (less than 4.0 hours).

- The study also provides a detailed discussion on other factors that are used to confirm the above stated findings, such as the shaking acceleration, settlement (vertical displacement), horizontal deformation (displacement), and changes in effective stress by monitoring the changes in electrical conductivity, volumetric water content, temperature, and suction (before shaking, during shaking, and after shaking).

- Microstructural analysis was also used for comprehending the obtained results.

- The relatively large-scale 1-g shaking table tests on CPB materials that were conducted in this study are time consuming and expansive. However, they provided significant contribution to the understanding of cyclic behavior and liquefaction potential of CPB at early ages.

- The results obtained in this study can contribute to cost effective and safer design of CPB structures in mining area and reduce the susceptibility of liquefaction-induced failure of these structures under seismic conditions.

- The obtained results can contribute to eliminate the risks related to human lives in the mine area, negative environmental impacts, and the associated economic damages that may occur duo to the seismic-induced failure of CPB structures.

8.2 Recommendations

Taking into consideration the experimental limitations, time consumption and high cost of the experimental tests conducted in this study, the following recommendations are proposed for future works.

- Investigating the seismic behavior of CPB and/or soils undergoing cementation with cyclic parameters or seismic loading conditions different than those applied in this study. These conditions should be close to conditions induced by natural earthquakes. Indeed, cyclic loading conditions selected in this study were not intended to simulate a natural earthquake. Unlike natural earthquakes, the signal used in this study was one-dimensional, of uniform amplitude, constant frequency, and of long duration. In natural earthquakes, the number of cycles is a function of the earthquake magnitude (and is commonly of the order of 5 to 20), and the motion amplitudes have a gradual increase, and a gradual decrease. However, the dynamic loading conditions selected

in this study allowed to gain a deeper insight into the seismic behavior of CPB material as well as provide key information necessary for the future development of model to describe the seismic behaviour of CPB.

- Investigating the seismic behavior of CPB materials that are prepared with mix designs that are different from which was used in this study. For instant, CPB prepared using different binder material (such as Slag and/or Flay Ash), different binder content, and/or different w/c ratio.
- Studying the seismic behavior of CPB and/or soils undergoing cementation under the effect of the different conditions described below:
  - ✓ The effect of sulphate on the seismic behavior of CPB materials that are cured for 10.0 hours.
  - ✓ Combined effect of the presence of sulphate and high initial temperature on CPB materials that are cured for 2.5 hours and 4.0 hours.
  - ✓ Studying the effect of the presence of sulphate within the CPB materials that are filled using discontinuous filling strategy.
  - ✓ Investigating the liquefaction potential of CPB materials that contain different initial chemical components, such as different dosages of sodium silicate and/or superplasticizer.
  - ✓ Investigating the seismic behavior of CPB materials that are prepared and cured with sub-zero initial temperature and cured for more than 4.0 hours.
- Constitutive modeling and simulation of the seismic behavior and liquefaction response of CPB materials under seismic loadings

APPENDIX

Experimental Setup

APPENDIX: Experimental setup

In this appendix, the experimental setup, its design and development, and CPB sample preparation are explained in detail.

1. Shaking Table and Fexibale Laminar Shear Box (FLSB)

The cyclic behavior of fresh CPB was investigated in this study by exposing CPB samples to seismic (cyclic) loadings using the shaking table of the University of Ottawa (Figure Appendix.1). This shaking table consists of a rigid steel base and has a platform of (~1200 mm × ~1060 mm), with steel C-channels between them. The cyclic loading of this is driven by an MTS hydraulic actuator (Figure Appendix.2) that provides a series of one dimensional (longitudinal) sinusoidal cyclic motion with one degree of freedom of horizontal displacement. The cyclic loading range, maximum base shear capacity, and displacement limit of this table are 1 to 17 Hz, 27 kN, and 120 mm, respectively. The MTS actuator is controlled by a digital control module (MTS module). The input data that have to be provided to the MTS module to operate are the maximum amplitude (horizontal displacement), displacement time (movement frequency), and desired shaking period.

In order to achieve the goals of this study, and to simulate shaking events in semi-realistic conditions, a flexible laminar shear box (FLSB) (Figure Appendix.3) was developed for this research program, and fabricated and assembled at the facilities of the University of Ottawa. The FLSB consists of 30 horizontal laminae made of (31.7 mm × 31.7 mm) aluminum alloy box sections. The inner dimensions of each lamina are (75 mm × 750 mm), and the clearance spacing between lamina was arranged to be (2 mm) to ensure the independent movement of each lamina. Accordingly, the total capacity of assembled FLSB is 750 mm × 750 mm (in plan) and 1,000 mm (in depth).

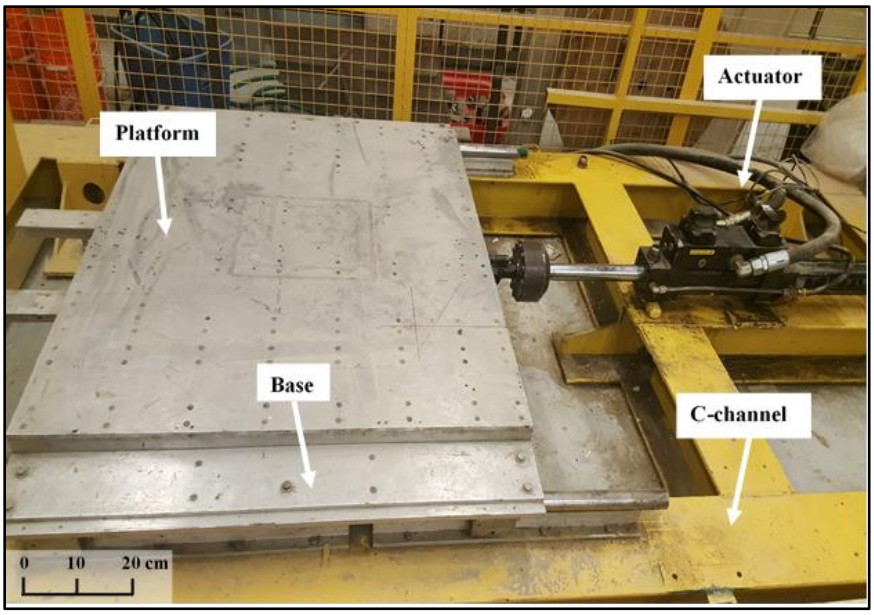

Figure Appendix.1 Shaking table of the University of Ottawa

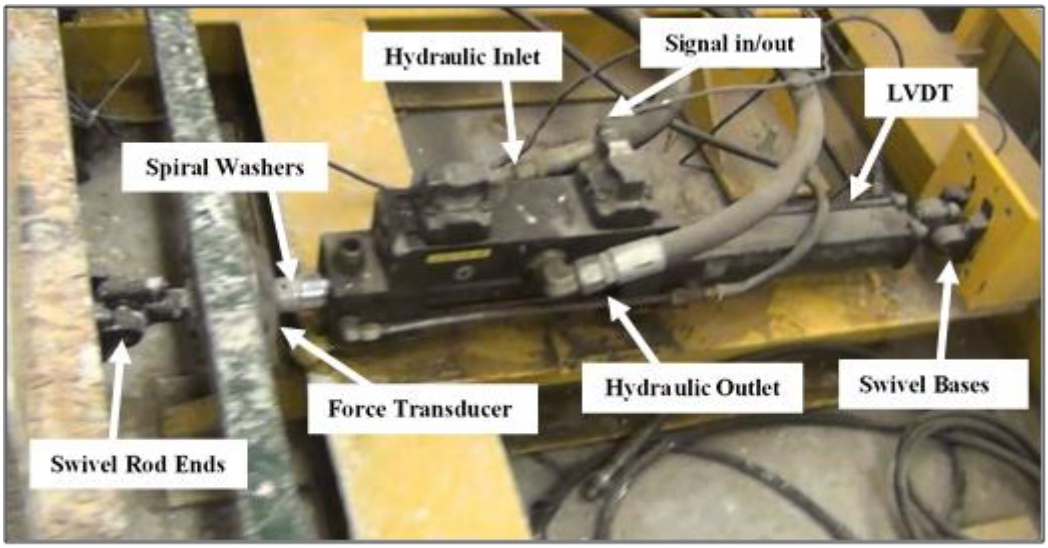

Figure Appendix.2 MTS actuator used in this study

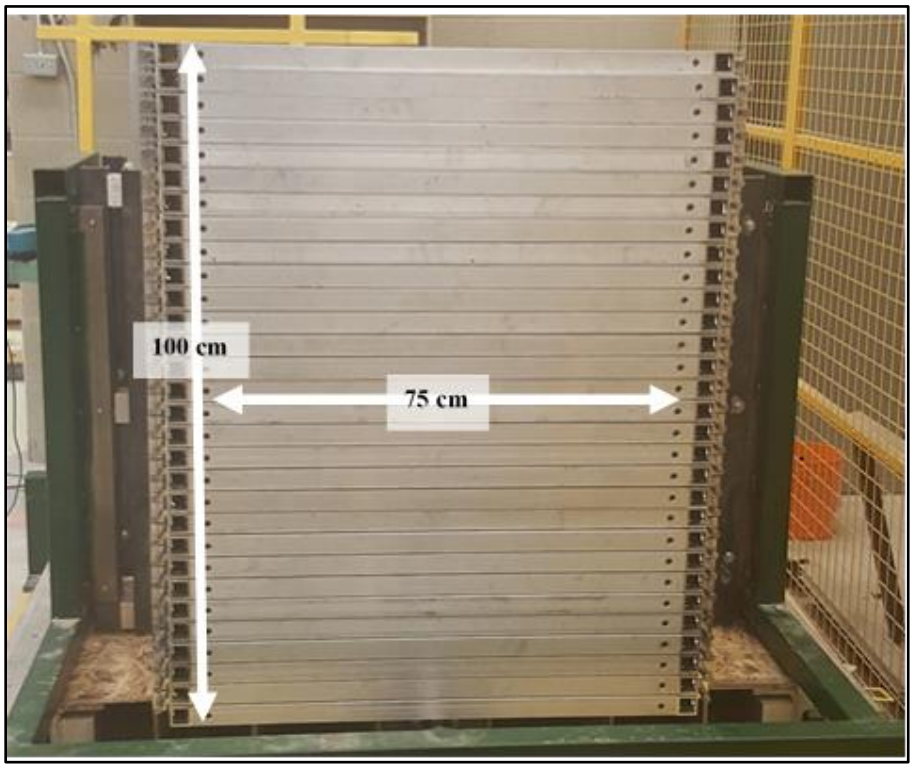

Figure Appendix.3 Flexible Laminar Shear Box (FLSB) designed and built at the University of Ottawa for this study

A flexible polyethylenic membrane of 0.5 mm thickness was placed in the FLSB to contain/hold the CPB mixture (Figure Appendix.4). The high flexibility of this membrane causes no (or negligible) effect on the movement of the FLSB. The FLSB and the membrane were securely attached to the platform of the shaking table.

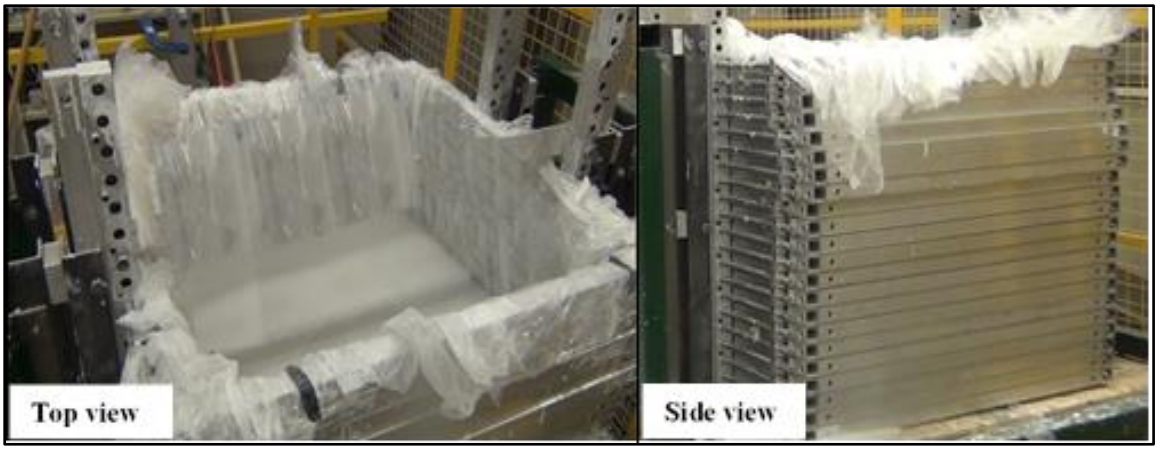

Figure Appendix.4 Flexible membrane placed in the FLSB.

2. Instrumentation Setup

The FLSB was instrumented with numerous sensors and transducers to determine/measure the desired characteristics of CPB material before, during, and after applying the cyclic loading.

In order to design an instrumentation setup that is suitable for this research, it was necessary to study the available setups that were developed/adopted in previous studies from the literature. Specially those studies that dealt with shaking table, laminar box, tailings, and/or fresh CPB. Also, because the behavior and consistency of any cemented soil changes with the progress of time (due to cement hydration), it was important to try these setups by conducting a series of trial tests on uncemented tailing slurry (with same mix design of CPB, but without cement) (Figure Appendix.5). However, due to the consistency of the mixture and the high water content, none of these setups properly worked in the current research. Accordingly, it was necessary to develop a new setup that appropriately works with the fresh CPB mixture.

Finally, and after conducting several trial tests, a suitable setup was developed for this study (Figure Appendix.6). The design of this setup is described in the following sub-sections:

2.1 Vertical Displacement Transducers

The vertical displacement transducers are divided into two system groups: (i) surface settlement, at which a linear variable differential transformer (LVDT) was used. The HCD-1000 LVDTs of 25.4 mm range were used and was placed on top of a lightweight perforated plastic plate, which is placed on the CPB models surface. To avoid uncontrolled movement of the LVDT during shaking, it was connected through a plastic bridge that is attached to the side of the FLSB (Figure Appendix.7); and (ii) layered settlement, at which three Celesco SP2-12 compact string Cable transducers (CTs) with 317 mm range were used to determine the shaking-induced settlement within the CPB material at various depths. These CTs have an accuracy of ±0.25 to ±1.0%, and they operate in temperature and vibration ranges of -18 to +71^{o}C and 2000 Hz, respectively.

Figure Appendix.5 Trial tests and trial instrumentation setups

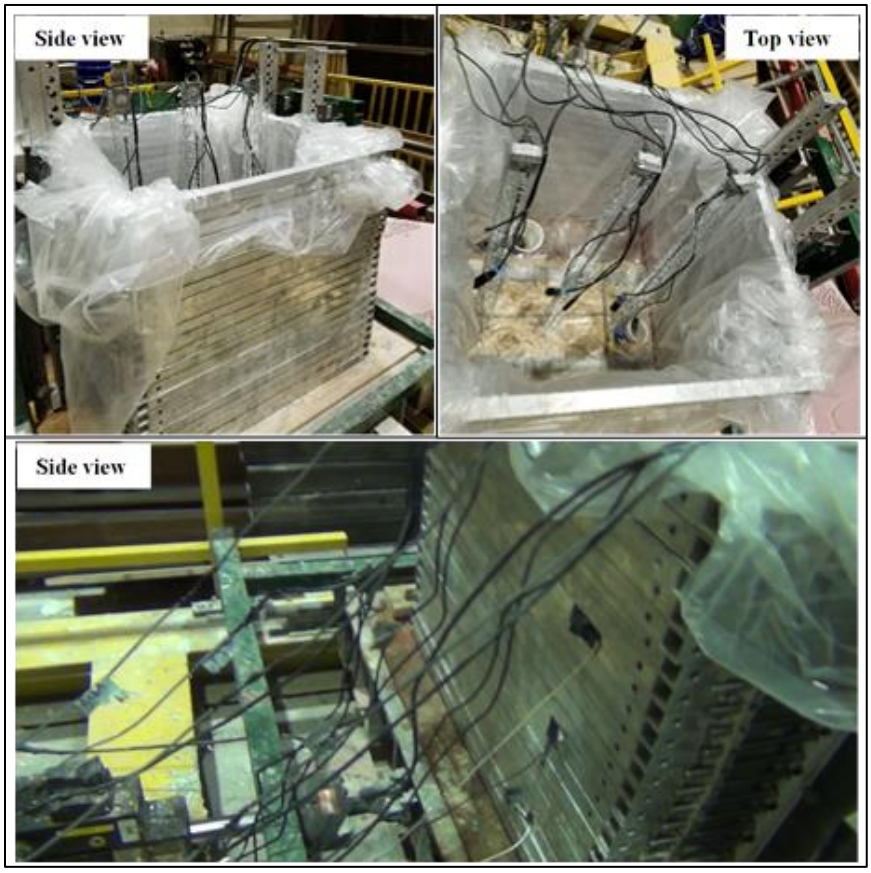

Figure Appendix.6 Instrumentation setup used in this study

CTs were attached to a thin metal rods connected to lightweight perforated plastic plates that were installed at the three different depths. The CTs, metal rods and plastic plates were installed within a cylindrical guidance towers (made of thin mesh sheets) to avoid unwanted tilting/ movement during shaking. To allow the whole system to follow the same motion rhythm, the guidance towers were connected to the shaking table horizontal bracing bridge and vertical supporting guides (Figure Appendix.8).

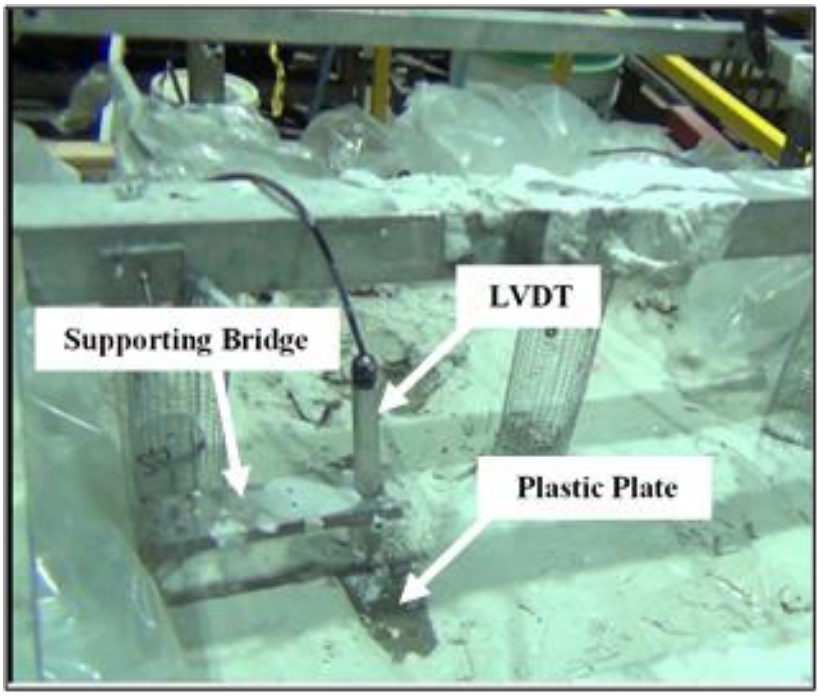

Figure Appendix.7 Surface settlement measuring system.

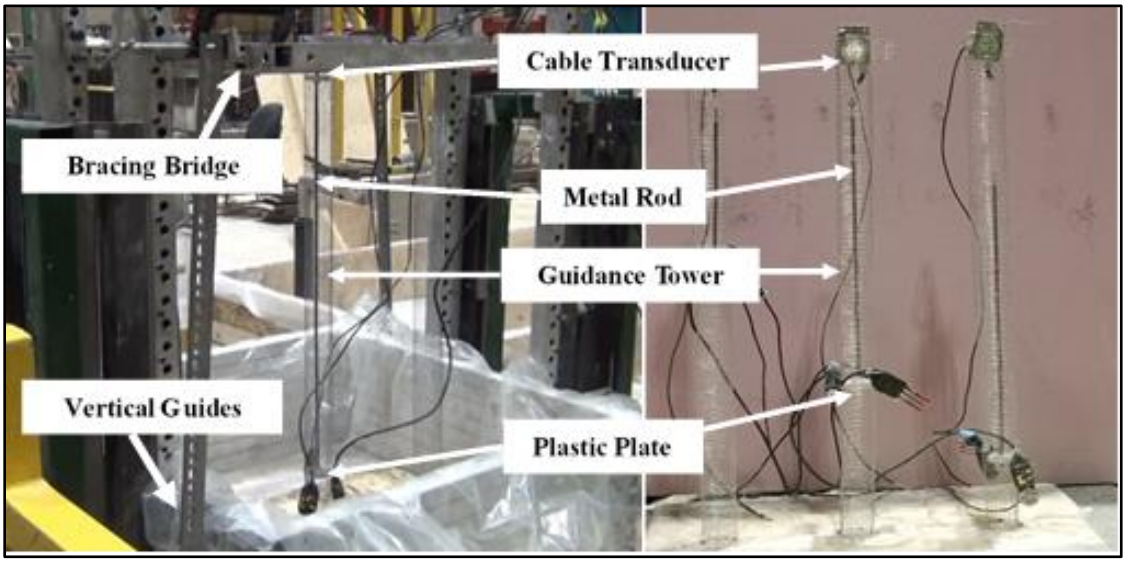

Figure Appendix.8 Layered settlement measuring system.

2.2 Horizontal Displacement Transducers

The horizontal displacement during shaking was also determined using the cable transducers (CTs). The CTs were attached to the shaking table frame and their strings were attached to the outside of the FLSB at depth-related-laminas (Figure Appendix.9).

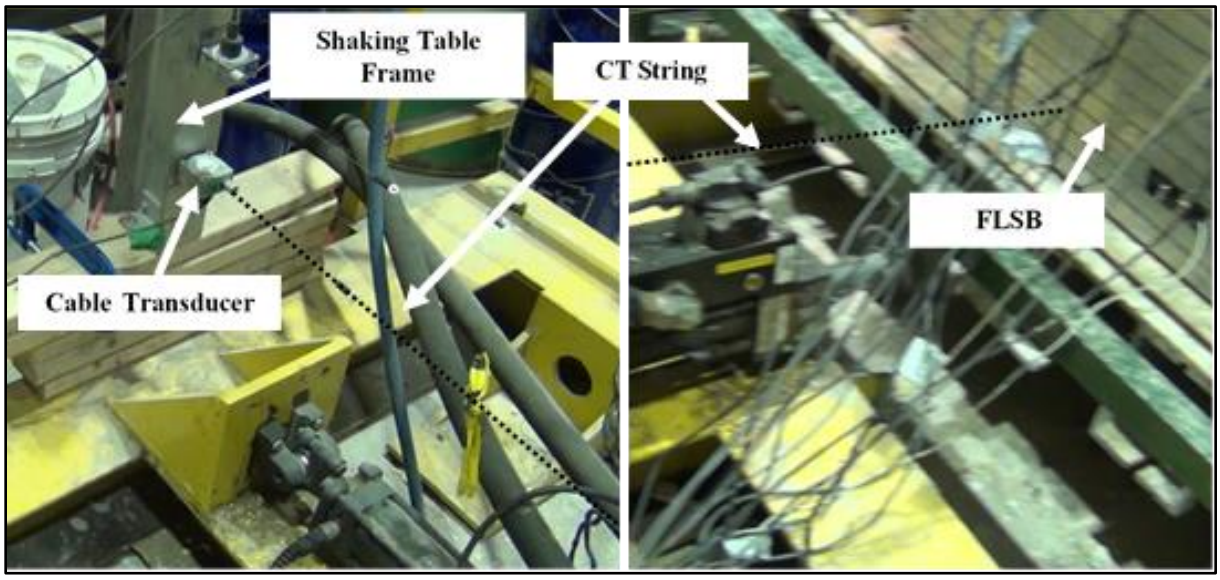

Figure Appendix.9 Horizontal displacement measuring system.

2.3 Puressure Transducers

Omega PX309 Pressure transducers were used to monitor the change in PWP at each depth before, during, and after shaking. The measuring range of these transducers is -15 to +15 PSI and the static accuracy is ±0.25%, and they operate in temperature range of -40 to +85^{o}C. To maintain its position, pressure transducers were attached to guidance towers (Figure Appendix.10).

2.4 ECH2-5TE Sensors

ECH2-5TE sensors were used to monitor the change in electrical conductivity (EC), volumetric water content (VWC), and temperature at each depth within the CPB models before, during, and after shaking. This sensor determines the EC in the range of 0-23 dS/m with the accuracy of ±0.1. It measures the VWC in the range of 0-80% with the accuracy of ±0.15% from 40-80 (VWC), whereas the temperature measurement range and accuracy are -40 to 50^{o}C and ±1°C, respectively. To maintain its position, these sensors were also attached to guidance towers (Figure Appendix.10). These sensors were placed at different depths (0.20 m, 0.40 m and 0.60 m) within the sample.

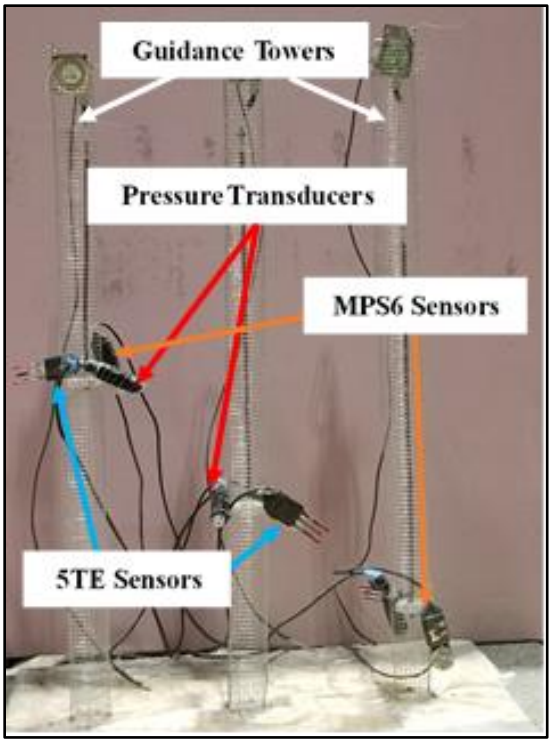

Figure Appendix.10 Pressure transducteurs, 5TE, and MPS6 sensors.

2.5 ECH2-MPS6 Sensors

ECH2-MPS6 sensors were used to monitor the water suction within the CPB models at each depth before, during, and after shaking. Measurement range of these sensors are -9 to -100,000 kPa with a resolution of 0.1 kPa, and its accuracy is ±10% of reading + 2 kPa, from -9 to -100 kPa. To maintain its position, these sensors were also attached to guidance towers (Figure Appendix.10).

2.6 Accelerometers

Endevco-7593A accelerometers were used to determine/maintain the shaking acceleration. Three accelerometers were attached to the outside of the FLSB at each depth-related-laminas, and one accelerometer was attached to the shaking table (Figure Appendix.11). The full-scale range and frequency response of these accelerometers are ±2g and 0-50 Hz, respectively. These accelerometers operate over a temperature range of -40 to 125^{o}C.

2.7 Data Acquisition System and Data Loggers

LVDT, CTs, Pressure transducers, and accelerometers were all connected to signal conditioning and Data Acquisition System (DAQS), while 5TE and MPS6 sensors were connected to Decagon Em50 series data logger. DAQS was connected to external power supplies, while the Em50 is designed to work on batteries. DAQS and Em50 were connected to a computer to record/analyze the required data during the whole test period (Figure Appendix.12). Furthermore, a digital camera was used to record each step of the testing program.

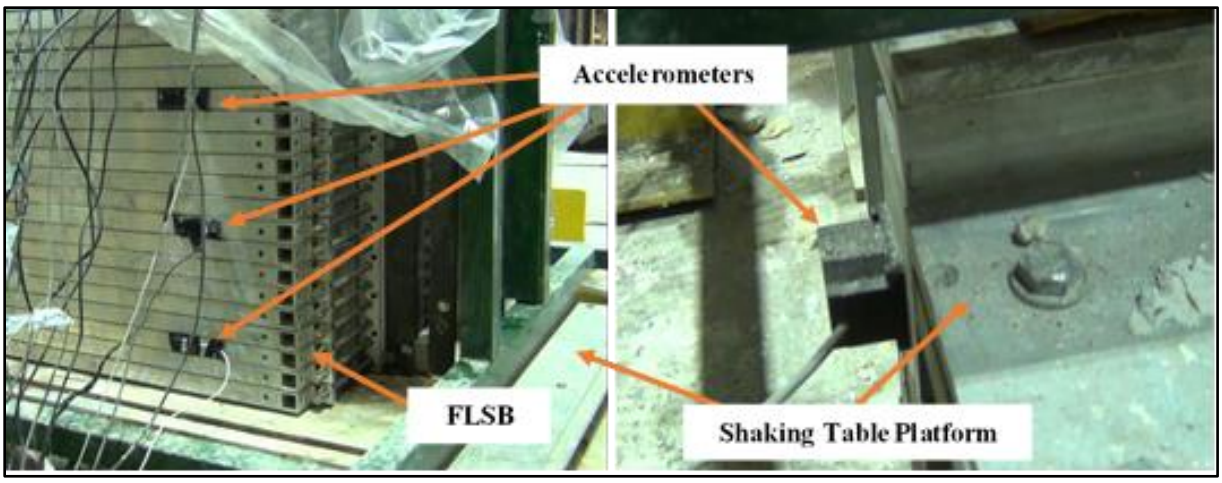

Figure Appendix.11 Shaking accelerometers.

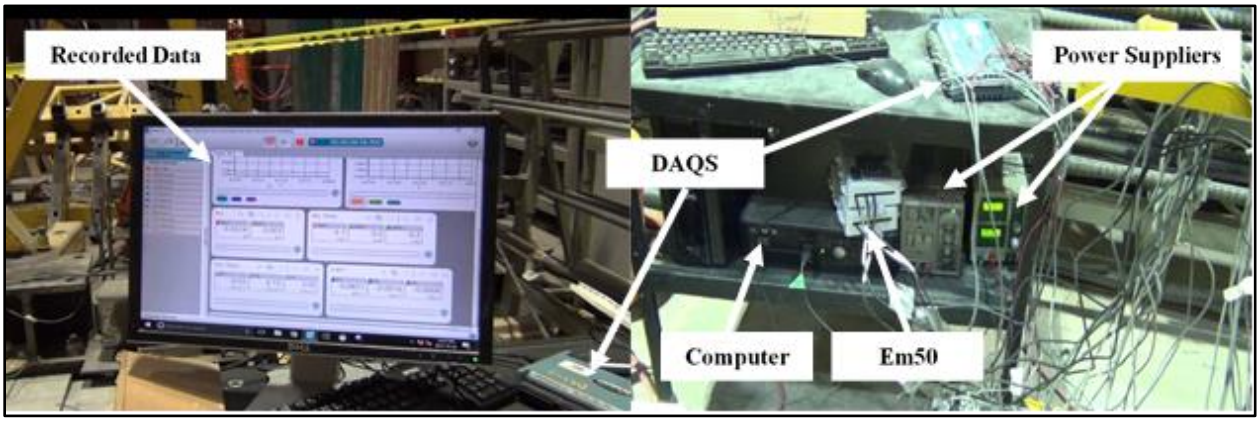

Figure Appendix.12 Data collection system.

3. Instruments Calibration

Prior to conduct and experimental test, it is very important to calibrate all instruments. In this study, the shaking table was calibrated, before placing the CPB material, by entering the input data (maximum amplitude, shaking frequency, and shaking period) to the MTS system, performing the shaking operation and measuring the maximum displacement of the table platform, frequency (number of movement per second), and total shaking period.

Although they have manufacturer calibration sheets, it was necessary to manually calibrate all sensors and transducers used in this research. For instance, pressure transducers were placed under multiple known PWP conditions, and compared it with the values recorded in the DAQS. Same procedure was applied on other sensors and transducers. However, it was difficult to check the manually calibration of the accelerometers, so that the manufacturer calibration sheet was adopted in this case.

4. Models Preparation

After constructing experimental setup, CPB samples were then prepared for each test of the experimental program. In this study, CPB mixtures were prepared and mixed by using a 3.5 Cubic ft mixer (1/3 electric cement mixer) (Figure Appendix.13 and Appendix.14) and then poured into the FLSB (Figure Appendix.15) with final demotion of each CPB model of 75 cm × 75 cm × 70 cm. CPB samples were then securely cured under stable temperature conditions until reaching the desired age (curing time).

5. Shaking Table Test

After curing for the desired age (Figure Appendix.16), shaking table test was performed on each CPB sample. The cyclic loading applied to the shaking table tests of this study encompassed 0.13 g acceleration, 1 Hz frequency, and 32 mm shaking amplitude. Shaking table was conducted for 30 minutes (1800 sec). After shaking, all CPB samples were monitored for 24 hours to capture the post loading behavior. The CPB behavior at each test was recorded by the digital camera, which allows to better evaluate/understand the observed behavior.

6. Microstructure Analysis

In addition to the CPB models prepared for the shaking table tests, CP specimens (CPB material prepared without tailings) were prepared at the same condition of each tested CPB model for microstructural analysis, such as thermal analysis and X-ray diffraction. This allowed better understanding for the effect of microstructural evolution of CPB on its cyclic behavior.

Figure Appendix.13 Mixer used in this study

Figure Appendix.14 CPB mixing process

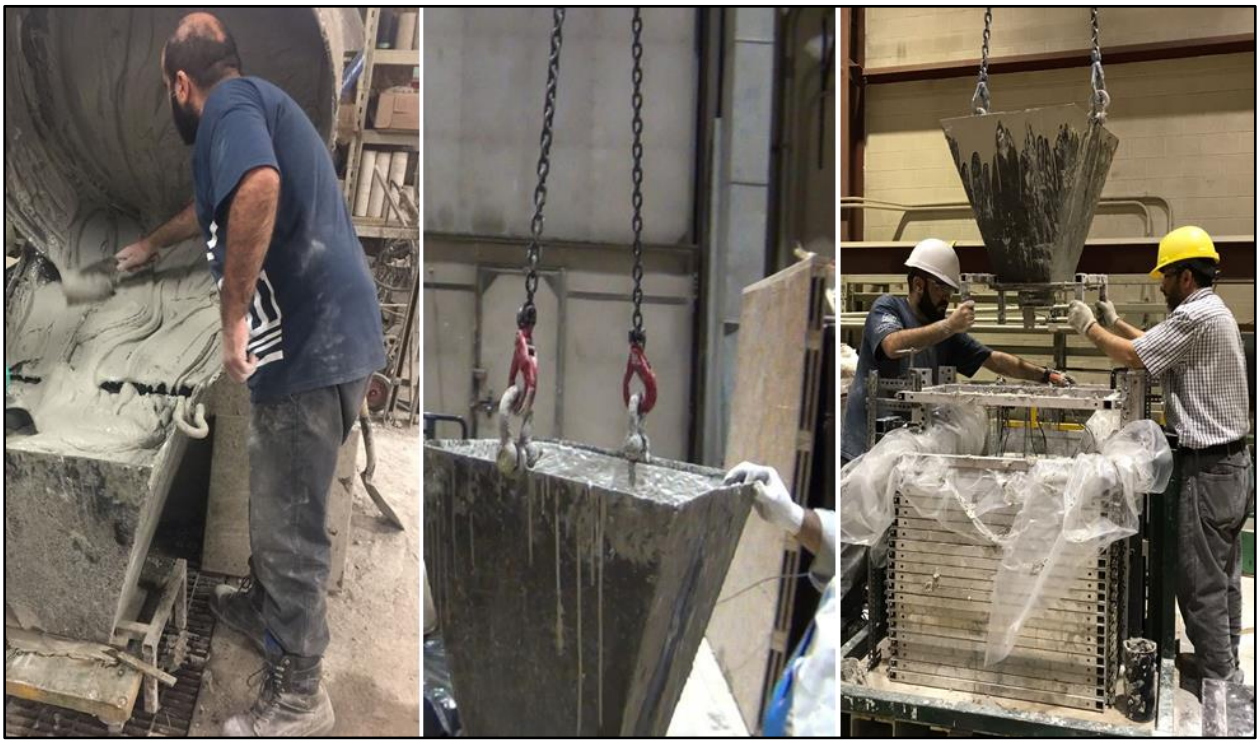

Figure Appendix.15 Pouring fresh CPB mixture inside the FLSB

Figure Appendix.16 CPB sample ready for test